DOCTORAL DISSERTATION

THE PRETREATMENT OF AMMONIUM AND MICROPOLLUTANTS IN DRINKING WATER TREATMENT PLANTS USING NITRIFYING EXPANDED-BED REACTOR WITH BIOLOGICAL ACTIVATED CARBON MEDIA

DAO THI MINH NGUYET

February 2020

THE UNIVERSITY OF KITAKYUSHU

GRADUATE SCHOOL OF ENVIRONMENTAL ENGINEERING

THE PRETREATMENT OF AMMONIUM AND MICROPOLLUTANTS IN DRINKING WATER TREATMENT PLANTS USING NITRIFYING EXPANDED-BED REACTOR WITH BIOLOGICAL ACTIVATED CARBON MEDIA

by

DAO THI MINH NGUYET

Februray 2020

This dissertation is submitted for the degree of Doctor of Engineering

DECLARATION

This dissertation is the result of my own work and contains no material which has been accepted for the award of any other degree or diploma in my name, in any university or other tertiary institution. It contains no material previously published or written by another person, except where due reference has been made in the text. This dissertation has not been previously submitted, in part or whole, to any university or other tertiary institution for any degree, diploma, or the other qualification.

Author

Dao Thi Minh Nguyet

Supervisor

Professor Hidenari Yasui

February 2020

Kitakyushu, Japan

ACKNOWLEDGEMENTS

The PhD journey is a special and unforgettable experience of a life-time to me. When I write these words to close the journey, I would like to take a moment to thank the people who accompanying me during my PhD works.

First and foremost, I would like to express my deepest appreciation to my supervisor Professor Hidenari Yasui for his dedicated support and guidance. I feel very proud of being your PhD student. Your approach in training independent researchers is not easy to say the least; however, I do gain a lot of knowledge and skills through the trials and errors. Thank you for asking the questions that sharpen my insights and raised my works to a higher level. Your responsive feedbacks and tireless efforts in correcting my manuscripts and thesis are very meaningful to me. I also highly appreciate the opportunity of working in your laboratory where we have everything in hands to satisfy our science curiosity.

I would also like to extend my sincere gratitude to Associate Professor Mitsuharu Terashima for his insight comments throughout my study. Your explanations are always simple and efficient which helped me to overcome the research challenges. Your kind supports and encouragements mean a lot to me.

I am deeply indebted to Professor Kiwao Kadokami, without whom my research would not have been possible. Thank you for allowing me to use your laboratory in most of my experimental works. You do not mind showing me how to proceed the cumbersome analysis properly, or spending time to answer to any of my questions. Your generosity, kindness and warm smiles are always cheering up anyone around you including myself.

I am very grateful to Professor Nguyen Viet-Anh in the University of Civil Engineering in Hanoi, Vietnam. He was the one who introduced me to the PhD work, and always give me the advice and encouragement from distance. His analytical thinking, enduring enthusiasm for academic science and perseverance have always been an inspiration to me.

My special thanks go to Associate Professor Changhee Cho in the jury committee for his

valuable comments on my research.

My gratitude also sends to the Vietnam International Education Development (VIED) for the financial supports which made my PhD oversea possible.

I wish to thank my lab-mates in Yasui-Terashima laboratory for supporting me during my PhD works. We have been working together days and nights, running breathlessly for the weekly and monthly reports. I wish you achieve all your goals and success in your future research career.

I always feel like home in Japan thanks to my surrounding Vietnamese friends whom I could not mention all their names here. I am very happy to be part of our “big family”, to share my joys and sorrows with you. You made my four years in Kitakyushu unforgettable.

Words could not express my deepest gratitude to my dearest husband and children, and our families in Vietnam. Your trust and encouragement made me stronger to overcome all the challenges. We have experienced this together, and I am grateful to have your presents in every moment of my PhD journey.

ABSTRACT

At present, the quality of the drinking water supply source is degraded by the pollutants originated from various human activities. Among those contaminants, ammonium and micropollutants are of critical concern due to their toxic and harmful effects to public health and aquatic system, as well as troubles induced in the operation of drinking water treatment processes. Different treatment methods could successfully remove ammonium and micropollutants from water; however, a technology that balanced the treatment efficiency, cost-effectiveness, and sustainability is desirable.

In this regard, a nitrifying expanded-bed reactor using biological activated carbon (BAC) media appeared to be responsive to the demand. Rather than focusing on the adsorption capacity, this process uses exhausted granular activated carbon (GAC) media as the carrier for microbial colonization. This naturally occurring biofilm can biodegrade a wide variety of contaminants such as ammonium, micropollutants, disinfection by-products precursors, and other organic/inorganic substances. In this way, the service life of BAC media could be significantly extended. The up-flow direction also offers advantages, such as improvement of contact between water influent and the biomass in the whole expanded-bed, or reduction of head loss and backwashing frequency.

In the first part, a kinetic model of a nitrifying expanded-bed reactor for the pretreatment of drinking water was developed to analyze its behavior under different concentrations of influent dissolved oxygen, ammonium, and organic substrate. In the laboratory, an up-flow expanded-bed reactor was initially fed with synthetic water containing 1 mg NH_x-N/L to stimulate nitrifiers growth, followed by varied NH_x-N loadings (1–2 mg NH_x-N/L with a fixed linear velocity). From tracer tests, the hydraulic regime of the expanded-bed reactor was simulated to be 11 tanks-in-series. To model the even distribution of media in the expended-bed height, a mathematical internal recycle flow allowing the movement of media between the cell tanks was made. The performances were also studied on the pilot-

and full-scale reactors receiving river water in two water treatment plants in Vietnam. A single set of biological kinetic and stoichiometric parameters was elaborated that successfully reproduced the five different datasets over the lab-, pilot- and full-scale reactors. The attachment/detachment specific rates of the biofilm were estimated during filtration cycles and backwash events. The graphical guidance and empirical equation were provided to obtain the reactor treatment efficiency under variable influent and temperature.

Additionally, the dissertation summarized the principles of the biofilm and biological model with a focus on the Integrated Fixed-film Activated Sludge (IFAS) object on the GPS-X software. The sensitivity analysis of the numerical calculation and operational parameters on the calculation results was also carried out.

In the second part, the possibility of degrading the pesticides using nitrifying expanded-bed reactor was investigated. The field analysis demonstrated that four pesticides Flutolanil, Buprofezin, Chlorpyrifos, and Fenobucard, were removed at the removal efficiencies of 82%, 55%, 54%, and 52% respectively, while others were not significantly removed. Under controlled laboratory conditions with continuous and batch experiments, the adsorption onto the biological activated carbon media was demonstrated to be the main removal pathway of the pesticides. The contribution of microorganisms to the pesticide removals was rather limited. The pesticide removals observed in the field reactor was speculated to be the adsorption on the suspended solids in the influent water or to the biofilm in the reactor. The obtained results highlighted the need to apply a more efficient and cost-effective technology to remove the pesticides in the drinking water treatment process.

TABLE OF CONTENTS

LIST OF FIGURES

LIST OF TABLES

CHAPTER 1. INTRODUCTION

1.1. AMMONIUM OCCURRENCE AND THE NEED OF REMOVAL IN DRINKING WATER TREATMENT

At present, elevated concentrations of ammonium (NH_x-N) are often encountered in different surface water sources worldwide. NH_x-N is considered one of the most critical contaminants in freshwater due to its highly toxic nature and ubiquity in the water systems [1]. NH_x-N of natural sources is mainly produced from the decomposition of organic nitrogen, such as animal excrements and dead plants or animals. However, NH_x-N of anthropogenic sources are the primary factors contributing to freshwater degradation. In the industrial sectors, NH_x-N is primarily used as the nitrogen source in fertilizers in agriculture land, with direct application of anhydrous NH_x-N being the largest method of consumption [2]. To a lesser extent, NH_x-N is also applied in various industrial activities, such as plastics, cleaning products, explosives, animal feed, and food additives. In addition, the discharge of untreated domestic and industrial sewage and runoff from areas with intensive animal husbandry are also major sources of NH_x-N in the environment [3]. The principle emission sources of NH_x-N to the water environment were illustrated in Figure 1. The specific origins and fate of NH_x-N could be identified by analyzing the stable N isotopic compositions in water sources [4].

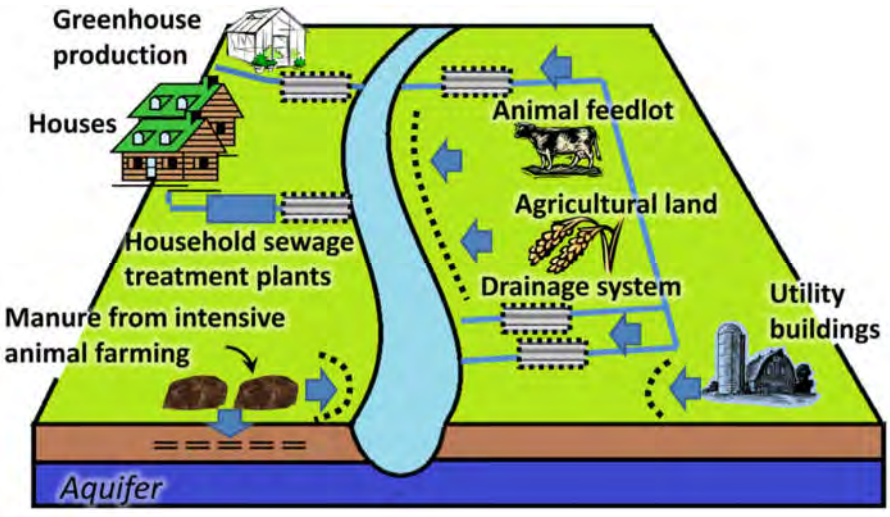

Figure 1. Principle emission sources of ammonium to water environment [5]

In water, NH_x-N is presented in two chemical forms, in which the ammonium ion (NH_4-N) is more abundant than the unionized ammonia (NH_3). The concentration of total ammonia, denoted as NH_x-N, is the sum of NH_4-N and NH_3 concentrations. The ratio of these species depends on the pH and temperature of the aqueous solution, as shown in Figure 2. At the pH around 7 almost the total ammonia is presented as NH_4-N; therefore, the term ammonium is often adopted for this contaminant in water.

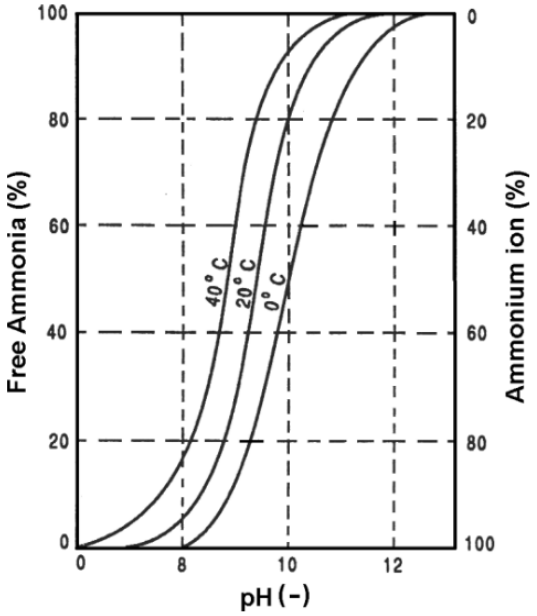

Figure 2. The fraction of ammonium ion and free ammonia as a function of temperature and pH [6]**.**

Annually domestic wastewater released about 20 million tons of NH_x-N into the environment, occupying nearly 10% of the total world emission. The figure is projected to further increase to 35 million tons annually by the middle of 21st century [7]. Consequently, various studies have observed growing trends of NH_x-N contaminants in water sources, especially in developing countries. In Vietnam, the NH_x-N concentrations in major rivers were higher than 0.3 mgN/L, which is the national threshold for drinking water purposes. In particular, very high concentrations of NH_x-N of 6.5mgN/L were monitored in Cau River basin, where industrial wastewater was discharged without proper treatment [8]. In China, the NH_x-N pollution issues in freshwater have drawn significant attention in the main river

basins such as Liao River, Yellow River, Songhua River, etc. For instance, the NH_x-N concentrations were ranged from 0.32 to 8.12 mgN/L in winter and 0.91 to 6.95 in summer in Liao River [9]. In another study carried out in Tongshun River, another large and important river in Jianghan Plain in China, the NH_x-N concentrations were ranged from 0.07 to 10.25 mgN/L mainly due to the discharge of industrial and municipal wastes [4]. In Mongolia, a very high concentration of NH_x-N reached 29.5 mgN/L was recorded in Tuurl River in the North center of the country due to anthropogenic discharge sources [10]. The NH_x-N pollutants in rivers and canals in and around Dhaka City, the capital and the largest city of Bangladesh, were found to be varied from 6.35 to 34 mgN/L in 2008 and 2009, threatening the water supply source of Saidabad Water Treatment Plant.

Opposing pictures relating to NH_x-N pollutants have been drawn in the countries where adequate wastewater treatment facilities are in place. For example, over 21 years from 1992 to 2012, the average NH_x-N concentration in European rivers was decreased by 0.231 mgN/L, which was equivalent to 3.5% per year thanks to implementing the Urban Waste Water Treatment Directive and national legislation [11]. In Canada, the NH_x-N concentrations were found to be lower than 0.1 mgN/L in surface water systems[12]. In Japan, the NH_x-N concentrations met the Water Environment Quality Standard, in which the allowable total nitrogen was ranged from 0.1 to 1 mgN/L, in almost all surface water monitoring sites [13][14]. These examples suggested that the NH_x-N pollution situation in the aquatic environment and supply drinking water sources could be remedied with appropriate integrated water resources management, in which the removal of NH_x-N from water sources played a critical role.

The presence of NH_x-N at high concentrations in surface water ecosystems represented one of the most harmful issues besides oxygen depletion. It could directly impact individual species, typically death, reduced growth rate, or reduced reproduction success. Indirect impacts are those that affect the ecosystem by changing the living conditions of organisms, for instance, eutrophication or acidification [2],[9]. Therefore, the ecology risks assessment caused by NH_x-N has been carried out worldwide. In Liao River in China, the acute and

chronic water quality criteria of NH_x-N based on the toxicity of the Liao River species were found to be 16.86 and 4.39 mgN/L. In Korea, an acute predicted no effect concentration value of 22 mgN/L for NH_x-N was proposed based on short-term toxicity data of Korean native aquatic species. In the USA, the acute and chronic criteria of 17 and 1.9 mgN/L were updated since 2013 for NH_x-N water quality criteria [9]. As for human health, the NH_x-N in potable water is not of significant concern because of its lower concentration than the human capacity to detoxify [15]. Therefore the World Health Organization does not provide health-based guideline value for NH_x-N [16]. However, the presence of NH_x-N might induce objectionable taste and odor; therefore, its maximum concentration is regulated in several drinking water standards, such as 0.3 mgN/L in Vietnamese QCVN01-1:2008/BYT [17].

The elevated concentrations of NH_x-N at the supply drinking water sources are of particular concern for the operators of drinking water treatment plants (WTP). In biological nitrification, NH_x-N will be decomposed into an intermediate nitrite (NO_2-N) and final product nitrate (NO_3-N). In some countries, NO_2-N and NO_3-N are regulated at strict values. For instance, Japan requests 0.04 mgN/L as NO_2-N and 10 mgN/L for total NO_2-N and NO_3-N, while Vietnam requires 0.05 mgN/L as NO_2-N and 2 mgN/L as NO_3-N. Because the formation of NO_2-N and NO_3-N indicates the loss of NH_x-N following a ratio of 1:1:1, their regulated values could be used as a secondary drinking water standard for NH_x-N [18]. In particular, when chlorination disinfection is applied in the water treatment process, a large amount of chlorine would be needed to remove the NH_x-N. A dose of 8 – 10 $mgCl_2/mgNH_x$-N is often recommended to reach the chlorination breakpoint and obtain the free chlorine residual [19]. Therefore, high influent NH_x-N is directly engaged to the increase in the operational costs. Additionally, in case that the influent dissolved oxygen (DO) is limited, the incomplete removal of NH_x-N may result in the accumulation of NO_2-N in the system. The high concentration of NO_2-N in tap water can cause methemoglobinemia in infants [20]. Consequently, more chlorine should be dosed to oxidize the generated NO_2-N.

Therefore, effective technologies to remove NH_x-N from water have been extensively studied, as presented in section 2.1.

1.2. MICROPOLLUTANT OCCURRENCE AND THE NEED OF REMOVAL IN DRINKING WATER TREATMENT

In addition to the NH_x-N contaminants, the micropollutants are of critical concern in the degradation of freshwater quality. As indicated in Figure 3, the surface and groundwater are being degraded by various due to multiple human activities.

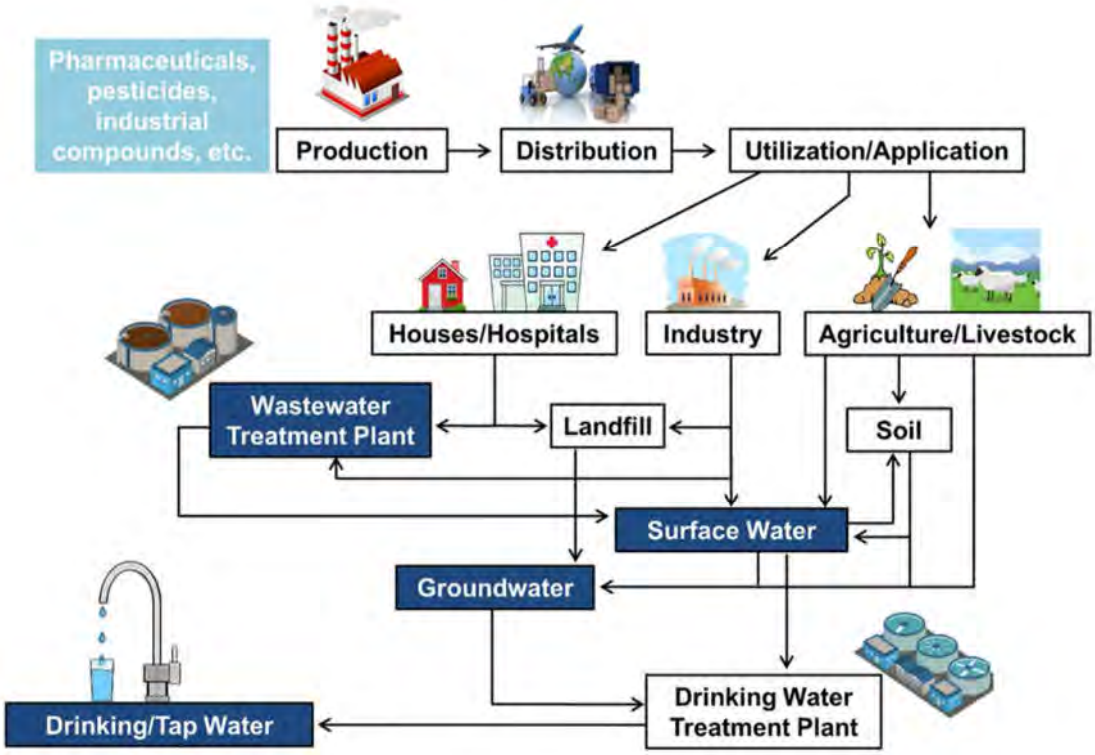

Figure 3. Typical sources and routes of micropollutants in the environment [21]

The release of effluent from wastewater treatment plants to the aquatic environment contributes significantly to the increasing concentrations of contaminants of emerging concern (CECs) in surface water. Those wastewaters originated from domestic, industrial, and hospitals [21]. In developed countries, a high portion of generated wastewater is treated adequately to reduce the harmful effects. However, the discharge of untreated sewage to water bodies occurs in many regions of the world, representing a severe concern to public health and the ecosystem. Conventional wastewater treatment plants were not designed for dealing with these CECs; therefore, they could only be removed to a certain extend. Other

sources of CECs are the leakages from landfills, septic tanks, etc. Additionally, the management of industrial effluents from the production sectors of pharmaceuticals, personal care products, pesticides, and other compounds are not handled properly in some places, which increases the appearance of CECs in water. The runoffs from agriculture and livestock areas are also essential sources of micropollutants [21].

In this study, the concurrence of pesticides in water supply sources was focused. Pesticides are one of the few toxic substances released deliberately into the environment to kill living organisms. Although the term pesticide is often misunderstood to refer only to insecticides, it is also applicable to herbicides, fungicides, and various other substances used to control pests [22]. Several hundred pesticides of different chemical compositions are currently used for agricultural and vector control purposes worldwide [23]. Newer pesticides that are more selective and less toxic to humans and the environment, which require fewer application dosages, are in the trend in developed countries. Meanwhile, significant use of older broad-spectrum pesticides continues in many parts of the world. It was suggested that the mobilization of nutrients might have been surpassed the thresholds that will cause dramatic changes in continental-to-planetary-scale systems, including the pollution of ground and surface waters [24].

The most common way to classify the pesticides is based on their chemical structure, in which the pesticides are divided into four main groups as follows.

Table 1. Typical examples of chemical pesticides with their definition and applications [25]

Pesticide group	Definition and applications
Organochlorines	Stable compounds are too persistent in the environment and tend to accumulate in fatty tissue. Its primary use is in the eradication of disease vectors such as malaria, dengue, and malaria. They are also used in the cultivation of grapes, lettuce, tomato, alfalfa, corn, rice, sorghum, cotton, and wood, for preservation. Its way of

Pesticide group	Definition and applications
	exposure is mainly on insects by contact or by ingestion
Organophosphates	They are esters derived from phosphoric acid. Organophosphorus compounds are most commonly used in agriculture; most are insecticides and miticides. Their way of joining these organizations is by ingestion and contact. They are used in vegetable crops, fruit trees, grains, cotton, sugarcane, among many others.
Carbamates	They are esters derived from acids or dimethyl N-methyl carbamic acid are used as insecticides, herbicides, fungicides, and nematicides. They are less persistent than organochlorines and organophosphates, and likewise, the latter inhibit acetylcholinesterase
Pyrethroids	They originate from natural insecticides derived from pyrethrum extract derived from chrysanthemum flowers, known as pyrethrins.
Others	Other pesticides are triazine herbicides, ureic, hormonal, amides, nitro compounds, benzimidazoles, ftalamidas, bipyridyl compounds, ethylene dibromide, sulfur-containing compounds, copper or mercury, etc.

The presence of pesticides in surface waters has been reported in many regions in the world, such as in Malaysia, Chile, Canada, India, Japan, Greece, Brazil, China, and Vietnam [26]–[34]. Different stages in which pesticides could reach the aquatic environment are illustrated in Figure 4. Pesticide contaminants in surface water are often generated from diffused pollution sources, such as runoff, leaching, and chemical spilling from agricultural zones.

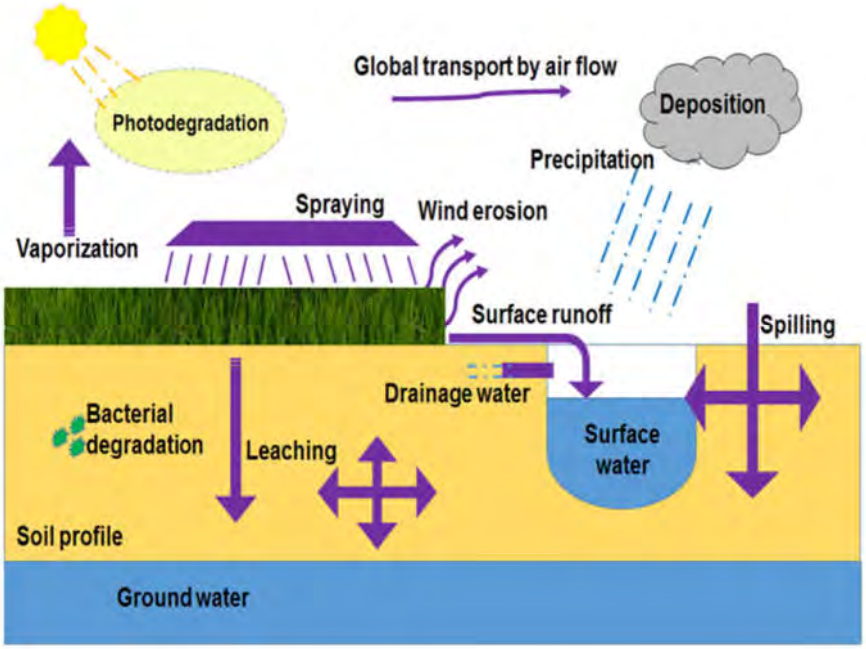

Figure 4. The pathways of pesticides to the aquatic environment [29]

As pesticides are designed to be toxic to particular groups of organisms, they can have considerable adverse environmental effects on other living creatures as well as diverse media, including air, soil, or water [25]. The hazardous effects of pesticides on human health by direct exposures have been well documented in [22], [29]. However, pesticides in drinking water are often of trace levels; hence the concern is primarily for their potential for causing chronic health problems. To the best of our knowledge, there is no scientific publication on the non-carcinogenic health risk, defined as the pesticide thresholds below which the effect does not occur, due to the human ingestion of pesticides in the finished water from WTPs [26]. The studies on the chronic exposure of pesticides were often based on laboratory animals for the measurement of incidence of cancer, birth defects, genetic mutations, or other problems such as damage to the liver or central nervous system. The information were interpreted in the context of its potential hazard under actual field conditions, providing the health-based data for the policy makers [35].

The drinking water guidelines are aimed at keeping pesticides at levels below those that are considered to cause any health effects in humans [35]. In 2017, the World Health Organization (WHO) had provided the guideline values for 31 pesticides presented in

drinking water, which were of health significance [16]. In Europe, a proposal for a revised drinking water directive has been adopted since 2018, in which a maximum concentration of 0.1 μg/L for individual pesticide and 0.5 μg/L for total pesticides were regulated [36]. In the United States, the Environmental Protection Agency has identified 18 types of pesticides and herbicides with their maximum contaminant levels and potential health effects from long-term exposure in the National Primary Drinking Water Regulations [37]. In Japan, pesticides were not listed in the Drinking Water Standards but referred to the category of "Complimentary Items to Set the Target for Water Quality Management" [38]. In Vietnam, the Ministry of Health has recently listed 27 pesticides with their maximum limits in the National Technical Regulation on Drinking Water Quality (QCVN01-1:2018/BTY) [17].

Therefore, effective technologies to remove the pesticides from drinking water sources are beneficial to improve the finished water quality and fulfill the drinking water standards.

1.3. INTRODUCTION ON GRANULAR ACTIVATED CARBON AND APPLICATION IN WATER TREATMENT

Activated carbon (AC) is produced from rich-carbonaceous precursors, such as wood, coal, coke etc., via two main processes, which are thermal activation and chemical activation. Thermally activated carbon has high reactivity towards oxygen, which can induce catalytic reaction to convert the nonbiodegradable substances into biodegradable ones. On the other hand, chemically activated carbon showed better desorbability than thermally AC and resulted in enhanced adsorption capacity of AC for nonbiodegradable compounds. Therefore, the selection of AC types significantly affected the treatment performance purposes and could help to extend the service life of AC [39].

AC is manufactured in three main forms of powder AC (PAC), granular AC (GAC) and pelletized AC, which are differentiated by the particle size. GAC is more often adopted in water treatment due to its cost-effectiveness in continuous and extensive scale-systems. Typically, GAC's effective sizes in water treatment ranged from 0.5 to 0.7 mm, and 0.8 to 1 mm [40]. The pore size distribution of GAC significantly affects its specific surface area and adsorption capacity. The pore diameters could be categorized as primary micropores (<0.8 nm), secondary micropores (0.8-2 nm), mesopores (2 – 50 nm), and macropores (>50 nm) [41]. GAC' irregular crevices and porous particle shape offer an extremely high number of adsorption sites for the adsorption of various water contaminants.

GAC was firstly used in drinking water treatment in the late 1920s to remove the taste and odor in finished water. The undesirable taste and odor in drinking water were mainly attributed to the presence of chlorophenol formed in water as a result of the chlorination of phenols at the disinfection stage. Currently, problems in drinking water treatment extend beyond the scope of taste and odor control [42]. CECs appear to be one of the most problematic issues as the quality of drinking water supply sources is gradually degraded. Additionally to the GAC adsorption, which has been employed for decades, the biological activated carbon (BAC) process, which uses exhausted GAC media for microbial colonization, has also received much attention. This naturally occurring biofilm can

biodegrade a wide variety of contaminants such as organic carbon, organic/inorganic substances, and disinfection by-products precursors [39], [43], [44]. Detailed on AC's technologies adopted in water treatment will be presented in section 2.3.

1.4. BIOFILM MODEL IN ACTIVATED SLUDGE MODEL (ASM1)

The development and application of the International Water Association (IWA) Activated Sludge Models (ASMs) have created fruitful transformation and achievement in water and wastewater treatment research and practice. The models offer efficient means to combine the knowledge of science, engineering, and practice into an executable tool. The design criteria of a model are to keep the complexity as low as possible while encompassing crucial components and processes. Their application progress relies on the continuous accumulation of successful and failure experiences. Additionally, their widespread application has created a common language between the researchers and practitioners [45], which pave the way for further model development and improvement.

While the mathematical model of suspended-growth processes has been soundly investigated in various publications [46]–[48], the model of biofilm-based processes is more complicated due to increased complexity in describing the fate of wastewater constituents (i.e. particulate versus soluble substrate), differences in biofilm reactor configuration and operation, the impact of bulk-liquid hydrodynamics, and diffusional biofilm resistances. Over the last 30 years, the biofilm models have become more complex and more computationally intensive [49], with the model resolutions range from 1-dimension (1-D) to 3-dimension (3-D), as indicated in Figure 5. A 1-D model allows property gradients in one direction, usually over the biofilm depth, i.e., from the bulk liquid to the substratum. Meanwhile, the 2-D and 3-D models are needed to reproduce complex spatial distributions of the components, complex biofilm geometries, etc. [50]; however, they also demand heavy computing resources and deep programming expertise [45]. The 1-D model can capture the dominant processes of microbial reactions and mass transport [45]; therefore, it has been widely adopted in water treatment engineering,

At present, different process simulators are offered for biofilm modeling, as listed in Table 2. Among the available simulators, the GPS-X software was selected for the biofilm model in this study.

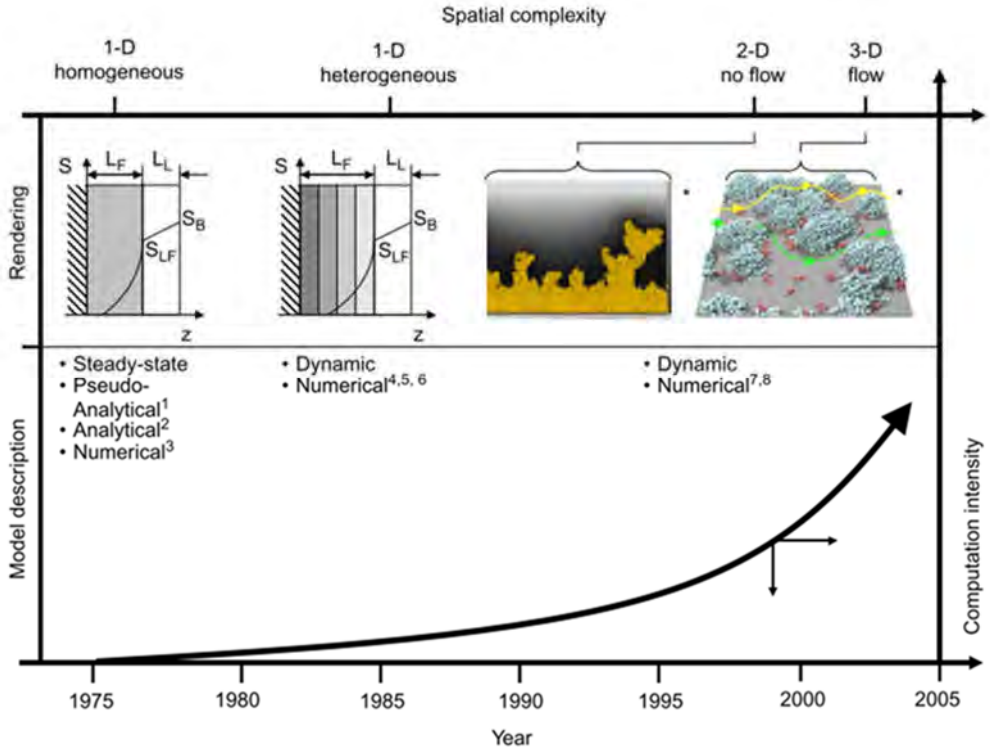

Figure 5. Biofilm models development over the last 30 years [49]

Table 2. Available simulators for biofilm models and wastewater treatment plants [51]

Name	Source	Model type and biomass distribution*
AQUASIM	EAWAG, Swiss Federal Institute of Aquatic Science and Technology, Du¨ bendorf, Switzerland (www.eawag.ch/index_EN)	1-D, DY, N; Heterogeneous
AQUIFAS	Aquaregen, Mountain View, California (www.aquifas.com)	1-D, SE, N, Heterogeneous
BioWin	EnviroSim Associates Ltd., Flamborough, Canada (www.envirosim.com)	1-D, DY, N, Heterogeneous 1-D,
GPS-X	Hydromantis, Inc., Hamilton, Canada (www.hydromantis.com)	1-D, DY, N, Heterogeneous 1-D,
Pro2D	CH2M HILL, Inc., Englewood, Colorado (www.ch2m.com/corporate)	1-D, SS, N(A), Homogeneous
Simba	ifak GmbH, Magdeburg, Germany (www.ifak-system.com)	1-D, DY, N, Heterogeneous
STOAT	WRc, Wiltshire, England (www.wateronline.com/storefronts/ wrcgroup.html)	1-D, DY, N, Heterogeneous
WEST	MOSTforWATER, Kortrijk, Belgium (www.mostforwater.com)	1-D, DY, N(A)

* Note: SS = steady-state, DY = dynamic, SE = semi-empirical, N = numerical, and N(A) = numerical using analytical solutions.

1.5. DISSERTATION STRUCTURE

The dissertation is organized into nine chapters. Each chapter focused on a specific objective as briefly introduced below:

In Chapter 1, the occurrences of ammonium and micropollutants were reported with their harmful effects on public health and the aquatic system. The granular activated carbon offered the capacity of adsorption and biodegradation that could respond to the treatment purpose. The mathematical biofilm model could provide insights on the biological reactions and mass transport processes that occurred in the attached-growth-process systems.

In Chapter 2, the existing technologies to remove ammonium and micropollutants in drinking water treatment were documented together with their advantages and limitations. The nitrifying expanded-bed reactor using biological activated carbon media appeared to be a promising alternative to respond to the treatment request.

In Chapter 3, a model concept used to simulate the nitrifying expanded-bed reactor was presented. The principles of biofilm and biological models on the platform of Activated Sludge Model 1 (ASM1) were summarized. A combined model with two-step-nitrification was proposed to simulate the nitrifying expanded-bed reactor.

In Chapter 4, a physical model was developed to identify the physical boundaries in which the biological reactions occurred. An internal recycle flow with media was first introduced to simulate the even distribution and moving of media within the expanded-bed.

In Chapter 5, an incorporated physical, biofilm, and biological model was applied to simulate the ammonium and organics removals of the nitrifying expanded-bed reactor on five different datasets of lab-, pilot- and full-scale reactors. A single set of kinetic and stoichiometric parameters were proposed for the oligotrophic heterotrophs and autotrophs. The complex biofilm attachment and detachment were investigated. The reactor performance was also studied under variation of influent water quality and temperature.

In Chapter 6, a sensitivity analysis of the numerical calculation and operational parameters

on the calculation results of the Integrated Fixed-film Activated Sludge (IFAS) object was carried out.

In Chapter 7, the possibility of the nitrifying expanded-bed reactor to remove the pesticides were investigated. The removal mechanisms of the pesticides in drinking water biofilm were revealed by the continuous and batch experiments on the full- and lab-scale reactors.

In Chapter 8, a summary of the key findings was provided. The recommendations for further studies were also discussed.

CHAPTER 2. EXISTING RESEARCHES

2.1. REMOVAL OF AMMONIUM IN WATER TREATMENT

Due to the harmful effects of NH_x-N on the aquatic ecosystem, intensive studies have been carried out to remove NH_x-N from water. Various processes have been used for NH_x-N removal from wastewater, such as air/steam stripping, vacuum distillation, chemical precipitation as struvite, membrane filtration, etc. [6]; however, those which are frequently used in drinking water treatment will be focused in this study. In the following sections, a review of these processes with their advantages and limitations will be summarized.

2.1.1. Physico-chemical technologies

2.1.1.1. Breakpoint chlorination

Breakpoint chlorination is a well-known method that has been applied for decades for the removal of NH_x-N. In this section, the chemistry of chlorine in water treatment will be presented [52].

Chlorine is often added to water under gaseous or liquid forms of sodium or calcium hypochlorite. These substances are rapidly hydrolyzed to hypochlorous acid according to the following equations:

$$Cl_2 + H_2O \rightarrow HOCl + H^+ + Cl^- \quad \textbf{Eq (1)}$$

$$Ca(OCl)_2 + 2H_2O \rightarrow Ca^{2+} + 2HOCl + 2OH^- \quad \textbf{Eq (2)}$$

$$NaOCl + H_2O \rightarrow Na^+ + HOCl + OH^- \quad \textbf{Eq (3)}$$

The two chemical species formed by chlorine in water, hypochlorous acid (HOCl) and hypochlorite ion (OCl^-) are commonly referred to as free available chlorine. Hypochlorous acid is a weak acid and will disassociate to H^+ and OCl^-. In waters with a pH between 6.5 and 8.5, the reaction is incomplete, and both species (HOCl and OCl^-) will be present.

As a relatively strong oxidizing agent, chlorine can react with a wide variety of compounds. As indicated in Figure 6, after adding chlorine to the water, the following processes will

happen [18] :

- Zone 1: Initial chlorine demand is caused by reducing agents (Fe^{+2}, Mn^{+2}, H_2S, $NO2^-$) that consume most of the chlorine applied prior to forming combined residuals.
- Zone 2: Additional chlorine combines with available total ammonia and reactive organics until forming maximum monochloramine residual. At the same time, uncombined free NH_3 is being depleted until it reaches zero [52]:

$$NH_3 + HOCl \rightarrow NH_2Cl \text{ (monochloramine)} + H_2O \quad \textbf{Eq (4)}$$

- Zone 3: More chlorine dosage converts monochloramine into odorous dichloramine and nitrogen trichloride. Total combined chloramine residual decreases, and total NH_x-N concentration approaches zero at the breakpoint.

$$NH_2Cl + HOCl \rightarrow NHCl_2 \text{ (dichloramine)} + H_2O \quad \textbf{Eq (5)}$$

$$NHCl_2 + HOCl \rightarrow NCl_3 \text{ (trichloramine)} + H_2O \quad \textbf{Eq (6)}$$

- Zone 4: True free chlorine residual is obtained and provides the least nuisance odor when free residuals make up 85 % of the total chlorine concentration. Nuisance combined chlorine residuals survive, and the potential for disinfection by-products (trihalomethane and haloacetic acid) formation remains as free chlorine residual develops further. Continuous adding of chlorine after the breakpoint will convert trichloramine to nitrogen gas. The overall reaction for chlorination breakpoint is given as:

$$NH_4^+ + 1.5\ HOCl = 0.5\ N_2 + 1.5\ H_2O + 2.5\ H^+ + 1.5\ Cl^- \quad \textbf{Eq (7)}$$

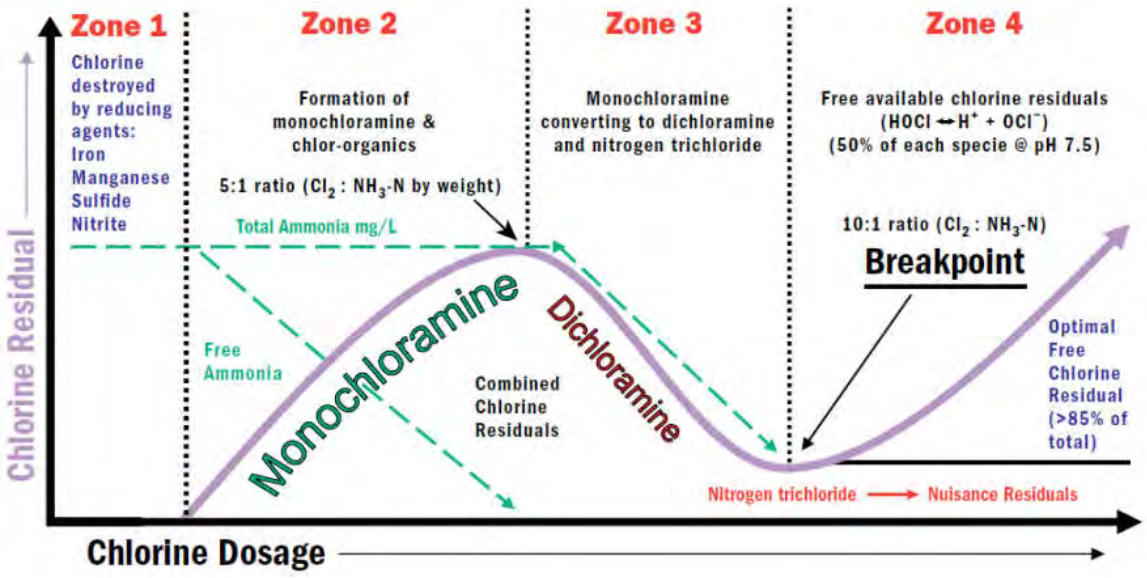

Figure 6. Interpretation of Breakpoint Chlorination Curve [18]

The free chlorine residual concentration is regulated in drinking water standards as an indicator for sufficient disinfection, targeting pathogen killing

As shown in Eq (7), the amount of chlorine to entirely oxidize NH_x-N is stoichiometrically 7.6 mgCl_2 to 1 mgNH_x-N. However, in practice, a dose of 8 – 10 mgCl_2/mgNH_x-N is often recommended to reach the chlorination breakpoint and obtain the free chlorine residual [19].

The chlorination breakpoint for NH_x-N is a simple and well-established technique. However, in the case of high NH_x-N concentrations, an increased dose of chlorine would be needed to fully oxidize such an amount, leading to high chemical reagent costs. Further, the side-effects of chlorination, such as unpleasant taste and odor, or the formation of harmful and carcinogenic disinfection by-products should be considered.

2.1.1.2. Adsorption

Adsorption is a process in which the substances are accumulated or concentrated at a surface or interface. In water treatment, the removal of NH_x-N often occurs between the interface of the liquid phase and solid adsorbent materials. Because NH_x-N is highly miscible with water, the primary driving force of adsorption is due to the high affinity of

NH_x-N for the particular solid adsorbents rather than the solvent disliking character. The adsorption is induced by van der Waals attraction or chemical interaction of NH_x-N with the adsorbent [53]. Hence, the efficiency of the adsorption process depends mainly on selecting suitable adsorbent media. Additionally, recent studies also highlighted the importance of other operational parameters, such as adsorbent dosage, pH, contact time, and coexisting ions [7].

The adsorption of NH_x-N onto solid media provided many advantages, including high removal efficiency, simple operation, and low energy consumption. It is suitable for a wide range of NH_x-N concentrations from low-strength categories, such as in fish pond water (~ 10 mgN/L), domestic wastewater (~ 40 – 60 mgN/L) to very high NH_x-N loadings in landfill leachate (~ 100 – 1000 mgN/L) [7]. However, adsorption could not be used in the water pretreatment with high influent suspended solids (maximum tolerance of 20 mg/L) due to the blockages or pressure loss [54]. The major limitation of adsorption pertains to the saturation or exhaustion of adsorbent materials in which the breakthrough and exhausted points are reached. Regeneration of adsorbents is needed, including chemical washing, biological regeneration, electrochemical regeneration, mild heating, or electric field [7].

Numerous adsorbents have been studied so far for the adsorption of NH_x-N in water treatment. They could be roughly categorized as conventional materials such as clay and carbonaceous matters, or nanostructured materials such as metal-organic frameworks, as shown in Figure 7. The conventional adsorbents are abundant and cost-effective; however, their bindings with NH_x-N are relatively weak. The new materials, such as nanostructured materials, provides high adsorption capacity and rapid adsorption kinetics; however, they require expensive precursors, tedious preparation, and uncertainty [7]. Additionally, the adsorbents prepared from agricultural wastes or residues, such as strawberry leaf powder, were also studied intensively due to their abundance and cheap price [54]

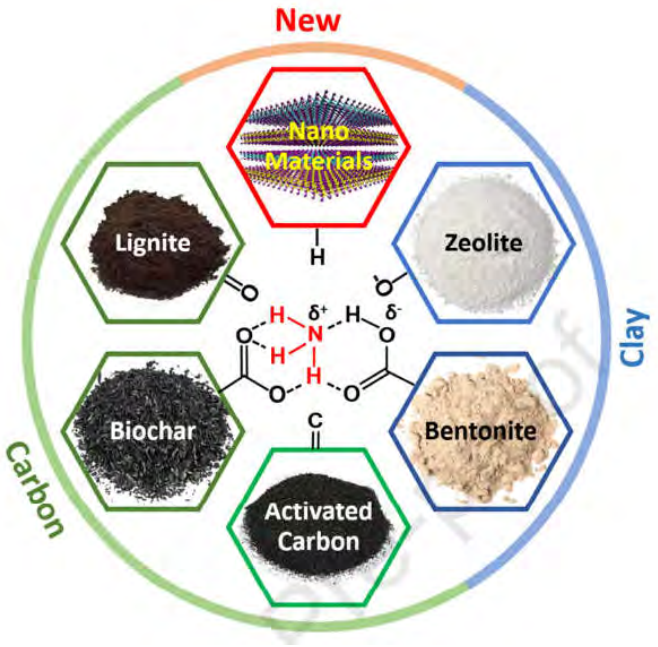

Figure 7. Typical adsorbent materials for ammonium in water treatment [7]

Among those adsorbents, activated carbon is considered a versatile material due to high specific surface area, porous structure, and rich surface chemistry. However, the bindings between activated carbon and NH_x-N are relatively weak due to the lacking of sufficient surface acidity. Further, it should be noted that the average pore size of activated carbon is much higher than that of NH_x-N molecule of 0.3 nm. Therefore, activated carbon is a less effective adsorbent for NH_x-N [7].

2.1.1.3. Ion exchange process

The ion exchange process consists of reversible chemical reactions in which dissolved ions in a solution are replaced with other similar charged ions [54]. In the case of removing NH_x-N from water, a cation exchanger using zeolitic minerals such as clinoptilolite, sepiolite, betonite, and mordenite, is commonly applied.

In the conventional design, the ion exchange column consists of zeolite particles in the packed-bed through which the influent is tricked until a specific NH_x-N breakthrough concentration is reached. This process is efficient at a wide range of temperature and NH_x-

N concentration and is responsive to NH_x-N shock loading. However, significant use of chemical regenerants and rinse water are required to restore and reuse of the exchange column, leading to high operational costs. Further, at least one duplicate column is needed to maintain the continuous operation [54], [55].

Most of the studies on the ion exchange process investigated the primary treatment of wastewater containing high NH_x-N loading. Focusing on the low-strength NH_x-N concentrations from 2 to 10 mgN/L, research was carried out using several zeolites of Na-form, such as Na-mordenite, Na-ferrierite, NaZSM-5, Na-Y, and Na-β [56]. The result demonstrated that Na-modernite was an efficient cation-exchanger for the removal of low NH_x-N concentration comparing to the remaining materials. The NH_x-N uptake on Na-modernite was neither impacted by the temperature at the range of 278 to 333 K, nor the presence of coexistent K^+ and Na^+ in water. However, the presence of Ca^{2+} and Mg^{2+} significantly reduced the NH_x-N uptake.

2.1.2. Biological technologies

Aerobic nitrification consists of two-step microbial processes. In the first step, NH_x-N will be oxidized to NO_2-N by ammonium-oxidizing organisms (AOO) following the equation:

$$2NH_4^+ + 3\ O_2 = 2\ NO_2^- + 4H^+ + 2H_2O \qquad \textbf{Eq (8)}$$

In the subsequent step, NO_2-N will be converted into NO_3-N by nitrite-oxidizing organisms (NOO) following the equation:

$$2\ NO_2^- + O_2 = 2\ NO_3^- \qquad \textbf{Eq (9)}$$

The global nitrification reaction is given as follows:

$$NH_4^+ + 2\ O_2 = NO_3^- + 2H^+ + H_2O \qquad \textbf{Eq (10)}$$

The stoichiometric oxygen demands of the above three equations are 3.43, 1.14, and 4.57

mgO_2 per 1 mgN, respectively. As nitrifying bacteria are obligate aerobes, the dissolved oxygen (DO) concentration is one of the decisive factors that control the process performance.

On the other hand, NH_x-N can be reduced anaerobically by anammox bacteria following the equation:

$$NH_4^+ + NO_2 = N_2 + 2H_2O \qquad \textbf{Eq (11)}$$

When dealing with high NH_x-N concentrations as in wastewater treatment, various technologies have been developed using biological nitrification process, such as anaerobic ammonia oxidation (ANAMMOX), completely autotrophic nitrogen removal over nitrite (CANON), single reactor high activity ammonia removal over nitrite (SHARON), Oxygen-limited nitrification and denitrification (OLAND), "NOX process", and "aerobic de-ammonification process" [54]. However, these techniques are not in the scope of study and will not be further discussed.

In the drinking water sources where the substrates for microorganism growth are very limited, the oligotrophic bacteria with very low half-saturation coefficients (K_S) [57], [58] such as AOO/NOO are favored. In this regard rather than ordinary heterotrophic organisms (OHO), nitrifiers are known to be sensitive to various environmental factors [59]. Their growth on the carrier might provide a more hospitable environment [60] and nitrifying biomass concentration in the reactor could be significantly increased. Therefore, most of the nitrifying reactors applied in drinking water treatment were of the attached-growth process and are referred to as "biologically active filter" or "biofilter" due to filtration capacity, with variation in the flow direction. Down-flow biofilters were widely used due to their simplicity. However, the high head loss, or uneven distribution of biomass in the bed, and the possible leakages of bacteria-attached particles were the main disadvantages that limited their acceptance in practice [61]. The up-flow or expanded-bed biofilters were proposed to overcome such limitations. In the expanded-bed biofilter, better contact of

water influent and the biomass was maintained in the whole fluidized bed, and bed clogging was reduced due to limited capture of suspended solids particles [62]. In this study, the performance of an expanded-bed nitrifying reactor to remove NH_x-N and micropollutants from the water was investigate.

However, unlike biological wastewater treatment systems, DO competition between nitrifiers and heterotrophs, and each reaction rate in low-strength influent have not been well formulated. Hence, at present, it is difficult to calculate the removable NH_x-N and organic substrates and possible NO_2-N accumulation in the pretreatment of WTPs. Additionally, there is little information regarding the kinetic and stoichiometric parameters of the AOO/NOO/OHO in drinking water treatment, which might be considerably different from those applied in wastewater treatment.

The most significant advantage of the conventional nitrification process is the low-cost requirement. However, the bio-conversion process is low, and a long start-up period is needed before initiating the treatment [54]. Further, nitrifying bacteria are susceptible to environmental changes, such as DO, substrates, pH, temperature, etc, and are easily outcompeted by the heterotrophs in the presence of organic substrates. Therefore, the biological nitrification process is not responsive to influent variations.

2.2. REMOVAL OF MICROPOLLUTANTS IN WATER TREATMENT

The conventional drinking water treatment process consists of coagulation, flocculation, sedimentation, filtration, and disinfection, as shown in Figure 8. Additionally, some other processes, such as advanced oxidation, adsorption onto activated carbon, or biofiltration, could also be used for micropollutant removals.

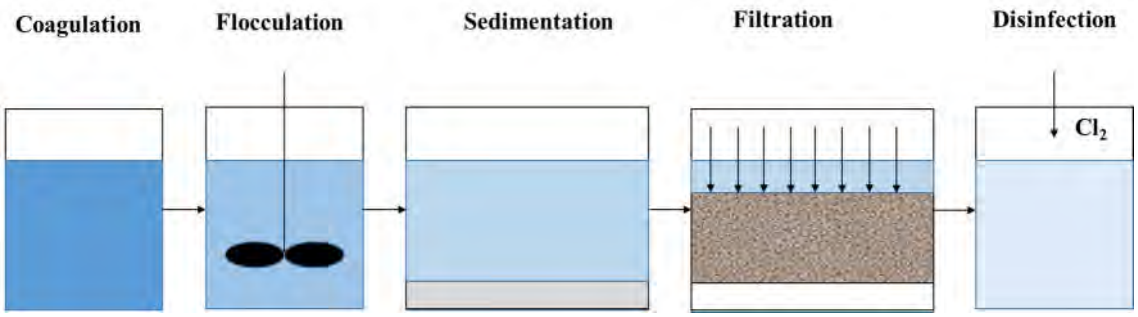

Figure 8. Conventional drinking water treatment process

The removal of micropollutants in WTPs depends on various factors, such as configurations of systems, operation schedules, treatment conditions, and influent loadings in the influent source. The removal mechanisms of micropollutants in each treatment process should be studied at both field conditions in WTPs and laboratory-controlled conditions [63].

In this section, the micropollutant removal efficiencies in each process of WTPs will be discussed.

2.2.1. Physico-chemical technologies

2.2.1.1. Coagulation – Flocculation – Sedimentation

The coagulant, flocculation, and sedimentation are subsequent processes to remove colloidal and suspended solids particles from water. Opposing viewpoints have been raised regarding the removal efficiencies of micropollutants in these processes. On the one hand, some researchers investigated the removals of pharmaceutical substances in the coagulation process, and the removal efficiencies reported were ranged from 8 to 30% [64], [65]. On

the other hand, others demonstrated that their removals obtained in the coagulation stage was not only by coagulation itself. In fact, it was reported that adsorption to the particles, direct sunlight photolysis, and hydrolysis are the main micropollutant removal mechanisms that operate during the coagulation process in a WTP. A broad range of removal efficiencies from 9 to 100% was observed when the turbidity of influent water was higher than 10 NTU [63].

2.2.1.2. Sand filtration

The sand filtration is designed to remove the remaining residual particles from the sedimentation process. Previous studies suggested that adsorption can be the dominant mechanism in accordance with the hydrophobicity of the compound during sand filtration. It was reported that compounds with $\log K_{ow}$ less than 1 had lower removal efficiencies (<50%) while hydrophobic compounds with $\log K_{ow}$ higher than 2.5 had higher removal efficiencies (>80%). Hydrophobicity is a controlling factor in the removal of micropollutants during the sand filtration stage. However, some micropollutants, even with $\log K_{ow}$ higher than 2.5, showed inefficient reductions during the filtration stage and sometimes negative removal efficiencies. Negative removal during sand filtration can be explained by the timing differences or desorption of accumulated pollutants in the filter bed. The filter bed could only temporarily capture the micropollutants by partitioning during filtration [63].

2.2.1.3. Advanced oxidation and disinfection

Depending on the quality of the source water as well as on the requirements of the finished drinking water, drinking water treatment is often completed with one or more final polishing steps prior to distribution. Disinfection and oxidation processes are often employed to stabilize the biological quality of the finished water, remove color and odor, or to inactivate pathogens. These processes rely on the addition of either chemical oxidants such as hydrogen peroxide, free chlorine, chloramines, or ozone or UV radiation. The chlorination was previously presented in section 2.1.1.1. Ozonation or other advanced

oxidation techniques (e.g., combining ozonation with hydrogen peroxide and/or UV radiation to produce a high yield of reactive hydroxyl radicals) are popular alternatives to chlorination. However, both techniques have been shown to create a variety of persistent oxidation products that may have equal or more significant toxicity as the parent chemical [66].

2.2.1.4. Adsorption onto granular activated carbon

The adsorption onto granular activated carbon process is presented in detail in 2.3.1.

2.2.2. Biological technologies

Based on the above background, it was shown that the contribution of conventional drinking water treatment process to micropollutant removals was rather limited and uncertain. Some techniques might be useful in removing these compounds, such as adsorption onto activated carbon, however expensive operational costs are needed [66]. In this regard, the biotransformation approach emerges as a cost-effective and sustainable alternative targeting the persistent chemicals in drinking water sources.

In biological technologies, single strains or microbial consortia that have the ability to degrade or mineralize target micropollutants partially were employed [66]. Their metabolic and co-metabolic strategies were illustrated as follows:

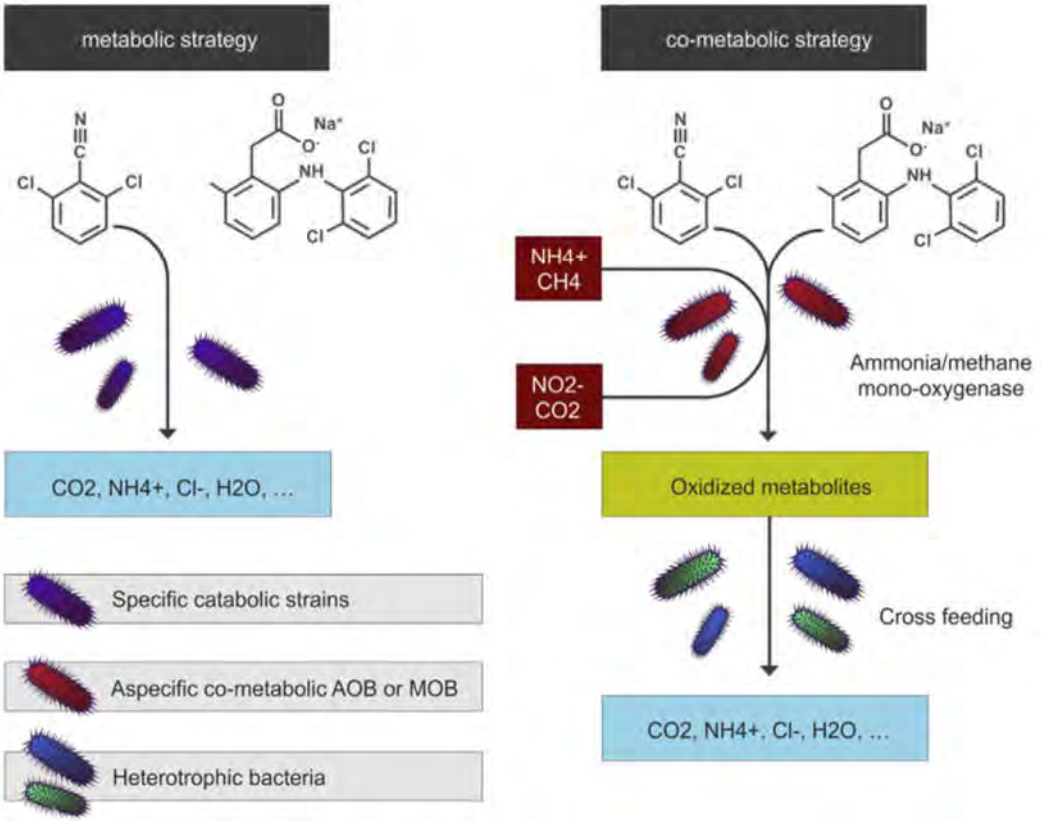

Figure 9. Schematic of the metabolic and co-metabolic biotransformation strategies [66]

In the metabolic strategy, microorganisms interact with target micropollutants in growth-linked processes that result in the mineralization of the micropollutants. In the co-metabolic strategy, microorganisms interact with non-target micropollutants in biochemical processes that result in the formation of oxidized metabolites. These oxidized metabolites can then be used as primary for heterotrophic members of the population [66].

As mentioned above, the raw drinking water sources are of oligotrophic conditions where the substrates are found at trace levels. Their concentrations are very low compared to that of the primary substrates; therefore, cometabolic might be the degradation pathway [67].

The attached-growth process was often adopted with various kinds of carriers, such as sand, activated carbon or anthracite. Several studies have reported the possibility of removing micropollutants using biologically active filters with varying removal efficiencies depending on the characteristics of micropollutants [61], [67]–[70]. Empty bed contact time, pH and DO, backwashing regime are among the parameters that influence the performance of biologically active filters [39]. Additionally, the association between nitrification rate and micropollutant removals has been documented in nitrifying activated sludge systems of wastewater treatment [71]–[74]. Nevertheless, there is still questionable if the nitrifying biofilms could remove the pesticides in drinking water treatment. The pesticide removals using biological activated carbon process were reported in [75], [70], [76], [77], in which the removal mechanism was thought to be simultaneous adsorption and biodegradation. However, because the removal mechanism is affected by various factors such as configurations of systems, operating conditions, and influent loadings in influent water, the examination and comparison should be carried out to reveal the removal pathways [63].

2.3. APPPLICATION OF ACTIVATED CARBON IN DRINKING WATER TREATMENT

2.3.1. Adsorption onto granular activated carbon process

Adsorption is considered to be an important phenomenon in most natural physical, biological, and chemical processes, and GAC is the most widely used adsorbent material in water treatment. In GAC adsorption process, the adsorption occurs between two phases, which are the GAC adsorbent in solid and the adsorbate compounds in liquid. In an adsorption system, equilibrium is established between the adsorbent and the adsorbate in the bulk phase. The transport mechanisms consist of four stages, including the bulk solution transport, external diffusion, internal diffusion, and adsorption, as illustrated in Figure 10 [53]:

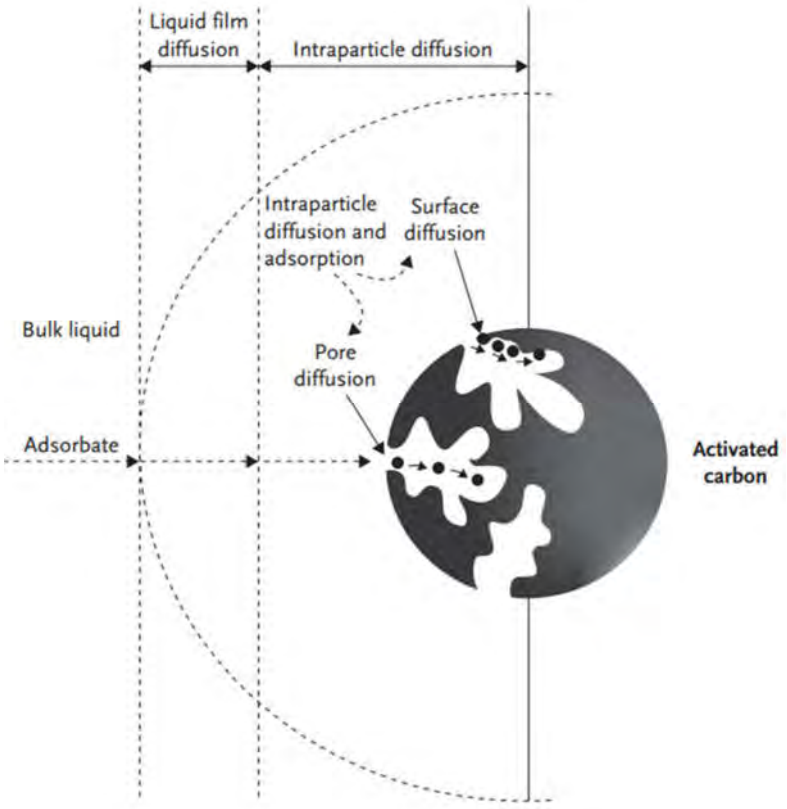

Figure 10. External and internal transport of an adsorbate in activated carbon particle [53]

The irregular and porous shape of GAC provides an extensive network of adsorption sites. Various studies have focused on the ranges of pollutants that can be adsorbed onto the GAC surface, as shown in Table 3.

Table 3. Classes of organic compounds adsorbed on activated carbon [42]

Organic chemical class	Examples
Aromatics	Benzene, Toluene, Ethylbenzene, Xylene
Polynuclear Aromatics	Naphthalene, Anthracenes, Biphenyls
Chlorinated Aromatics	Chlorobenzene, Polychlorinated biphenyls
Phenolics	Phenol, Cresol, Chlorophenols, Nitrophenols
High-molecular-weight hydrocarbons	Gasoline, Kerosene
Chlorinated aliphatics	Trichloroethylene, Carbon tetrachloride
Aliphatic and aromatic acids	Tar acids, Benzoic acids
Ketones, esters, ethers, and alcohols	Hydroquinone, Polyethylene glycol
Surfactants	Alkyl benzene sulfonates
Soluble organic dyes	Methylene blue, Indigo carmine

The factors affecting the adsorption capacity are as follows [41], [42]:

- Specific surface area of GAC: which is proportional to the extent of adsorption,
- Physical and chemical properties of the adsorbate: the adsorbability of a compound increases with increasing molecular weight and increasing number of functional groups such as double bonds or halogens. Additionally, hydrophobic and non-polar molecules adsorb better on GAC,
- pH: Adsorption of most organic materials is higher at neutral conditions,

- Temperature: The extent of adsorption should increase with decreasing temperature because the adsorption reactions are exothermic. However, increased temperature also increases the rate of diffusion of the solute through the liquid to the adsorption sites, which eventually leads to increased adsorption,
- Porosity of GAC: The adsorption performance is dependent on the condition of internal surface accessibility, defined as the pore size distribution,
- Chemical Surface Characteristics of GAC: depends on their heteroatom content (oxygen, sulfur, and nitrogen), and mainly on their oxygen complex content. Heteroatoms are brought during the activation, providing charged groups with stronger valence forces in the carbon structure at which chemisorption may occur.

Adsorption on GAC process has been used for decades due to its effectiveness and simplicity. Additionally, the adsorption process does not add undesirable by-products to drinking water [41]. However, the main limitation of GAC adsorption pertains to its saturation and exhaustion over time. In this regard, regeneration or frequent dosing is needed to reuse the materials, leading to high operational costs.

2.3.2. Biological activated carbon process

The introduction of the biological activated carbon (BAC) process could overcome the limitation of GAC adsorption. This process uses GAC as filtration media to physically remove undesired matters. As the GAC media is gradually exhausted, microbial colonization is developed on the surface of the media [43]. This naturally occurring biofilm can biodegrade a wide variety of contaminants such as organic carbon, organic/inorganic substances, and disinfection by-products precursors [39], [43], [44]. Among the targeting contaminants, organic micropollutants and NH_x-N are of top concerns for WTP operators, and their removal efficiencies in the BAC process needed to be investigated.

The macro-porous structure and irregular surface of GACs are suitable sites for bacterial attachment, providing good protection from shear stress. Meanwhile, microporous GACs may not be adequate for microorganisms penetration due to because of their larger size

compared to those of microorganisms. However, the extracellular material from biofilm can be established in the GAC micropores. The biofilm formation on GAC comprises microbial cells either immobilized on the carbon surface or embedded in an extracellular organic polymer matrix of microbial origin. The attachment of bacteria to a solid surface is governed by different types of interactions, which include van der Waals forces, electrostatic forces, steric interactions, hydrophobic bonding, and hydrogen bonds [78].

Furthermore, when compared to other media such as anthracite or sand, GAC has a much higher effective surface area and a better surface texture for biofilm attachment. These characteristics may increase the potential to hold a greater amount of biomass and the possibility of higher biodegradation rates [78].

As mentioned in section 2.1.2, the biofilters using BAC media could be designed as down-flow or up-flow configuration, each with their advantages and limitations.

The operating aspects affecting the performance of BAC process includes reactor configuration, environmental factor such as influent water quality and temperature, and operating condition such as hydraulic loading and backwashing regime. The performance of BAC process depends largely on how the biological reactions occurred in the reactor with interactions of oligotrophic OHO and AOO/NOO, or how the operational conditions affected microbial activities. Such knowledge in drinking water treatment is currently lacking.

The most advantages of BAC process over GAC adsorption pertain to the cost-effectiveness, in which spent GAC could be reused without regeneration or frequent dosing. In this way, the service life of the BAC bed could be extended from 6-12 months to several years [43], [79]. However, the biological process might be of low-speed and require a long start-up period before treatment initiation. Further, the biological system is susceptible to influent variation, so the reactor is not responsive in the case of influent shocks.

2.4. CONCLUSION

From literature review, it was concluded that the biological active filters could be used as a low-cost technology to remove NH_x-N and micropollutants in the pretreatment of drinking water. The attachment-growth process could be applied to increase the biomass concentration in the reactor, especially for the low-yield growers AOO/NOO. The biological activated carbon was selected as the media for the microbial colonization. The up-flow configuration, or expanded-bed reactors, could provide advantages in terms of reducing the head loss, better contacting between biomass and the influent, or distributing evenly the biomass in the expanded-bed media. However, the kinetics and interactions between the biomass AOO/NOO/OHO in the oligotrophic conditions of drinking water treatment were not well estimated. Additionally, the possibility of removing the pesticides in the biological active filters in drinking water treatment were still questionable.

Based on the above-mentioned background, this study investigate the performance of a nitrifying expanded-bed reactor in the pretreatment of drinking water treatment plants. In the first part, a mathematical model will be developed which aimed at removing the NH_x-N and organics from water. In the second part, the removal mechanisms of the pesticides in the reactor were examined.

CHAPTER 3. MATERIALS AND METHODS (PLATFORM OF BIOCHEMICAL MODEL)

3.1. INTRODUCTION AND OBJECTIVES

The nitrifying expanded-bed reactor could be expressed by an Integrated Fixed-Film Activated Sludge (IFAS) object in the GPS-X software simulator (Hydromantis Inc., Canada). The performance of the reactor could be modeled by a combined physical, biofilm and biological model. The existing biofilm model in GPS-X software was constructed and adapted from a biokinetic model developed by Spengel and Dzombak in 1992 [80] for rotating biological contactors. The theory and structure of the biofilm model were presented in different technical manuals of GPS-X; however, there is still a need to organize and summarize various sources of information to provide a better understanding of the biofilm model, especially for first learners.

The biological model was used to calculate the removal of the substrates, e.g. NH_x-N, NO_2-N, organic substrates and DO, in relation to the growth of responsible microorganisms (AOO, NOO, and OHO). In the ASM1 model, the nitrification process was represented in a single-step process with the direct conversion of NH_4-N to NO_3-N by the autotrophs biomass. However, in case the undesired product NO_2-N was concerned, such a model could not provide an adequate response.

In the combination of biological and biofilm model, the available substrates in the biofilm layers were engaged with the substrate diffusion and microbial utilization governed in the biofilm model. In each biofilm layer, the biological reactions were simplified to be a dense suspended-growth system with a set of mass transfer from/to the next biofilm layers.

The objectives of this chapter were:

1. To illustrate the combined physical, biofilm and biological model for NH_x-N and organics removals.

2. To introduce the biofilm model on GPS-X software with a set of mass balances of soluble and particulate materials,

3. To develop an ASM1-based biological model with two-step-nitrification and continuity checking of the model.

3.2. PHYSICAL DESCRIPTION OF THE REACTORS AND THE MODEL CONCEPT

A lab-scale expanded-bed reactor with a cross-section area of 85 cm^2 was installed in the laboratory. About 12.7 L of spent GAC media (diameter: 0.4-0.5 mm) collected from an identical biological expanded-bed filter in Anou WTP (Kitakyushu, Japan) was filled to the reactor until 1.5 m of designed height in a packed basis. The feeding water was controlled at a constant flow rate (Q) of 2.2 L/min, which was also a designed linear velocity of 15.5 m/h. The bed height was expanded to 2.0 m, showing a working volume of 17.0 L.

A pilot-scale reactor using BAC media of identical configuration and linear velocity as the lab-scale reactor was set up at Hoa Phu WTP (Ho Chi Minh City, Vietnam) for the pretreatment of the river water.

A full-scale reactor using BAC media was studied in the headworks of Vinh Bao WTP (Hai Phong, Vietnam), receiving river water taken from an irrigation channel. The packed-bed was of dimension (W×L×H = 2.6 × 2.6 × 1.5 (m)), operating at the same velocity as that of the lab- and pilot-scale reactors with a working volume of 13.5 m^3.

A photo of the lab-, pilot- and full-scale reactors were shown in Figure 11 and Figure 12.

Figure 11. Lab-scale reactor at the University of Kitakyushu, Japan

Figure 12. Pilot-scale reactor in Hoa Phu WTP (left) and Full-scale reactor in Vinh Bao WTP (right)

The performance of the lab-, pilot- and ful-scale reactors could be modeled using the combined physical, biofilm and biological model, as illustrated in Figure 13.

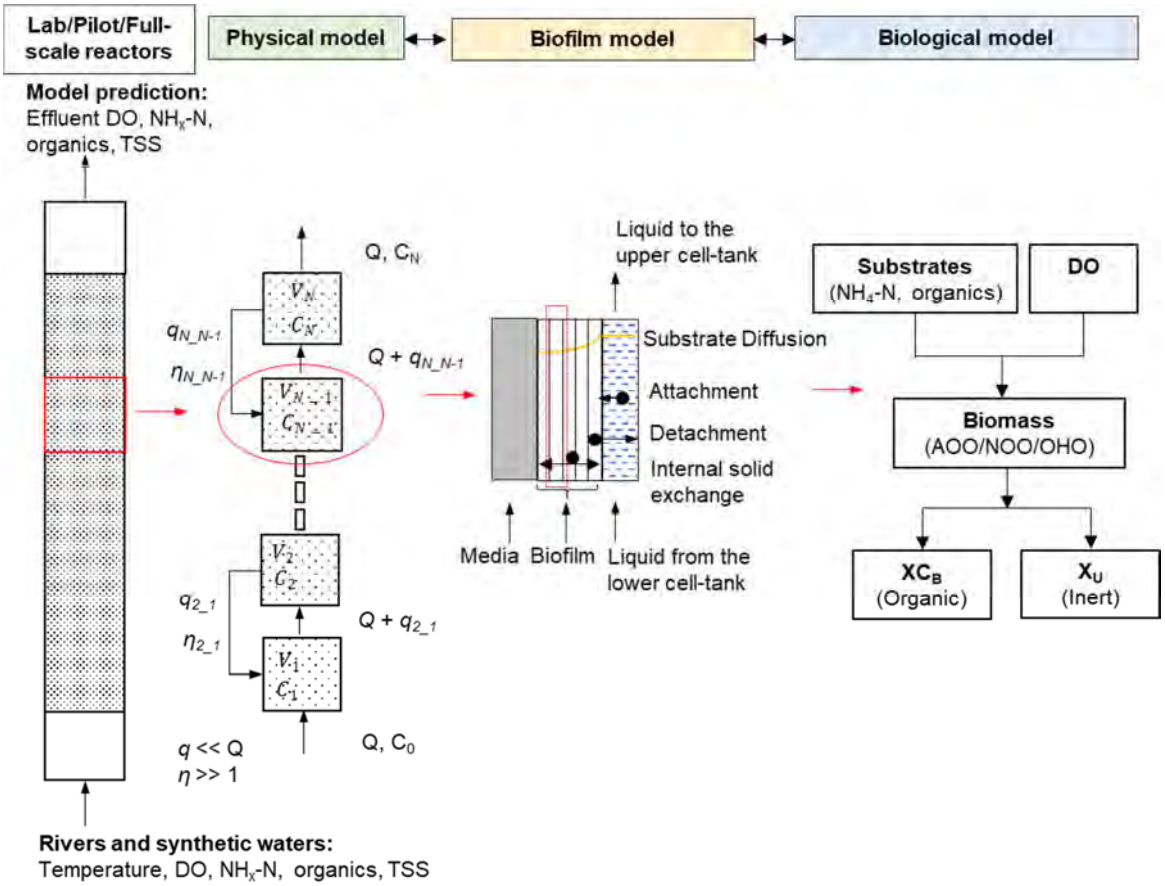

Figure 13. Schematic illustration of the model concept

The reactor was described as a plug-flow configuration composed of several tanks-in-series with the media traveled along the expanded-bed. The physical properties of the reactor will be modeled in the CHAPTER 4, while the mass transport and biological reactions will be expressed in CHAPTER 5.

3.3. BIOFILM MODEL IN GPS-X SOFTWARE

3.3.1. Introduction of the biofilm model in GPS-X software

The 1-D biofilm model consists of five biofilm layers and one attached liquid layer, as illustrated in

Figure 14. Each biofilm layer was modelled as an individual CSTR reactor, in which the biological reactions were simplified to be a dense suspended-growth system with a set of mass transfer from/to the next biofilm layers. Based on the specific surface area, the media in the reactor was simulated to be a giant and homogenized surface, on the top of which the biofilm layers were placed.

The mass transport in the biofilm model governed the following processes:

- The diffusion of soluble components to the biofilm layers
- The attachment and detachment of particulate components to/from the biofilm layers
- The internal solids exchange of particulate components among the biofilm layers
- The biological reactions in the biofilm layers

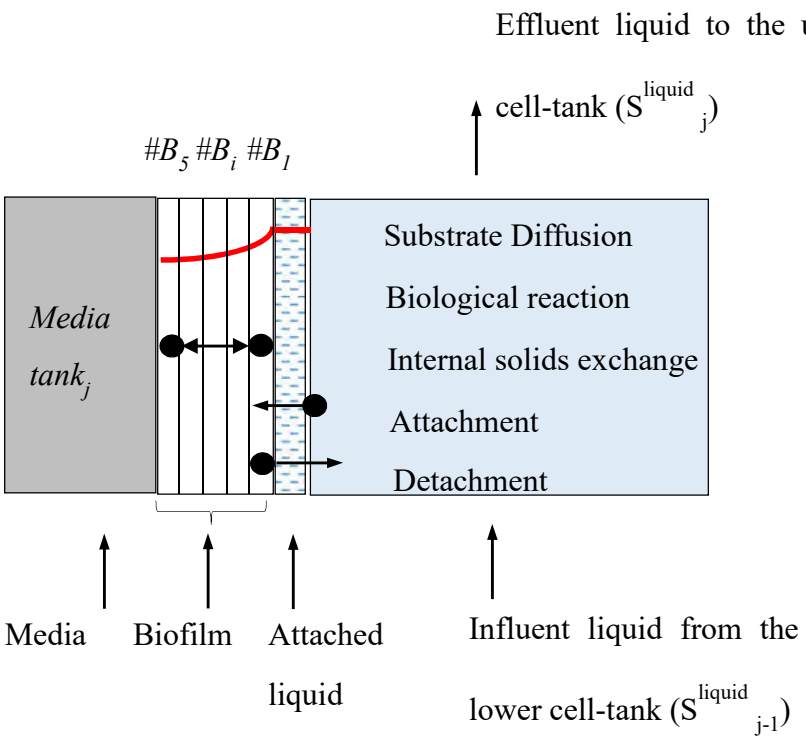

Figure 14. Illustration of biofilm processes in the expanded-bed reactor

3.3.2. The mass balances for soluble and particulate components

3.3.2.1. For soluble components

a. The tank equation: Mass balance for substrate transported into or out of the bulk liquid

Accumulation in the tank	Influent/effluent advection	Liquid layer advection	Diffusion into biofilm	Air/liquid exchange

$$V_j\left(\frac{dS_j^T}{dt}\right) = Q.(S_j^{Inf} - S_j^{Eff}) + Q_L(S_{j-1}^L - S_j^L) - K_M A_S(S_j^T - S_j^{BL}) + K_{MT} A_S(S_j^* - S_j^T) \quad \textbf{Eq (12)}$$

Where

t	Times	day
A_S	Media surface area in the tank j	m^2
V_j	Working volume of reactor j	m^3
Q	Volumetric flow rate of influent/effluent	m^3/d
Q_L	Liquid flow rate to the liquid layer	m^3/d
S_j^T	Substrate concentration in the bulk liquid in the tank j	g/m^3
S_j^{Inf}	Substrate concentration in the influent in the tank j	g/m^3
S_j^{Eff}	Substrate concentration in the effluent in the tank j	g/m^3
S_{j-1}^L	Substrate concentration in the liquid film in the tank (j-1)	g/m^3
S_j^L	Substrate concentration in the liquid film in the tank j	g/m^3
S_j^{BL}	Substrate concentration at biofilm-liquid interface in the tank j	g/m^3
S_j^*	Saturated liquid substrate concentration for oxygen in the tank j	g/m^3
K_M	Mass transfer coefficient from liquid to biofilm	m/d
K_{MT}	Oxygen transfer coefficient from air to bulk liquid	m/d

In GPS-X software, the mass transfer coefficient from liquid to biofilm (K_M) was calculated as follows:

$$K_M = \frac{D_S \times R_{diff\_biofilm}}{\delta_L} \qquad \textbf{Eq (13)}$$

Where

D_S	Diffusion constant	m^2/d
$R_{diff\_biofilm}$	Reduction in diffusion in biofilm	
δ_L	Attached liquid film thickness	m

b. Liquid film equation: Mass balance of substrates in/out the attached liquid film

Accumulation in liquid film	Liquid film advection	Diffusion into biofilm	Air/liquid exchange

$$A_S\delta_L\left(\frac{dS_j^L}{dt}\right) = Q_L(S_{j-1}^L - S_j^L) - K_M A_S(S_j^L - S_j^{BL}) + K_{ML}A_S(S_j^* - S_j^L) \quad \textbf{Eq (14)}$$

where:

K_{ML}	Oxygen transfer coefficient from air to liquid film	m/d

c. Biofilm equation: Mass balance for a biofilm layer

The biofilm equation governed the substrates in/out that biofilm layer and the substrates utilized by the biomass. The diffusion occurred in one direction from the bulk liquid to the attached liquid film, next to the adjacent biofilm layer, and then to the concerned biofilm layer.

Accumulation in biofilm	Diffusion into biofilm	Biofilm layer advection	Microbial utilization

$$\frac{\partial S}{\partial t} = -D_S\frac{\partial^2 S}{\partial y^2} + \frac{Q_B}{A_S\delta_B}(S_{j-1}^B - S_j^B) - R_S \quad \textbf{Eq (15)}$$

where:

δ_B	Thickness of biofilm layers	m
y	Thickness of individual biofilm film layer	m
Q_B	Liquid flow rate to the biofilm layer	m^3/d
S_j^B	Substrate concentration at biofilm layer in the tank j	g/m^3
R_S	Substrate utilization rate	$g/m^3.d$

Each biofilm layer was considered as a CSTR where the utilization rate occurred as in a suspended growth system, as expressed in the following equation:

$$R_S = \frac{\mu_{\max}.X_a.A_S}{Y.A_S.\delta_B}.\frac{S}{K_S + S}.\frac{S_{O2}}{K_{S\_O2} + S_{O2}} \qquad \textbf{Eq (16)}$$

where:

R_S	Substrate utilization rate	$g/(m^3.d)$
S	Substrate concentration in one biofilm layer	g/m^3
S_{O2}	Oxygen concentration in one biofilm layer	gO_2/m^3
K_S	Substrate half-saturation coefficient	g/m^3
$K_{S,O2}$	Oxygen half-saturation coefficient	gO_2/m^3
μ_{max}	Maximum specific growth rate	d^{-1}
Y	Yield or coefficient of biomass production	gCOD/gCOD
X_a	Surface concentration of microorganism in one layer	g/m^2

3.3.2.2. For particulate components

a. Attachment from liquid to biofilm

The attachment phenomenon, described by a rate constant k_{attach}, was defined as the entrapment of particulate matter from the bulk liquid to the biofilm layers [81].

$$R_{attach} = k_{attach}.X_j.A_S \quad \textbf{Eq (17)}$$

where:

R_{attach}	Attachment rate	g/d
k_{attach}	Specific attachment rate of particulates from liquid to biofilm layer	m/d
X_j	Particulates concentration in the liquid in the tank j	g/m^3

b. Detachment from biofilm to liquid

The detachment phenomenon, described by the specific detachment rate k_{detach}, was determined as the loss of solids components from the outermost biofilm layer to the bulk liquid. This kinetic parameter affected the biofilm thickness and the biomass concentration in the biofilm 1st layer [81].

$$R_{detach} = k_{detach}.X_{j\_B\#1}.A_S.(\frac{\delta_{B,\max}}{\delta_{B,\max} - \delta_B} - 1) \quad \textbf{Eq (18)}$$

where:

R_{detach}	Detachment rate	g/d
k_{detach}	Specific detachment rate of particulates from the first biofilm layer to the liquid	m/d
$X_{j\_B\#1}$	Particulates concentration in the first biofilm layer	g/m^3
$\delta_{B,max}$	The maximum biofilm thickness, defined by users	m

In GPS-X software, the detachment was adjusted by adding a product to the right part of Eq (18). This allowed the growth of biomass in biofilm but not exceeding the maximum biofilm thickness defined by the users.

c. Internal solids exchange

The internal solids exchange was designed to provide the means to circulate the particulates such as biomass, etc., among the biofilm layers. The process was calculated as follow [81]s:

$$R_{inter\_exchange} = \frac{k_{inter\_exchange}.(X_{j\_B\#k-1} - 2.X_{j\_B\#k} + X_{j\_B\#k+1}).A_S^2}{\delta_B^2} \quad \textbf{Eq (19)}$$

where:

$R_{inter\text{-}exchange}$	Internal solids exchange rate	g/d
$k_{inter\_exchange}$	Specific internal solids exchange rate of particulates among biofilm layers	m/d
$X_{j\_B\#k}$	Particulates concentration in the biofilm layer #k	g/m^3

3.4. BIOLOGICAL MODEL WITH TWO-STEP-NITRIFICATION PROCESS

3.4.1. Introduction of the biological model with a two-step-nitrification process on GPS-X software

In this study, a biological model with a two-step-nitrification process was proposed based on the ASM1 cryptic growth model, including 12 biological reactions. Recently, the bacteriology studies revealed the growth of strictly NOO bacteria of *Nitrospira* genus on NO_2-N as the sole substrate and nutrient source [82], [83]. In this study, a reaction (r6) was newly added to stimulate this process, although it was highly limited.

The continuity of the proposed model was verified using a systematic approach of Hauduc et al. [47] to avoid the errors, such as typing, inconsistencies, gaps, or conceptual errors that occurred in generating such a numerical model. In this approach, all the state variables are expressed in terms of COD, nitrogenous element, and charge. A composition matrix was developed, in which the conversion for all the state variables was put in rows, and the observables (e.g. S_{NHx}) were placed in columns. The continuity checking was carried out by multiplying the stoichiometric matrix with the composition matrix, as illustrated in Figure 15. The results should be zeros or having accepting tolerance of 10^{-15}.

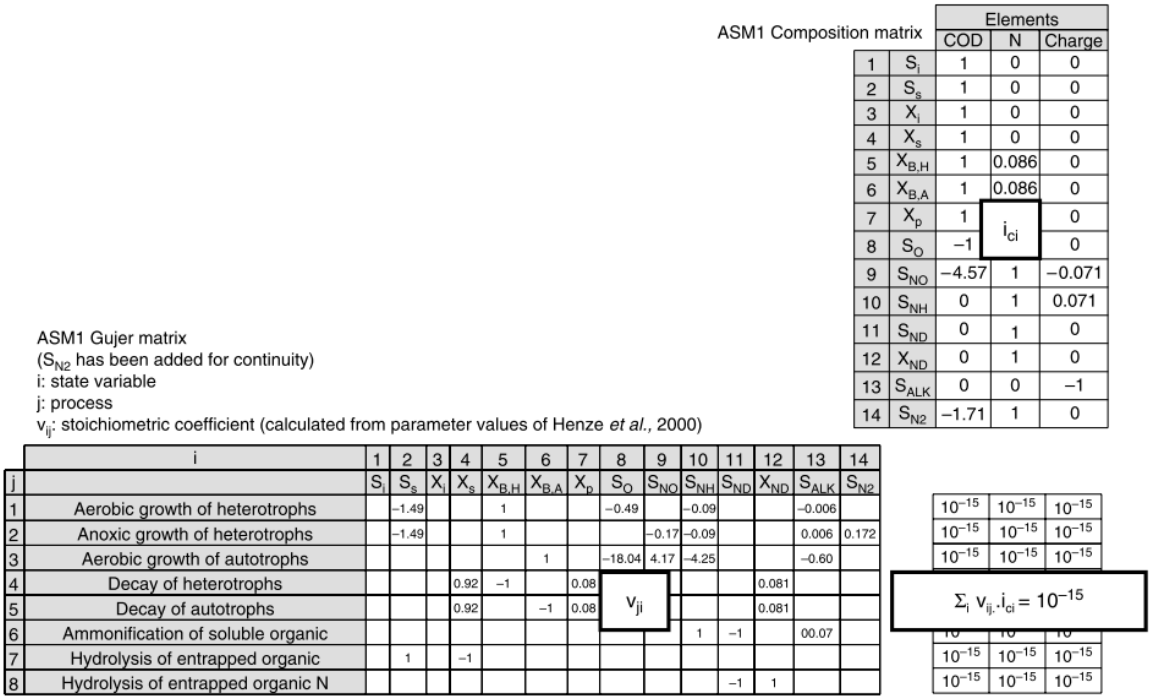

	ASM1 Composition matrix		COD	N	Charge
1	S_I		1	0	0
2	S_S		1	0	0
3	X_I		1	0	0
4	X_S		1	0	0
5	$X_{B,H}$		1	0.086	0
6	$X_{B,A}$		1	0.086	0
7	X_P	i_{ci}	1		0
8	S_O		−1		0
9	S_{NO}		−4.57	1	−0.071
10	S_{NH}		0	1	0.071
11	S_{ND}		0	1	0
12	X_{ND}		0	1	0
13	S_{ALK}		0	0	−1
14	S_{N2}		−1.71	1	0

i		1	2	3	4	5	6	7	8	9	10	11	12	13	14	
j		S_I	S_S	X_I	X_S	$X_{B,H}$	$X_{B,A}$	X_P	S_O	S_{NO}	S_{NH}	S_{ND}	X_{ND}	S_{ALK}	S_{N2}	
1	Aerobic growth of heterotrophs		−1.49			1			−0.49		−0.09			−0.006		10^{-15} 10^{-15} 10^{-15}
2	Anoxic growth of heterotrophs		−1.49			1				−0.17	−0.09			0.006	0.172	10^{-15} 10^{-15} 10^{-15}
3	Aerobic growth of autotrophs						1		−18.04	4.17	−4.25			−0.60		10^{-15} 10^{-15} 10^{-15}
4	Decay of heterotrophs				0.92	−1		0.08					0.081			
5	Decay of autotrophs				0.92		−1	0.08					0.081			
6	Ammonification of soluble organic										1	−1		00.07		10^{-15} 10^{-15} 10^{-15}
7	Hydrolysis of entrapped organic		1		−1											10^{-15} 10^{-15} 10^{-15}
8	Hydrolysis of entrapped organic N											−1	1			

Figure 15. Illustration of continuity checking approach [47]

3.4.2. The Peterson matrix and reaction rates for a biological model with two-step-nitrification

Comparing to the original ASM1 model, some modifications were made to better describe the biological process that occurred in the reactor, as shown in Table 4. Accordingly, the Peterson matrix and reaction rates were developed in Table 5 and Table 6.

Table 4. Comparison of original ASM1 model and the proposed model

Original ASM1 model	Proposed model
The aerobic growth of heterotrophs on readily biodegradable substrate (S_B) with NH_4-N as nutrient	The direct growth of OHO on S_B required nutrients. In case NH_4-N was depleted, NO_x could be used as a nutrient source [84]. Therefore the process was separated into three reactions (r1 to r3), in which the nutrient was NH_4-N, NO_2-N and NO_3-N, respectively

Original ASM1 model	**Proposed model**
The aerobic growth of autotrophs	The autotrophs were separated into AOO and NOO. Accordingly, the process was divided into the growth of AOO (r4); and the growth of NOO with NH_4-N as a nutrient (r5) and with NO_2-N as a nutrient (r6)
The decay of autotrophs	The decay of autotrophs was separated into the decay of AOO (r8) and the decay of NOO (r9)

Table 5. Peterson matrix on two-step-nitrification

		S_B	XC_B	$X_{U,E}$	X_{OHO}	X_{AOO}	X_{NOO}	S_{O2}	S_{NHx}	S_{NO2}	S_{NO3}	$S_{B,N}$	$XC_{B,N}$	S_{Alk}
1	Aerobic growth of heterotrophs on S_b with S_{NHx} (as N source)	$-1/Y_{OHO}$			1			$-(1-Y_{OHO})/Y_{OHO}$	$-i_{N\_XBio}$					$-i_{N\_XBio}*i_{Charge\_SNHx}$
2	Aerobic growth of heterotrophs on S_b with S_{NO2} (as N source)	$-1/Y_{OHO}+i_{COD\_NO2}*i_{N\_Xbio}$			1			$-(1-Y_{OHO})/Y_{OHO}$		$-i_{N\_Xbio}$				$-i_{N\_Xbio}*i_{Charge\_SNOx}$
3	Aerobic growth of heterotrophs on S_b with S_{NO3} (as N source)	$-1/Y_{OHO}+i_{COD\_NO3}*i_{N\_Xbio}$			1			$-(1-Y_{OHO})/Y_{OHO}$			$-i_{N\_Xbio}$			$-i_{N\_Xbio}*i_{Charge\_SNOx}$
4	Aerobic growth of active ammonia-oxidizing biomass					1		$-(-i_{COD\_NO2}-Y_{AOO})/Y_{AOO}$	$-i_{N\_XBio}-1/Y_{AOO}$	$1/Y_{AOO}$				$(-i_{N\_Xbio}-1/Y_{AOO})*i_{Charge\_SNHx}+($

		S_B	XC_B	$X_{U,E}$	X_{OHO}	X_{AOO}	X_{NOO}	S_{O2}	S_{NHx}	S_{NO2}	S_{NO3}	$S_{B,N}$	$XC_{B,N}$	S_{Alk}
														$1/Y_{AOO}$) $*i_{Charge\_SNOx}$
5	Aerobic growth of active nitrite-oxidizing biomass with S_{NHx} (as N source)						1	$-(i_{COD\_NO2}-i_{COD\_NO3}-Y_{NOO})/Y_{NOO}$	$-i_{N\_Xbio}$	$-1/Y_{NOO}$	$1/Y_{NOO}$			$-i_{N\_XBio}*i_{Charge\_SNHx}$
6	Aerobic growth of active nitrite-oxidizing biomass with S_{NO2} (as N source)						1	$(Y_{NOO}+i_{COD\_NO3}-i_{COD\_NO2}-i_{COD\_NO2}*i_{N\_Xbio}*Y_{NOO})/Y_{NOO}$		$-i_{N\_Xbio}-1/Y_{NOO}$	$1/Y_{NOO}$			$[-i_{N\_Xbio}-(1/Y_{NOO})]*i_{Charge\_SNOx}+(1/Y_{NOO})*i_{Charge\_SNOx}$
7	Decay of heterotrophs		$1-f_{XU\_Bio,lys}$	$f_{XU\_Bio,lys}$	-1								$i_{N\_XBio}-f_{XU\_Bio,l}$	

		S_B	XC_B	$X_{U,E}$	X_{OHO}	X_{AOO}	X_{NOO}	S_{O2}	S_{NHx}	S_{NO2}	S_{NO3}	$S_{B,N}$	$XC_{B,N}$	S_{Alk}
													$_{ys}*i_{N\_X}$ $_{bio}$	
8	Decay of active ammonia-oxidizing biomass		$1-f_{XU\_Bio,lys}$	$f_{XU\_Bio,lys}$		-1							$i_{N\_XBio}-f_{XU\_Bio,l}$ $_{ys}*i_{N\_X}$ $_{bio}$	
9	Decay of active nitrite-oxidizing biomass		$1-f_{XU\_Bio,lys}$	$f_{XU\_Bio,lys}$			-1						$i_{N\_XBio}-f_{XU\_Bio,l}$ $_{ys}*i_{N\_X}$ $_{bio}$	
10	Ammonification of soluble organic Nitrogen								1			-1		i_{Charge_S} $_{NHx}$
11	Hydrolysis of slowly hydrolyzable substrate	1	-1											
12	Hydrolysis of particulate											1	-1	

		S_B	XC_B	$X_{U,E}$	X_{OHO}	X_{AOO}	X_{NOO}	S_{O2}	S_{NHx}	S_{NO2}	S_{NO3}	$S_{B,N}$	$XC_{B,N}$	S_{Alk}
	biodegradable organic nitrogen													
		Readily biodegradable substrate, gCOD/m^3	Slowly biodegradable substrate, gCOD/m^3	Unbiodegradable particulates from cell decay, gCOD/m^3	Active heterotrophic biomass, gCOD/m^3	Active ammonia oxidizing biomass, gCOD/m^3	Active nitrite oxidizing biomass, gCOD/m^3	Dissolved oxygen, gO_2/m^3	Free and ionized ammonia, gN/m^3	Nitrite, gN/m^3	Nitrate, gN/m^3	Soluble biodegradable organic nitrogen, gN/m^3	Particulate biodegradable organic nitrogen, gN/m^3	Alkalinity, mol $HCO3^-/m^3$

Table 6. Process rate in Peterson matrix for two-step-nitrification

#	Process rates
1	$\mu_{OHO,Max}.\frac{S_B}{K_{S_B,OHO}+S_B}.\frac{S_{O2}}{K_{O2,OHO}+S_{O2}}.\frac{S_{NHx}}{K_{NHx,nutrient}+S_{NHx}}.X_{OHO}$
2	$\mu_{OHO,Max}.\frac{S_B}{K_{S_B,OHO}+S_B}.\frac{S_{O2}}{K_{O2,OHO}+S_{O2}}.\frac{S_{NO2}}{K_{NO2,nutrient}+S_{NO2}}.\frac{K_{NHx,nutrient}}{K_{NHx,nutrient}+S_{NHx}}.X_{OHO}$
3	$\mu_{OHO,Max}.\frac{S_B}{K_{S_B,OHO}+S_B}.\frac{S_{O2}}{K_{O2,OHO}+S_{O2}}.\frac{S_{NO3}}{K_{NO3,nutrient}+S_{NO3}}.\frac{K_{NHx,nutrient}}{K_{NHx,nutrient}+S_{NHx}}.X_{OHO}$
4	$\mu_{AOO,Max}.\frac{S_{NHx}}{K_{NHx,AOO}+S_{NHx}}.\frac{S_{O2}}{K_{O2,AOO}+S_{O2}}.\frac{S_{NHx}}{K_{NHx,nutrient}+S_{NHx}}.X_{AOO}$
5	$\mu_{NOO,Max}.\frac{S_{NO2}}{K_{NO2,NOO}+S_{NO2}}.\frac{S_{O2}}{K_{O2,NOO}+S_{O2}}.\frac{S_{NHx}}{K_{NHx,nutrient}+S_{NHx}}.X_{NOO}$
6	$\mu_{NOO,Max}.\frac{S_{NO2}}{K_{NO2,NOO}+S_{NO2}}.\frac{S_{O2}}{K_{O2,NOO}+S_{O2}}.\frac{S_{NO2}}{K_{NO2,nutrient}+S_{NO2}}.\frac{K_{NHx}}{K_{NHx,nutrient}+S_{NHx}}.X_{NOO}$
7	$b_{OHO}.X_{OHO}$
8	$b_{AOO}.X_{AOO}$
9	$b_{NOO}.X_{NOO}$
10	$q_{am}.S_{B,N}X_{OHO}$
11	$q_{XCB\_Sb,hyd}.\frac{\frac{XC_B}{X_{OHO}}}{K_{S,XC_B}+\frac{XC_B}{X_{OHO}}}.\frac{S_{O2}}{K_{O2,OHO}+S_{O2}}.X_{OHO}$
12	$r_{11}.\frac{XC_{B,N}}{XC_B}$

3.4.3. The continuity checking of the proposed model

By applying the stoichiometric parameters defined in section 5.3, the composition matrix of the proposed model was shown in Table 7.

Table 7. Composition matrix of the proposed model

	COD	**N**	**Charge**
S_U	1	0	0
S_B	1	0	0
XC_B	1	0	0
$X_{U,E}$	1	0.086	0
X_{OHO}	1	0.086	0
X_{AOO}	1	0.086	0
X_{NOO}	1	0.086	0
S_{O2}	-1	0	0
S_{NHx}	0	1	0.071
S_{NO2}	-3.43	1	-0.071
S_{NO3}	-4.57	1	-0.071
$S_{B,N}$	0	1	0
$XC_{B,N}$	0	1	0
$X_{U,N}$	0	1	0
S_{Alk}	0	0	-1

By applying the calibrated stoichiometric parameters, the numerical stoichiometry of Peterson matrix for two-step nitrification was presented in Table 8.

Table 8. Numerical stoichiometry of the Petersen matrix for two-step nitrification

		S_B	XC_B	$X_{U,E}$	X_{OHO}	X_{AOO}	X_{NOO}	S_{O2}	$S_{\_NH}$	$S_{\_NO2}$	$S_{\_NO3}$	$S_{B,N}$	$XC_{B,N}$	$S_{\_ALK}$
1	Aerobic growth of heterotrophs on Sb with S_{NHx} (as N source)	-1.49			1.00			-0.5	-0.086					-0.006
2	Aerobic growth of heterotrophs on Sb with S_{NO2} (as N source)	-1.79			1.00			-0.5		-0.086				0.006
3	Aerobic growth of heterotrophs on Sb with S_{NO3} (as N source)	-1.89			1.00			-0.5			-0.086			0.006
4	Aerobic growth of active ammonia-oxidizing biomass					1.00		-15.3	-4.85	4.76				-0.69
5	Aerobic growth of active nitrite-oxidizing biomass with S_{NHx} (as N source)						1.00	-11.7	-0.086	-11.11	11.11			-0.01
6	Aerobic growth of active nitrite-oxidizing biomass with S_{NO2} (as N source)						1.00	-11.4		-11.20	11.11			0.01
7	Decay of heterotrophs		0.92	0.08	-1.00								0.08	
8	Decay of active ammonia-oxidizing biomass		0.92	0.08		-1.00							0.08	

		S_B	XC_B	$X_{U,E}$	X_{OHO}	X_{AOO}	X_{NOO}	S_{O2}	$S_{\_NH}$	$S_{\_NO2}$	$S_{\_NO3}$	$S_{B,N}$	$XC_{B,N}$	$S_{\_ALK}$
9	Decay of active nitrite-oxidizing biomass		0.92	0.08			-1.00						0.08	
10	Ammonification of soluble organic Nitrogen								1.00			-1.00		0.07
11	Hydrolysis of slowly hydrolyzable substrate	1.00	-1.00											
12	Hydrolysis of particulate biodegradable organic nitrogen											1.00	-1.00	

The results of continuity checking was presented in Table 9. As indicated, the continuity of the proposed model was reserved, because all the terms of COD, N and charge were found to be zero or lower than the tolerance of 10^{-15} for each process.

Table 9. Continuity checking of the Petersen matrix for two-step nitrification model

		COD	N	Charge
1	Aerobic growth of heterotrophs on Sb with S_{NHx} (as N source)	5.55E-17	0.00E+00	0.00E+00
2	Aerobic growth of heterotrophs on Sb with S_{NO2} (as N source)	-5.55E-17	0.00E+00	0.00E+00
3	Aerobic growth of heterotrophs on Sb with S_{NO3} (as N source)	1.11E-16	0.00E+00	0.00E+00
4	Aerobic growth of active ammonia-oxidizing biomass	0.00E+00	0.00E+00	0.00E+00
5	Aerobic growth of active nitrite-oxidizing biomass with S_{NHx} (as N source)	0.00E+00	0.00E+00	2.52E-17
6	Aerobic growth of active nitrite-oxidizing biomass with S_{NO2} (as N source)	0.00E+00	0.00E+00	0.00E+00
7	Decay of heterotrophs	0.00E+00	0.00E+00	0.00E+00
8	Decay of active ammonia-oxidizing biomass	0.00E+00	0.00E+00	0.00E+00
9	Decay of active nitrite-oxidizing biomass	0.00E+00	0.00E+00	0.00E+00
10	Ammonification of soluble organic Nitrogen	0.00E+00	0.00E+00	0.00E+00
11	Hydrolysis of slowly hydrolyzable substrate	0.00E+00	0.00E+00	0.00E+00
12	Hydrolysis of particulate biodegradable organic nitrogen	0.00E+00	0.00E+00	0.00E+00

3.5. CONCLUSION

In this chapter, a combined biofilm and biological model with two-step nitrification on IFAS object was introduced on GPS-X software. The main results were as follows:

1. An illustration of the combined physical, biofilm and biological model for NH_x-N and organics removals for a nitrifying expanded-bed reactor was presented.

2. The biofilm model principles are presented, together with the mass transport processes and the mass balance equations for soluble and particulate components in the bulk liquid, attached liquid film, and biofilm layers,

3. A biological model with Peterson matrix and reaction rates for two-step nitrification was built. The continuity checking of the proposed model was reserved.

CHAPTER 4. PHYSICAL MODEL OF AN EXPANDED-BED REACTOR WITH GRANULAR ACTIVATED CARBON MEDIA

CHAPTER 4 PHYSICAL MODEL OF AN EXPANDED-BED REACTOR WITH GRANULAR ACTIVATED CARBON MEDIA

4.1. INTRODUCTION AND OBJECTIVES

The ultimate goal of this study is to develop a mathematical model of a nitrifying expanded-bed reactor to remove NH_4-N and micropollutants in drinking water treatment. The first step was to create a physical model that defined the physical boundaries in which the biological reactions took place.

In the existing modeling studies with moving media, such as those of IFAS and Moving Bed Biofilm Reactor (MBBR) [51], [85], [86], the movement of carriers was isolated in separate compartments of the reactors. In this study, we first introduced the definitions of internal recycle flow with the media concentration factor, which simulated media movement between the compartments. CHAPTER 6 will present the detailed inputs and operation of the IFAS object on GPS-X. Here, we determined the basic physical parameters relating to the media and the reactor's hydraulic regime, which will be used in building up the physical model.

The objectives of this chapter were:

1. To estimate the media fraction of granular activated carbon media in packed-bed condition,

2. To determine the specific surface area of the granular activated carbon media,

3. To study the hydraulic regime in the reactor, including the number of tanks-in-series, the internal recycle flow with concentration factor,

4. To evaluate the influences of internal recycle flow with a media concentration factor to the media and biomass distribution in the expanded-bed.

4.2. MEDIA FRACTION OF GRANULAR ACTIVATED CARBON IN THE PACKED-BED CONDITION

The apparent volume fraction of media without micro-pores was determined in the packed-bed condition. As shown in Figure 16, the wet granular activated carbon media was carefully placed on a paper to remove the attached water on the surface. Next, the material was placed on a measuring cylinder. Water with known volume was poured to the top of the cylinder, making the volume of the packed-bed increase. From the volume of added water and topwater beyond the packed-bed, the volume of water filled into the packed-bed was calculated. Triplicate tests were carried out, and their average value of 35.7% was used for the media fraction in the modeling (void fraction of the packed bed = 64.3%).

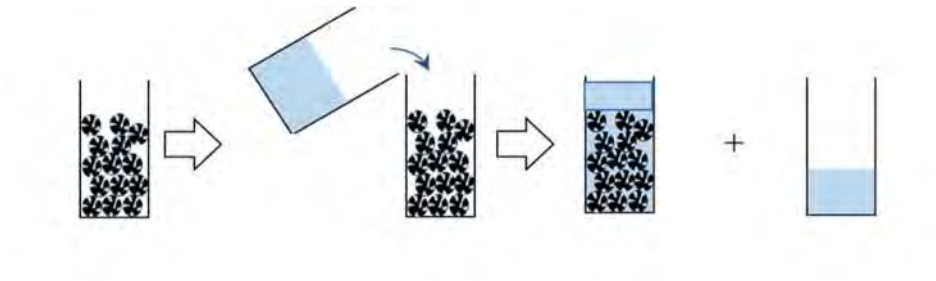

Figure 16. Determination of media fraction in packed-bed condition

4.3. SPECIFIC SURFACE AREA OF GRANULAR ACTIVATED CARBON MEDIA

To estimate the media's specific surface area, the irregular shape of GAC particles was considered as spheres for simplification. This assumption was acceptable since most of the microorganisms were assumed to be distributed mainly at the GAC's outer surface area due to their larger sizes compared to the ones of GAC's intraparticle pores [75]. A series of photos of dried GAC particles were taken using a microscope and then analyzed using binary image processing software (Quick Grain, Inotech Inc., Japan), as shown in Figure 17.

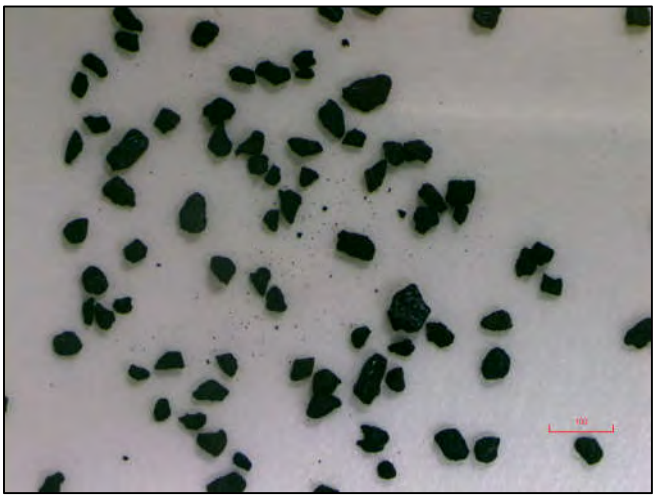

Figure 17. Microscopic image of granular activated carbon media

The equivalent circle area diameter d_p, defined as the diameter of the circle having the same area as of the particle, was determined for each GAC granule. The particle size distribution for the GAC sample was evaluated, as shown in Figure 18.

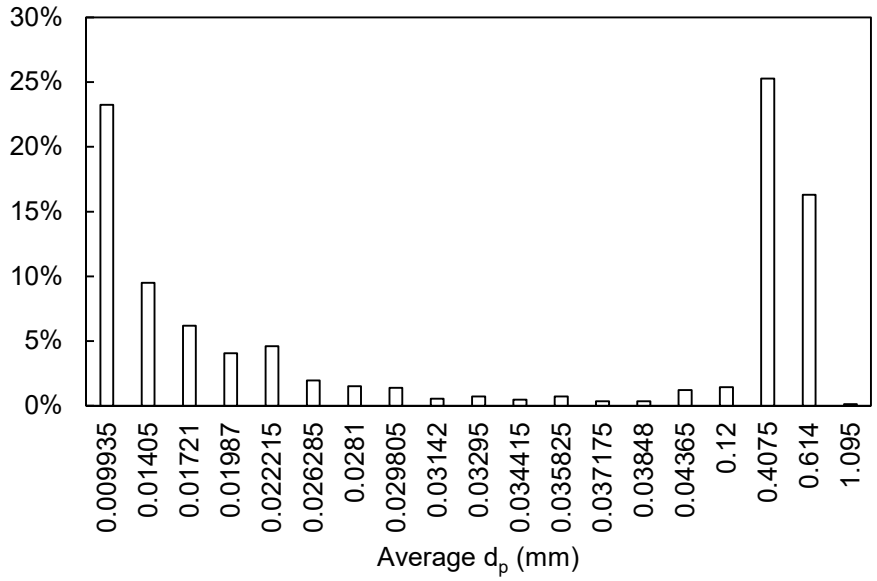

Figure 18. The particle size distribution of the granular activated carbon media

From the particle size distribution, the average d_p was calculated to be 0.431 mm.

The specific surface area of the carriers in the expanded-bed was calculated according to Eq (20)

$$Specific\_surface\_area = \frac{\sum_{1}^{N} n_i.\pi.(d_{p,i})^2}{\sum_{1}^{N} n_i.\frac{1}{6}.\pi.(d_{p,i})^3} \qquad \textbf{Eq (20)}$$

Where n_i: Number of GAC particles having the $R_{a,i}$, N: the group of a particle having $d_{p,i}$ (N = 19), $\sum_{1}^{N} n_i = 3,778$

The packed-basis specific surface area was found to be 5,587 m^2/m^3.

4.4. HYDRAULIC REGIME OF THE REACTOR

4.4.1. The tracer test

To catch the hydraulic regime, a tanks-in-series model was applied over the 2-m of the expanded-bed height of the lab-scale reactor. The reactor was assumed to be composed of several identical completely stirred tanks (CSTR), which were connected in series ($1 \ldots i \ldots N$) [87]. A pulse of NaCl liquid (30 g/L, 80 mL) was prepared as a tracer and injected into the reactor. A conductivity probe (CM-31P, DKK-TOA, Japan) was placed at 2 cm below the expanded bed surface. The conductivity of the effluent was recorded every 30 seconds. Prior to the test, the calibration curve of conductivity of NaCl solution was obtained ($y = 169.25x + 25.8$, $R^2 = 0.998$). Based on this, the tracer conductivity (mS /m) recorded in the effluent was converted into mass concentration (g/L). The experiment of the tracer test was presented in Figure 19.

In total, six tracer tests were carried out under identical experimental conditions. The non-dimensional mean residence time ($\bar{\theta}$) and non-dimensional time distribution functions (E_θ) curve in each test was calculated. The average E_θ curve was built and compared with the curves of several numbers of tanks-in-series. The curve of 11 tanks was closest to the average E_θ curve; therefore, the N equaled to 11 was selected for the hydraulic modeling. The measured and simulated E_θ curves of the tracer test was shown in Figure 20.

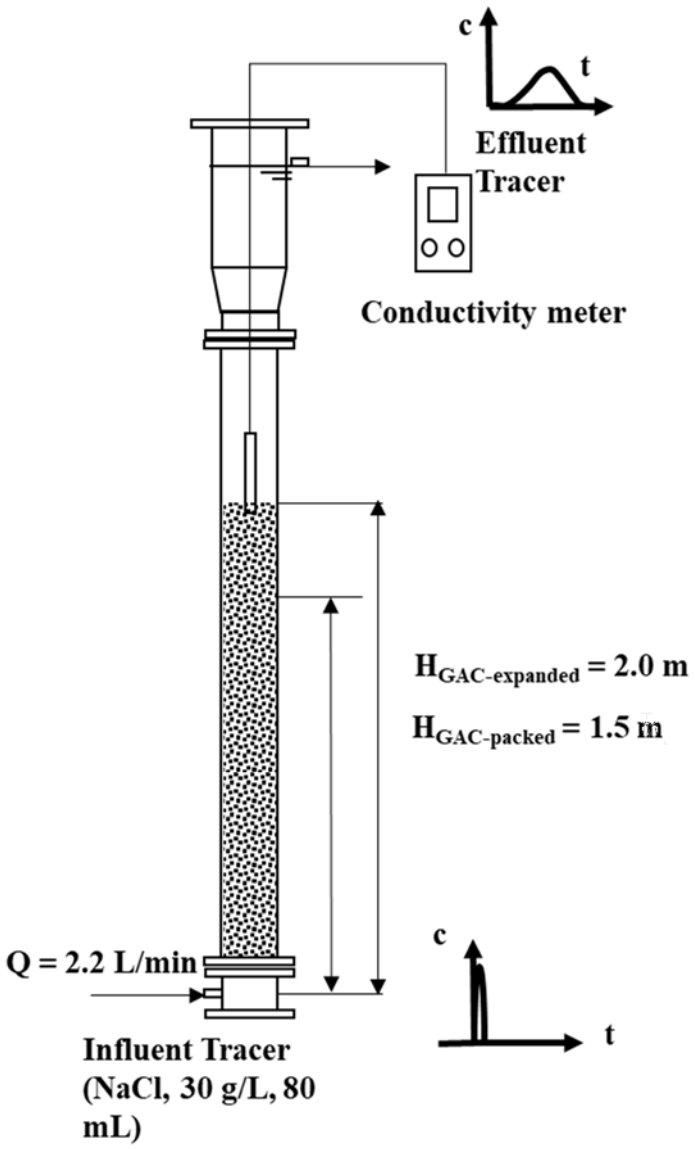

Figure 19. Tracer test experiment

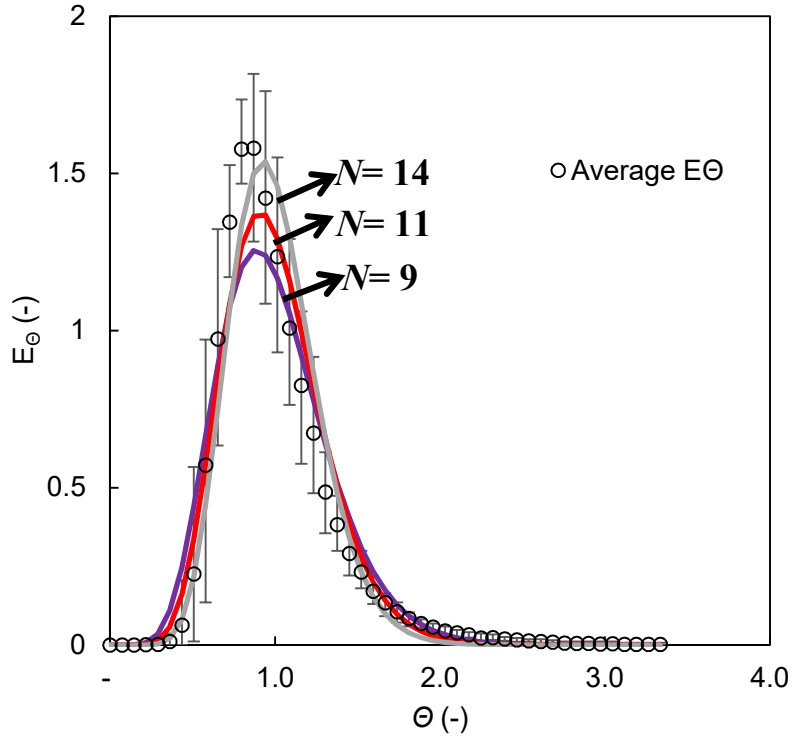

Figure 20. Measured and simulated non-dimensional time distribution functions (E_θ) curves of the tracer

4.4.2. The internal recycle flow and concentration factor

The physical model was incorporated into the combined biofilm and biological model, as illustrated in Figure 13. In the tanks-in-series, the biomass media circulated from the tank *i* to the tank *i+1* where the biomass media again recycled back to the tank *i* with a very small portion of liquid. The biological reactions took place in each tank where the influent was defined from the bottom (1st tank) to the top (11th tank) of the reactor.

Using the definitions of the internal recycle flow rate (q_{i_i-1}) and the concentration factor (η), the material balance equations for the 1st tank, the tank i and the last tank were given respectively in Eq (21) as below:

$$\begin{cases} \frac{1}{C_0}.\frac{dC_1}{dt} = \frac{1}{\tau_{H,1}}.S_0 + \eta_{2-1}.\frac{1}{\tau_{R,2\_1}}.S_2 - (\frac{1}{\tau_{H,1}} + \frac{1}{\tau_{R,2\_1}}).S_1 \\ \frac{1}{C_0}.\frac{dC_i}{dt} = (\frac{1}{\tau_{H,i}} + \frac{1}{\tau_{R,i\_i-1}}).S_{i-1} - (\frac{1}{\tau_{H,i}} + \frac{1}{\tau_{R,i+1\_i}}).S_i + \eta_{i+1\_i}.\frac{1}{\tau_{R,i+1\_i}}.S_{i+1} - \eta_{i\_i-1}.\frac{1}{\tau_{R,i\_i-1}}.S_i \\ \frac{1}{C_0}.\frac{dC_N}{dt} = (\frac{1}{\tau_{H,N}} + \frac{1}{\tau_{R,N\_N-1}}).S_{N-1} - \eta_{N\_N-1}.\frac{1}{\tau_{R,N\_N-1}}.S_N - \frac{1}{\tau_{H,N}}.S_{Final} \end{cases} \quad \textbf{Eq (21)}$$

In which $\tau_{H,i} = \frac{Q}{V_i}$; $\tau_{R,i\_i-1} = \frac{q_{i\_i-1}}{V_i}$; $S_i = \frac{C_i}{C_0}$

Where: In case of liquid: $\eta = 1$, in case of media and biomass: $S_0 = 0$ and $S_{Final} = 0$;

t: time (second); C_0, C_i, C_{Final}: concentration at the influent, in the tank i and at the effluent (g/m^3 or m^3/ m^3); Q and q_{i_i-1}: mainstream flowrate and internal recycle flowrate from tank (i) to tank (i-1) (m^3/s); V_i: cell tank volume i (m^3); η_{i_i-1}: Concentration factor from tank (i) to tank (i-1).

For simplification, the individual values of q_{i_i-1} and η_{i_i-1} were assumed to be identical in all the cell tanks. The even distribution of media over the expanded-bed height would be ideally achieved following Eq (22):

$$\eta = \frac{Q}{q} + 1 = F + 1 \quad \textbf{Eq (22)}$$

Where F: the ratio of mainstream flowrate to internal recycle flowrate (dimensionless)

The F and η were calibrated based on the simulation of the tracer test using a process simulator, GPS-X ver. 8. (Hydromantis Inc., Canada).

The physical model was also applied to the pilot-scale reactor in Hoa Phu WTP, which of identical configuration, and to the full-scale reactor in Vinh Bao WTP, assuming the horizontally scale-up did not affect the vertical mixing.

4.5. MODELING MEDIA DISTRIBUTION IN THE EXPANDED-BED

4.5.1. Calibration of internal recycle flow and media concentration factor

A very high value of F was desirable to limit the effect of the internal recycle flow on the hydraulic retention time of the materials in the reactor. The calibration of F and η was based on the comparison of $\bar{\theta}$ in the tracer test. As shown in Figure 21, when the F was set at 5 and η was estimated to be 6, the tracer exited the reactor earlier, expressed by the $\bar{\theta}$ of 0.99989. At the doubled value of F and η equaled to 11, a shorter $\bar{\theta}$ of 0.99992 was still observed. When the F was increased to 1,000 and η increased to 1,001, the $\bar{\theta}$ was found to be 1, which was perfectly matched to the experimental data. The E_θ curve corresponding to F equaled to 1,000 was visually closest to the experimental curve. For the F higher than 1,000, tiny improvement on the E_θ curve and $\bar{\theta}$ were observed.

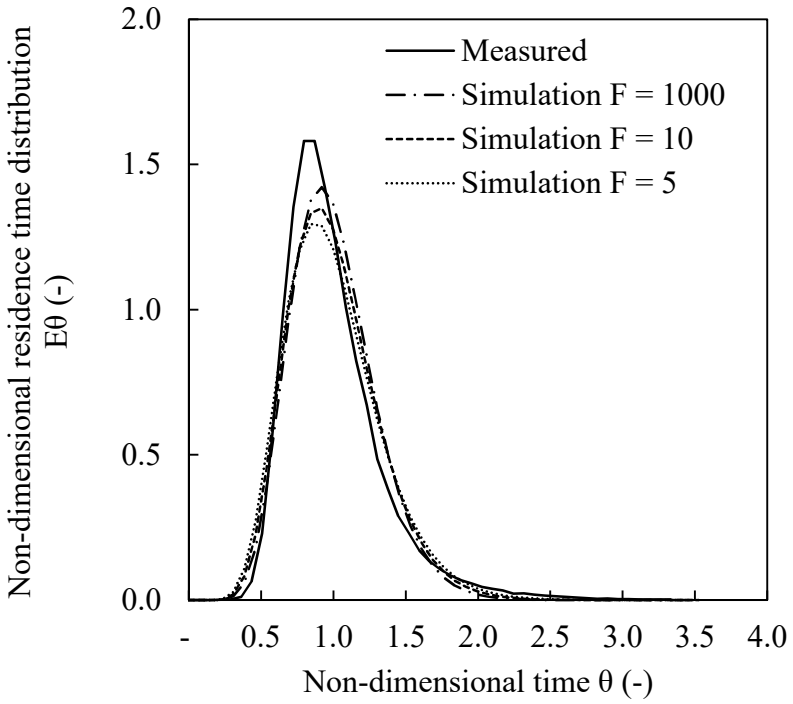

Figure 21. Non-dimensional residence time distribution curves of tracer test

4.5.2. Media distribution in the expanded-bed

By manipulating the η, the distribution of media over the expended-bed could be created.

However, due to the limited data, an even distribution of media was selected for modeling in this study. The permissive values of F and η were selected to be 1,000 and 1,001, respectively, which resulted in the media concentrations of 75% in all the cell CSTRs. In practice, because the media density is slightly higher than water density, the media concentrations at the bottom of the expanded column might be slightly higher than those in the top. To show the effect of η on media distribution, different simulations were carried out with various values of η. The influence of high or low values of concentration factor to the media distribution in the expanded-bed was illustrated in Figure 22.

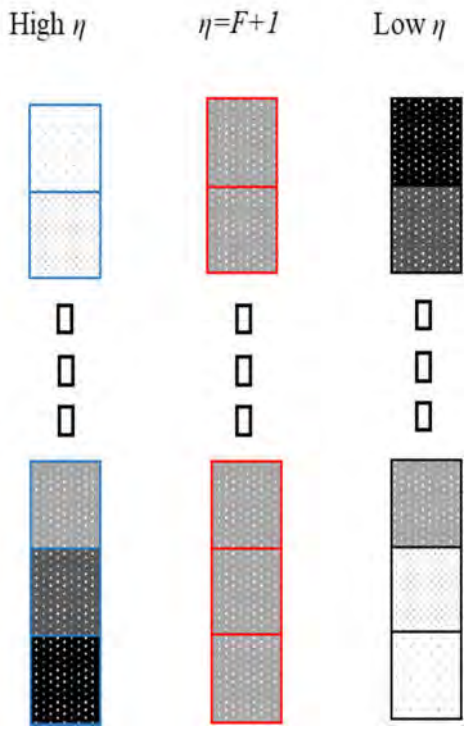

Figure 22. Illustration of the media distribution in the expanded-bed with different values of concentration factor

As shown in Figure 23, when η was set at 1,051 that was 5% higher than the selected η, a stronger movement of media toward the bottom was observed, in which the media concentration in the first tank was found to be 93.4% and smoothly decreased to 59.0% in the top tank. The opposite trend was made when η was fixed at 951 which was 5% lower than the selected η.

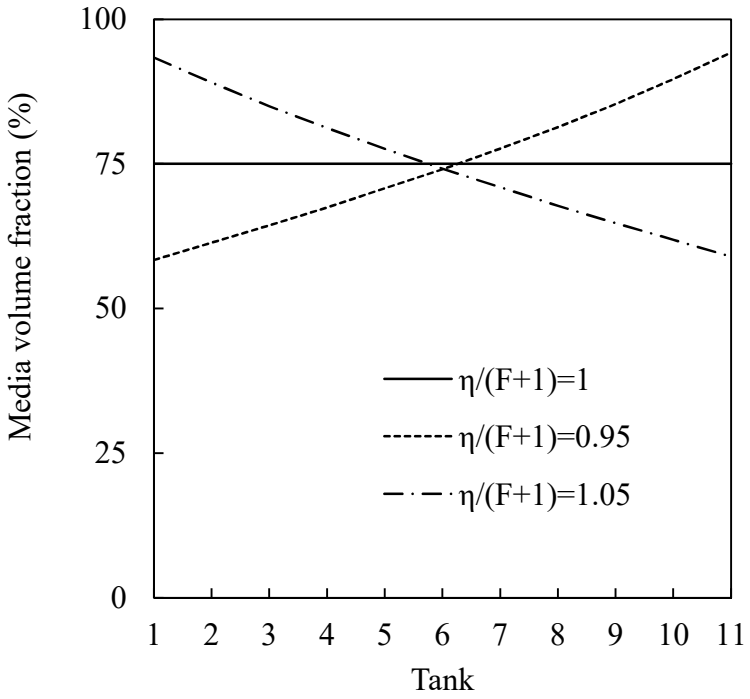

Figure 23. Media volume fraction distribution in the expanded-bed

4.5.3. The biomass distribution in the expanded-bed

To investigate the attached biomass concentration that was influenced by the media concentration, the steady-state simulation of the full-scale reactor was carried out with the set of kinetic and stoichiometric parameters, as presented in CHAPTER 5.

As shown in Figure 24, when the media was homogenized in the expanded-bed, the OHO biomass concentration in the biofilm was gradually decreased from 1,439 mgCOD/L in the first tank to 1,394 mgCOD/L in the final tank, which was aligned with the removal of pollutants along the reactor. When η was varied, a similar trend of decreased OHO biomass along the expanded-bed height was observed. In the case of higher η, increased media volume at the bottom resulted in a slightly elevated OHO biomass of around 1.5% in the cell tanks. In the case of lower η, the OHO biomass was reduced by around 1.1% in the cell tanks.

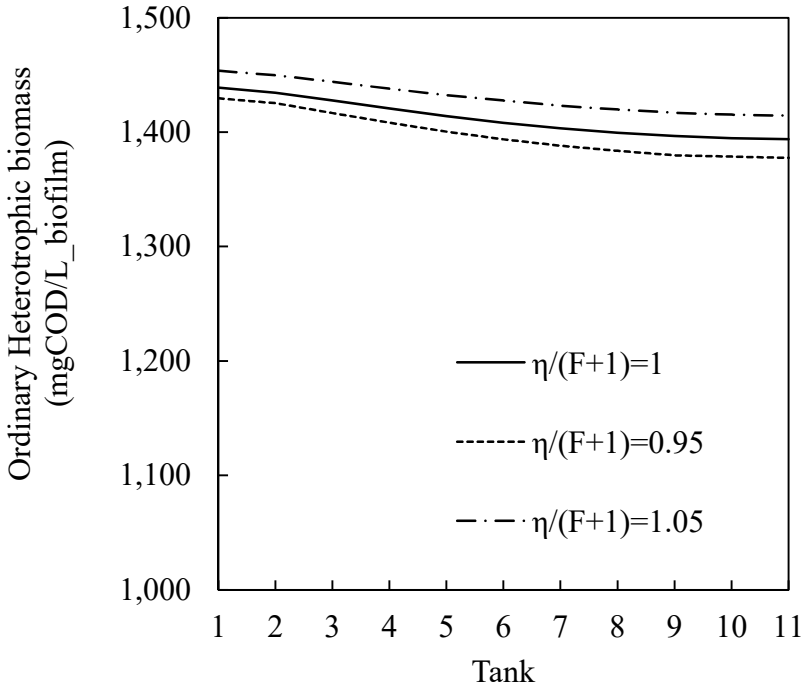

Figure 24. Ordinary heterotrophic biomass distribution in the expanded-bed

Conversely, the variation of η created less impact on the distribution of AOO and NOO biomass because they were mostly even in the reactor. It was because the AOO and NOO biomass concentrations were calculated to be only 530 and 105 mgCOD/L, respectively, which were significantly lower than those of OHO. Further, the OHO was dominant in the outer biofilm layers for available DO and substrates. Although the media volume was changed, the available space in the deeper biofilm layers was unlikely to affect the growth of AOO and NOO. For further application of the hydraulic model in the attached growth process, the demonstration suggested that the media and biomass concentration in the cell CSTR could be differentiated by varying the individual $\eta_{i,i-1,}$ to suit the evolution of pollutants along the reactor and meet the design criteria.

4.6. CONCLUSIONS

In this chapter, a physical model was developed to express an expanded-bed reactor using granular activated carbon media. The obtained results were as follows:

1. The media fraction of the packed-bed was estimated to be 35.7%,

2. The specific surface area of the media in the packed-basis was found to be 5,587 m^2/m^3.

3. From the tracer test, the number of tanks-in-series of the reactor (*N*) was estimated to be 11.

4. The homogenization of the media over the expanded-bed height was simulated. The evenest distribution of the media was found at the media concentration factor of 1,000 and the internal recycle flow equaled to 0.001Q. The influence of media distribution on the attached biomass was also evaluated.

CHAPTER 5. COMBINED BIOFILM AND BIOLOGICAL MODEL OF A NITRIFYING EXPANDED-BED REACTOR FOR AMMONIA AND ORGANICS REMOVALS

5.1. INTRODUCTION AND OBJECTIVES

At present, due to the discharge of inadequately treated wastewater to water bodies, a large number of drinking water treatment plants (WTPs) in developing countries face with high concentrations of ammonium (NH_x-N) at the supply sources. When chlorination disinfection is applied, a large amount of chlorine would be needed to remove the NH_x-N. To reach the chlorination breakpoint and obtain the free chlorine residual, a dose of 8 – 10 $mgCl_2/mgNH_x$-N is often recommended [19]. Therefore, high influent NH_x-N is directly engaged to the increase in the operational costs. Additionally, in case that the influent dissolved oxygen (DO) is limited, the incomplete removal of NH_x-N may result in the accumulation of nitrite (NO_2-N) in the system. The high concentration of NO_2-N in tap water can cause methemoglobinemia in infants [20]. Therefore, more chlorine should be dosed to oxidize the generated NO_2-N.

Among the available pretreatment technologies, biological nitrification is considered to be a promising and cost-effective option to remove NH_x-N from water sources. In principle, nitrification is composed of a two-step microbiological process, in which ammonium-oxidizing organisms (AOO) and nitrite-oxidizing organisms (NOO) convert NH_x-N to NO_2-N and NO_2-N to nitrate (NO_3-N), respectively. In the drinking water sources where the substrates for microorganism growth are very limited, the oligotrophic bacteria with very low half-saturation coefficients (K_S) [57], [58] are favored. In this regard rather than ordinary heterotrophic organisms (OHO), nitrifiers are known to be sensitive to various environmental factors, such as temperature, pH, available DO, and substrates [59]. Their growth on the carrier might provide a more hospitable environment [60], and nitrifying biomass concentration in the reactor could be significantly increased. However, unlike biological wastewater treatment systems, DO competition between nitrifiers and heterotrophs, and each reaction rate in low-strength influent have not been well formulated. Hence, at present, it is difficult to calculate the removable NH_x-N and organic substrates and possible NO_2-N accumulation in the pretreatment of WTPs.

Based on the above background, a mathematical model of two-stage oligotrophic nitrification and heterotrophic reactions was developed for an expended-bed reactor aiming to remove NH_x-N from drinking water. The model was incorporated by physical, biofilm and biological models explained in CHAPTER 3 and CHAPTER 4 on the framework of Activated Sludge Models (ASMs) developed by IWA Task Group [46]. At present, different scales from 0-dimensional (0-D) to multi-dimensional (2-D and 3-D) resolutions could be used for biofilm modeling. In water and wastewater engineering, the application of the 0-D model might cause discrepancies in the simulation results due to oversimplifications. On the other hand, the 2-D and 3-D model could provide insights into the biofilm's heterogeneous morphology and inter-species microbial interactions; however, interdisciplinary expertise and a huge amount of experimental data are needed in building such a fine-resolution model. In the shortage of experimental data on how the species spatially existed in the biofilm, the 1-D model that still well captures the dominant biofilm process has become the most attractive option [45].

In the nitrifying expanded-bed reactors, the granular activated carbon (GAC), which then transformed into biological activated carbon due to the biofilm coating, was used as the carrier for the biofilm. Rather than its adsorption capacity which was eventually expired during long-term operation, the diverse and stable bacterial culture developed on the biofilm was proven to remove NH_x-N [88] and a wide range of biodegradable organic matters [39]. In the biofilm model, instead of considering the overall biofilm-detachment loss as previous research [60], [89], this study examined the dynamic attachment and detachment separately in their interrelation. The detachment was examined in the experiment with limited suspended solids, while the attachment was estimated from the capture of suspended solids in the field study. The reactive biofilm thickness and internal biomass exchange were calibrated to reproduce comparable effluent concentrations. Their implications to the biofilm performance were also investigated in initial biofilm development, steady-state operation, and backwash events. The model calibration was

carried out based on five different datasets of both synthetic and rivers water over the lab-, pilot- and full-scale reactors. It aimed at obtaining a single set of kinetic and stoichiometric parameters for the oligotrophic AOO/NOO/OHO, which might be considerably different from those applied in wastewater treatment. Once the single set was obtained, it could be used as a set of default parameters in future designing water treatment with low-strength NH_x-N and organic substrates.

The objectives of this chapter were:

1. To investigate the attachment, detachment, and internal solids exchange of suspended solids to/from the biofilm layers,

2. To obtain a single set of kinetic and stoichiometric parameters for the oligotrophic AOO/NOO/OHO from the calibrations of five different datasets, which reflected the biofilm performance in different circumstances,

3. To create the graphical guidance on the reactor performance at variable influent conditions.

5.2. MATERIALS AND METHODS

5.2.1. Monitoring campaigns for the lab-, pilot- and full-scale reactors

The physical properties of the lab-, pilot- and full-scale reactors were previously presented in CHAPTER 4.

As for the lab-scale reactor, the influent was made with NH_4Cl solution of 2,200 mgN/L and dechlorinated tap water using metering and centrifugal pumps respectively (IWAKI, Japan). In the start-up period of 90 days, the reactor was fed with synthetic water containing 1 mg NH_x-N/L to stimulate nitrifiers' growth. The temperature of tap water was ranged from 10°C to 20°C in 3 months. In the subsequent continuous operation for 90 days, the NH_x-N loading was varied from 1 to 2 mg NH_x-N/L in a stepwise manner. During this period, the temperature was changed from 20°C to 30°C.

The pilot-scale reactor in Hoa Phu WTP was located in the semi-diurnal tidal zone. The intake point of the plant was found at different depths from the water surface because of the tidal effect, resulting in the sinusoidal trends of DO and temperature of influent water in a day. Intensive monitoring was carried out for 4.5 days in January when the temperature was around 30°C.

As for the full-scale reactor in Vinh Bao WTP, the influent was pumped from an irrigation channel that received the water from the main river. The water quality was said to be degraded in the rainy season, especially from July to August. In this period, the crops were harvested and their roots were still on the field. Due to the precipitations, part of the substances (fertilizer, etc.) remained in the field were washed-out to the channel, resulting in the polluted water source for both organics and nitrogen. To investigate the reactor performance, two intensive monitoring campaigns were carried out at different influent circumstances. The first survey for 3 days was carried out in dry season in January (hereinafter Vinh Bao WTP (D)). The water quality was fairly acceptable, and the reactor

was operated at the designed flow rate of 105 m^3/h with the water temperature at around 20°C. The second monitoring for 7 days was carried out in the rainy season in August (hereinafter Vinh Bao WTP (R)). In the first 3 days, because of the poor influent water quality, the reactor was run at 50 m^3/h with a lowered linear velocity. From day 4, the influent quality was improved due to the release of the freshwater from the main river to the channel. The flow rate of the reactor was then increased to 70 m^3/h. During the campaign, the water temperature was kept at around 30°C.

The monitored parameters and their ranges of values were listed in Table 10.

Table 10. Summary of influent water quality and objectives of modeling

No	Dataset	Objectives of modeling	Temp. (°C)	DO (mgO_2/L)	NH_x-N (mgN/L)	NO_2-N (mgN/L)	NO_3-N (mgN/L)	TSS (mg/L)	VSS (mg/L)	Total COD (mg/L)
1	Lab-scale start up	Biofilm initial formation	11.3 – 20.2	8 – 10	0.6 – 1.2	0 – 0.04	0 – 1.2	0	0	0
2	Lab-scale continuous operation	NO_2-N accumulation in low DO	17.8 – 29.7	5.5 – 9.2	0.7 – 2.1	0 – 0.03	0.1 – 0.8	0	0	0
3	Pilot-scale Hoa Phu WTP	Estimation of influent readily biodegradable substrate from DO consumption	27.2 – 34.3	2.9 – 6.5	0 – 0.6	NA	NA	NA	NA	NA
4	Full-scale Vinh Bao WTP (D)♣	Same as above	19.2 – 21.2	6.6 – 8.0	0 – 0.5	NA	NA	NA	NA	NA
5	Full-scale Vinh Bao WTP (R)♦	Biofilm in long-term operation Biofilm attachment and detachment	28.3 – 31.0	4.4 – 7.9	0 – 6.5	0 – 0.4	0 – 1.9	22 – 120	2.2 – 17.7	7.2 – 36.6

♣ in the dry season ***♦ in the rainy season*** ***NA: Not measured***

5.2.2. Analytical procedures

For the lab-scale reactor, influent and effluent samples were collected daily for analysis. NH_x-N concentrations were measured according to #4500-NH_3 F in Standard Methods [90]. NO_2-N and NO_3-N were analyzed using Ion Chromatography (ICS-1500, Dionex, California, USA). The accuracy of NO_3-N measurement at the concentration as low as 1 to 2 mgN/L was rather limited. DO was monitored using the DO meter (TOX-999, TOKO, Tokyo, Japan). The temperature was recorded using a thermometer. The batch experiments on the oxygen uptake rates (OUR) were carried out using the media sampled from the reactor after the system reached a steady-state condition. The amounts of 20 g of wet media were taken from the lab-scale reactor and washed by the effluent water in which the NH_x-N and NO_2-N concentrations were highly limited. The media were transferred into the Winkler bottles, which were then filled up with an air-saturated solution containing 2 mgN/L of NH_x-N concentration. Under the gently stirring, the DO decrement in the Winkler bottles was recorded using the DO meter until the DO reached to 0 mg O_2/L. The batch experiments were controlled at the temperature of 20^{o}C, 30^{o}C, and 35^{o}C using a water bath. Based on the results of OUR, the detachment of biofilm, the amount of biomass, and the temperature correction factor for AOO were obtained.

As for the pilot reactor at Hoa Phu WTP, the DO and temperature at the influent and effluent chambers were automatically recorded at every 15 minutes using optical DO sensors (FDO 925-P probes and Multimeter 3430, WTW, Germany). The accuracy of the DO and temperature probes in the field conditions were ± 0.2 mgO_2/L and ± 0.2^{o}C, respectively. The NH_x-N concentration was also automatically measured using dual on-line portable meters LAQUAact-D73 (Horiba, Japan). The influent and effluent samples were mixed with sodium hydroxide solution 20% to increase the pH to more than 12. In this condition, ammonium ion in the water was converted into ammonia gas, which was then recorded using high polymer membrane ammonia electrodes 5002A (Holiba, Japan). Influent and

effluent electrodes were calibrated every day, showing acceptable linearity with R^2 from 0.977 to 0.998. The pH of the mixture solutions was checked periodically to ensure that the pH higher than 12 was maintained.

For the full-scale reactor at Vinh Bao WTP, in the first and second monitoring campaigns, the water temperature, DO and NH_x-N concentrations were automatically recorded using comparable materials to those used in Hoa Phu WTP. Particularly, during the second survey, the influent and effluent water samples were collected hourly with two units of autosampler (Avalanche, Teledyne ISCO, USA) for the lab analysis. The inorganic nitrogen was measured using reflectometric with test strips (RQflex 10, Merck, Germany). The measuring ranges were 0.16 – 5.4 mg NH_x-N/L, 0.2 – 7.6 mg NO_2-N/L and 0.7 – 20.3 mg NO_3-N/L respectively. Prior to the analysis, the calibration curves were created with acceptable linearity for NH_x-N. The measured NO_2-N and NO_3-N were closed to the low detection limits of the test papers, resulting in the poor linearities. The total chemical oxygen demand (COD) was measured using digestion vials of ultra-low range of 0.7 – 40 mgO_2/L (Hach, USA). The total and volatile suspended solids (TSS and VSS) were measured according to #2540 B and #2540 E respectively in the Standard Methods [90].

5.3. RESULTS AND DISCUSSIONS

5.3.1. Detachment and amount of biomass in the lab-scale experiment

The dynamic simulations were carried out for the three OUR tests using the set of kinetic and stoichiometric parameters listed in Table 11. The biomass concentrations obtained from the dynamic simulation of the lab-scale reactor at the steady-state condition were used as the initial conditions for the design of the batch experiments. As shown in Figure 25, the DO decrements with time at different temperatures could be fairly reproduced. The biomass concentrations of AOO and NOO in the biofilm were estimated to be 1,373.5 mgCOD/L$_{\text{-biofilm}}$ and 590 mgCOD/L$_{\text{-biofilm}}$, respectively. Based on the slopes of DO decrement, the temperature correction factor for AOO was estimated to be 1.072. The batch OUR experiment might slightly overestimate the microbial activities compared to the continuous operation with limiting-substrate conditions.

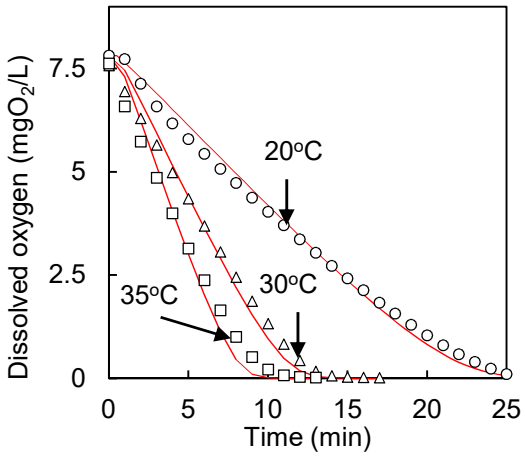

Figure 25. Measured and simulated oxygen uptake batch experiment at different temperature

(Biofilm media: 20 g, NH_4-N = 2 mgN/L, saturated DO)

The detachment was examined based on the dataset of the lab-scale start-up period, in which the effects of attachment were highly limited. When the k_{detach} was set at $1 \cdot 10^{-3}$ m/d, the biomass was washed-out from the biofilm, resulted in the NH_x-rich effluents. When

k_{detach} was reduced to $1 \cdot 10^{-5}$ m/d, complete removal of NO_2-N was wrongly achieved earlier than the experimental observation. The value of k_{detach} of $1 \cdot 10^{-4}$ m/d (biomass detach rate per area ≅ 10 g/(m^2·d) could fairly reproduce the effluent NH_x-N and NO_2-N concentrations, as shown in Figure 26. Because the pilot- and full-scale reactors were also operated at a similar linear velocity, the same value of k_{detach} of $1 \cdot 10^{-4}$ m/d was was used to simulate the detachment in the filtration runs. In the low substrate conditions, the biofilm thickness in the lab-scale reactor was estimated to be 0.002 mm. Such thin biofilm was calculated because the biofilm was modelled to evenly cover the large surface of the area.

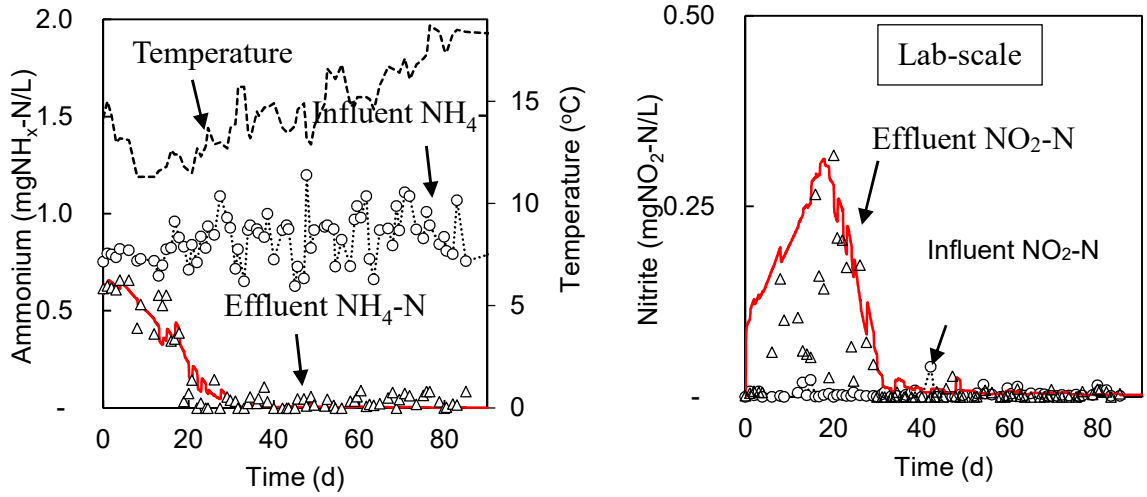

Figure 26. Ammonium removal and nitrite accumulation in the initial biofilm formation

Influent Measured effluent Simulated effluent Temperature

5.3.2. Attachment, detachment and internal solids exchange of the field reactors

In the monitoring of Vinh Bao WTP (R), the TSS and VSS of influent and effluent samples were collected every 1 h during the filtration cycle. Especially in backwash events, four samples of influent and backwash water were collected. In the surveying for 6.7 days (161 h), the backwash was conducted at day 2 (48^{th} h) and day 5 (122^{th} h). In the backwash of 1

hour, the strong water and air scouring (5.5 L/min) were applied to remove the excessive biofilm and repair the filter performance.

The dynamic attachment of particulates in the biofilm would depend on the nature of influent suspended solids. Most of the previous research only focused on the attachment at the initial biofilm development rather than the steady-state operation [43], [91]. In Vinh Bao WTP (R), the influent inert inorganic suspended solids were observed to be 37.6 mg/L on average. Using the experimental data of the effluent inert inorganic suspended solids, the k_{attach} was dynamically calibrated from 0.15 to 0.85 m/d as shown in Figure 27 (a). In the backwash events, a high value of $2.5 \cdot 10^{-3}$ m/d (biomass detach rate per area ≅ 250 g/(m^2·d) was applied to simulate the strong release of solids from the biofilm. The experimental plots of effluent suspended solids were reasonably reproduced in both three filtration cycles and two backwash events, as shown in Figure 28.

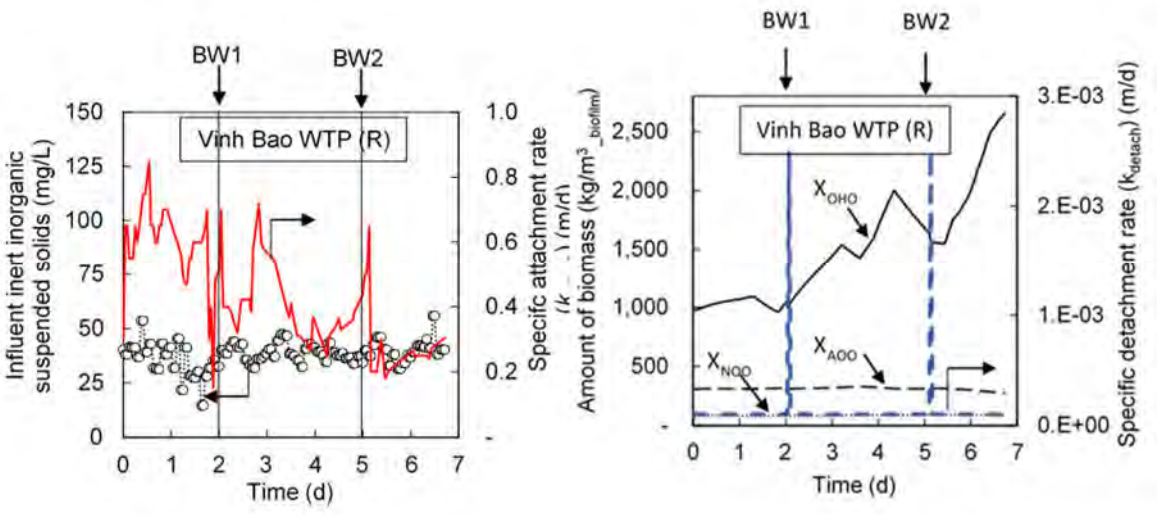

Figure 27. Influent inert inorganic suspended solids and specific attachment rates (a), Estimated amount of biofilm and specific detachment rates (b).

As shown in Figure 27 (b), in the field reactor of Vinh Bao WTP (R), the OHO was dominant over the AOO and NOO in the biofilm at the concentration from 1,000 mgCOD/$L_{\text{-biofilm}}$ to more than 2,500 mgCOD/$L_{\text{-biofilm}}$. The OHO was distributed in the outer

biofilm layers, therefore their concentration was found to be decreased after the backwashes. Meanwhile, the AOO and NOO was located in the inner biofilm layers and less affected by the strong detachment. The concentrations of AOO and NOO were around 325 mgCOD/$L_{\text{-biofilm}}$ and 90 mgCOD/$L_{\text{-biofilm}}$, respectively. Due to the influent suspended solids, the major portion of the biofilm was inert solids. The biofilm thickness in the field reactor was estimated to be around 0.315 mm. The calculation was based on a maximum biofilm thickness of 0.5 mm, as further explained in section 6.4.2.2. Unfortunately, the OUR test was not conducted on the biofilm media in the full-scale reactor to experimentally check the appropriate biofilm thickness.

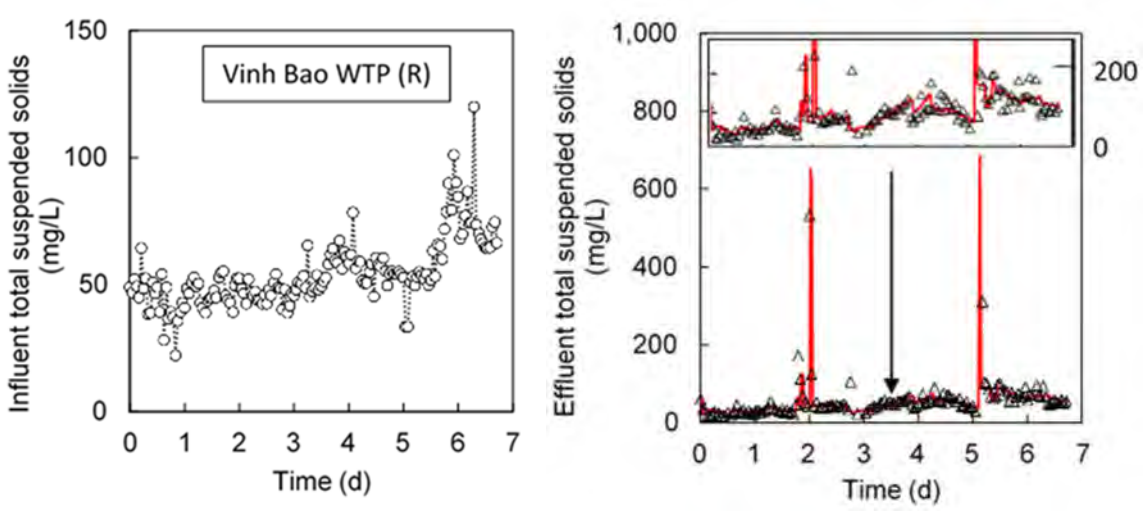

Figure 28. Measured and simulated influent and effluent total suspended solids for attachment and detachment

.....o..... Influent Δ Measured effluent ____ Simulated effluent

For the internal solid exchange, the $k_{inter\text{-}exchange}$ was found to be sensitive to the biofilm response when high concentrations of NH_x-N, organics and suspended solids were present in the influent, as in Vinh Bao WTP (R). The implication of $k_{inter\text{-}exchange}$ in Vinh Bao WTP (R) was related to the spatial competition among AOO/NOO/OHO while a large portion of the biofilm layers was already occupied by the inert solids. When a high value of $k_{inter\text{-}}$

$_{exchange}$ was applied, a uniform distribution of all biomass was created in the biofilm layers (0-D). In the case of the limiting substrates, the low-yield growers AOO/NOO could not compete with the high-yield grower OHO in the outer biofilm layers, leading to the lowered DO consumption of the system. In this study, the value of $k_{inter\text{-}exchange}$ of $2 \cdot 10^{-5}$ m/d was able to simulate the effluent concentrations.

In Hoa Phu WTP and Vinh Bao WTP (D), the influent water taken from the rivers that also contained the suspended solids. However, because these monitorings were mainly focused on the NH_x-N removal efficiencies, the TSS parameter was not measured. Therefore, the TSS was treated as no-react material in the dynamic simulation. Even the k_{attach} was a site-specific parameter in most of the case, when the average value of 0.43 m/d obtaining from the Vinh Bao WTP (R) was applied, together with the above-mentioned values of k_{detach} and $k_{inter\text{-}exchange}$, the effluent experimental plots in these datasets were also reproduced. A reactive biofilm thickness of around 0.004 mm was created in the two plants, similar to that of the lab-scale reactor.

5.3.3. Biological kinetic parameters of the biofilm in the nitrifying expanded-bed reactor

The calibration of the biological parameters was carried out on the five datasets of both synthetic and river waters. As shown in Table 11, a single set of kinetic and stoichiometric parameters of AOO, NOO, and OHO was elaborated, including the physical kinetics of attachment and detachment. Even a wide range of water qualities and water temperature, the set created comparable effluent concentrations to all the datasets, as shown from Figure S 1 to Figure S 8 in the ANNEX, in which the concentrations of influent and effluent for the five datasets were summarized together with each dynamic simulation.

Table 11. Kinetic and stoichiometric parameters and mass transport for oligotrophic biofilm

Characterization	Symbol	This study	Reference	Unit
Active Ammonia Oxidizing Biomass				
Active ammonia oxidizing biomass maximum specific growth rate	$\mu_{AOO,Max}$	0.40	0.46 – 2.2 [48], [59], [60]	d^{-1}
Ammonia (as substrate) half saturation coefficient	$K_{NHx,AOO}$	0.10	0.06 – 5.6 [48]	gN/m^3
Oxygen half-saturation coefficient for active ammonia-oxidizing biomass	$K_{O2,AOO}$	0.25	[92]	mgO_2/L
Active ammonia oxidizing biomass organism decay rate	b_{AOO}	0.08	0.03 – 0.15 [48], [60]	d^{-1}
Active Nitrite Oxidizing Biomass				
Active nitrite oxidizing biomass maximum specific growth rate	$\mu_{NOO,Max}$	0.65	0.28 – 3 [48], [60]	d^{-1}
Nitrite half saturation coefficient	$K_{NO2,NOO}$	0.10	0.05 – 3 [48]	gN/m^3
Oxygen half-saturation coefficient for active nitrite-oxidizing biomass	$K_{O2,NOO}$	0.40	[92]	mgO_2/L
Active nitrite oxidizing biomass organism decay rate	b_{NOO}	0.08	0.03 – 0.15 [48], [60]	d^{-1}
Active Heterotrophic Biomass				
Heterotrophic maximum specific growth rate	$\mu_{OHO,Max}$	3.00	1 – 6 [93]	d^{-1}
Readily biodegradable substrate half saturation coefficient	$K_{S_B,OHO}$	0.10	< 1 [93]	$gCOD/m^3$
Aerobic oxygen half-saturation coefficient for heterotrophs	$K_{O2,OHO}$	0.20	[92]	$gO2/m^3$

Characterization	Symbol	This study	Reference	Unit
Heterotrophic decay rate	b_{OHO}	0.50	[92]	d^{-1}
General Half-Saturation Coefficients				
Ammonia (as nutrient) half saturation coefficient	$K_{NHx,nutrient}$	0.005	[92]	gN/m^3
Nitrite (as nutrient) half saturation coefficient	$K_{NO2,nutrient}$	0.05	[92]	gN/m^3
Nitrate (as nutrient) half saturation coefficient	$K_{NO3,nutrient}$	0.05	[92]	gN/m^3
Hydrolysis				
Slowly biodegradable substrate maximum specific hydrolysis rate	$q_{XC_B\_Sb,hyd}$	3	[92]	d^{-1}
Slowly biodegradable substrate half saturation coefficient	$K_{XC_B,hyd}$	0.10	[92]	gCOD/gCOD
Ammonification Ammonification rate	q_{am}	0.08	[92]	m^3/gCOD/d
Temperature coefficient (θ)				
θ for $\mu_{AOO,Max}$, $\mu_{OHO,Max}$, q_{am}		1.072	[92]	
θ for $\mu_{NOO,Max}$		1.058	[92]	
θ for b_{AOO} , b_{NOO} , b_{OHO}		1.029	[92]	
θ for $K_{XC_B,hyd}$		1.116	[92]	
Stoichiometry				
Active ammonia oxidizing biomass yield	Y_{AOO}	0.21	0.03 – 0.33 [48], [59], [60]	gCOD/gN
Active nitrite oxidizing biomass yield	Y_{NOO}	0.09	0.02 – 0.09 [48], [59],	gCOD/gN

Characterization	Symbol	This study	Reference	Unit
			[60]	
Active Heterotrophic Biomass yield	Y_{OHO}	0.67	0.46 – 0.69 [48]	gCOD/gCOD
Heterotrophic endogenous fraction	$f_{XU\_Bio,lys}$	0.08	[92]	gCOD/gCOD
Nitrogen content of active biomass	i_{N_XBio}	0.086	[92]	gN/gCOD
Conversion factor for NO_2 in COD	i_{COD_NO2}	-3.43		gCOD/gN
Conversion factor for NO_3 in COD	i_{COD_NO3}	-4.57		gCOD/gN
Conversion factor for NH_x in charge	i_{Charge_SNHx}	0.071		Charge/gN
Conversion factor for NO_3 in charge	i_{Charge_SNOx}	-0.071		Charge/gN
Mass transport of biofilm				
Specific attachment rate	k_{attach}	0.43	average in this study	m/d
Specific detachment rate	k_{detach}	$1 \cdot 10^{-4}$		m/d
Specific exchange rate	$k_{inter-exchange}$	$2 \cdot 10^{-5}$		m/d
Maximum biofilm thickness	$\delta_{B,max}$			
Lab-scale reactor (start-up, continuous operation)		0.3		mm
Pilot-scale reactor of Hoa Phu WTP		0.3		mm
Full-scale reactor of Vinh Bao WTP (Dry, rainy season)		0.5		mm

Each attached microorganism in AOO/NOO/OHO groups was modelled as a single state variable or species having fixed kinetics and stoichiometry. This approximation might be supported in the literature [94], in which a single genus of *Pseudomonas* was found to be dominant in the oligotrophic biofilm for the degradation of different carbonaceous substrates. As the kinetic and stoichiometric parameters obtained in this study were supposed to be globally applicable, this set was expected to be as default in designing water treatment with low-strength NH_x-N and organic substrates.

During the simulations, K_S was found to be more sensitive than the maximum specific growth rate (μ_{max}). In the oligotrophic conditions where the substrate concentrations were limited, the K_S was a crucial factor for microbial substrate utilization [58]. The K_S of AOO and NOO for N-substrate were calibrated to be both 0.1 mgN/L, whilst their μ_{max} were estimated to be 0.40 and 0.65 d^{-1} respectively, which were at the lower ranges that found in wastewater treatment systems [48]. Dissolved oxygen was also the rate-limiting factor and highly affected the response of the nitrification process. Previous studies presented that the activity of NOO was considerably lowered at low DO concentration compared to the one of AOO [59]. Based on this, the half-saturation coefficients of oxygen (K_{O2}) for NOO and AOO were calibrated to be 0.4 and 0.25 mgO_2/L respectively. Because of the inferiority of NOO to AOO in the competition for oxygen and substrates, the specific decay rate (b) became also influential in determining their appropriate concentrations in the biofilm. In the simulation, this kinetic parameter was assumed to be 0.08 d^{-1} for both NOO and AOO.

With respect to the OHO, the K_S was calibrated to be 0.1 mgCOD/L, whereas its μ_{max} was found to be 3.0 d^{-1} which was considerably lower than the ordinary OHO in wastewater treatment systems [48], [58]. Furthermore, the K_{O2} for OHO was known to be relatively low, leading to their competitive growth to AOO and NOO in presence of organic substrate [59]. In this study, the K_{O2} for OHO was estimated to be 0.2 mgO_2/L, which was comparable to those in wastewater treatment systems.

5.3.3.1. Measured versus predicted data over all the datasets

When the set of kinetic and stoichiometric parameters listed in Table 11 was applied to the dynamic simulation of five datasets, the predicted data were in a good agreement with the measured data, as shown in Figure 29. The effluent DO ranged from 0 to 8 mgO_2/L was reasonably simulated in the model with a coefficient of determination (R^2) of 0.86 with 937 data plots in all the five datasets. NH_4-N was also predicted at a high R^2 of 0.97 with 937 of data plots. A moderate prediction was obtained for NO_2-N with a R^2 of 0.55 with 323 data plots, which might be due to the challenges in producing intermediate product in the model. The predicted NO_3-N was highly scattering with a low R^2 of 0.154 at the similar data plots as those of NO_2-N. This might be attributed by the poor calibration curve of the test papers for NO_3-N in the field study, in addition to the low precision of NO_3-N measurement in the lab analysis. Nevertheless, because the production of NO_3-N directly engaged in the removal of NH_4-N that was well simulated, the model output for NO_3-N was thought to be reasonable. For the TSS, an acceptable R^2 of 0.73 was obtained over the 147 data plots.

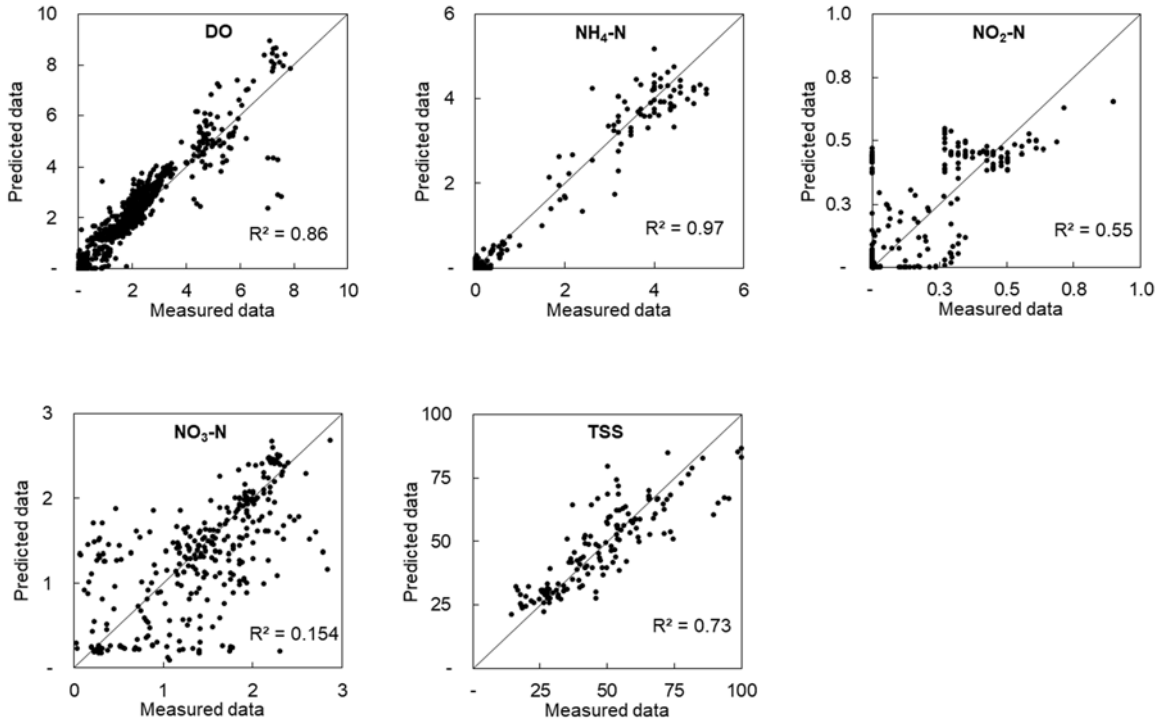

Figure 29. Measured versus simulated outputs in the five datasets

5.3.3.2. Nitrifying biofilm formation in the start-up period

In the lab-scale reactor, during the start-up period of 90 days with ranging temperature between 11 and 20ºC, high influent DO concentration from 8 to 10 mgO_2/L and influent NH_x-N concentration of around 1 mgN/L, the AOO and NOO were found to be gradually developed on the media. As shown in Figure 26, during the first 20 days of operation, NH_x-N concentration in the effluent was consistently reduced whilst NO_2-N was accumulated in the system due to the imbalance growth rate of AOO and NOO in the biofilm. At the starting time, a small amount of NH_x-N was converted into NO_3-N indicating that a small amount of active AOO and NOO were already present in the media taken from the WTP. In the dynamic simulation, the initial biomass concentrations in the biofilm layers of AOO and NOO were determined to reproduce the initial effluent concentration. After day 20, NH_x-N was totally converted into NO_3-N. The high removal efficiency of 96% was obtained during the remaining period of 70 days. The biomass concentrations of AOO and NOO in

the biofilm layers at the end of the start-up period were used for the dynamic simulation in the next analysis of the continuous operation.

5.3.3.3. Nitrite accumulation due to low dissolved oxygen

Once the activities of AOO and NOO were stably developed on the media in the lab-scale reactor, in the next 90 days, the NH_x-N loading was intentionally varied from 1 to 2 mgN/L and from 2 to 1 mgN/L in a stepwise manner, as shown in the top of figures of Figure 30. Because of temperature change of the influent for the long-term operation, the DO in the influent was around 6 mgO_2/L in the first 15 days and gradually increased from 7 to 9 mgO_2/L in the next 75 days. When the influent NH_x-N was maintained at around 1 – 1.5 mgN/L, NH_x-N was entirely converted into NO_3-N. During this period, the NH_x-N removal was obtained at around 95%. However, when the NH_x-N reached 2 mgN/L, which required a stoichiometric DO of about 9 mgO_2/L, the limited DO of below 0.1 mgO_2/L in the effluent resulted in the NO_2-N accumulation in the system. Even at the high loading rate of NH_x-N, the reactor was proved to remove NH_x-N with the utilization rate of 4,118 $gN/m^3/d$. Due to NOO's higher K_{O2} than that of AOO, NOO could not outcompete with AOO. The dynamic simulation could fairly reproduce the NO_2-N accumulation. A slight gap between experimental data of the effluent (around 0.25 mgN/L) and simulated data (around 0.13 mgN/L) was observed. To match the experimental data, the NOO biomass in the biofilm should be slightly reduced. For instance, the specific decay rate of NOO was especially needed to adjust to 0.12 d^{-1} from the global calibration of 0.08 d^{-1} (data not shown). However, since the mismatch of the effluent nitrite concentration was only 0.12 mgN/L, it was decided that the global parameter was applied to the simulation without modification.

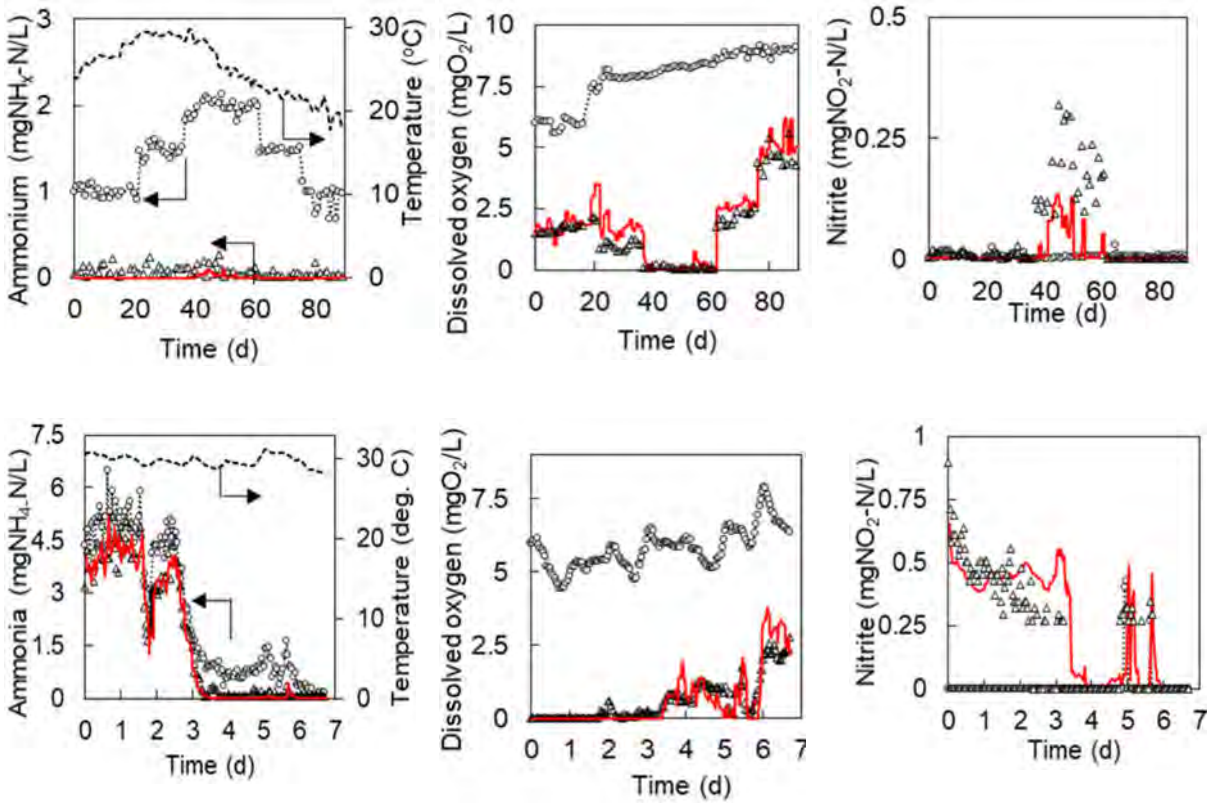

Figure 30. Ammonium removal and nitrite accumulation due to low dissolved oxygen (Top: Lab-scale reactor in continuous operation, Bottom: Full-scale reactor in Vinh Bao (R))

5.3.3.4. Overall biofilm responses in the field reactors

In the pilot- and full-scale reactors, the initial biomass concentrations in the reactor were estimated under each steady-state simulation to reproduce the effluent concentrations at the starting time.

For the dataset of Vinh Bao WTP (R), during the first 3 days, the surface water quality was seen to be poor and turbid, in which the influent DO, NH_x-N and COD were detected to be around 5.3 mgO_2/L, 4.4 mgN/L and 18.4 mgCOD/L respectively, as shown in bottom figures of Figure 30 and top figures of Figure 31. Because of this low DO, only around 1

mg NH_x-N/L could be stoichiometrically removed from the influent, and NO_2-N accumulation was also recognized. After day 4 when the surface water quality was improved, the influent NH_x-N was significantly decreased to around 0.75 mgN/L. During this measurement, it appeared that around 5 mgO_2/L of DO was still consumed, indicating the presence of the organic substrate in the influent. Again, when the effluent DO decrease to almost zero between days 5 and 6, the accumulation of NO_2-N was observed. As the biodegradable organic substance concentration was not experimentally measured, the organic substrate in the first 3 days was speculated to be varied from 1 to 5 mgCOD/L in the dynamic simulation. High organic substrate input to the reactor showed a comparable effect on reducing the effluent DO, which built an unrealistically high biomass concentration of OHO in the system. Under such simulation, the activity of NOO in the following days was suppressed, resulting in the overestimated concentration of effluent NO_2-N. From day 4, the organic substrate was speculated to be varied from 0.1 to 9 mgCOD/L to match the effluent DO.

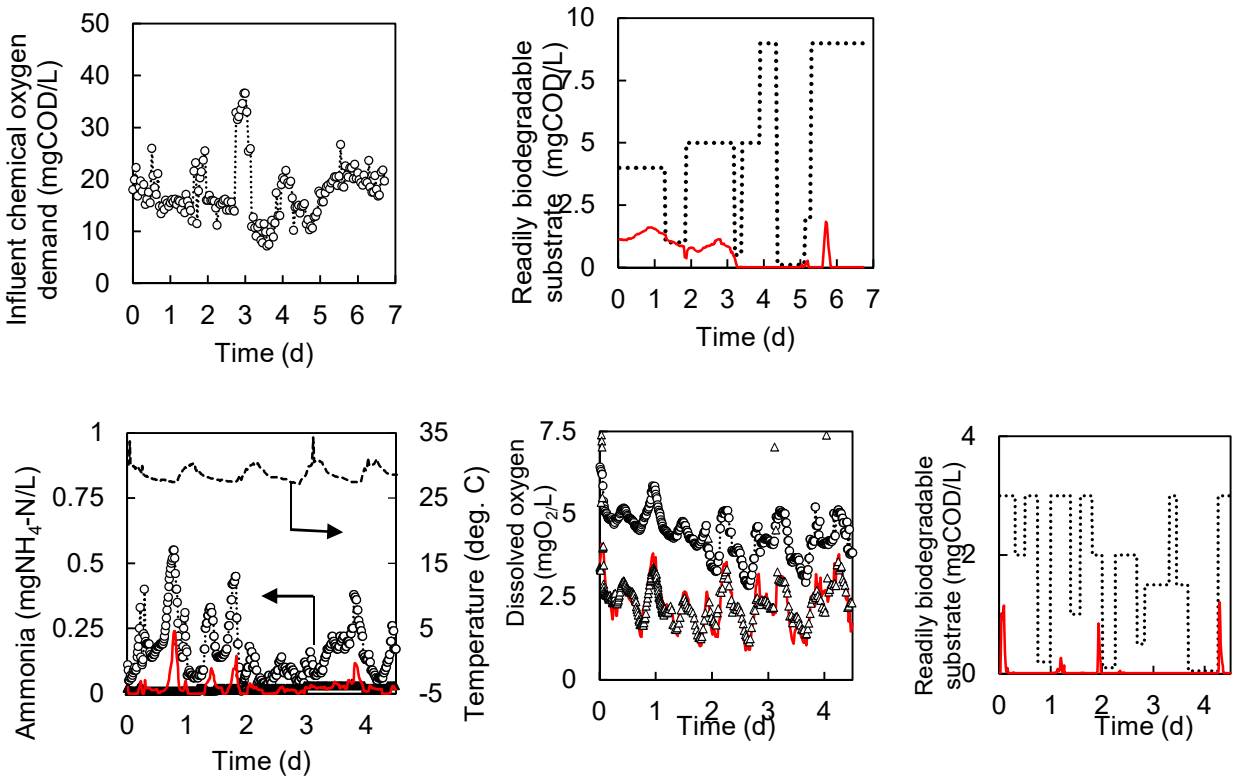

Figure 31. Estimation of the influent readily biodegradable substrate from dissolved oxygen consumption (Top: Full-scale reactor in Vinh Bao (R); Bottom: Pilot-scale reactor in Hoa Phu WTP)

The datasets in Hoa Phu WTP and in Vinh Bao WTP (D) were comparable to those in the lab-scale reactor, in which the influent NH_x-N was relatively low and almost completely removed from the effluent. Even the organic substrate was not measured, its presence in the influent could be estimated from the DO consumption in the system as described above. However, the growth of OHO required not only the organic substrate but also nitrogen as the nutrient. Because of limited NH_x-N in the influent, it was obligated to assume the presence of soluble biodegradable organic nitrogen to provide the required additional NH_x-

N source through the ammonification. In this way, in Hoa Phu WTP, the organic substrate was calculated to be varied from 0.05 to 3 mgCOD/L, as shown in Figure 31.

5.3.3.5. The biomass fraction in the steady-state operation

The short period of the intensive monitoring could only provide the snapshots of biofilm response in the dynamic operations. To catch the biofilm performance in the long-term operation, steady-state simulations were carried out using averaged influent concentrations listed in Table 12. As shown in Figure 32, it appeared that biomass fraction of each reactor was distinct and dependent on influent characteristics (e.g. high and low influent DO, NH_x-N, organic substrate, suspended solids).

Table 12. Influent concentrations for steady-state simulations

No	Dataset	Temp. (^oC)	DO (mgO_2/L)	NH_x-N (mgN/L)	Organic substrate (mgCOD/L)	TSS (mg/L)
1	Lab-scale start up	14.7	8.9	0.87	0	0
2	Pilot-scale Hoa Phu WTP	28.9	4.6	0.2	2	0
3	Full-scale Vinh Bao WTP (D)	20.6	7.2	0.1	6.8	0
4	Full-scale Vinh Bao WTP (R)	30.0	5.3	4.4	7.1	35.7

In the lab-scale reactor, because of no organic substrate in the influent, the OHO biomass was very limited in the biofilm. When the influent NH_x-N and DO were fixed to be 0.87 and 8.9 mg/L respectively, the NH_x-N was totally removed without accumulation of NO_2-N in the effluent. The active biomass of AOO and NOO were found to be 23.3 and 9.6% respectively in the biofilm. The slowly biodegradable substrate (XC_B) which was produced from endogenous decay of AOO and NOO was the major component in the biofilm, occupied more than 60% of the total biomass. Although XC_B was supposed to be degraded by OHO and became a source of its cryptic growth, due to competition of DO between

OHO and nitrifiers, OHO seemed not to grow much in the system.

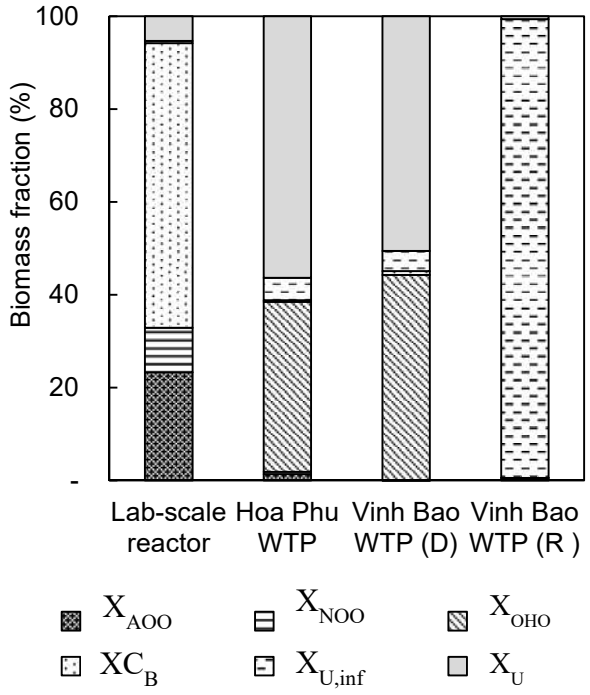

Figure 32. Biomass fraction in steady-state operation

For Hoa Phu WTP and Vinh Bao WTP (D), the biomass fractions were found to be comparable. The influent organic substrate was present at the concentration of 2 mgCOD/L and 6.8 mgCOD/L respectively, whilst NH_x-N was very low. Due to enough influent DO, both of organic substrate and NH_x-N were almost removed in the effluent. The OHO was found to be dominant over the AOO and NOO. The OHO biomass fractions were calculated to be 36.6 and 44.3% in both plants respectively, whilst the growth of AOO and NOO were very limited. The unbiodegradable particulates from the decay of OHO (X_U) occupied the largest portion in the biofilm with more than 50%.

A totally different biofilm was created in Vinh Bao WTP (R). The moderate influent DO of 5.3 mgO_2/L was insufficient to oxidize the high influent concentrations of NH_x-N and organic substrate which were fixed at 4.4 mgN/L and 7.1 mgCOD/L respectively. As a result, the removal efficiencies of NH_x-N and organic substrates were only 72.7% and

32.7% respectively. Further, due to the influent inert inorganic suspended solids concentration of 35.7 mg/L, more than 98 % of the biofilm was occupied by the inert inorganic suspended solids ($X_{U,inf}$). Consequently, the active biomass of AOO, NOO and OHO accounted for only 0.6% of the total biomass. It suggested that the occupation of influent suspended solids in the biofilm could limit the growth of active biomass. The frequent backwash was therefore required to repair filter-bed performance. Additionally, the particulates, such as sand and silt, should be carefully removed before the influent entering the biofilter to improve the treatment efficiency of the reactor.

5.3.4. Graphical guidance on the reactor performance at variable influent and temperature

Based on the set of global kinetic and stoichiometric parameters obtained in this study, graphical guidance was developed to estimate the reactor performance under different influent concentrations and water temperature, which aimed at providing simple and quick tools for the designers and practitioners of nitrifying expanded-bed reactors.

As shown in Figure 33, the influence of water temperature to the biological NH_x-N removal was examined, according to the steady-state simulations under the temperature ranged from 10 to 35ºC, varied influent NH_x-N from 2 to 10 mgN/L with fixed influent DO at 8 mgO_2/L and organic substrate at 0 and 5 mgCOD/L. Without the presence of organic substrate, when the influent NH_x-N was fixed at 2 mgN/L, the NH_x-N removal was almost constant at 1.9 mgN/L within the temperature range. However, a slightly higher nitrification rate was observed along with the temperature increase when the influent NH_x-N was from 3 to 10 mgN/L. When the temperature beyond 30 – 35 ºC, the highest and lowest values of NH_x-N influent created the NH_x-N decrement of 2.1 and 1.9 mgN/L respectively. When the organic substrate was fixed at 5 mgCOD/L, the NH_x-N removal was dropped to a constant value of 1.5 mgN/L over the temperature range. The highest removal of NH_x-N was found to be 1.68 mgN/L when both influent NH_x-N and temperature were at the maximum values.

Overall, the insignificant improvement on nitrification rate suggested that the process was not considerably influenced by the hydraulic retention time and the specific surface area of the media in the experimental condition, in case the influent DO concentration was almost saturated in air

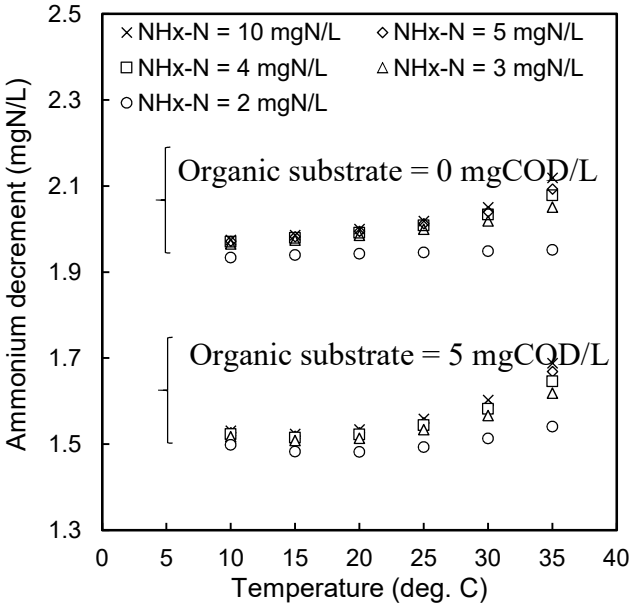

Figure 33. Impact of temperature on ammonium removal (Influent DO = 8 mgO_2/L and influent organic substrate = 0 and 5 mgCOD/L).

Considering the simulation result, the permissive influent DO to totally remove NH_x-N and organic substrate, and suppression of NO_2-N accumulation was estimated, where the water temperature was fixed at 20ºC and 35ºC respectively, and the influent NH_x-N was ranged 0 to 3 mgN/L whilst the influent organic substrate was ranged from 0 to 5 mgCOD/L. As shown in Figure 34, at the temperature of 20ºC and influent DO of 8 mgO_2/L, it appeared that the range of NHx-N at which the reactor could entirely remove was from 1.20 to 1.92 mgN/L when the influent organic substrate was ranged between 0 to 5 mgCOD/L. The similar applicable range for NHx-N was used in the empirical equation at the temperature of 35ºC, which could be found in a graphical manner in Figure 35**.**

Based on the analysis, an empirical equation to estimate permissive DO from the influent

NH_x-N and organic substrate was made as shown in Eq (23).

Required DO (mgO_2/L) = a x *influent NH_x-N (mgN/L) + b* x *influent organic substrate (mgCOD/L)*

Eq (23)

Where a = 4.16 gO_2/gN; b = 0.60 $gO_2/gCOD$ at the temperature 20°C;

a = 4.17 gO_2/gN; b = 0.82 $gO_2/gCOD$ at the temperature 35°C.

In the empirical equation, the lines were not perfectly matched to the data plots, resulting in the overestimations of required DO in some operating conditions. Nevertheless, the overestimations were mostly less than 10%, which can be treated as a safety margin in the designing procedure. The empirical equation was applicable at NHx-N higher than 0.25 mgN/L without the presence of organic substrate, at NH_x-N higher than 0.5 mgN/L whilst organic substrate was from 1 to 2 mgCOD/L and at NH_x-N higher than 1.0 mgN/L whilst organic substrate was from 3 to 5 mgCOD/L.

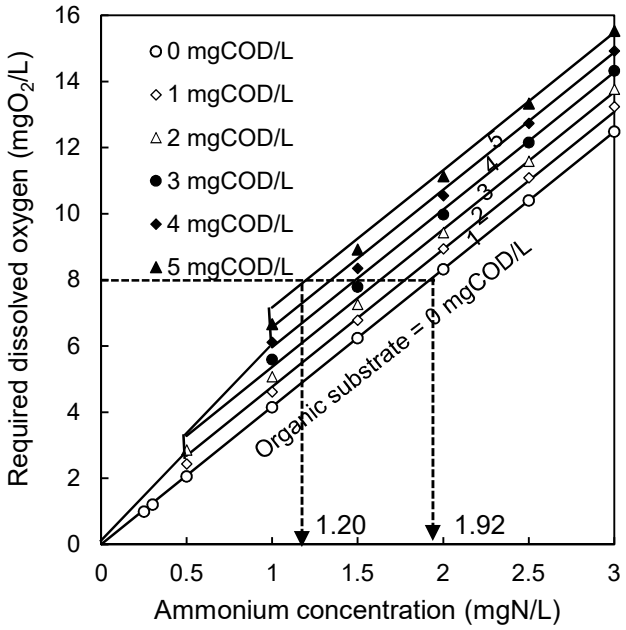

Figure 34. Dissolved oxygen requirement for variable influent ammonium and organic substrate at temperature 20^0C (line: empirical required dissolved oxygen, markers = simulated required dissolved oxygen).

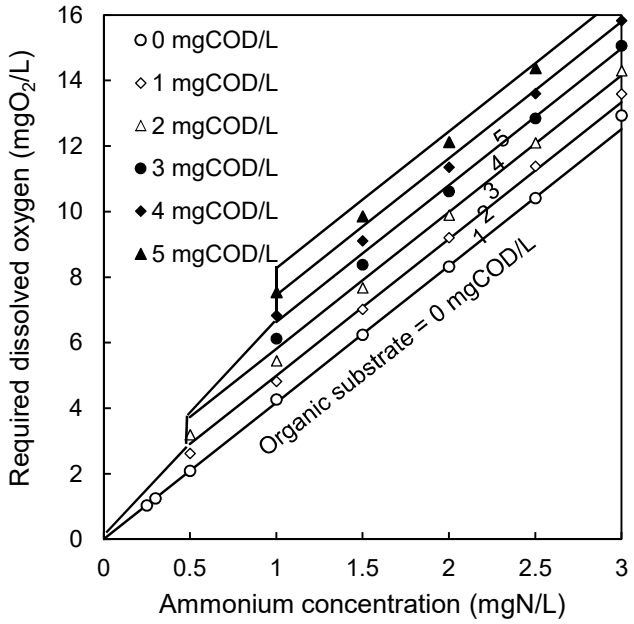

Figure 35. Dissolved oxygen requirement for variable influent ammonium and organic substrate at temperature 35^0C (line: empirical required dissolved oxygen, markers = simulated required dissolved oxygen).

Based on the above guidance, the required influent DO could be estimated if field information for NH_x-N and organic substrate was obtained. In case that the influent DO was not enough to meet the biological oxygenation of the influent materials, the configuration of the expanded-bed reactor might be needed to modify into a multi-series reactor where aeration was conducted at the effluent of the reactor to maintain DO for the subsequent reactor.

5.4. CONCLUSIONS

A combined biofilm and biological model of biological NH_x-N removal for the nitrifying expanded-bed reactor was developed. The findings obtained from the study were:

1. The detachment of the biofilm was estimated in the experiment with limited suspended solids, while the attachment was estimated based on the capture of suspended solids of the field reactor. The detachment rate was found to be $1 \cdot 10^{-4}$ m/d at the normal operation of filtration and $2.5 \cdot 10^{-3}$ m/d at the backwash events. The attachment rate was varied from 0.15 to 0.85 m/d depending on the influent suspended solids. The internal solid exchange rate of particulate among the biofilm layers was estimated to be $2 \cdot 10^{-5}$ m/d.
2. A single set of kinetic and stoichiometric parameters for AOO/NOO/OHO was elaborated to reproduce the five distinct datasets obtained from synthetic and rivers influent water, respectively. Due to the oligotrophic environment in the drinking water sources, most of the calibrated parameters were found at the lower range of those collected from wastewater treatment systems. The set could be used as default in the designing of nitrifying expanded-bed reactor in the treatment of low-strength NH_x-N and organics.
3. A graphical guidance was provided with an empirical equation to estimate the required dissolved oxygen to totally remove influent NH_x-N (from 0 – 3 mgN/L) and organic substrate (from 0 – 5 mgCOD/L) at the temperature of 20ºC and 35ºC, respectively. The impact of temperature from 10 to 35ºC to the nitrification rate was also examined.

CHAPTER 6. SENSITIVITY ANALYSIS OF NUMERICAL CALCULATION AND OPERATIONAL PARAMETERS ON THE CALCULATION RESULTS

6.1. INTRODUCTION AND OBJECTIVES

In this study, the Integrated Fixed-Film Activated Sludge (IFAS) object was used to model the nitrifying expanded-bed reactor. Although there was a section dedicated to IFAS object in Hydromantis' Technical Reference, it could not cover all its operational aspects. As shown in 4.4.2., novelty functions of internal recycle flow, and media's concentration factor were added in which needed to be explained. In this regards, a list of optimized parameters to reach the reasonable calculation results could be helpful.

The simulation with the IFAS object appeared to be one of the most complicated works on GPS-X due to the combination of biofilm and biological model and the high number of tanks-in-series in the physical model. Additionally, not all the terminologies in the models were well defined and explained in the technical documents. Therefore, a thoughtful understanding of the physical, biofilm and biological inputs was a prerequisite for building a proper model layout. During the simulations, the calculation outputs from GPS-X should be checked and evaluated to ensure the same expectations between the users and programmers. In this section, the tips to avoid unexpected calculation results or lessons learned were summarized based on the personal experience in dealing with the issues from GPS-X.

The model calibration was carried out based on the datasets obtained from the experimental model. A complete set of influent and effluent compositions was desirable; however, multiple analytical and experimental tasks were required which were both expensive, labor-intensive and time-consuming. In this section, a list of key parameters to be monitored in the experimental model was proposed. Such a list was sufficient to provide adequate answers to the model input. The remaining parameters could be hypothetically estimated based on the collected data.

The objectives of this section were:

1. To provide a list of key parameters to be monitored in the experimental model,

2. To provide a list of optimized parameters to reach a reasonable calculation results,

3. To carry out the sensitivity analysis of numerical calculations on the calculation results.

The model layout developed in this study with application of the IFAS object was shown in Figure 36 as follows:

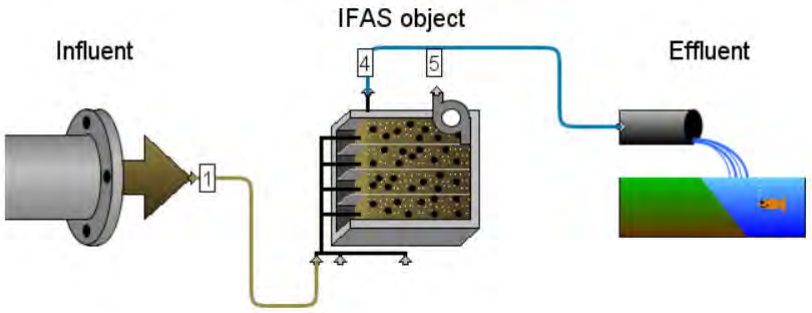

Figure 36. The model layout of an IFAS object on GPS-X software

6.2. CHARACTERIZATION OF THE INFLUENT COMPOSITION

Due to the configuration complexity, the IFAS object was simulated in the simplest Carbon – Nitrogen Library (CNLIB) of GPS-X software, which consists of sixteen state variables, as shown in Figure 37. The influent composition of IFAS object was divided into four main components, which were the inorganic suspended solids, organic matters, dissolved oxygen and nitrogenous matters. These state variables are the fundamental components that are acted upon by the processes described in the model, as shown in Table 5 and Table 6.

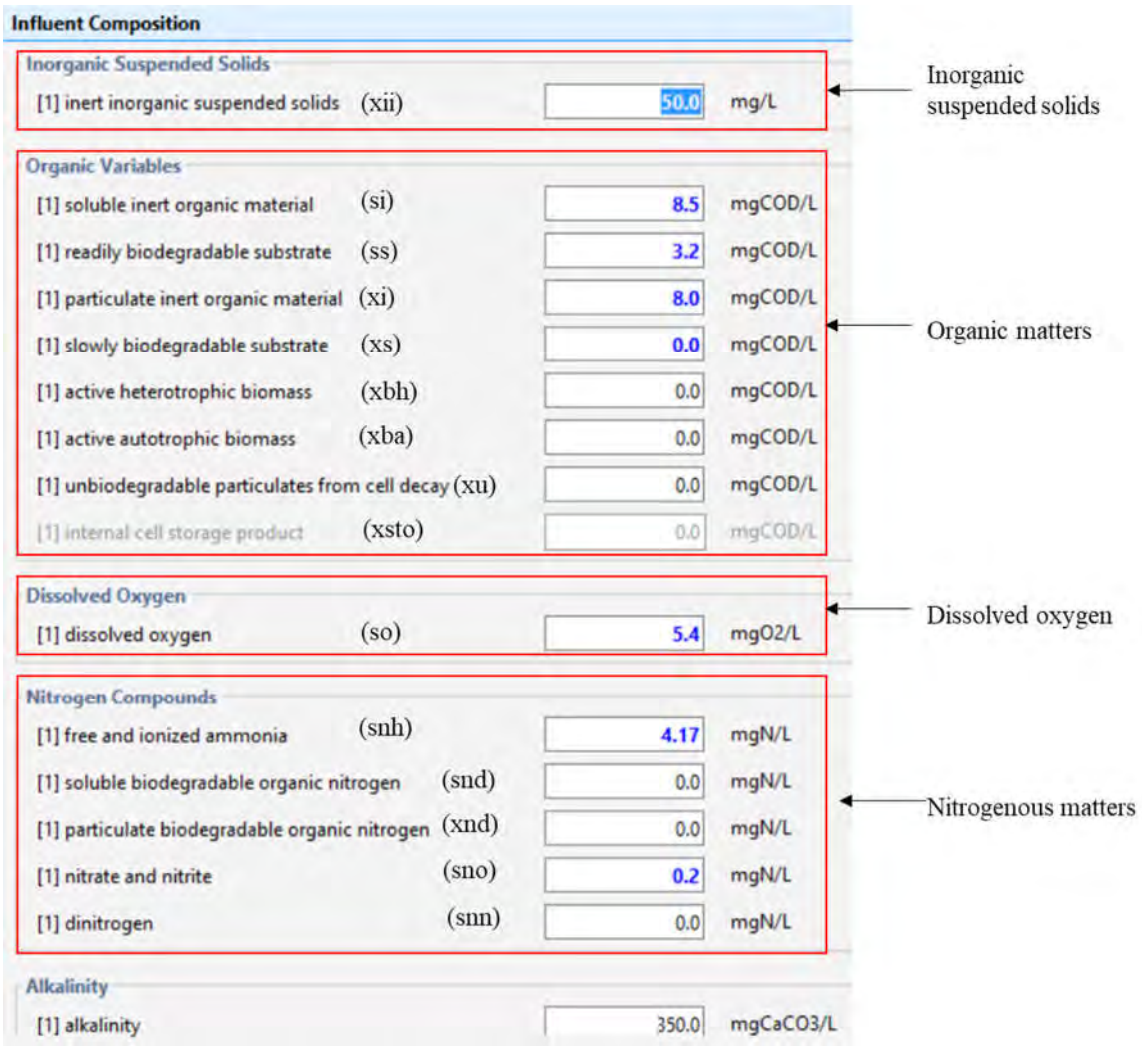

Figure 37. Influent composition input and their cryptic names for IFAS object in CNLIB library

However, it should be noted that the state variables were not always easily measurable or interpretable in the field conditions. Therefore, they could be obtained indirectly from the composite variables, such as TSS, VSS, COD, BOD, and Total Kjeldahl Nitrogen (TKN), by adding some conversion factors. The relationship between the state and composite variables in CNLIB was presented as below [95].

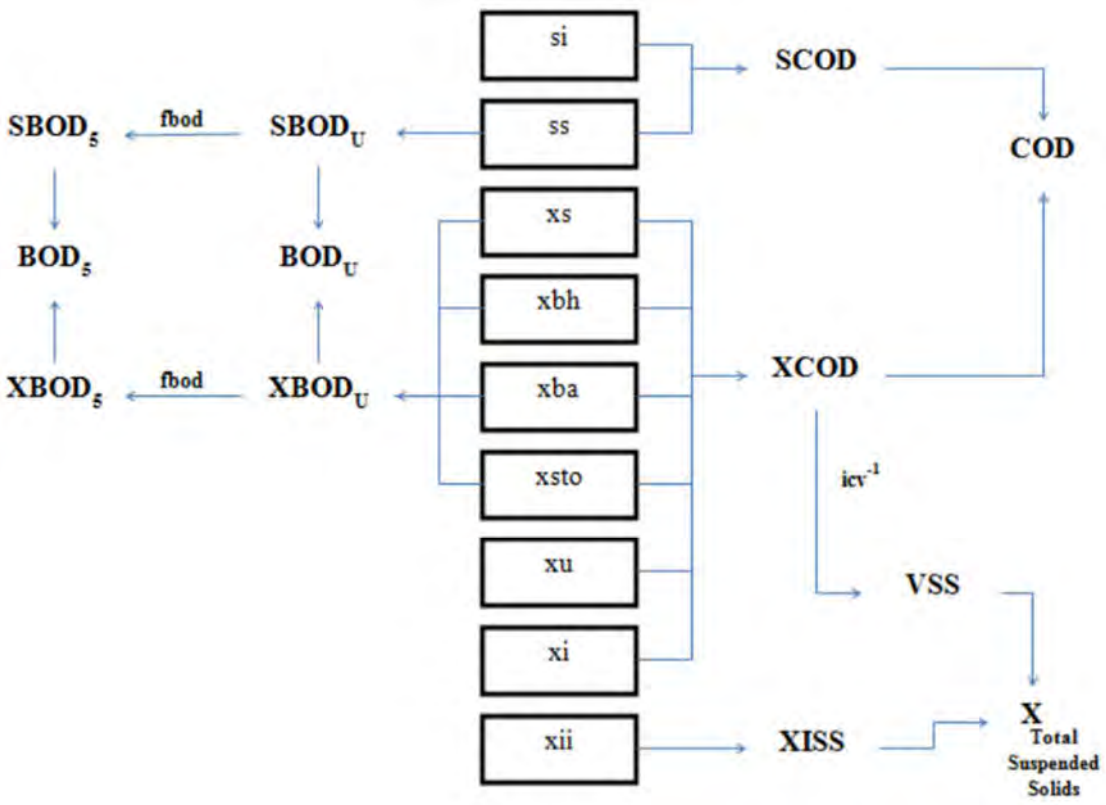

Figure 38. Relationship between composite and state variables in CNLIB [95]

In this study, the simulations of IFAS object were carried out based on five different datasets, as indicated in Table 10. Based on the knowledge of the influent sources, as well as the specific monitoring purposes, the datasets were differentiated from the simplest ones in Hoa Phu WTP and Vinh Bao (D) WTP, which included the temperature, DO and NH_x-N, to a more complete set in Vinh Bao (R) WTP, which covered the above-mentioned parameters as well as NO_2-N, NO_3-N, TSS, VSS, and total COD.

Based on the experience acquired in the simulation process, some lessons learned on the necessary monitored parameters were presented as below:

- Temperature, DO, and NH_x-N are the primary parameters that allowed to estimate the ammonium removal efficiency of the IFAS object in one-stage nitrification,
- As experienced in Hoa Phu WTP and Vinh Bao (D) WTP, the low NH_x-N in the water influent might not be sufficient for the biomass activities when compared to the DO consumption. In this case, the supplementary source of NH_x-N might be derived from the organic nitrogen present in water influent through the ammonification process. Therefore, the knowledge of the organic nitrogen concentration, which could be obtained indirectly from the TKN measurement, could be beneficial,
- As related to organic matters, soluble COD was preferable to the total COD. The soluble COD was engaged directly to the readily biodegradable substrate, which supported the growth of the heterotrophs as indicated in r1, r2, and r3 of Table 5. The difference between total and soluble COD allowed estimating the particulate organic components, which could also be double-checked with the VSS parameter. The measurement of both soluble and total COD would reduce the assumptions; therefore, more realistic simulation results could be provided. Further, it was necessary to note that the presence of heterotrophs and autotrophs biomass in the water influent should be neglected because they could not corporate into the existing biomass of the reactor due to the competition and differences in species.
- The measurement of TSS and VSS allowed simulating the particulate components in the biofilm. The difference between TSS and VSS was defined as the inert inorganic suspended solids (xii) variable in the input menu. When the TSS and VSS data were available, the kinetic parameters related to the biofilm mass transport, such as attachment, detachment and internal solid exchange rates, become sensitive

parameters in the simulation because they were related to the spatial competition among the different biomass,

- As shown in Figure 38, the ratio of XCOD and VSS was denoted as “icv factor”. The “icv factor” should be calibrated to match the measured VSS and XCOD. For example, the value of “icv factor” was calibrated to be 1.0 from its default value of 1.8.

The list of the monitored parameters depending on the simulation purposes was summarized as below:

Table 13. List of monitored parameters and objectives of modeling

Objectives of modeling	Temp. (°C)	DO (mgO_2/L)	NH_x-N (mgN/L)	NO_2-N (mgN/L)	NO_3-N (mgN/L)	TKN (mgN/L)	TSS (mg/L)	VSS (mg/L)	Soluble COD (mg/L)	Total COD (mg/L)
Ammonium removal in one-step nitrification	○	○	○							
Ammonium removal in one-step nitrification with possible organic nitrogen uptake	○	○	○			○				
Ammonium removal in two-step nitrification	○	○	○	○	○					
Ammonium removal in two-step nitrification and organics removal	○	○	○	○	○				○	○
Ammonium removal in two-step nitrification and organics removal, with biofilm attachment and detachment	○	○	○	○	○	○	○	○	○	○

6.3. OPTIMIZED PARAMETERS FOR REASONABLE CALCULATION RESULTS

The Input Parameters for IFAS objects composed of the following items:

- Physical
- Operational
- Mass Transport
- Composite variable Stoichiometry
- Model Stoichiometry
- Kinetic
- High concentration inhibition
- Consistency
- Operating cost

Among these items, the Physical, Operational, Mass Transport, and Kinetic were required to be customized according to the studied reactor. The following paragraphs will focus on the parameters to be optimized in the simulation process.

6.3.1. Physical menu

This menu subjected to the physical properties of the reactor, as well as the media characteristics. The appropriate data for physical menu was critical to the simulation results, because it defined the surface area based on which the biofilm layers and biomass were attached.

Item	Definition/Discussion	How to obtain data
Dimension		
Tanks in series	The number (N) of tanks-in-series	Conduct the tracer test
Volume		
Tank depth	Tank depth with media in working condition	Measure the bed-height in working condition
Maximum volume	Tank volume in working condition	Calculate the tank volume in working condition
Media initial volume		
Reator portion filled by media	The volume of media in the reactor in empty-bed condition	Calculate the volume of media in the reactor in empty-bed condition
Biofilm related parameters		
Specific surface of media	The specific surface area of the media	From media manufacturer, measurement, etc.
Water displaced by media	Media fraction in packed-bed condition	Measurement
Specific density of media		From media manufacturer, measurement, etc.
Attached liquid film thickness		Literature [45]
Maximum biofilm thickness	A user input which is related to the detachment and biomass concentration in the first biofilm layer.	• From literature [45] • By estimating from the VSS of attached biomass in the reactor, the media surface area, and biofilm density, then adding a safety margin of 10 to 20%
Speed		
Soluble integration period	How long the soluble state variables are integrated.	In short-term monitoring, such as in batch experiments, the soluble integration period should be equaled to

Item	Definition/Discussion	How to obtain data
Soluble integration length	How long the soluble state variables are integrated.	the soluble integration length and be the same as the data recorded interval for the accuracy of the output results.

It was suggested that the practitioners should check the simulation results of IFAS object in the output menu to avoid any misleading input data. The concerned parameters and their calculation formula in each cell tank were presented as below:

Table 14. Some physical properties of the reactors and their calculation formula

Parameter	Unit	Formula
Media Surface Area	m^2	(V_{total}/N_{tank}) x (Reactor media fill) x (Specific surface area)
Reactor media fill	%	$(V_{media\_packed}/V_{reactor})$
Media displaced volume	m^3	(V_{total}/N_{tank}) x (Reactor media fill) x (water displaced by media)
Liquid volume	m^3	(V_{total}/N_{tank}) – (Media displaced volume)

Additionally, some notifications should be mentioned on the soluble integration length and period. As explained in the Technical Reference [95], these parameters were designed to adjust the frequency of the integration for soluble components in diffusing into the biofilm, as shown from Eq (12) to Eq (16), without loss of accuracy. The illustration of soluble integration length and period was presented as below:

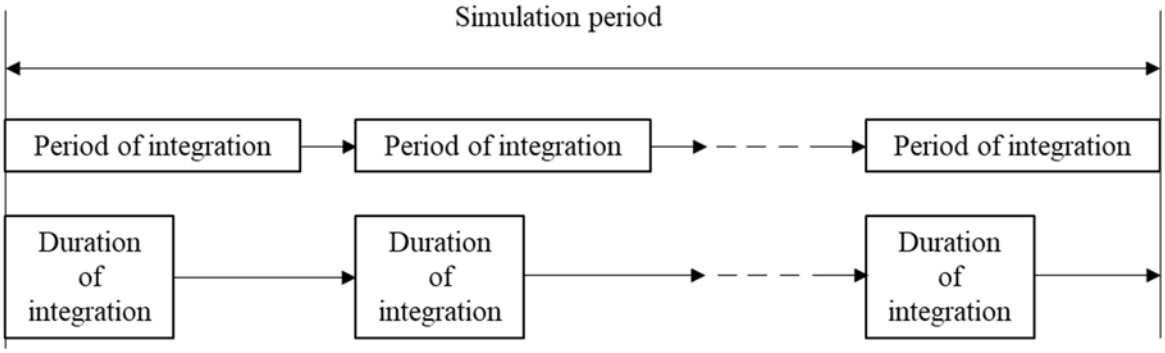

Figure 39. Illustration of soluble integration length and period over the simulation period

When the duration of integration was shorter or equaled to the period of integration, the continuous integration was conducted, resulting in a more accurate simulation results. However, the speed of the calculation would be relatively low. The continuous integration is suitable for short-term simulation when the data logging is more frequently (in seconds, minutes, etc.).

When the duration of integration was shorter than the period of integration, the soluble components in Eq (12) to Eq (16) would be integrated during the duration of integration, and the derivations were kept at constant in the remaining period of the integration. The discrete integration is suitable for long-term simulation when the data logging is less frequently (in hour, day, etc.).

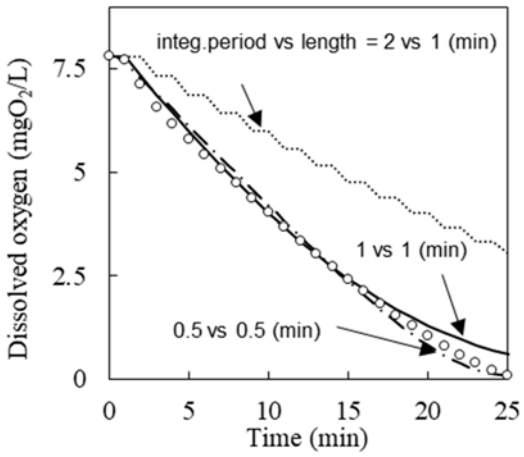

Figure 40. Influence of soluble integration length and period parameters to simulation results

For illustration, different paired values of the duration and period of integration were applied for the OUR test at 20°C explained previously in section 5.3.1. As shown in Figure 40, the data was logged every 1 minute in the total period of 26 minutes of the experiment. When both the paired values were fixed at 0.5 or 1 minute, the simulation results fairly reproduced the experimental data for DO. However, when the period of integration was increased to 2 minutes and the duration of integration was kept at 1 minute, a high discrepancy was observed between simulation and measured data.

6.3.2. Operational Menu

This section will mainly focus on the Internal Flow Distribution sub-menu, which was related to the Internal Recycle Flow, and was not defined in existing technical support documents. The labels of IFAS object and different sub-menu in Internal Flow Distribution were presented as follows:

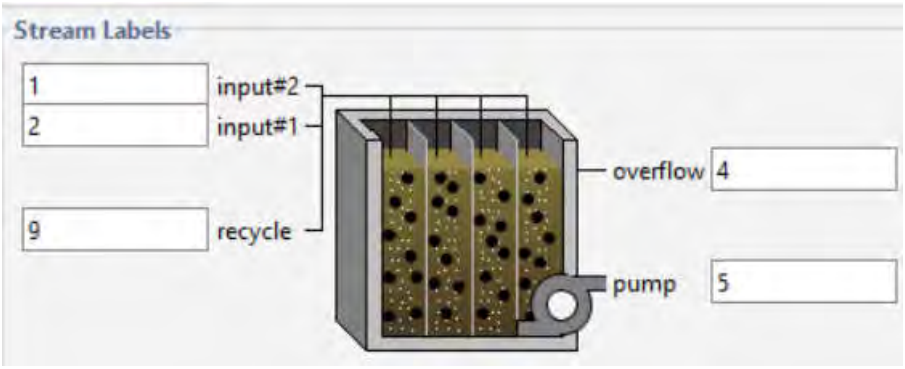

Figure 41. The labels of IFAS object

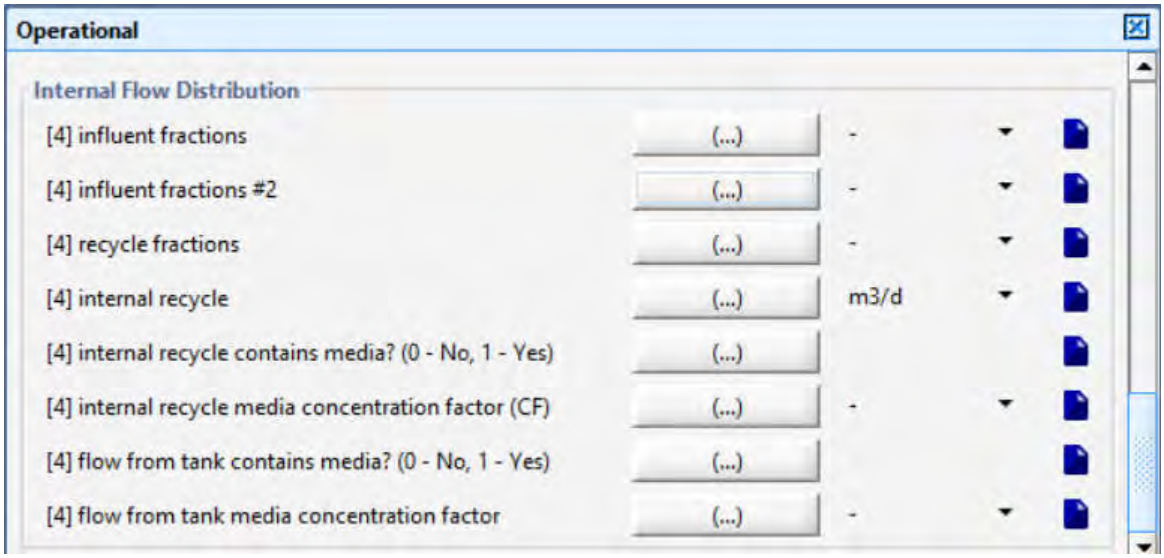

Figure 42. Internal Flow Distribution menu

Due to the missing definition of labels of IFAS object in the technical documents, the following figures explained how they were transferred to the reactor.

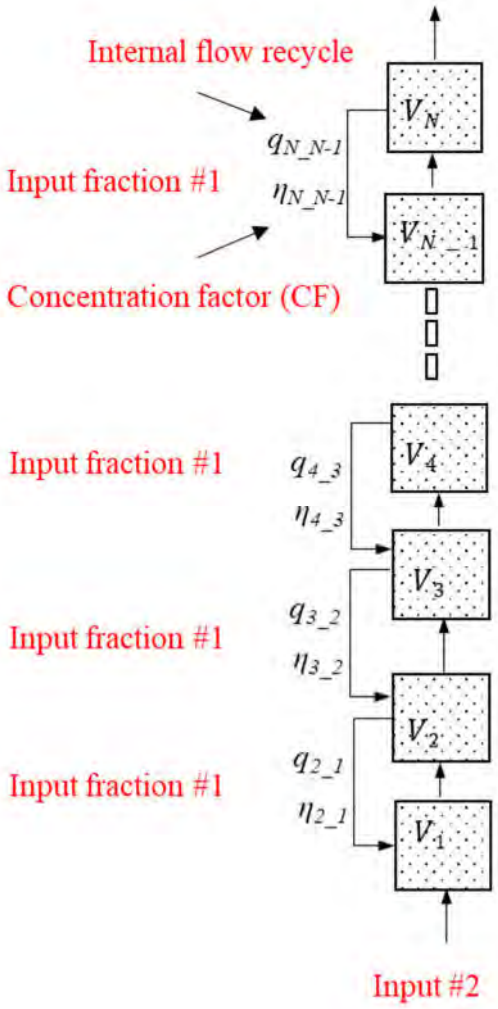

Figure 43. Definition of labels of Internal Flow Distribution sub-menu on the reactor

As shown in Figure 42, in the sub-menu of Internal Flow Distribution, the "Influent fractions", "Influent fractions #2" and "Recycle fractions" required the totals of input fractions equaled to 1. In the model, their values were distributed as below:

- "Influent fractions" related to the internal flow recycle. Because the internal flows were split evenly among the cell tanks, the value equaled to $1/N$ (equaled to 1/11 in this study) were distributed to each fraction,
- "Influent fractions #2" related to the main flow rate, which was connected to the 1st cell tank. Therefore, the value of 1 was distributed to the 1st cell tank, and the zero was distributed to the remaining cell tanks,

- "Recycle fractions" was not considered in the model because there was no recycle from other boundaries to the reactor.

For the remaining items, their values were defined as follows:

- "Internal recycle": the internal flow rate q_{i_i-1} (m^3/d) should be filled in from the cell-tank *i* to the cell-tank (*i-1*). As explained in section 4.5.1, the value q_{i_i-1} equaled to Q/1000 was selected in this study,
- "Internal recycle contains media?": because the media was recycled, the value of 1 was selected from the cell-tank *i* to the cell-tank (*i-1*),
- "Internal recycle media concentration factor (CF)", as explained in section 4.5.1, the value equaled to (Q/q+1) was selected from the cell-tank *i* to the cell-tank (*i-1*) in this study,
- "Flow from tanks contain media": as shown in Figure 43, the media flow from the tank *i* to the tank *i+1* and then recycled back to the tank *i* together with a small portion of liquid. Therefore the value of 1 (Yes) was selected for the flows from the cell tank 1 to (*N*-1), and zero for the one from cell tank *N*. If the value of the cell tank *N* was wrongly selected to be 1, the media will be withdrawn and gradually emptied from the reactor,
- "Flow from tank media concentration factor": as explained in Eq (21), when targeting the liquid, the concentration factor should be 1 for all the flows.

6.3.3. Mass Transport Menu

This menu is dedicated to the mass transfer of soluble and particulate materials from/to and between biofilm layers to the bulk liquid, as shown in Figure 44. In this study, the calibration of "Attachment rate", "Detachment rate" and "Internal solids exchange rate" was explained in sections 5.3.1 and 5.3.2.

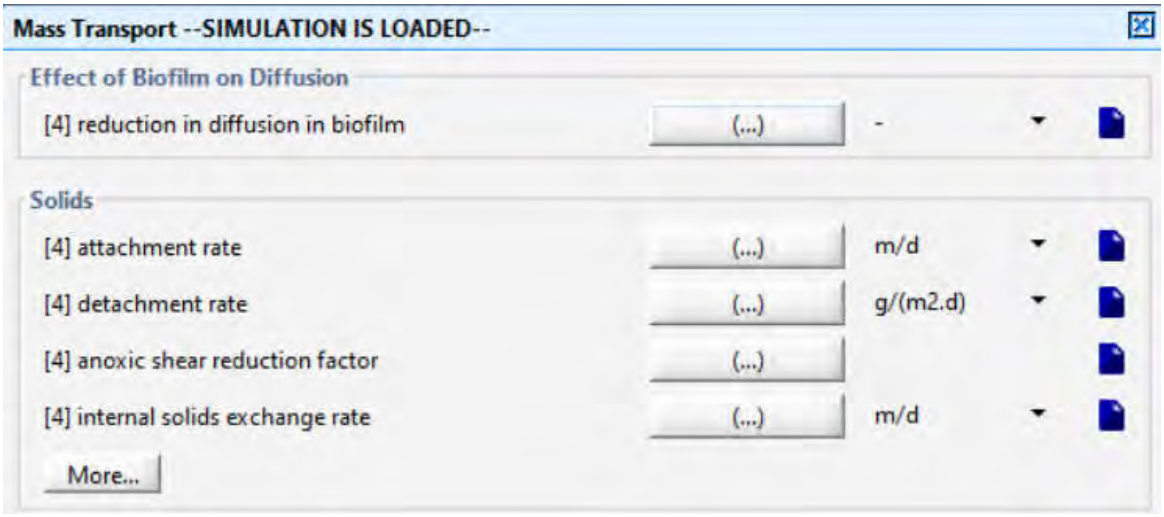

Figure 44. Mass transport menu

6.3.4. Kinetic Menu

The kinetic menu is related to the growth of OHO/AOO/NOO and other biological processes defined in the Peterson matrix. As mentioned in the 5.3.3, the following kinetics and stoichiometric parameters were applicable to five different datasets over the lab-, pilot- and full-scale reactors.

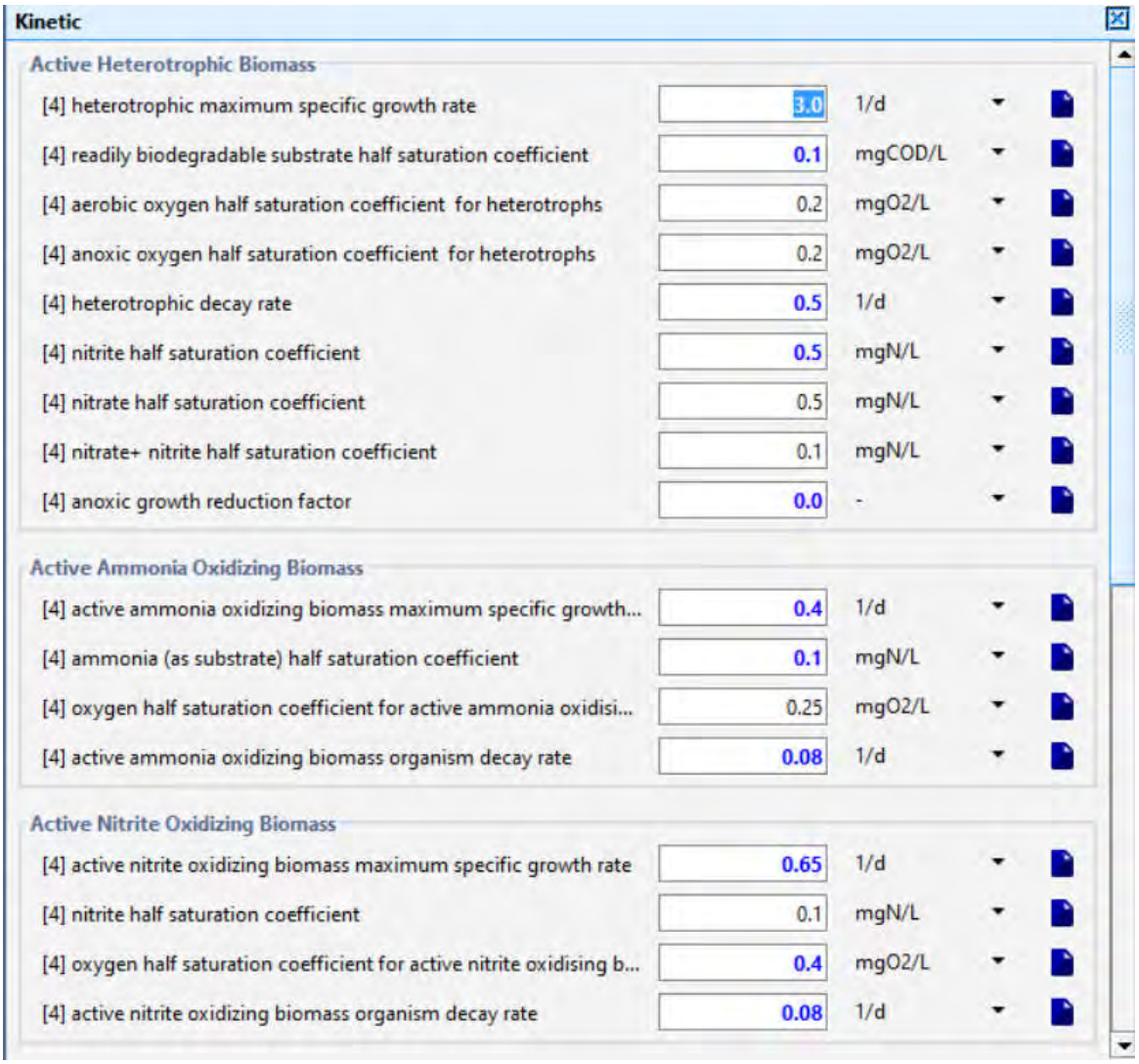

Figure 45. Kinetic menu

6.4. SENSITIVITY ANALYSIS OF NUMERICAL CALCULATIONS TO THE CALCULATION RESULTS

6.4.1. Unstable convergence of steady-state simulation

In the dynamic simulation for short periods, such as in hours, days, and weeks, the initial biomass concentrations were critical, which induced the effluent concentrations at the starting point of the simulation. If the initial biomass concentrations were unknown, they might be calculated in steady-state simulation with an assumption on the influent concentrations. This trial-error process was time-consuming until acceptable effluent concentrations at t=0 were obtained.

In the case of a complicated model, the steady-state convergence might be slow or diverged. The following steps could be used to avoid such problems:

In the **Layout > General Data > System > Input Parameters > Steady-State Solver Settings**:

- Adjusting the **iteration termination criteria:** As stated in GPS-X's Technical Reference, the steady-state convergence is triggered when the solver achieves a sum of state variable derivatives below the **iteration termination criteria.** Therefore, the **iteration termination criteria** might be increased to a higher value, e.g. 100 or 50, compared to the default value of 10, in the condition that the convergence was stable in each simulation.
- Adjusting the **maximum number of iterations**: increase this value will set up higher loop counters for the steady-state solver until the convergence is solved.
- Adjusting the **maximum number of unsuccessful iterations**: increase this value will prolong the termination of the steady-state solver.

6.4.2. Sensitivity analysis of the maximum biofilm thickness

6.4.2.1. Calculation approach of simulated biofilm thickness

The biofilm attachment, detachment, and corresponding biofilm thickness could significantly influence the biofilm reactor performance under some conditions. The detachment has a substantial impact on the biofilm thickness and the activities of low-growing bacterial within the biofilm, such as AOO and NOO. Meanwhile, the attachment of particulates from the bulk liquid to the biofilm layers influences to the availability of the organic substrate within the biofilm and the seeding of the biofilm by the suspended biomass. Unfortunately, up to date, such issues were not well-understood and explained [45].

In GPS-X software, the simulated biofilm thickness was modeled not to exceed the "maximum biofilm thickness" value, as explained in the Eq (18). In this way, both the simulated biofilm thickness, attachment, and detachment were controlled by the "maximum biofilm thickness" value, which is user input. Therefore, in some cases, appropriate data of the "maximum biofilm thickness" is critical to the simulation results. Ideally, the data could be obtained directly by measuring the attached biofilm on the media in the full-scale reactor, then adding 10 to 20% to the value for the marginal. Sometimes, the separation of biomass from the media might be unfeasible. In this study, the measurement of VSS for the attached biomass was impractical because the BAC media would be destroyed during the ignition process. In such a case, the "maximum biofilm thickness" could only be retrieved from the literature [45]. However, the uncertainty of the simulated biofilm thickness, attachment, and detachment was unavoidable.

In GPS-X software, the biofilm was constructed in five biofilm layers and one attached liquid layer as default, as indicated in Figure 46. The particulate components "filled" into the biofilm from the most outer biofilm layer (B#1) to the inner biofilm layers (to B#5). From the "maximum biofilm thickness" data ($\delta_{B,max}$), the "maximum biofilm thickness per

layer" ($\delta_{B,max,layer}$) was calculated, based on which the "maximum biofilm volume per layer" ($V_{B,max,layer}$) was estimated. When the particulate concentration in the biofilm layer B#1 reached the "dry material content of biofilm", which was fixed at 102 g/L [95], the simulated biofilm thickness and volume also reached to their maximum value. Due to the internal solids exchange, the particulate components were transferred to the adjacent biofilm layers (B#2 to B#5). The simulated biofilm thickness ($\delta_{B,layer}$) in layer B#i was estimated based on the following equation:

$$\delta_{B\#i,layer} = \frac{(total\_particulates_{B\#i}) x \delta_{B,max\_layer}}{dried\_material\_content\_of\_biofilm} \quad \textbf{Eq (24)}$$

It should be noted that the above equation was resulted from our manual checking on the calculation of GPS-X. In fact, neither the $\delta_{B,layer}$ nor the "total particlulates$_{B\#i}$" was displayed at the output of the simulation. The "total particlulates$_{B\#i}$" was manually determined by summing the particulate components (inert inorganic suspended solids, particulate inert organic material, slowly biodegradable substrate, active AOO, active NOO, active OHO, unbiodegradable particulates from cell decay) in the biofilm B#i in the (Output Variables > 2-D state variables) in the reported files.

In this way, the sum of five $\delta_{B,layer}$ was calculated, which was also the simulated biofilm thickness provided in GPS-X output display. In this calculation approach, the biofilm thickness in each layer was not even, in which the thicker biofilm layers were found in the outer while thinner biofilm layers were placed in the inner of the biofilm.

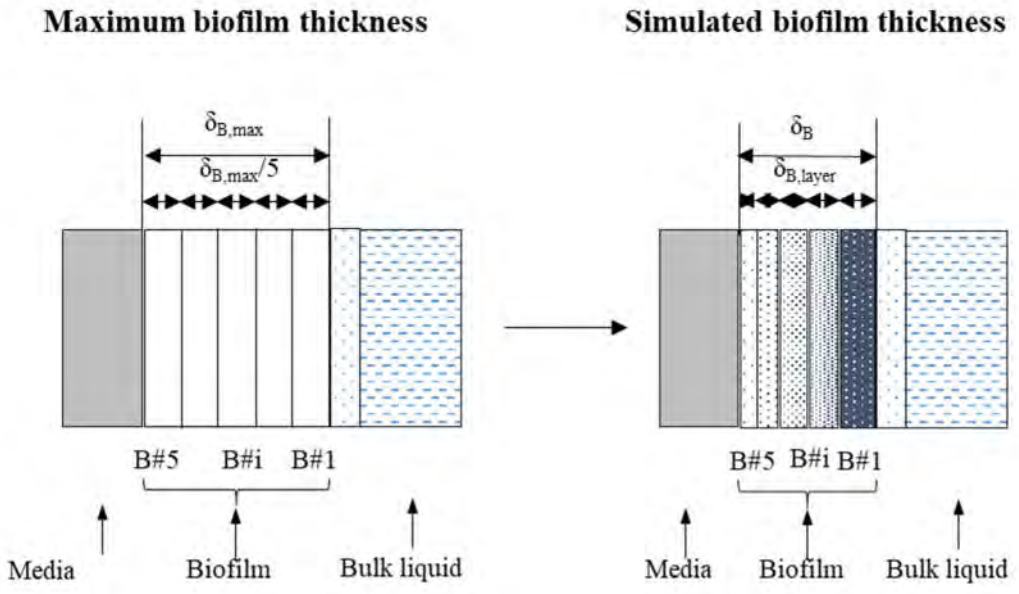

Figure 46. Biofilm thickness calculation

6.4.2.2. Sensitivity analysis of the maximum biofilm thickness to simulated biofilm performance

To investigate the influence of the $\delta_{B,max}$ to the simulation results of the full-scale reactor in Vinh Bao (R) WTP, the simulations were carried out at different values of $\delta_{B,max}$, while the set of attachment and detachment rates were similar as described in section 5.3.1 and 5.3.2. In section 5.3, the value of $\delta_{B,max}$ was kept at 0.5 mm, which resulted in the simulated δ_B of 0.315 mm and reproduced acceptable predicted data at reasonable simulation time. When the $\delta_{B,max}$ was reduced to 0.2 mm, the simulated δ_B was found to be 0.126 mm. The simulation speed becomes very low, due to the impact of the small value of $\delta_{B,max,layer}$ to the integration process. When the value of $\delta_{B,max}$ was increased to 0.7 mm, the simulated δ_B was estimated to be 0.443 mm, and the simulation speed was faster. The $\delta_{B,layer}$ in each scenario was presented in Figure 47 (a). The influence of $\delta_{B,max}$ to the total particulate and active biomass concentration in the biofilm was also investigated. As shown in Figure 47 (a), the total particulate concentrations in the biofilm were found at 320 g/L, which were manually calculated from the particulates components in the biofilm B#i (Eq (24)), were not significantly different over the three simulations. It was because the parameters

determined the total particulate concentrations in the biofilm layers, which were the growth and decay of the biomass, the attachment, detachment, and internal solid exchanges between the biofilm layers and the bulk liquids, were fixed. Additionally, due to the different simulated δ_B, the biomass per surface area were varied at 40.72, 100.08, and 142.67 g/m^2, when the $\delta_{B,max}$ were increased from 0.2 to 0.7 mm. It indicated that the simulated biomass per surface area would again depend on the $\delta_{B,max,}$ leading to the uncertainty of the results.

In another viewpoints, the impacts of $\delta_{B,max}$ on the $\delta_{B,layer}$ and the total particulates in each layers could be displayed in Figure 47 (b). It was clearly shown that in the most outer layer, both the $\delta_{B,layer}$ and the total particulates reached their maximum values, and gradually decreased in the inner biofilm layer, given the "dry material content of biofilm" was always fixed at 102 g/L.

The composition and concentration of active biomass AOO/NOO/OHO were rather fluctuated. When the biofilm thickness was reduced, the volume of biofilm per layer was also decreased, leading to an increase in the active biomass concentrations. However, more active biomass was washed-out from the biofilm layers, leading to a decrease of the active biofilm mass. Consequently, the effluent DO in the case of $\delta_{B,max}$ equaled to 0.2 mm was slightly increased compared to the other scenarios, as indicated in Figure 49. Interestingly, the variation of $\delta_{B,max}$ from 0.2 to 0.5 mm was not influenced the NO_2-N effluent. However, as the biofilm layer become thicker, it was likely that the NOO could not compete with the dominant OHO, leading to the deterioration of NO_2-N effluent quality.

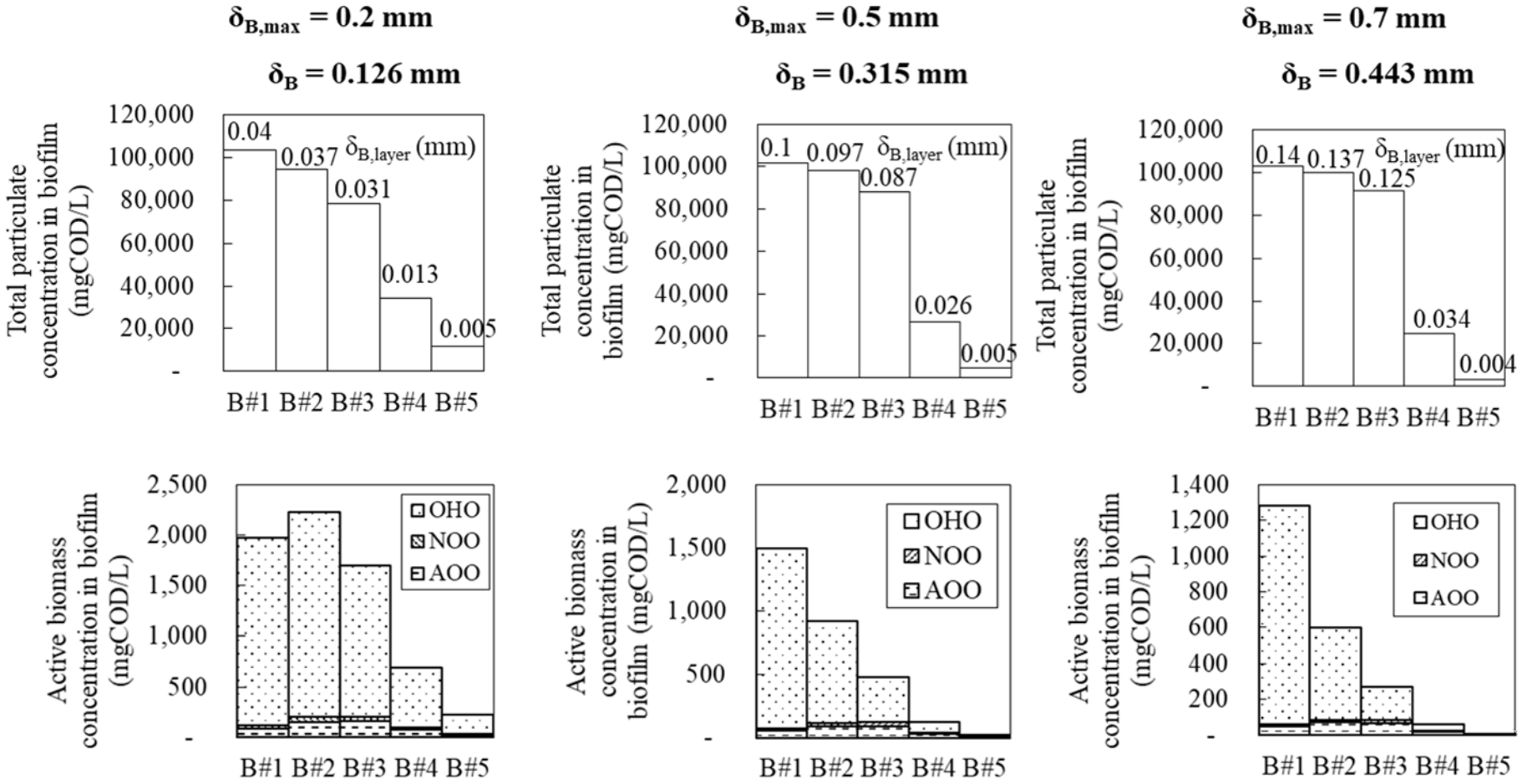

Figure 47 (a) Impacts of max. biofilm thickness values to the particulates and active biomass concentration and calculated biofilm thickness

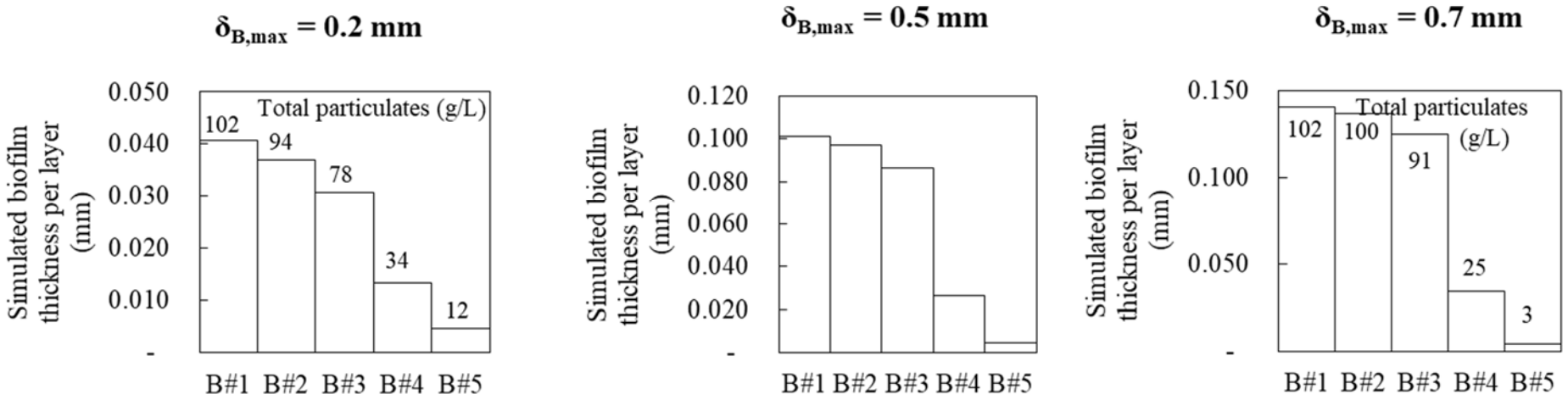

Figure 48 (b) Impacts of max. biofilm thickness values to the calculated biofilm thickness and total particulates

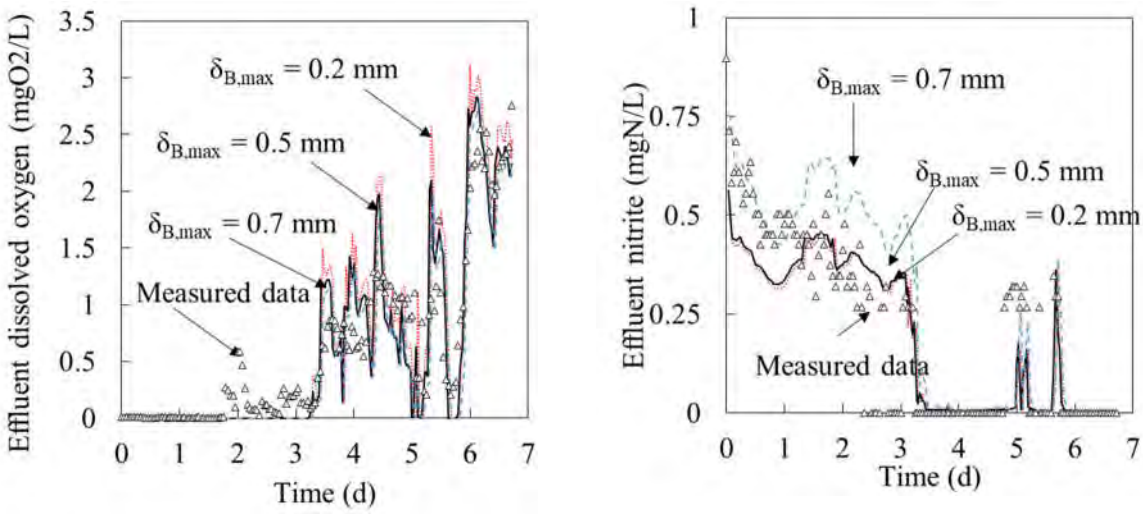

Figure 49. Impact of maximum biofilm thickness to the effluent dissolved oxygen and nitrite concentration

Therefore, the experimental evidence were absolutely needed to validate the reliability of the $\delta_{B,max}$. The simple OUR test for the biofilm media, such as those indicated in Figure 25, could provide some useful information. Given the short duration of the OUR test, the calibrated biofilm thickness could reproduce the reasonable volumetric reaction rate to meet the experimental data. It should be noted that this OUR test was carried out on the biofilm media sampled from the lab-scale reactor where the presence of influent suspended solids were rather limited. Here, the impact of difference $\delta_{B,max}$ to the volumetric reaction rate was investigated, as shown in Figure 50. When a small value of 0.2 mm was applied, the limited volumetric reaction rate resulted in the elevated effluent DO. On the contrary, when the $\delta_{B,max}$ was increased to 0.5 or 0.7 mm, the simulated volumetric reaction rates were higher than expected. The value of $\delta_{B,max}$ equaled to 0.3 mm reproduced the experimental volumetric reaction rate, and was applied to the simulations of the lab-scale reactors.

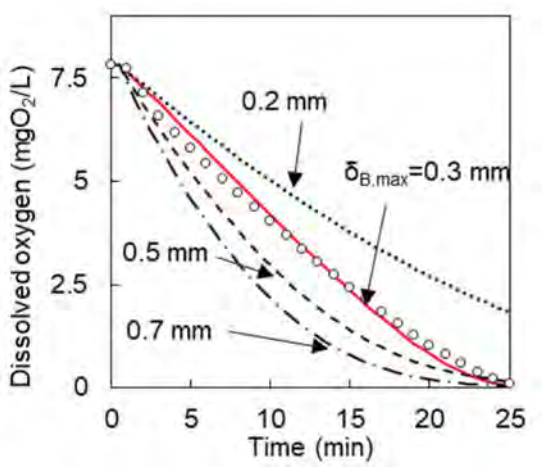

Figure 50. Impact of maximum biofilm thickness to the volumetric reaction rate

6.4.2.3. State-of-the-art in biofilm thickness simulation

As the results of simulated biofilm thickness in this study were considered with caution, we have investigated how this data was solved in other existing simulators.

To the best of our knowledge, the relationship between attachment, detachment and corresponding biofilm thickness are still not well understood in the research; therefore, their mathematical transformations hold some uncertainties. Based on the simulator programming, the modeler must either fix a certain biofilm thickness (e.g., based on measurements in the full-scale reactor) or have the model predict biofilm thickness (e.g., by fixing the value of the detachment and attachment rate coefficients [45].

From literature review, a summary of simulator functions for biofilm attachment, detachment and biofilm thickness was provided as follows [49]:

Name	Source	Type and biomass distribution	Type	Biofilm detachment rate function ($g\,m^{-2}\,d^{-1}$)	Bulk-phase particulate attachment rate function ($g\,m^{-2}\,d^{-1}$)
AQUASIM[79]	EAWAG, Swiss Federal Institute of Aquatic Science and Technology, Dübendorf, Switzerland (www.eawag.ch/index_EN)	1-D, DY, N; heterogeneous	DY, N	User defined	User defined
AQUIFAS[78]	Aquaregen, Mountain View, California, USA (www.aquifas.com)	1-D, DY, SE and N, heterogeneous	DY, N	$r_{de,X_k} = k_{de,X_k} \cdot X_{F,k} \cdot L_F$ or $r_{de,X_k} = k_{de,X_k} \cdot X_{F,k} \cdot L_F^2$	$r_{at} = k_{at} \cdot \frac{X_L}{X_L + K_{at}}$ for substrates that hydrolyze
BioWin[59]	EnviroSim Associates Ltd., Flamborough, Canada (www.envirosim.com)	1-D, DY, N, heterogeneous	DY, N	Included but function not reported	Included but function not reported
GPS-X[59]	Hydromantis, Inc., Hamilton, Canada (www.hydromantis.com)	1-D, DY, N, heterogeneous	DY, N	$r_{de,X_k} = k''_{de,X_k} \cdot \frac{X_{F,k}}{X_F} \cdot \left(\frac{L_{F,max}}{L_{F,max} - L_F} - 1\right)$	$r_{at} = k'_{at} \cdot X_L$
TRIFL[79]	The Penn State University, University Park, Pennsylvania, USA (www.engr.psu.edu/ce/enve/logan/bioremediation/trickling_filter/model.htm)	1-D, SS, N, homogeneous	N/A	Biofilm thickness and detachment are not taken into account explicitly	Biofilm thickness and attachment are not taken into account explicitly
Pro2D[78]	CH2M HILL, Inc., Englewood, Colorado, USA (www.ch2m.com/corporate)	1-D, SS, N(A), homogeneous	SS, N	$r_{de,X_k} = \sum_{k=1}^{x} \{r_{g,k} + r_{dec,k} + r_{hyd,k}\}$ Constant L_F. Biofilm growth balanced by decay and hydrolysis. Biofilm fragments assumed to detach from biofilm surface. The assumed homogenous biofilm biomass distribution does not result in preferential detachment of biomass types based on location	IFAS: Influent particulates assumed to bioflocculate with MLSS after mixing with RAS. Hydrolysis is the rate-controlling process. MBBR: Published model may not well describe system receiving influent wastewater with high sbCOD
		1-D, SS, N(A), Homogeneous	SS, N		$r_{at} = k'_{at} \cdot X_L$
Simba[58]	ifak GmbH, Magdeburg, Germany (www.ifak-system.com)	1-D, DY, N, heterogeneous	DY, N	$r_{de} = k'_{de} \cdot X_F \cdot L_F^2$, or user defined	$r_{at} = k'_{at} \cdot X_L$
STOAT[74]	WRc, Wiltshire, England (www.wateronline.com/storefronts/wrcgroup.html)	1-D, DY, N, heterogeneous	DY, N	$r_{de} = 0.5 \cdot \left(k''_{de} \cdot \bar{\mu}_k \cdot X_F \cdot L_{F,g}^2 + k'''_{de} \cdot X_F \cdot L_F^2\right)$	$r_{at} = k'_{at} \cdot X_L$
WEST[59]	MOSTforWATER, Kortrijk, Belgium (www.mostforwater.com)	1-D, DY, N(A)[a], N[b], homogeneous[a], heterogeneous[b]	DY, N	[a] $r_{de} = k'_{de} \cdot X_{F,k}$ (constant r_{de}), [b] $r_{de} = k'_{de} \cdot X_{F,k} \cdot L_F^2$	[a] $r_{at} = k'_{at} \cdot u_F$, [b] $r_{at} = k'_{at} \cdot X_L$ [b]

where:

1-D	one dimensional
DY	dynamic
N	numerical
sbCOD	slowly biodegradable chemical oxygen demand
SS	steady state
SE	semi-empirical
N(A)	numerical solution using analytical flux expressions
$L_{F,max}$	maximum biofilm thickness (m)
L_L	mass transfer boundary layer thickness (m)
r_{at}	attachment rate ($g\,m^{-2}\,d^{-1}$)
r_{de}	detachment rate ($g\,m^{-2}\,d^{-1}$)
r_{de,X_k}	detachment rate ($g\,m^{-2}\,d^{-1}$)
X_F	total biomass concentration inside the biofilm ($g\,COD\,m^{-3}$)
$X_{F,k}$	concentration of biomass type k inside the biofilm ($g\,COD\,m^{-3}$)
X_L	particulate concentration near the biofilm surface ($g\,m^{-3}$)
k	biomass type
k_{at}	attachment rate coefficient, max ($g\,m^{-2}\,d^{-1}$)
k'_{at}	attachment rate coefficient ($m\,d^{-1}$)
k''_{at}	attachment rate coefficient ($m^{-3}\,d^{-1}$)
k_{de}	detachment rate coefficient (d^{-1})
k'_{de}	detachment rate coefficient ($m^{-1}\,d^{-1}$)
k''_{de}	detachment rate coefficient ($g\,m^{-3}$)
k'''_{de,X_k}	detachment rate coefficient of particulate type k ($g\,m^{-2}\,d^{-1}$)
k'^{m}_{de}	detachment rate coefficient (m^{-1})
k''^{m}_{de}	detachment rate coefficient ($m^{-1}\,d^{-1}$)
$K_{at,k}$	attachment constant, half-saturation concentration of particulate (type k) ($g\,m^{-3}$)
L_c	characteristic length (m)
L_F	biofilm thickness (m)
$L_{F,g}$	biofilm thickness, in addition to a base L_F, where growth occurs (m)

The above expressions failed to explain each steps involved in the attachment and detachment. Further basic research on these complex phenomenon is needed to pave the way for their mathematical description. Until then, the mechanical components of the biofilm reactors could be developed or optimized to control the process [49].

6.4.2.4. Conclusion

In this section, the calculation approach of δ_B in GPS-X software was explained. The implications of the $\delta_{B,max}$, which is user input, to the simulated δ_B and biofilm performance were also investigated. Ideally, the data could be obtained directly by measuring the attached biofilm on the media in the full-scale reactor. Otherwise, the information could be referred in the literature. The $\delta_{B,max}$ was selected based on acceptable biofilm response within reasonable simulation time. Due to the uncertainty of the $\delta_{B,max}$ and its implications, the simulated results of δ_B, attachment, and detachment should be carefully considered. Experimental evidence, such as the OUR test of the biofilm media, were absolutely needed to validate the calibrated δ_B. It was expected that future research would enlighten the attachment and detachment process in the biofilm, and such understanding could be well transferred into the modeling language.

CHAPTER 7. REMOVAL MECHANISMS OF PESTICIDES IN THE NITRIFYING EXPANDED-BED REACTOR

7.1. INTRODUCTION

In Vietnam and worldwide, intensive cultivation and increasing application rates of fertilizers, pesticides, herbicides, and other related crop protection products are being practiced to meet the growing food demand and assure food security. Accordingly, numerous studies have been focused on the degradation at the surface, groundwater, soil, and air quality due to the release of surplus pesticides and herbicides to the environment. A survey by Duong H.T. et al. in four big cities in Vietnam including Hanoi, Hai Phong, Da Nang, and Ho Chi Minh Cities in 2011 detected the occurrence of 38 pesticides in river waters and 14 pesticides in groundwater, some of which have been banned from use since the 1990s [34]. An investigation by Chau et al. from 2011 to 2013 also revealed the widespread of pesticide pollutions in both private and public drinking water sources in the Mekong Delta in Vietnam [96]. Regulations and guidelines take effect at national and international levels to monitor and control the occurrence and thresholds of emerging chemicals in drinking water. In 2017, the World Health Organization (WHO) had provided the guideline values for 31 pesticides presented in drinking water, which were of health significance [16]. In Europe, a proposal for a revised drinking water directive has been adopted since 2018, in which a maximum concentration of 0.1 μg/L for individual pesticide and 0.5 μg/L for total pesticides were regulated [36]. In the United States, the Environmental Protection Agency has identified 18 types of pesticides and herbicides with their maximum contaminant levels and potential health effects from long-term exposure in the National Primary Drinking Water Regulations [37]. In Japan, pesticides were not listed in the Drinking Water Standards but referred to the category of “Complimentary Items to Set the Target for Water Quality Management” [38]. In Vietnam, the Ministry of Health has recently listed 27 pesticides with their maximum limits in the National Technical Regulation on Drinking Water Quality (QCVN01-1:2018/BTY) [17].

The conventional drinking water treatment process alone, which includes

coagulation/flocculation, sedimentation, and filtration, could partly remove the pesticides [97]. At present, available technologies to remove such persistent chemicals from drinking water sources are chemical oxidation, chemical precipitation, membrane, activated carbon adsorption and/or biofilter. Traditionally, granular activated carbon (GAC) was effectively used to adsorb the pesticides and other organic pollutants due to its irregular crevices and porous particle shape that bind those specific contaminants [43]. Thuy et al. (2013) demonstrated that pesticides (Chlorpyrifos, Diazinon, and Carbofuran) could be adsorbed on the low-cost GAC generated from local products (bamboo and coconut shell) at the pilot-scale upgraded from a typical drinking water treatment plant (WTP) in Vietnam [97]. However, a major set-back pertains to GAC saturation overtime when all of its available adsorption sites could not bound with either organic matters and/or microorganisms [43]. Consequently, frequent regeneration or continuous dosing of GAC are needed to renew the adsorption capacity [75], [98], leading to high operational costs. To overcome such limitation, the biological activated carbon (BAC) process, which is transformed from GAC after a long operation period, has received much attention [39], [43], [75], [99]. This process uses GAC as filtration media to physically remove undesired matters. As the GAC media is gradually exhausted, microbial colonization is developed on the surface of the media [43]. This naturally occurring biofilm can biodegrade a wide variety of contaminants such as organic carbon, organic/inorganic substances, and disinfection by-products precursors [39], [43], [44]. In this way, the service life of the BAC bed could be extended from 6-12 months to several years [43], [79]. The pesticide removals using the BAC process were reported in [75], [70], [76], [77], in which the removal mechanism was thought to be simultaneous adsorption and biodegradation. The biotransformation of persistent compounds such as pesticides at trace level is possibly due to the co-metabolism, in which pesticides might be biodegraded by non-specific enzymes generated by the primary substrate metabolism [67]. Some parameters such as the type of activated carbon, hydraulic retention time, and backwashing regime on the performance of BAC process [29]; however,

a critical role of ammonia-oxidizing organism (AOO) in the enhancement of micropollutants removal in nitrifying activated sludge of wastewater treatment [71]–[74] was focused in this study. However, there is still questionable if the nitrifying biofilms could remove the pesticides in drinking water treatment.

Nitrifying expanded-bed filter using BAC media is widely used at the pretreatment of drinking water in Japan and recently installed at the pilot and full-scale in several WTPs in Vietnam to remove NH_x-N, dissolved manganese, and organic substances [62]. Because the process focuses on the biological activities rather than the adsorption of media, the spent GAC could be used without regeneration or frequent adding of virgin adsorbent, making this process a very cost-effective option. In addition to the treatment efficiency for NH_x-N and organics that were previously demonstrated [44], this study aimed to investigate the possibility of degrading the pesticides of the reactor. Based on the prominent results in the full-scale reactor receiving river water, the reactor was implemented in the laboratory to study the pesticide removal mechanism and the contribution of nitrifying bacteria to the removal efficiency.

7.2. MATERIALS AND METHODS

7.2.1. Monitoring campaigns for the full-scale and lab-scale reactor

As for the full-scale reactor, the monitoring of pesticide removals was carried out in the rainy season for 7 days. Eighteen pairs of influent and effluent water samples were taken at AM 8:00, AM 12:00, and PM 16:00 every day, aiming to investigate the representative samples in different moments of a day for pesticide analysis. The organic and nitrogenous pollutions were also monitored, and the results were shown in section 5.3.3.

In the lab-scale reactor, the reactor was continuously fed with synthetic influent water composed of 1 mgN/L as ammonium nitrogen, 0.5 mgP/L as phosphate, 3-5 mg DOC/L mixed from acetone and ethanol, pesticides solution at the range of ng/L, and dechlorinated tap water in 2 months. The pesticide stock solution was prepared in acetone and kept in an amber glass bottle at room temperature. The influent and effluent samples were collected every 2 to 3 days for pesticide analysis. Similarly, DO, and NH_x-N were also monitored to check the biomass activity in the reactor. When the biomass was stably developed on the BAC granules, a series of batch experiments were carried out to examine the pesticide removal mechanisms. The first batch experiment aimed to estimate the contribution of microbial activity to the pesticide removal using a microbial inhibitor. A series of Erlenmeyer flasks of 500 mL were filled with solution similar to the influent in the continuous experiment. Fresh BAC was taken from the lab-scale reactor and washed by deionized tap water several times to remove the remaining substrates. The wet BAC was placed on a paper to remove the water attached to the surface, then weighted 10 g before putting it in each mesh bag. In the first group, where the microbial activity was promoted, the BAC bags were placed into the flasks, and oxygen gas was continuously injected. In the second group, which inhibited the biomass, together with the BAG bags, 500 mg/L of sodium azide was added in, and nitrogen gas was continuously purged. The third group of control flasks was designed as the inhibited flasks without the presence of BAC. For better

contact between the biomass and substrates, all the flasks were operated under gentle stirring. The samples were taken for pesticides and NH_x-N analysis at the starting time in the controlled flasks, and after 1, 2, 3 and 4 hours of the experiment for the other flasks. The first batch experiment was carried out in triplicate. The second batch experiment aimed at investigating the association of the nitrification reaction rate to the pesticide removals. While the controlled flasks were designed exactly as mentioned above, in two groups of experimental flasks the NH_x-N concentrations were varied at 1 and 5 mgN/L and oxygen gas was continuously injected. Rather than changing the NH_x-N as above, the third batch experiment aimed at estimating the impact of biomass concentration on the pesticide removals by using different BAC amounts of 10 g and 30 g. The statistical analysis was carried out for the data obtained from the triplicated batch experiments using a programming language R developed by the R Core team (CRAN project) [100].

7.2.2. Studied pesticides

In this research, eight pesticides from different classes that are frequently used in a wide range of crops in Vietnam were selected for monitoring. The occurrence of these pesticides was reported in [34] in Chanh Duong River in 2011. Among them, two pesticides Atrazine and Chlorpyrifos are listed in the Vietnamese National technical regulation on Domestic Water Quality (QCVN 01-1:2018/BYT) for allowable concentrations of 100 and 30 µg/L, respectively. The list of targeted pesticides and some of their physical properties were presented in Table 15.

Table 15. Some physical characteristics of targeted pesticides and maximum allowable limits in drinking water regulations

No	Pesticide	Class	Chemical formula	Molecular weight (g/mol)	Octanol-Water Partition Coefficient log K_{ow}♣	Maximum allowable limit (µg/L)
1	Atrazine	1,3,5-triazine	$C_8H_{14}ClN_5$	215.69	2.5	100[1,2], 3[3], 0.1[4]
2	Fenobucard	Carbamate	$C_{12}H_{17}NO_2$	207.27	2.79	0.1[4]
3	Flutolanil	Carboxamide	$C_{17}H_{16}F_3NO_2$	323.31	3.7	0.1[4]
4	Isoprothiolane	Dithiolane	$C_{12}H_{18}O_4S_2$	290.39	3.3	0.1[4]
5	Chlorpyrifos	Organophosphate	$C_9H_{11}Cl_3NO_3PS$	350.57	4.7	30[1,2], 0.1[4]
6	Fipronil	Fiprole	$C_{12}H_4Cl_2F_6N_4OS$	437.14	4	0.1[4]
7	Fenbuconazole	Triazole	$C_{19}H_{17}ClN_4$	336.82	3.23	0.1[4]
8	Buprofezin	Unclassified	$C_{16}H_{23}N_3SO$	305.44	4.3	0.1[4]

♣: *The Pesticide Manual: a world compendium* [101]

[1]: *National technical regulation on Domestic Water Quality (QCVN01-1:2018/BTY), Ministry of Health, Vietnam.*

[2]: *Guidelines for Drinking-water Quality, WHO (2017).*

[3]: *National Primary Drinking Water Regulation, EPA (2009)*

[4]: *Proposal for a revised drinking water directive, European Commission (2018): maximum concentration of 0.1 µg/L for individual pesticide and of 0.5 µg/L for total pesticides*

7.2.3. Analytical procedures

As for the pesticides, the glass sampling bottles were prewashed by acetone, purified water, and the water samples. After collecting, 500 mL of water sample was filtered by glass-fiber filters (Whatman, 47 mm, Grade GF/F, prewashed with purified water, and dried at 105 °C in 3 hours). The filtrate was passed through a PS-2 Sep-Pak cartridge (Waters Associates, USA, preconditioned with acetone, methanol, and purified water) at the flow rate of 10 mL/min, then finished by adding 20 mL of purified water. The cartridges were stored at 4 °C and delivered to the laboratory for further analysis. The cartridges were dried by air for 1 hour. They were eluted by 5 mL of acetone, then concentrated to 1 mL under a gentle nitrogen stream. Next, 5 mL of hexane was added, and the concentration continued until the eluate volume was reduced to 0.9 mL. Finally, the eluates were spiked with 100 µL of internal standards solution (10 µg/mL, Sigma-Aldrich, Japan) before being analyzed using the Gas Chromatography-Mass Spectrometry (GC-MS, QP-2100 Plus, Shimadzu, Japan). The measurement conditions of GC-MS can be referred to in [102]. As for the continuous and batch experiments of the lab-scale reactor, the pesticide analysis was carried out with the same procedure as mentioned above. Duplicated samples were taken and the average values were reported for data analysis.

7.3. RESULTS AND DISCUSSION

7.3.1. Pesticide removals in the full-scale reactor

As mentioned in section 5.3.3, the water quality was degraded during the first 3 days and then significantly improved in the last 4 days due to the release of freshwater from Luoc River. As shown in Figure 51 , the average influent DO was found to be 5.50 (SD=0.56) mgO2/L, while the NH_x-N concentration was relatively high at around 4.27 (SD=0.94) mgN/L between day 0 and day 3, and then dropped to about 1.58 (SD=1.28) mgN/L in the remaining day. The biological activities of the BAC bed was described in 5.3.3, in which about 0.76 (SD=0.38) mgN/L and 2.81 (SD=1.51) mgCOD/L were removed in the first 3 days due to limited influent DO and almost removed in the last 4 days when DO was sufficient [44]. The nitrifying expanded-bed filter could remove some pesticides to a certain extent, as indicated in Figure 52. Four pesticides, which were Flutolanil, Buprofezin, Chlorpyrifos and Fenobucard were removed at 82% (SD=6.03), 55% (SD=14.50), 54% (SD=18.31), and 52% (SD=12.77), respectively. The other pesticides were not considerably removed at removal rates lower than 50%. Comparing to those regulated in Vietnamese drinking water standard, the concentrations of Atrazine and Chlorpyrifos were lower than the threshold values. However, the pesticides Atrazine, Fenbuconazole and Isoprothiolane were found at elevated concentrations of 1,000 ng/L, 6,000 and 400 ng/L respectively, which were far higher than their reported values in Chanh Duong River in 2011 [34].

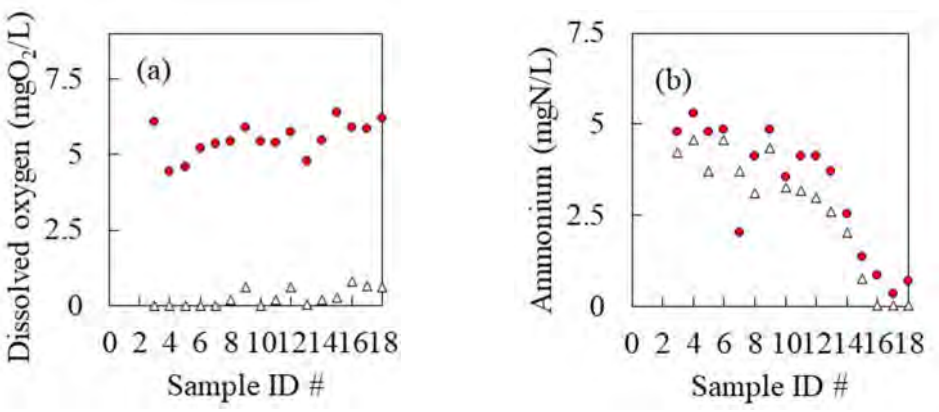

Figure 51. Influent and effluent dissolved oxygen (a) and ammonium (b) in the full-scale reactor

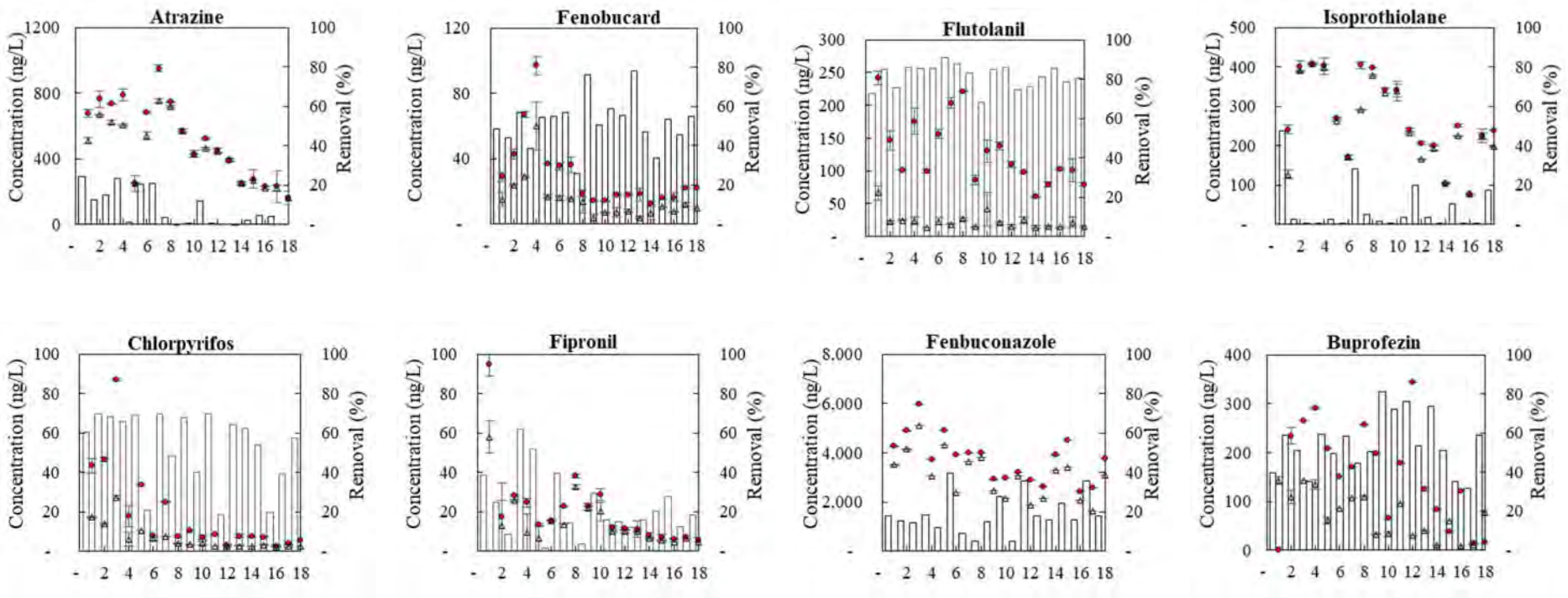

Figure 52. Influent and effluent pesticides and removal efficiencies in the full-scale reactor in the rainy season in Vinh Bao WTP (red circle = influent, white triangle = effluent, bar = removal efficiency)

In this full-scale, it was unclear if the pesticides were removed due to adsorption or biodegradation. As adsorption is principally an exchange process, it is largely influenced by the physicochemical characteristics of both adsorbent which was BAC and the adsorbates, which were the pesticides. As for the BAC bed, there were opposing viewpoints related to its adsorption capacity over time. Some researchers believed that the physical adsorption capacity of BAC would be exhausted after 2 to 3 months [79], or after six months of operation [43]. However, others proved that adsorption in BAC was still partly responsible for micro-pollutants removal after four years of filtration [75]. In this study, the life-service of the BAC bed reached to more than 6 years at the time of the experiment, and it was unable to tell if there were still available adsorption sites on the BAC surface. For the pesticides, it was reported that the adsorption capacity could be enhanced in case (i) the small molecular size or low molecular weight, (ii) hydrophobic molecule, expressed by high Octanol-water distribution coefficient (log K_{ow}) and (iii) the electrostatic interactions with the GAC surface [41]. As shown in Table 1, all the pesticides could be considered as hydrophobic (log $K_{ow} > 2$). However, there was no correlation between the removals of the pesticides and the log K_{ow}. A similar lack of correlation between the physicochemical properties of the pesticides and their adsorption onto GAC was previously reported at a very diluted concentration (ng/L) [75]. Therefore, it was difficult to evaluate the adsorption of those pesticides based on the obtained results in this study.

In the dynamic simulation of the biological activities in the reactor, the available DO was recognized as a critical factor controlling the activities of nitrifiers and heterotrophs in the biofilm. However, no correlation could be drawn from the pesticide removals and DO consumption. As related to the micropollutants, previous studies have observed their higher removals when the nitrifying activated sludge system working at higher nitrogen loading rate (> 1 gNH_x-N/gVSS.d) [71], [72]. Because the micropollutants often presented at trace level which were insufficient to sustain the biomass growth, their removals were probably

due to the action of ammonium monooxygenase enzyme through the cometabolism of the main substrates [72]. In this study, no correlation was found between the pesticide removals and the influent NH_x-N. Even though the role of nitrifiers could not be confirmed, it should be noted that the reactor was operated at much lowered nitrogen rate comparing to those reported in wastewater treatment. Furthermore, as indicated in the simulation, the actitivity of nitrifiers were rather limited due to the dominance of the heterotrophs in the biofilm at limited DO condition. Therefore, further studies and experimental evidence should be conducted under laboratory-controlled conditions to reveal the degradation pathway of pesticides in the nitrifying expanded-bed filter.

Another factor might explain the pesticide removals in the field study. As demonstrated in [103], the pesticides might adsorb on the suspended solids (e.g. clay particles) and colloids presented in the river water. Additionally, a good correlation between removals of micropollutants by adsorption to the kaolin particles and their $\log K_{ow}$ values were demonstrated in laboratory-condition, indicating the contribution of water turbidity to the micropollutants removal efficiencies [63]. In this study, the total suspended solids concentration was found around 54.0 (SD=13.22) mg/L during the monitoring campaign [44]. All the four pesticides with removal rates higher than 50% also have high values of log K_{ow}, highlighting the possibility of adsorption onto the surface of suspended solids while no more accessible adsorption sites could be offered from the BAC bed.

7.3.2. Pesticide removals in the lab-scale reactor

7.3.2.1. Continuous experiment

As mentioned above, there was biomass developed on the used BAC at the start-up period in the lab-scale experiment. As shown in the bottom of Figure 53, there was about 5 mgO2/L consumed at day 0 and a small amount of NH_x-N was removed. After 10 days of acclimation, the influent NH_x-N of 1.11 (SD=0.13) mgN/L was removed entirely, and about 7.81 (SD=0.26) mgO2/L was stably consumed. Because the DO consumption for

nitrification was stoichiometrically 4.57 mgO_2/L for 1 mgN, it was believed that both nitrifiers and heterotrophs bacteria were stably settled onto the BAC media.

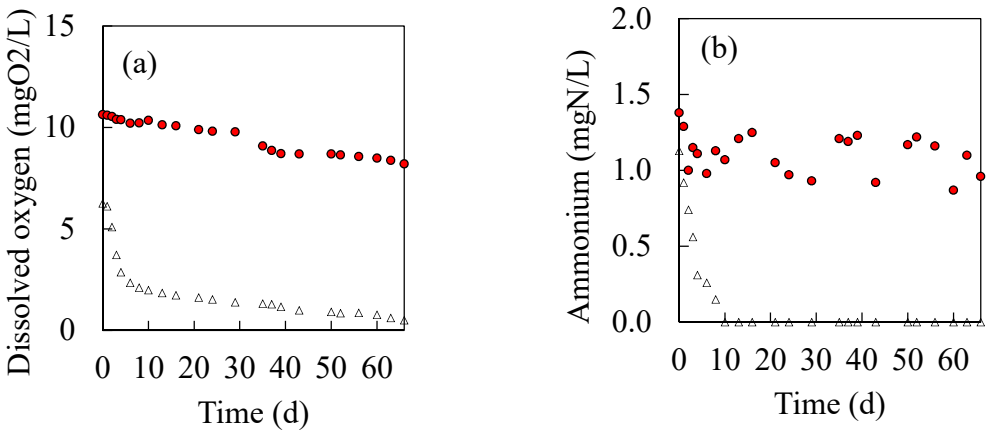

Figure 53. Influent and effluent dissolved oxygen (a) and ammonium (b) in the lab-scale reactor for pesticide removal monitoring

Regarding the pesticides, a very high removal was observed during the first several days. However, as shown in Figure 54, the removal efficiencies were gradually decreased. After 66 days of the experiment, most of the pesticide could not be removed or having removal rates lower than 20%. In the same period, better removal rates of around 40% were observed for Fenbuconazole and Buprofezin. Regarding the increasing trend of the effluent pesticides, it was speculated that the pesticide removals of Fenbuconazole and Buprofezin would reduce further as the experiment continued. While the activities of microorganisms were confirmed, the decreasing removal of the pesticides suggested that their removals might due to adsorption rather than biodegradation. It was likely that there were very limited adsorption sites on the BAC media after 2 months of the continuous experiment. To study the pesticide removal mechanisms, a series of batch experiments was carried out to evaluate the contribution of biomass to pesticide degradation.

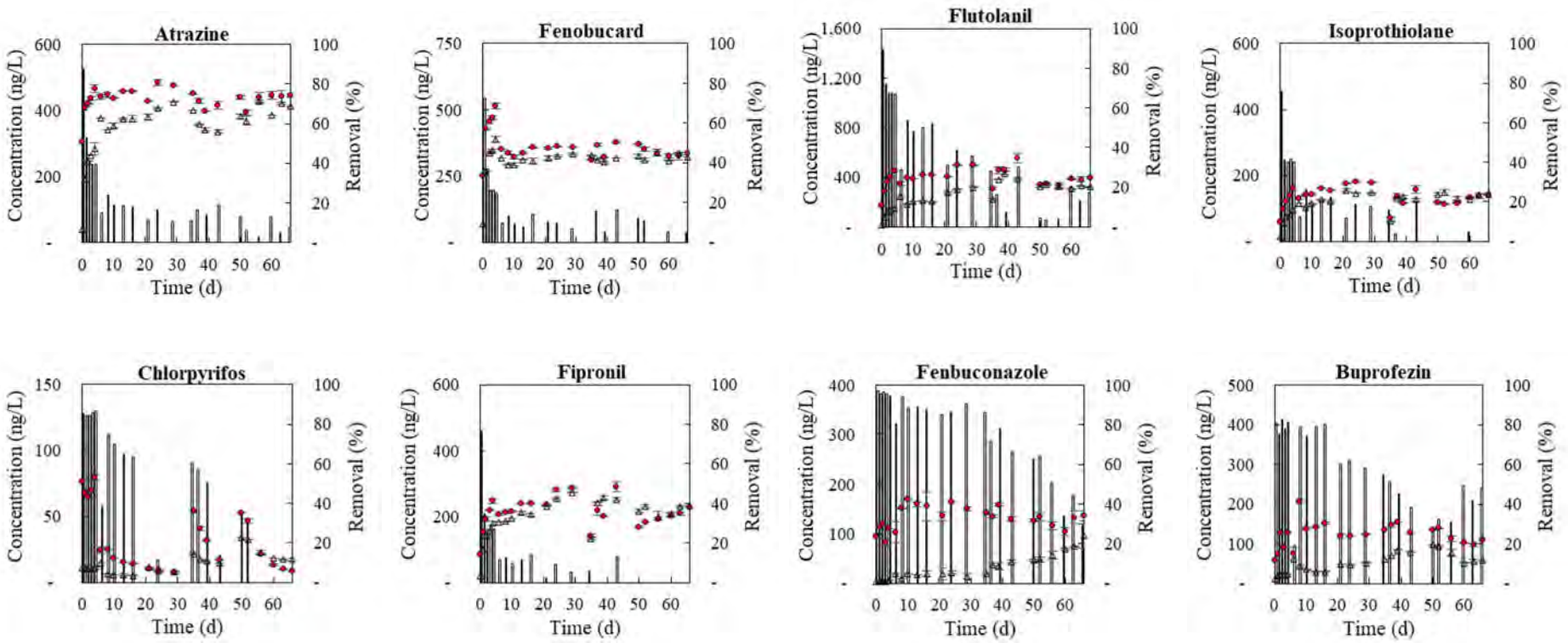

Figure 54. Influent and effluent pesticides and removal efficiencies in the lab-scale reactor (red circle = influent, white triangle = effluent, bar = removal efficiency)

7.3.2.2. Batch experiments: Contribution of biomass to pesticide removals

In the first batch experiment, the use of 500 mg/L NaN_3 successfully inhibited the biomass activities, as shown in Figure 55 (a), where the influent NH_x-N was kept almost constant during 4 hours of the experiment in control and inhibited flasks. In the non-inhibited flasks, as the DO was continuously purged in, the influent of 1 mg/L of NH_x-N was completely removed at the end of the batch experiment. As indicated in Figure 56, most of the pesticides showed no significant difference (p-value < 0.05) between the control, inhibited, and non-inhibited flasks in triplicated batch tests (Table 16). Further, the variation of pesticide concentrations in time were minor, except for Chlorpyrifos and Buprofezin. The results were consistent with those observed in the continuous experiment, confirming that the bacteria can not degrade the targeted pesticides and the removals would stop when the BAC media were saturated. As for Chlorpyrifos and Buprofezin, their concentrations were decreased in time, as proven by the highlighted p-values. However, higher degree of decline was observed when BAC media were present. It was noticeable that the log K_{ow} were 4.7 and 4.3 for Chlorpyrifos and Buprofezin, which are the highest values among those of targeted pesticides, suggesting the possibility of their adsorption onto the BAC media.

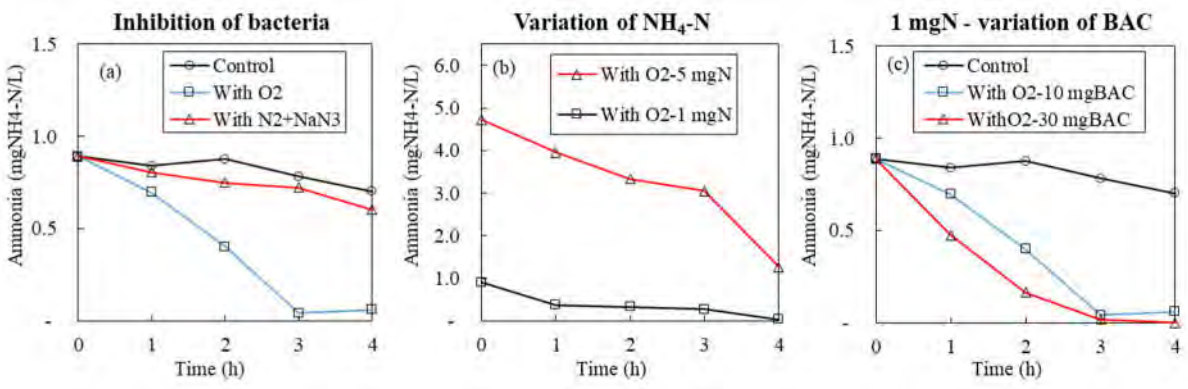

Figure 55. Ammonia concentrations in the batch experiments

Table 16 Statistical analysis for pesticide concentrations in triplicated batch experiment.

		P value			
No	Pesticide	1h	2h	3h	4h
1	Atrazine	0.11	0.59	0.89	0.45
2	Fenobucard	0.19	0.22	0.82	0.62
3	Flutolanil	0.19	0.67	0.09	0.17
4	Isoprothiolane	0.14	0.70	0.10	0.11
5	Chlorpyrifos	0.09	0.16	0.06	0.02
6	Fipronil	0.13	0.51	0.49	0.32
7	Fenbuconazole	0.11	0.63	0.48	0.01
8	Buprofezin	0.12	0.07	0.01	0.001

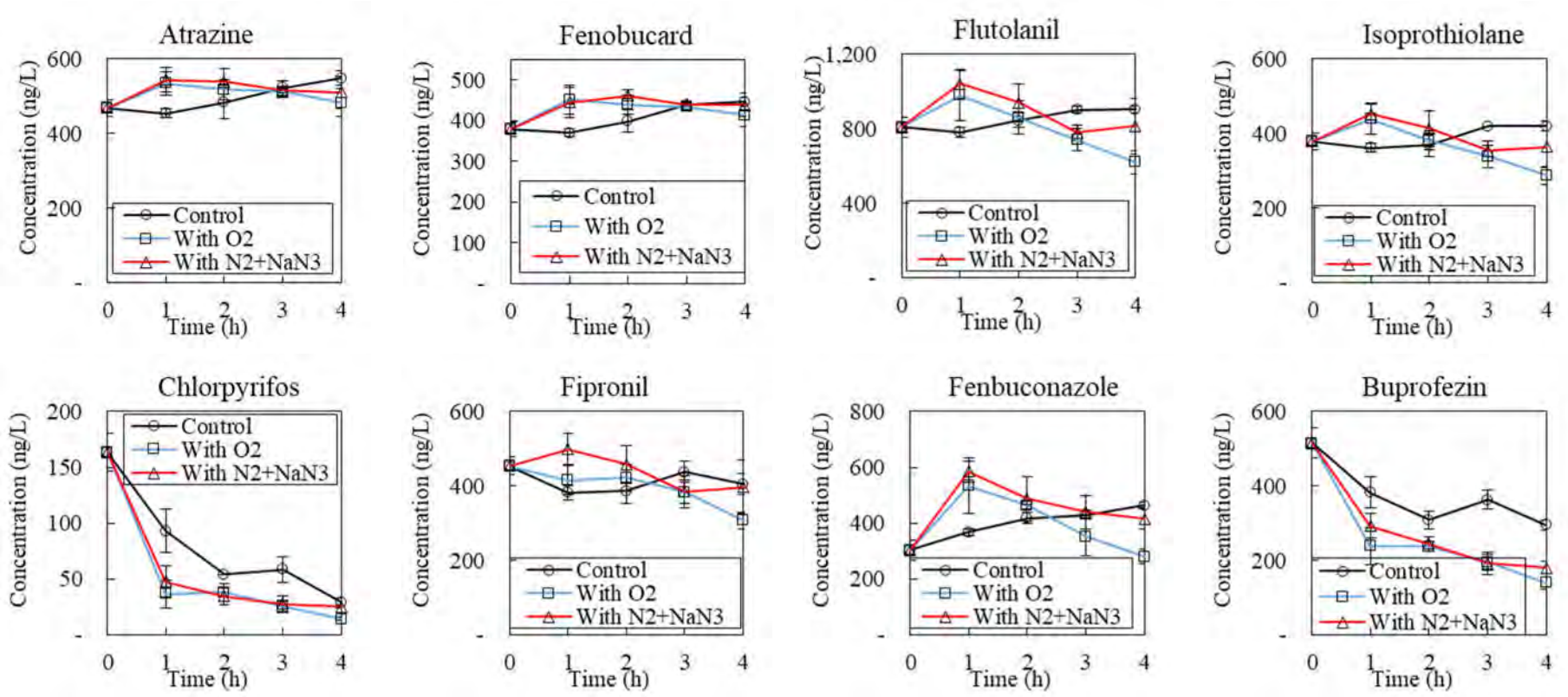

Figure 56. Influent and effluent pesticides and removal efficiencies in the lab-scale reactor (reported data = average value of triplicate measurements)

In the second and the third batch experiments, the nitrifiers activities were improved when the influent NH_x-N was increased from 1 to 5 mgN/L, or the weight of BAC media was increased from 10 to 30 g BAC, as seen in Figure 55 (b) and Figure 55 (c). However, neither changing the nitrification rates nor the biomass concentration induced any considerable influence on the pesticide removals. As shown in Figure 57, after 4 hours of the batch experiments, the pesticide concentrations were not significantly different in the control and experimental flasks. The observed maximum differences were around 20% for Flutolanil, Isoprothiolane, and Fenbuconazole. While the role of nitrifiers in improving the removals of micropollutants including pesticides in nitrifying activated sludge system [71]–[74], their insignificant contribution to the pesticide removals observed in this study might due to the different biomass composition in oligotrophic biofilm compared to those in wastewater treatment. Again, only Chlorpyrifos and Buprofezin showed a consistent decrease of concentrations in time. As for the others, the slight variations of concentration might be due to the analytical errors and instrument sensitivity, which were acceptable at these ranges of concentration.

From the results obtained in the batch experiments, the pesticide removals in the nitrifying expanded-bed reactor using BAC media was revealed. The adsorption was thought to be the main removal pathway of the pesticides. The used BAC media showed good pesticide removal efficiencies at the first beginning; however, most of the removals were gradually decreased to lower than 20% after two months of continuous operation. Although the nitrifiers were effective in removing the NH_x-N, their contribution to pesticide removals was rather limited. Therefore, the removals of some pesticides observed in the field reactor might result from the adsorption on the suspended solids in the influent water or the biofilm media in the reactor.

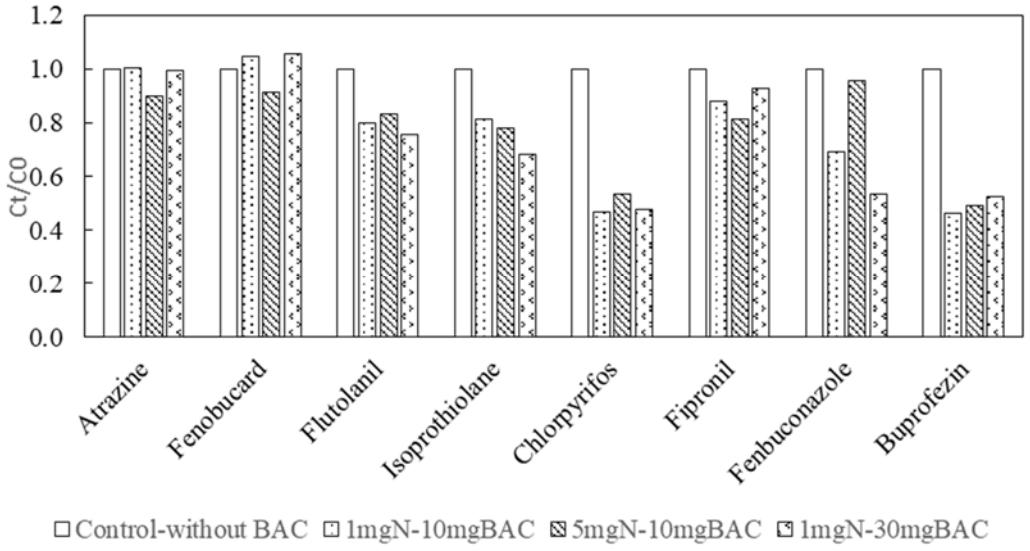

Figure 57. Pesticide ratios after 4 hours of batch experiment with variations of ammonia and biological activated carbon weight (C_t and C_0: concentrations of experimental and control flasks at 4h)

7.4. CONCLUSIONS

In this study, the pesticide occurrence and removals were monitored in a full-scale nitrifying expanded-bed reactor using BAC media. Although the recorded concentrations were relatively low comparing to regulated thresholds, detailed monitoring programs on pesticides is required at water utility taking water from pesticides related water sources. The full-scale reactor receiving river water could remove four pesticides, which were Flutolanil, Buprofezin, Chlorpyrifos, and Fenobucard at removal rates of 82%, 55%, 54%, and 52%, respectively.

While previous studies have reported the critical role of nitrifiers on the pesticide removals in wastewater treatment, this research successfully demonstrated that the nitrifying expanded-bed reactor using BAC media was not effective in removing the pesticides in drinking water treatment. In the controlled laboratory conditions, the batch experiments using microbial inhibitors or changing the nitrification rates and biomass concentrations showed insignificant differences in the removals of trace pesticides. Consequently, the adsorption onto BAC media was the main removal pathway for pesticides, which was quickly saturated after two months of operation. The obtained results highlighted the need to apply a more efficient and cost-effective technology targeting pesticide removals in drinking water treatment.

CHAPTER 8. CONCLUSIONS AND RECOMMENDATIONS

8.1. MAIN FINDINGS OF THE RESEARCH

This study investigated the pretreatment of NH_x-N and micropollutants in drinking water plants using the nitrifying expanded-bed reactor with biological activated carbon media.

The key findings of the research were as follows:

1. Among existing technologies to remove NH_x-N and micropollutants from drinking water, an up-flow biologically activated filter using activated carbon media appeared to be a suitable option regarding the treatment efficiency, cost-effectiveness, and simple operation.

2. A combined biofilm and biological model with Peterson matrix and reaction rates for two-step nitrification was developed on IFAS object in GPS-X software. The continuity of the proposed model was systematically checked and reserved

3. A physical model was developed to express an expanded-bed reactor using granular activated carbon media. A tanks-in-series model composed of 11 cell tanks, incorporated with an internal recycle flow of media, successfully demonstrated the physical and hydraulic properties of the reactor. The homogenization of the media over the expanded-bed height was achieved at the media concentration factor of 1,000 and the internal recycle flow equaled to 0.001Q. The influence of media distribution on the attached biomass was also evaluated.

4. The combined biofilm and biological model was applied for NH_x-N and organic removal in the pretreatment of drinking water. Based on the calibration of five datasets of both rivers and synthetic water, a single set of kinetic and stoichiometric parameters for AOO/NOO/OHO was elaborated that successfully demonstrated the biofilm performance, which could be used as default in designing water treatment with low-strength NH_x-N and organics. The specific rates of biofilm attachment, detachment, and internal solids exchange between biofilm layers were also examined in both filtration and backwashed cycles. A graphical guidance was provided with an empirical equation to estimate the

required dissolved oxygen to totally remove influent NH_x-N at different concentration and temperature ranges. The nitrifying expanded-bed reactor was able to remove NH_x-N and organics to some extent, depending on the influent concentration of the pollutants and DO.

5. The sensitivity analysis of numerical calculations and operational parameters on the calculation results was carried out.

6. The pesticide removal mechanisms in the nitrifying expanded-bed reactor were revealed. Adsorption appeared to be the main removal pathway, while the limited contribution of microorganisms to the pesticide degradation was observed. The pesticide removals observed in the full-scale reactor were possibly due to the adsorption onto the suspended solids particles in the influent water or to the biofilm media in the reactor.

8.2. RECOMMENDATIONS FOR FUTURE STUDIES

Based on these findings, the following topics could be develop in the future:

1. In this study, the media was simulated to be distributed evenly in the expanded-bed reactor. In the other circumstances, the media distribution in each compartment could be differentiated following the evolution of pollutants along the stream, or other specific design purposes. Using the proposed physical model with internal recycle flow with media, the equations which allows to calculate the media concentration in each compartment in their interrelation will be of beneficial for the designers.

2. The current configuration of the nitrifying expanded-bed reactor was not designed for dealing with high concentrations of NH_x-N and organics, or low concentration of DO in the water influent. As observed in the field monitoring in Vinh Bao WTP in rainy season, the intake water quality might be relatively poor and significant varied in a short period of time. More design options could be proposed to provide better reactor performance in the case of shock loading. For instance, the reactor could be designed into a multi-series reactor where aeration was conducted at the effluent of the reactor to maintain DO for the subsequent reactor. Simulations of the new configuration would help to visualize the reactor response under shock loading situations.

3. The sensitivity analysis in the modeling aims at validating the model results and identifying the parameters that have the greatest impact on the model prediction. Based on the results of the sensitivity analysis, useful guidelines could be provided to determine new experiments or data collection, or to explore operational strategies to optimize the reactor performance. At present, the IFAS object was not equipped with the sensitivity analysis function in the GPS-X software, possibly due to the complexity of the object and the function itself. In the future update of GPS-X, the sensitivity analysis could be carried out.

4. In the future, further studies should demonstrate the possibility of the nitrifying expanded-bed reactor to remove the THMs precursors (see Annex). In addition to the

natural dissolved organic compounds, the NH_x-N and organic nitrogenous substances removal in the influent water was also be uptake, resulted in the reduction of N-DBPs formation. However, the knowledge of the dominant microbial species involved in the biodegradation of DBPs, or the microorganisms involved in the cycling of nitrogen in the expanded-bed reactor is still limited. A greater understanding on how the operating conditions, such as filter media, empty bed contact time, backwashing and chemical addition could be beneficial on improving the DBPs removals in the nitrifying expanded-bed reactor [104].

REFERENCES

[1] EPA, "Aquatic Life Ambient Water Quality Criteria for Ammonia - Freshwater 2013," *United States Environ. Prot. Agency*, vol. 13, no. April, pp. 1–70, 2013.

[2] M. Constable, M. Charlton, F. Jensen, K. McDonald, G. Craig, and K. W. Taylor, "An ecological risk assessment of ammonia in the aquatic environment," *Hum. Ecol. Risk Assess.*, vol. 9, no. 2, pp. 527–548, 2003.

[3] European Food Safety Authority, "Health risk of ammonium released from water filters," *EFSA J.*, vol. 10, no. 10, pp. 1–16, 2012.

[4] Y. Du, T. Ma, Y. Deng, S. Shen, and Z. Lu, "Sources and fate of high levels of ammonium in surface water and shallow groundwater of the Jianghan Plain, Central China," *Environ. Sci. Process. Impacts*, vol. 19, no. 2, pp. 161–172, 2017.

[5] A. Bednarek, S. Szklarek, and M. Zalewski, "Nitrogen pollution removal from areas of intensive farming-comparison of various denitrification biotechnologies," *Ecohydrol. Hydrobiol.*, vol. 14, no. 2, pp. 132–141, 2014.

[6] A. G. Capodaglio, P. Hlavínek, and M. Raboni, "Physico-chemical technologies for nitrogen removal from wastewaters: a review," *Ambient. Água - An Interdiscip. J. Appl. Sci.*, vol. 10, 2015.

[7] B. Han, C. Butterly, W. Zhang, J. zheng He, and D. Chen, "Adsorbent materials for ammonium and ammonia removal: A review," *J. Clean. Prod.*, p. 124611, 2020.

[8] Vietnamese Ministry of Environment and Natural Resources, "Vietnamese National Environmental Report 2018," 2018.

[9] X. Wang *et al.*, "Water quality criteria of total ammonia nitrogen (TAN) and un-ionized ammonia (NH3-N) and their ecological risk in the Liao River, China," *Chemosphere*, vol. 243, 2020.

[10] Y. Kawabata, T. Ayush Munkhjargal, K. Shiraishi, M. Nagai, and Y. Katayama, "Water Pollution in the Rivers of Northern Central Mongolia Caused by Human Activity," *J. Arid L. Stud.*, vol. 19, no. 1, pp. 305–308, 2009.

[11] European Environment Information and Observation Network, "Indicator Assessment: Freshwater quality," 2017. [Online]. Available: https://www.eea.europa.eu/data-and-maps/indicators/freshwater-quality/freshwater-quality-assessment-published-may-2.

[12] Environment Canada, "Canadian Environmental Protection Act, 1999 - Priority Substances List Assessment Report," pp. 1–103, 1999.

[13] Water Environment Partnership in Asia, “State of water environmental issues in Japan.” [Online]. Available: http://www.wepa-db.net/policies/state/japan/japan.htm.

[14] Japanese Ministry of Enviroment, “Japanese Ministry of Enviroment - Environmental Quality Standards (EQS) for Water Pollution,” *Environmental quality standards for water pollution*. p. 2, 2013.

[15] World Health Organization (WHO), “Ammonia in Drinking-water,” *Heal. San Fr.*, vol. 2, no. 20th July, p. http://www.who.int/water_sanitation_health/dwq/che, 2003.

[16] World Health Organization, “Guidelines for Drinking-water Quality,” 2017.

[17] Vietnamese Ministry of Health, “QCVN 01-1:2018/BYT National technical regulation on Domestic Water Quality,” 2019.

[18] R. Spon, “ Do You Really Have a Free Chlorine Residual? ,” *Opflow*, vol. 34, no. 6, pp. 24–27, 2008.

[19] B. Halling-Sorensen and S. E. Jorgensen, *The Removal of Nitrogen Compounds from Wastewater*. Elsevier, 1993.

[20] World Health Organization, *Nitrate and Nitrite in Drinking Water*. 2016.

[21] M. O. Barbosa, N. F. F. Moreira, A. R. Ribeiro, M. F. R. Pereira, and A. M. T. Silva, “Occurrence and removal of organic micropollutants: An overview of the watch list of EU Decision 2015/495,” *Water Res.*, vol. 94, pp. 257–279, 2016.

[22] K. H. Kim, E. Kabir, and S. A. Jahan, “Exposure to pesticides and the associated human health effects,” *Sci. Total Environ.*, vol. 575, pp. 525–535, 2017.

[23] S. Bulut, S. F. Erdoğmuş, M. Konuk, and M. Cemek, “The organochlorine pesticide residues in the drinking waters of Afyonkarahisar, Turkey,” *Ekoloji*, no. 74, pp. 24–31, 2010.

[24] FAO and IWMI, *More people, more food, worse water? a global review of water pollution from agriculture*. 2018.

[25] F. Prieto Garcia, S. Y. Cortés Ascencio, J. C. G. Oyarzun, A. C. Hernandez, and P. V. Alavarado, “Pesticides: classification, uses and toxicity. Measures of exposure and genotoxic risks,” *J. Res. Environ. Sci. Toxicol.*, vol. 1, no. 11, pp. 2315–5698, 2012.

[26] N. Elfikrie, Y. Bin Ho, S. Z. Zaidon, H. Juahir, and E. S. S. Tan, “Occurrence of pesticides in surface water, pesticides removal efficiency in drinking water treatment plant and potential health risk to consumers in Tengi River Basin, Malaysia,” *Sci. Total Environ.*, vol. 712, 2020.

[27] M. J. Climent, E. Herrero-Hernández, M. J. Sánchez-Martín, M. S. Rodríguez-Cruz,

P. Pedreros, and R. Urrutia, “Residues of pesticides and some metabolites in dissolved and particulate phase in surface stream water of Cachapoal River basin, central Chile,” *Environ. Pollut.*, vol. 251, pp. 90–101, 2019.

[28] J. M. Montiel-León *et al.*, “Widespread occurrence and spatial distribution of glyphosate, atrazine, and neonicotinoids pesticides in the St. Lawrence and tributary rivers,” *Environ. Pollut.*, vol. 250, pp. 29–39, 2019.

[29] K. S. Rajmohan, R. Chandrasekaran, and S. Varjani, “A Review on Occurrence of Pesticides in Environment and Current Technologies for Their Remediation and Management,” *Indian J. Microbiol.*, vol. 60, no. 2, pp. 125–138, 2020.

[30] A. Derbalah, R. Chidya, W. Jadoon, and H. Sakugawa, “Temporal trends in organophosphorus pesticides use and concentrations in river water in Japan, and risk assessment,” *J. Environ. Sci. (China)*, vol. 79, pp. 135–152, 2019.

[31] E. N. Papadakis, A. Tsaboula, Z. Vryzas, A. Kotopoulou, K. Kintzikoglou, and E. Papadopoulou-Mourkidou, “Pesticides in the rivers and streams of two river basins in northern Greece,” *Sci. Total Environ.*, vol. 624, pp. 732–743, 2018.

[32] A. F. Albuquerque, J. S. Ribeiro, F. Kummrow, A. J. A. Nogueira, C. C. Montagner, and G. A. Umbuzeiro, “Pesticides in Brazilian freshwaters: A critical review,” *Environ. Sci. Process. Impacts*, vol. 18, no. 7, pp. 779–787, 2016.

[33] L. Kong, K. Kadokami, S. Wang, H. T. Duong, and H. T. C. Chau, “Monitoring of 1300 organic micro-pollutants in surface waters from Tianjin, North China,” *Chemosphere*, vol. 122, no. September, pp. 125–130, 2015.

[34] D. T. Hanh, “Occurence of organic micro-pollutants in the aquatic environment in Vietnam,” The University of Kitakyushu, Japan, 2015.

[35] Pesticide Safety Education Program, “Pesticides: Health Effects in Drinking Water,” *Cornell University*, 2012. [Online]. Available: http://psep.cce.cornell.edu/facts-slides-self/facts/pes-heef-grw85.aspx.

[36] European Commission, “Summary for Policymakers,” in *Climate Change 2013 - The Physical Science Basis*, Intergovernmental Panel on Climate Change, Ed. Cambridge: Cambridge University Press, 2018, pp. 1–30.

[37] U. Epa, “National Primary Drinking Water Regulations,” *Drink. Water Contam.*, 2009.

[38] K. Narita, Y. Matsui, K. Iwao, M. Kamata, T. Matsushita, and N. Shirasaki, “Selecting pesticides for inclusion in drinking water quality guidelines on the basis of detection probability and ranking,” *Environ. Int.*, vol. 63, pp. 114–120, 2014.

[39] S. M. Korotta-Gamage and A. Sathasivan, “A review: Potential and challenges of biologically activated carbon to remove natural organic matter in drinking water purification process,” *Chemosphere*, vol. 167, pp. 120–138, 2017.

[40] Activated Carbon Technologies Pty Ltd, “GAC - Granular Activated Carbon.” [Online]. Available: http://www.activatedcarbon.com.au/gac.htm. [Accessed: 06-Dec-2020].

[41] M. Rattier, J. Reungoat, and W. Gernjak, “Organic Micropollutant Removal by Biological Activated Carbon Filtration : A Review,” 2012.

[42] F. Çeçen and Ö. Aktaş, “Water and Wastewater Treatment: Historical Perspective of Activated Carbon Adsorption and its Integration with Biological Processes,” *Act. Carbon Water Wastewater Treat.*, pp. 1–11, 2011.

[43] D. R. Simpson, “Biofilm processes in biologically active carbon water purification,” *Water Res.*, vol. 42, no. 12, pp. 2839–2848, 2008.

[44] N. T.-M. Dao, T.-A. Nguyen, V.-A. Nguyen, M. Terashima, R. Goel, and H. Yasui, “A mathematical model of a nitrifying expanded-bed reactor for the pretreatment of drinking water,” *Biochem. Eng. J.*, vol. 158, 2020.

[45] B. E. Rittmann *et al.*, “A framework for good biofilm reactor modeling practice (GBRMP),” *Water Sci. Technol.*, vol. 77, no. 5, pp. 1149–1164, 2018.

[46] The IWA Task Group on Mathematical Modelling for Design and Operation of Biological Wastewater Treatment, *Activated Sludge Models ASM1, ASM2, ASM2D and ASM3*. IWA Publishing, 2000.

[47] H. Hauduc, L. Rieger, I. Takács, A. Héduit, P. A. Vanrolleghem, and S. Gillot, “A systematic approach for model verification: Application on seven published activated sludge models,” *Water Sci. Technol.*, vol. 61, no. 4, pp. 825–839, 2010.

[48] J. Makinia, *Mathematical Modelling and Computer Simulation of Activated Sludge Systems*. IWA Publishing, 2010.

[49] J. P. Boltz, E. Morgenroth, and D. Sen, “Mathematical modelling of biofilms and biofilm reactors for engineering design,” *Water Sci. Technol.*, vol. 62, no. 8, pp. 1821–1836, 2010.

[50] IWA Task Group on Biofilm Modeling, “Mathematical Modeling of Biofilms,” *IWA Publ.*, 2006.

[51] J. P. Boltz, B. R. Johnson, G. T. Daigger, and J. Sandino, “Modeling Integrated Fixed-Film Activated Sludge and Moving-Bed Biofilm Reactor Systems I: Mathematical Treatment and Model Development,” *Water Environ. Res.*, vol. 81,

no. 6, pp. 555–575, 2009.

[52] D. L. Harp, “Current Technology of Chlorine Analysis for Water and Wastewater, Technical Information Series,” in *Hach Company Inc, USA Booklet*, no. 17, 2002, p. 34.

[53] F. Çeçen and Ö. Aktaş, “Fundamentals of Adsorption onto Activated Carbon in Water and Wastewater Treatment,” *Act. Carbon Water Wastewater Treat.*, pp. 13–41, 2011.

[54] R. R. Karri, J. N. Sahu, and V. Chimmiri, “Critical review of abatement of ammonia from wastewater,” *J. Mol. Liq.*, vol. 261, no. 2017, pp. 21–31, 2018.

[55] A. Almutairi and L. R. Weatherley, “Intensification of ammonia removal from waste water in biologically active zeolitic ion exchange columns,” *J. Environ. Manage.*, vol. 160, pp. 128–138, 2015.

[56] Y. Wang, Y. Kmiya, and T. Okuhara, “Removal of low-concentration ammonia in water by ion-exchange using Na-mordenite,” *Water Res.*, vol. 41, no. 2, pp. 269–276, 2007.

[57] K. Dimitri Kits *et al.*, “Kinetic analysis of a complete nitrifier reveals an oligotrophic lifestyle,” *Nature*, vol. 549, no. 7671, pp. 269–272, 2017.

[58] B. E. Rittmann, L. Crawford, C. K. Tuck, and E. Namkung, “In situ determination of kinetic parameters for biofilms,” *Biotechnol. Bioeng.*, vol. 28, pp. 1753–1760, 1986.

[59] B. B. Ward, D. J. Arp, and M. G. Klotz, *Nitrification*. American Society for Microbiology Press, 2011.

[60] B. E. Rittmann and P. L. McCarty, *Environmental Biotechnology: Principles and Applications*. McGraw-Hill, 2001.

[61] L. Han *et al.*, “Comparison of NOM removal and microbial properties in up-flow/down-flow BAC filter,” *Water Res.*, vol. 47, no. 14, pp. 4861–4868, 2013.

[62] N. Nakamoto, *Progress in Slow Sand and Alternative Biofiltration Processes*. 2014.

[63] S. W. Nam, B. Il Jo, Y. Yoon, and K. D. Zoh, “Occurrence and removal of selected micropollutants in a water treatment plant,” *Chemosphere*, vol. 95, pp. 156–165, 2014.

[64] P. E. Stackelberg, J. Gibs, E. T. Furlong, M. T. Meyer, S. D. Zaugg, and R. L. Lippincott, “Efficiency of conventional drinking-water-treatment processes in removal of pharmaceuticals and other organic compounds,” *Sci. Total Environ.*, vol. 377, no. 2–3, pp. 255–272, 2007.

[65] N. Vieno, T. Tuhkanen, and L. Kronberg, “Removal of pharmaceuticals in drinking water treatment: Effect of chemical coagulation,” *Environ. Technol.*, vol. 27, no. 2, pp. 183–192, 2006.

[66] J. Benner *et al.*, “Is biological treatment a viable alternative for micropollutant removal in drinking water treatment processes?,” *Water Res.*, vol. 47, no. 16, pp. 5955–5976, 2013.

[67] T. L. Zearley and R. S. Summers, “Removal of trace organic micropollutants by drinking water biological filters,” *Environ. Sci. Technol.*, vol. 46, no. 17, pp. 9412–9419, 2012.

[68] L. Paredes, E. Fernandez-Fontaina, J. M. Lema, F. Omil, and M. Carballa, “Understanding the fate of organic micropollutants in sand and granular activated carbon biofiltration systems,” *Sci. Total Environ.*, vol. 551–552, pp. 640–648, 2016.

[69] L. juan Feng *et al.*, “Kinetic characteristics and bacterial structures in biofilm reactors with pre-cultured biofilm for source water pretreatment,” *Int. Biodeterior. Biodegrad.*, vol. 121, no. 1, pp. 26–34, 2017.

[70] L. T. J. Van Der Aa, R. J. Kolpa, L. C. Rietveld, and J. C. Van Dijk, “Improved removal of pesticides in biological granular activated carbon filters by pre-oxidation of natural organic matter,” *J. Water Supply Res. Technol. - AQUA*, vol. 61, no. 3, pp. 153–163, 2012.

[71] N. H. Tran, T. Urase, and O. Kusakabe, “The characteristics of enriched nitrifier culture in the degradation of selected pharmaceutically active compounds,” *J. Hazard. Mater.*, vol. 171, no. 1–3, pp. 1051–1057, 2009.

[72] E. Fernandez-Fontaina, F. Omil, J. M. Lema, and M. Carballa, “Influence of nitrifying conditions on the biodegradation and sorption of emerging micropollutants,” *Water Res.*, vol. 46, no. 16, pp. 5434–5444, 2012.

[73] M. Rattier, J. Reungoat, J. Keller, and W. Gernjak, “Removal of micropollutants during tertiary wastewater treatment by biofiltration: Role of nitrifiers and removal mechanisms,” *Water Res.*, vol. 54, pp. 89–99, 2014.

[74] J. Park, N. Yamashita, G. Wu, and H. Tanaka, “Removal of pharmaceuticals and personal care products by ammonia oxidizing bacteria acclimated in a membrane bioreactor: Contributions of cometabolism and endogenous respiration,” *Sci. Total Environ.*, vol. 605–606, pp. 18–25, 2017.

[75] M. Rattier, J. Reungoat, W. Gernjak, J. Keller, and A. Joss, “Investigating the role of adsorption and biodegradation in the removal of organic micropollutants during

biological activated carbon filtration of treated wastewater," *J. Water Reuse Desalin.*, vol. 2, no. 3, pp. 127–139, 2012.

[76] M. Herzberg, C. G. Dosoretz, S. Tarre, and M. Green, "Patchy biofilm coverage can explain the potential advantage of BGAC reactors," *Environ. Sci. Technol.*, vol. 37, no. 18, pp. 4274–4280, 2003.

[77] C. H. Liang, P. C. Chiang, and E. E. Chang, "Modeling the behaviors of adsorption and biodegradation in biological activated carbon filters," *Water Res.*, vol. 41, no. 15, pp. 3241–3250, 2007.

[78] P. R. S. L. A. Daniel, "A review : organic matter and ammonia removal by biological activated carbon filtration for water and wastewater treatment," *Int. J. Environ. Sci. Technol.*, no. 1995, 2019.

[79] B. P. Servais, "Biological Colonization of Granular Activated Carbon Filters in Drinking-Water Treatment," *J. Environ. Eng.*, vol. 120, no. 4, pp. 888–899, 1995.

[80] D. B. Spengel and D. A. Dzombak, "Biokinetic modeling and scale-up considerations for rotating biological contactors," *Water Environ. Res.*, vol. 64, no. 3, pp. 223–235, 1992.

[81] Hydromantis Environmental Software Solutions Inc., "Biofilm modeling in GPS-X (Recorded Webinars)," 2014. [Online]. Available: https://www.hydromantis.com/video-webinars.html.

[82] S. Lücker *et al.*, "A Nitrospira metagenome illuminates the physiology and evolution of globally important nitrite-oxidizing bacteria," *Proc. Natl. Acad. Sci. U. S. A.*, vol. 107, no. 30, pp. 13479–13484, 2010.

[83] S. Ehrich, D. Behrens, E. Lebedeva, W. Ludwig, and E. Bock, "A new obligately chemolithoautotrophic, nitrite-oxidizing bacterium, Nitrospira moscoviensis sp. nov. and its phylogenetic relationship," *Arch. Microbiol.*, vol. 164, no. 1, pp. 16–23, 1995.

[84] H. Hauduc *et al.*, "Critical review of activated sludge modeling: State of process knowledge, modeling concepts, and limitations," *Biotechnol. Bioeng.*, vol. 110, no. 1, pp. 24–46, 2013.

[85] M. Plattes, E. Henry, P. M. Schosseler, and A. Weidenhaupt, "Modelling and dynamic simulation of a moving bed bioreactor for the treatment of municipal wastewater," *Biochem. Eng. J.*, vol. 32, no. 2, pp. 61–68, 2006.

[86] G. Mannina, D. Di Trapani, G. Viviani, and H. Ødegaard, "Modelling and dynamic simulation of hybrid moving bed biofilm reactors: Model concepts and application to a pilot plant," *Biochem. Eng. J.*, vol. 56, no. 1–2, pp. 23–36, 2011.

[87] O. Levenspiel, *Tracer Technology*, vol. 96. 2012.

[88] C. Stoquart, P. Servais, and B. Barbeau, "Ammonia removal in the carbon contactor of a hybrid membrane process," *Water Res.*, vol. 67, pp. 255–266, 2014.

[89] L. Tijhuis, M. C. M. van Loosdrecht, and J. J. Heijnen, "Dynamics of biofilm detachment in biofilm airlift suspension reactors," *Biotechnol. Bioeng.*, vol. 45, no. 6, pp. 481–487, 1995.

[90] APHA/AWWA/WEF, *Standard Methods for the Examination of Water and Wastewater*, 23th ed. American Public Health Association, American Water Works Association, Water Environment Federation, 2017.

[91] X. Liu, "Drinking water biofiltration: Assessing Key and Improving Process Evaluation," University of WaterIoo, 2001.

[92] Hydromantis Environmental Software Solutions Inc., *GPS-X User's Guide Vers. 7.0*. 2017.

[93] J. Blok and J. Struys, "Measurement and validation of kinetic parameter values for prediction of biodegradation rates in sewage treatment," *Ecotoxicol. Environ. Saf.*, vol. 33, no. 3, pp. 217–227, 1996.

[94] K. Nakamura, M. Shibata, and Y. Miyaji, "Substrate affinity of oligotrophic bacteria in biofilm reactors," *Water Sci. Technol.*, 1989.

[95] Hydromantis Environmental Software Solutions Inc., *GPS-X Technical Reference Vers. 7.0*. 2017.

[96] N. D. G. Chau, Z. Sebesvari, W. Amelung, and F. G. Renaud, "Pesticide pollution of multiple drinking water sources in the Mekong Delta, Vietnam: evidence from two provinces," *Environ. Sci. Pollut. Res.*, vol. 22, no. 12, pp. 9042–9058, 2015.

[97] T. T. Pham, V. A. Nguyen, and B. Van Der Bruggen, "Pilot-scale evaluation of gac adsorption using low-cost, high-performance materials for removal of pesticides and organic matter in drinking water production," *J. Environ. Eng. (United States)*, vol. 139, no. 7, pp. 958–965, 2013.

[98] B. Van der Bruggen, K. Everaert, D. Wilms, and C. Vandecasteele, "The use of nanofiltration for the removal of pesticides from groundwater: An evaluation," *Water Sci. Technol. Water Supply*, vol. 1, no. 2, pp. 99–106, 2001.

[99] T. Alvarino, S. Suarez, J. Lema, and F. Omil, "Understanding the sorption and biotransformation of organic micropollutants in innovative biological wastewater treatment technologies," *Sci. Total Environ.*, vol. 615, pp. 297–306, 2018.

[100] R Core Team, "R: A Language and Environment for Statistical Computing." R

Foundation for Statistical Computing, 2020.

[101] C. D. S. Tomlin, *The pesticide manual : a world compendium*, Thirteen. Alton : British Crop Protection Council, 2003., 2013.

[102] H. T. Duong, K. Kadokami, S. Pan, N. Matsuura, and T. Q. Nguyen, "Screening and analysis of 940 organic micro-pollutants in river sediments in Vietnam using an automated identification and quantification database system for GC-MS," *Chemosphere*, vol. 107, pp. 462–472, 2014.

[103] T. T. Pham, "Assessment of Low Cost - High Performance Adsorbents for Safe Drinking Water Production from Polluted Surface Water . Application in Northern Vietnam," K.U. Leuven.

[104] C. Liu *et al.*, "The control of disinfection byproducts and their precursors in biologically active filtration processes," *Water Res.*, vol. 124, pp. 630–653, 2017.

[105] H. Zhang, H. Liu, X. Zhao, J. Qu, and M. Fan, "Formation of disinfection by-products in the chlorination of ammonia-containing effluents: Significance of Cl2/N ratios and the DOM fractions," *J. Hazard. Mater.*, vol. 190, no. 1–3, pp. 645–651, 2011.

[106] D. a Reckhow, D. Ph, and P. C. Singer, "Formation and Control of Disinfection By-Products," *Water Qual. Treat. A Handb. Drink. Water A Handb. Drink. Water*, pp. 1–60, 2010.

[107] Japanese Ministry of Health_Labour and Welfare, "Water quality in Japan," 2015. [Online]. Available: https://www.mhlw.go.jp/english/policy/health/water_supply/4.html. [Accessed: 04-Dec-2020].

[108] D. M. Golea *et al.*, "Influence of granular activated carbon media properties on natural organic matter and disinfection by-product precursor removal from drinking water," *Water Res.*, vol. 174, p. 115613, 2020.

[109] A. D. Shah and W. A. Mitch, "Halonitroalkanes, halonitriles, haloamides, and N-nitrosamines: A critical review of nitrogenous disinfection byproduct formation pathways," *Environ. Sci. Technol.*, vol. 46, no. 1, pp. 119–131, 2012.

[110] D. Liew, K. L. Linge, and C. A. Joll, "Formation of nitrogenous disinfection by-products in 10 chlorinated and chloraminated drinking water supply systems," *Environ. Monit. Assess.*, vol. 188, no. 9, 2016.

ANNEX

1. POSSIBILITY OF TRIHALOMETHANE PRECURSORS REMOVAL IN THE NITRIFYING EXPANDED-BED REACTOR

1.1. INTRODUCTION

Chlorination is a well-developed and widely applied process in water disinfection because of its cost-effectiveness, broad spectrum germicidal capacity, and simple practice [105]. However, chlorine oxidants also react with natural dissolved organic matters (DOM), such as humic and fulvic acids, leading to the formation of harmful and carcinogenic disinfection byproducts (DBPs). The chlorination DBPs include a wide range of halogenated and nonhalogenated organic compounds. Trihalomethane (THMs), a group of halogenated compounds, were the first class of DBPs identified in chlorinated drinking water in the 1970s [104], [106]. THMs are volatile and halogenated organic compounds, including four main compounds of chloroform ($CHCl_3$), dibromochloromethane ($CHBr_2Cl$), bromodichloromethane ($CHBrCl_2$), and bromoform ($CHBr_3$). The THMs comprise the major portion of the mass of halogenated DBPs and have been regulated in both international and national drinking water standards. In the Guidelines for drinking water quality, the WHO proposed separate values of 0.3, 0.1, 0.06, and 0.1 mg/L for $CHCl_3$, $CHBr_2Cl$, $CHBrCl_2$, and $CHBr_3$, respectively [16]. Those values were adopted in the Vietnamese drinking water standard [17]. In Japan and the EU, the regulation for THMs established the maximum permissible combined concentration of 0.1 mg/L [107], [108].

Recently, the interest in nitrogenous disinfection byproducts (N-DBPs) has been increased due to several reasons. First, the drinking water sources in many regions worldwide are gradually degraded with nitrogenous contaminants, which served as the sources for N-DBPs. Second, even present at lower concentrations, N-DBPs are significantly more toxic and have several hundred times higher cancer potency than regulated THMs [109]. However, most of these N-DBPs are not yet regulated, and the health significance of these occurrences requires further investigation. While there were no clear relationships between N-DBPs formation and organic nitrogen in the pre-disinfection water, N-DBP

concentrations were significantly correlated with dissolved organic carbon (DOC) and NH_x-N [110].

Biologically activated filters were designed to remove DOM, NH_x-N, and other contaminants in the water. Therefore, it is also possible to eliminate a fraction of biodegradable organic matters, thus preventing a reaction with chlorine to form DBPs. In the literature, the performance of biofiltration for DBP precursor removal depends on the concentration of attached biomass and precursor adsorption to filter media. The high concentration of biomass attached to the GAC media, as well as its rough and porous surface structure, offered a better reduction of trihalomethane formation potential (THMFP) compared to sand and anthracite materials. For example, biofiltration can decrease the THMFP from 80 mg/L to 71 or 68 mg/L for anthracite/sand or GAC/sand dual media fitler at the empty bed contact time of 4.5 minutes, respectively [104]. In another study, it was found that 30 % of the THM precursors were removed on BAC biofilter through long-term biodegradation. In general, the removal of THM precursors by biologically active GAC parallels the removal of DOC [106].

As shown in CHAPTER 5, the nitrifying expanded-bed reactor could remove the organic matter and NH_4-N to a certain extent, leading to possible reductions of the formation of THMs and N-DBPs. However, due to limited experimental conditions in the field study, a primary assessment on the reduction of chlorine dosage was carried out in the laboratory of Vinh Bao WTP on freshwater samples. Next, the same set of samples were stored and delivered to Japan for THMFP measurement. The production of N-DBPs was not yet analyzed in this monitoring campaign.

Rather than the DOC, previous studies suggested that UV absorbance is a good predictor of a water's tendency to form THMs [106]. Therefore, the analysis at UV absorbance of 260 nm (E260) was also conducted on the fresh samples and stored samples to estimate the loss of THM precursors during the storage and delivery process.

1.2. MATERIALS AND METHODS

In Vinh Bao WTP, five representative paired samples were taken in a day with 2 hours of an interval, at 8h, 10h, 12h, 14h, and 16h. Different doses of chlorine in the form of NaOCl solution were added to 100 mL of water samples. Using the digital residual chlorine tester (Tacmina, Japan) and the free chlorine N,N-diethyl-p-phenylenediamine (DPD) sachet reagents, the residual free chlorine ($R\text{-}Cl_2$) was measured at the time of addition, after 1 hour, and after 24 hours. The amount which resulted in 1 mg/L of free chlorine after 24 hours was used for the evaluation.

The analysis followed a Japanese protocol carried out at Water Quality Research Laboratory, Kitakyushu Water and Sewerage Bureau. The method was summarized as follows:

Table 17. Analysis protocol for THMFPs

Step	Content
Step 1	Adjust the water pH from 6.8 to 7.2
Step 2	Add NaOCl solution
Step 3	Incubate samples at 20^{o}C in 1 hour, measure the $R\text{-}Cl_2$
Step 4	Add more NaOCl if needed
Step 5	Incubate samples at 20^{o}C in 24 hours
Step 6	Measure the $R\text{-}Cl_2$, assuring the obtained value is from 1 to 2 mgCl_2/L
Step 7	Add ascorbic acid to remove $R\text{-}Cl_2$
Step 8	Measure THMs by the Purge and Trap GC-MS

Two groups of samples were designed to evaluate the loss of THMFP during storage and

delivery. In the first group, freshwater samples were treated from step 1 to step 6 to estimate the dose of chlorine to create 1 mgCl_2/L. The analysis of THMFPs was not carried out for those samples. In the second group, the fresh samples were stored for seven days, and the analysis from step 1 to step 8 was carried out at Anou WTP.

The on-site E260 analysis was carried out using a spectrophotometer in Vinh Bao WTP. The analysis on 7-day stored samples was conducted in the laboratory of the University of Kitakyushu using a spectrophotometer (Hitachi, U-5100, Japan).

1.3. RESULTS AND DISCUSSION

As shown in Figure 58, good linearity was obtained for the R-Cl_2 concentrations in five paired fresh samples. Based on this, the doses of applied NaOCl to obtain 1 mgR-Cl_2/L after 24 hours of quenching were interpolated. As indicated in Table 18, different reduction rates were observed on five paired samples. On average, it was estimated that about 40% of chlorine dosing could be saved as raw water passed through the nitrifying expanded-bed reactor. Correspondingly, the THMs precursors were also removed to some extent in the reactor.

Table 18. The dose of NaOCl applied on fresh samples to obtain 1 mgR-Cl_2 after 24h of quenching in Vinh Bao WTP

	Dose NaOCl (mg/L)					
Time (hour)	**8**	**10**	**12**	**14**	**16**	**Average**
Influent	0.10	0.11	0.13	0.11	0.11	0.11
Effluent	0.08	0.06	0.06	0.07	0.06	0.07
Reduction rate	17.7%	39.7%	54.5%	41.0%	46.5%	39.9%

In contrast, poor linearity was obtained for the R-Cl_2 concentrations in 7-day stored samples,

as shown in Figure 59. Therefore, the interpolated values to obtain 1 mgR-Cl_2/L after 24 hours of quenching were unreliable and could not be used to estimate the chlorine saving.

The THMFP analysis of the 7-day stored samples was shown in Table 19. Comparing to the Japanese water quality standard of 0.1 mg/L for THMs, the THMFP concentrations in all water samples were lower than the thresholds. On average, about 37.4% of THMs were removed by the nitrifying expanded-bed reactor.

Table 19. Trihalomethane formation potential analysis for 7-day stored sample in Vinh Bao WTP

	Time (hour)	8	10	12	14	16
Influent (mg/L)	THMs	0.059	0.051	0.052	0.051	0.047
	$CHCL_3$	0.052	0.043	0.043	0.043	0.04
	$CHBrCL_2$	0.006	0.007	0.008	0.007	0.006
	$CHBr_2CL$	0.001	0.001	0.001	0.001	0.001
	$CHBr_3$	<0.001	<0.001	<0.001	<0.001	<0.001
Effluent (mg/L)	THMs	0.032	0.03	0.036	0.032	0.032
	$CHCL_3$	0.026	0.024	0.029	0.025	0.025
	$CHBrCL_2$	0.005	0.005	0.006	0.006	0.006
	$CHBr_2CL$	0.001	0.001	0.001	0.001	0.001
	$CHBr_3$	<0.001	<0.001	<0.001	<0.001	<0.001
Reduction rate (%)	T-THM	45.8	41.2	30.8	37.3	31.9

** Detection limits: 0.001 mg/L*

However, regarding the poor linearity obtained in their R-Cl_2, it was speculated that the quality of water samples deteriorated to some extent during the seven days of storage. Additionally, during the delivery, the THMs precursors might also escape from the collected bottles.

A similar situation was observed for the E260 analysis. On average, the removal efficiencies among the five samples was found to be 16 %, as indicated in the following

table:

Table 20: The E260 analytical results on fresh samples in Vinh Bao WTP

Time (hour)	8	10	12	14	16	Average
Influent (ABS/cm)	0.051	0.044	0.04	0.041	0.038	0.043
Effluent (ABS/cm)	0.037	0.041	0.033	0.032	0.035	0.036
Reduction rate	27%	7%	18%	22%	8%	16%

However, after 7-day of storage, the removal efficiencies of E260 in all samples were negative, which suggested deterioration of water quality.

Unfortunately, there was no collected information regarding the N-DBPs production in this study. Future studies focusing on the removal efficiency and degradation mechanisms of THMs and N-DBPs precursors might enlighten their fates in the nitrifying expanded-bed reactor.

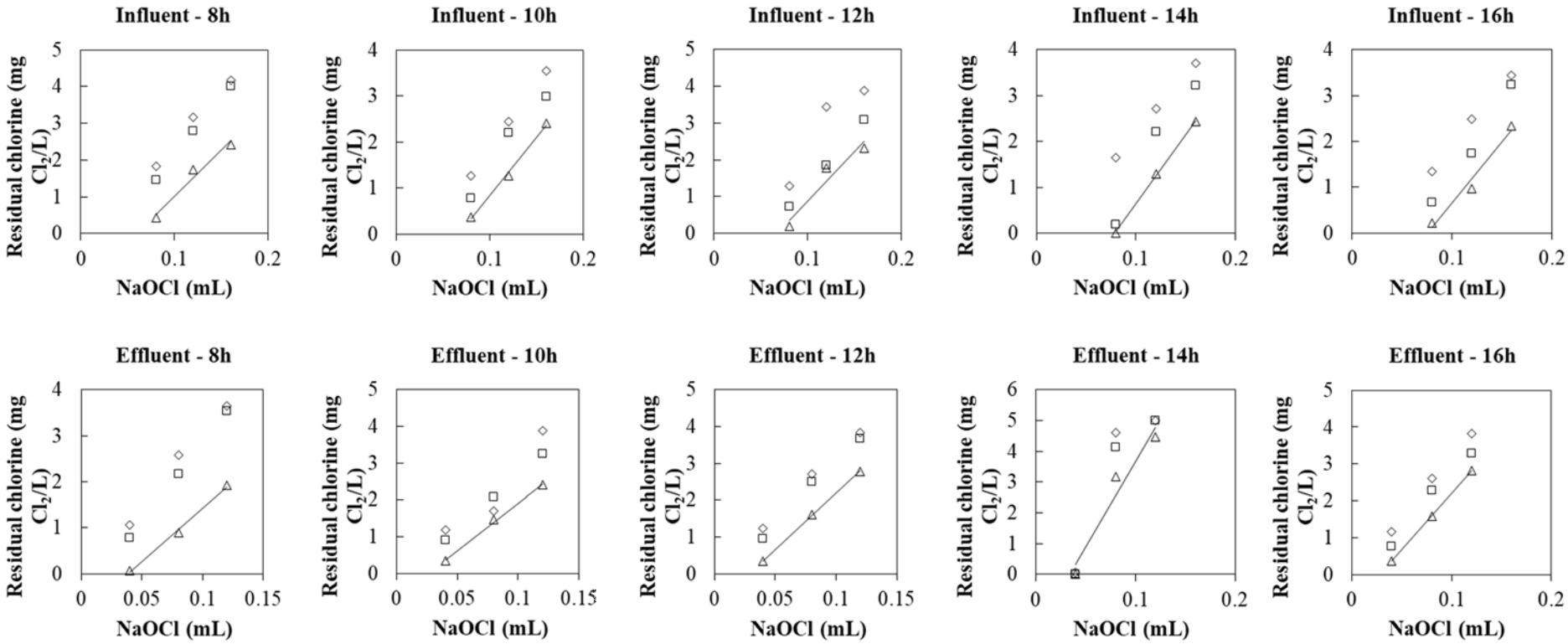

Figure 58. Free residual chlorine of fresh influent and effluent samples after 0, 1 and 24 hours of quenching in Vinh Bao WTP (rhombus = 0h, square = 1h, triangle = 24h)

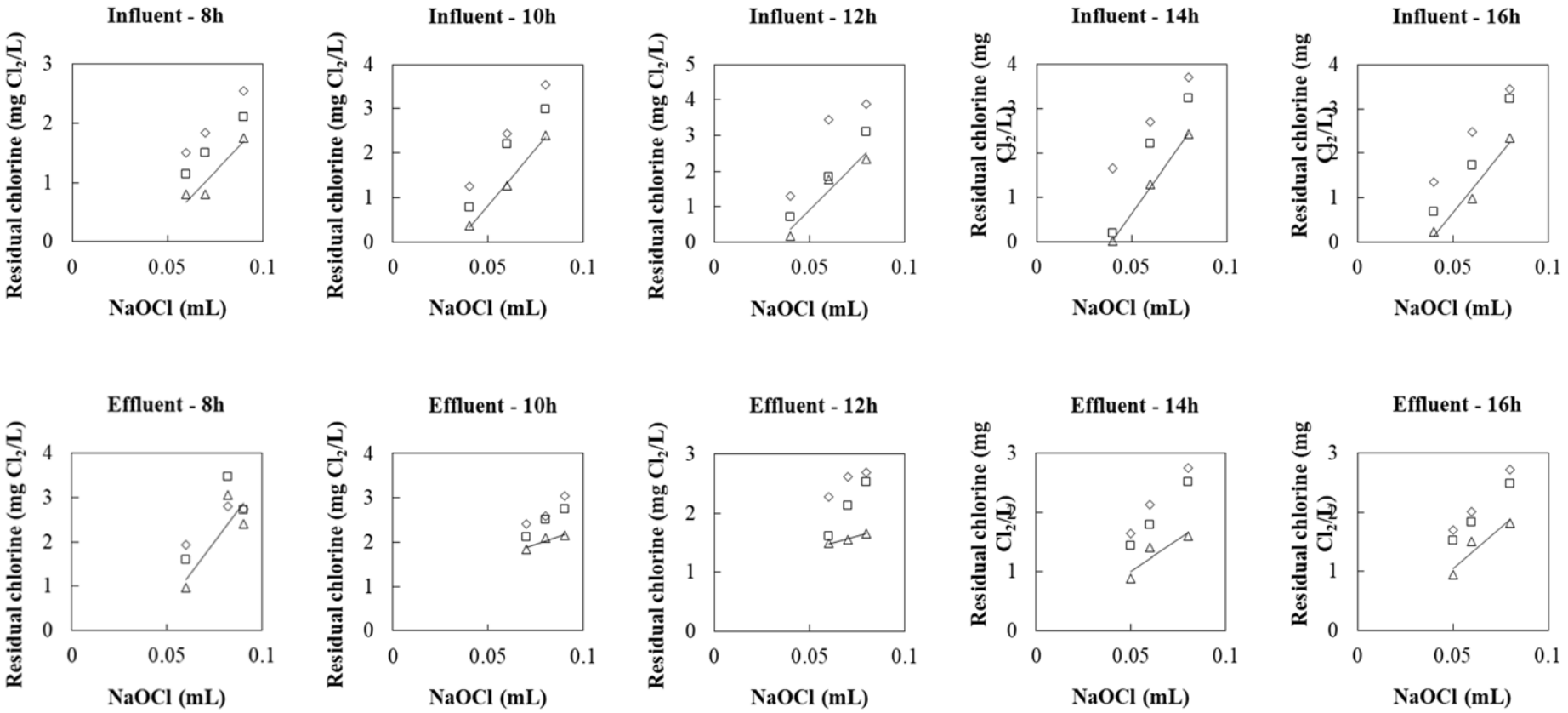

Figure 59. Free residual chlorine of 7-day stored influent and effluent samples after 0, 1 and 24 hours of quenching in laboratory (rhombus = 0h, square = 1h, triangle = 24h)

1.4. CONCLUSIONS

In this chapter, a preliminary assessment was carried out to evaluate the THMFP reduction by the nitrifying expanded-bed reactor. The analysis indicated that there was an average reduction of 37.4% of applied chlorine dosages to obtain 1 mg/L of R-Cl_2 in the influent and effluent samples. The concentrations of humic and fulvic acids which served as THMs precursors in the influent water were also decreased by 16%. Therefore it was speculated that the THMFP could be removed to some extent in the reactor. It should be noted that the sample storage and delivery could affect the sample quality. The THMFP analysis should be carried out as soon as possible to provide accurate results.

Regarding the nitrogenous pollutions in water sources, the chlorination disinfection may also produce N-DBPs together with THMs. Future studies focusing on the removal efficiency and degradation mechanisms of THMs and N-DBPs precursors might enlighten their fates in the nitrifying expanded-bed reactor.

2. COMPLETE INFORMATION FOR GPS-X SIMULATION

In total, five distinct simulation were carried out corresponding to five different datasets of:

(1). Lab-scale start-up period

(2). Lab-scale continuous operation

(3). Pilot-scale Hoa Phu WTP

(4). Full-scale Vinh Bao WTP (D)

(5). Full-scale Vinh Bao WTP (R)

The reactors from (1) to (3) have the same physical properties, while the reactors from (4) to (5) are identical.

2.1. MODEL LAYOUT

The simulations used a similar model layout as follows:

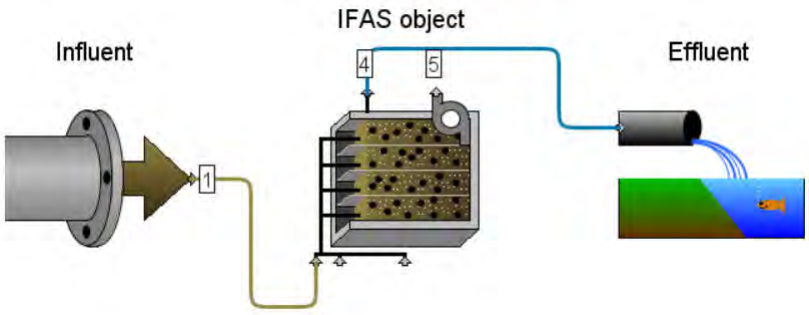

Figure 60. Model layout for five simulations

2.2. INPUT MENU

2.2.1. INFLUENT COMPOSITION

The influent composition defined in the input menu was critical, because they defined the initial biomass concentration at the time t = 0. The following data was obtained through the trials-errors approach

Content	Lab-scale start-up period	Lab-scale continuous operation	Pilot-scale Hoa Phu WTP	Full-scale Vinh Bao WTP (D)	Full-scale Vinh Bao WTP (R)
Influent Composition					
Inorganic Suspended Solids					
[1] inert inorganic suspended solids	0.0	0.0	0.0	0.0	50.0
Organic Variables					
[1] soluble inert organic material	0.0	0.0	0.0	0.0	8.5
[1] readily biodegradable substrate	0.0	0.0	3.0	8.0	3.2
[1] particulate inert organic material	0.0	0.0	0.0	0.0	8.0
[1] slowly biodegradable substrate	0.0	0.0	0.0	0.0	0.0
[1] active heterotrophic biomass	0.0	0.0	0.0	0.0	0.0
[1] active autotrophic biomass	0.0	0.0	0.0	0.0	0.0
[1] unbiodegradable particulates from cell decay	0.0	0.0	0.0	0.0	0.0
[1] internal cell storage product	0.0	0.0	0.0	0.0	0.0
Dissolved Oxygen					
[1] dissolved oxygen	8.87	6.0	6.45	7.57	5.4
Nitrogen Compounds					
[1] free and ionized ammonia	0.75	1.0	0.2	0.51	4.17
[1] soluble biodegradable organic nitrogen	0.0	0.0	0.2	0.5	0.0
[1] particulate biodegradable organic nitrogen	0.0	0.0	0.0	0.0	0.0
[1] nitrate and nitrite	0.0	0.004	0.0	0.0	0.2
[1] dinitrogen	0.68	0.4	0.0	0.0	0.0

Figure 61. Influent composition menu for five simulations

2.2.2. PHYSICAL MENU

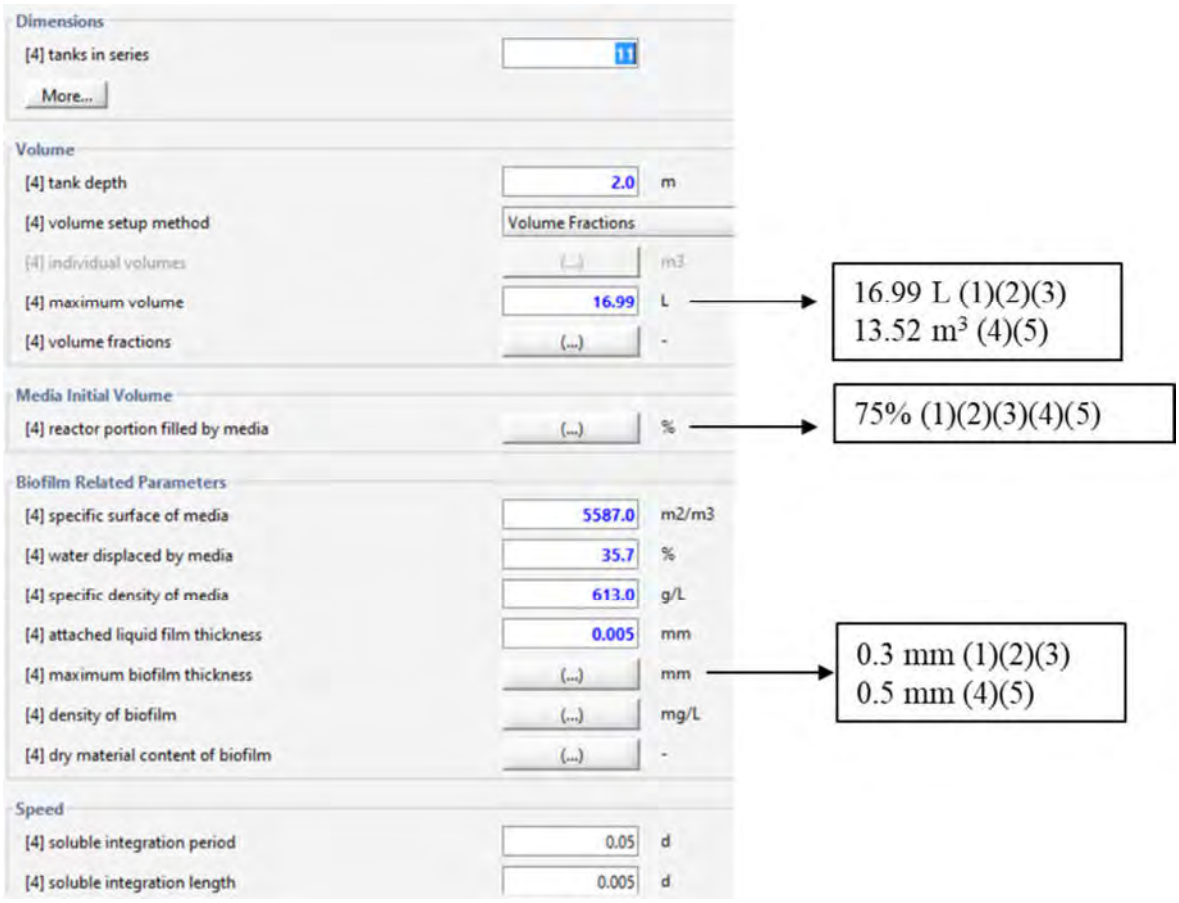

Figure 62. Physical menu for five simulations

2.2.3. OPERATIONAL MENU

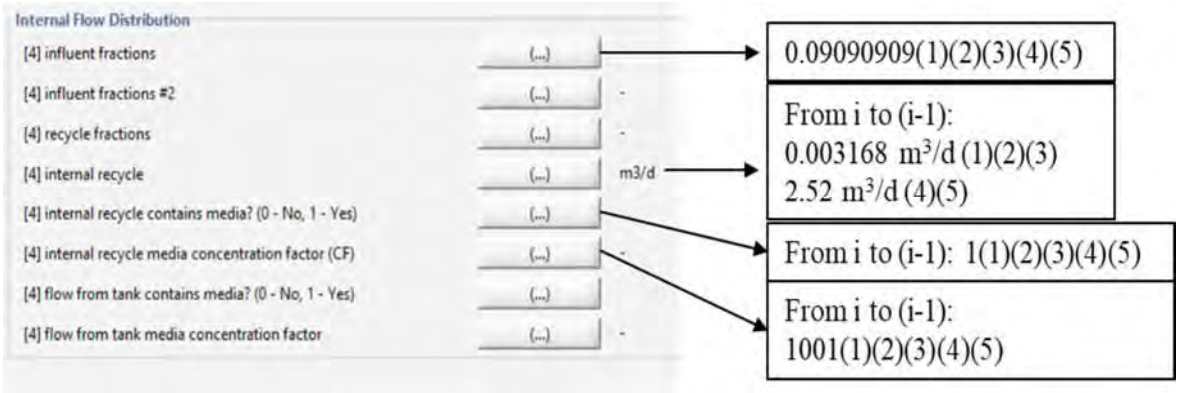

Figure 63. Operational menu for five simulations

2.2.4. MASS TRANSPORT MENU

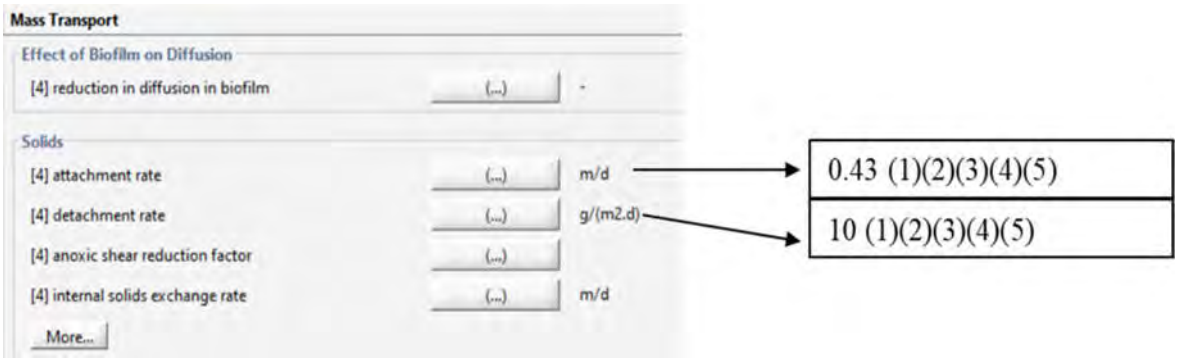

Figure 64. Mass transport menu for five simulations

2.2.5. KINETIC MENU

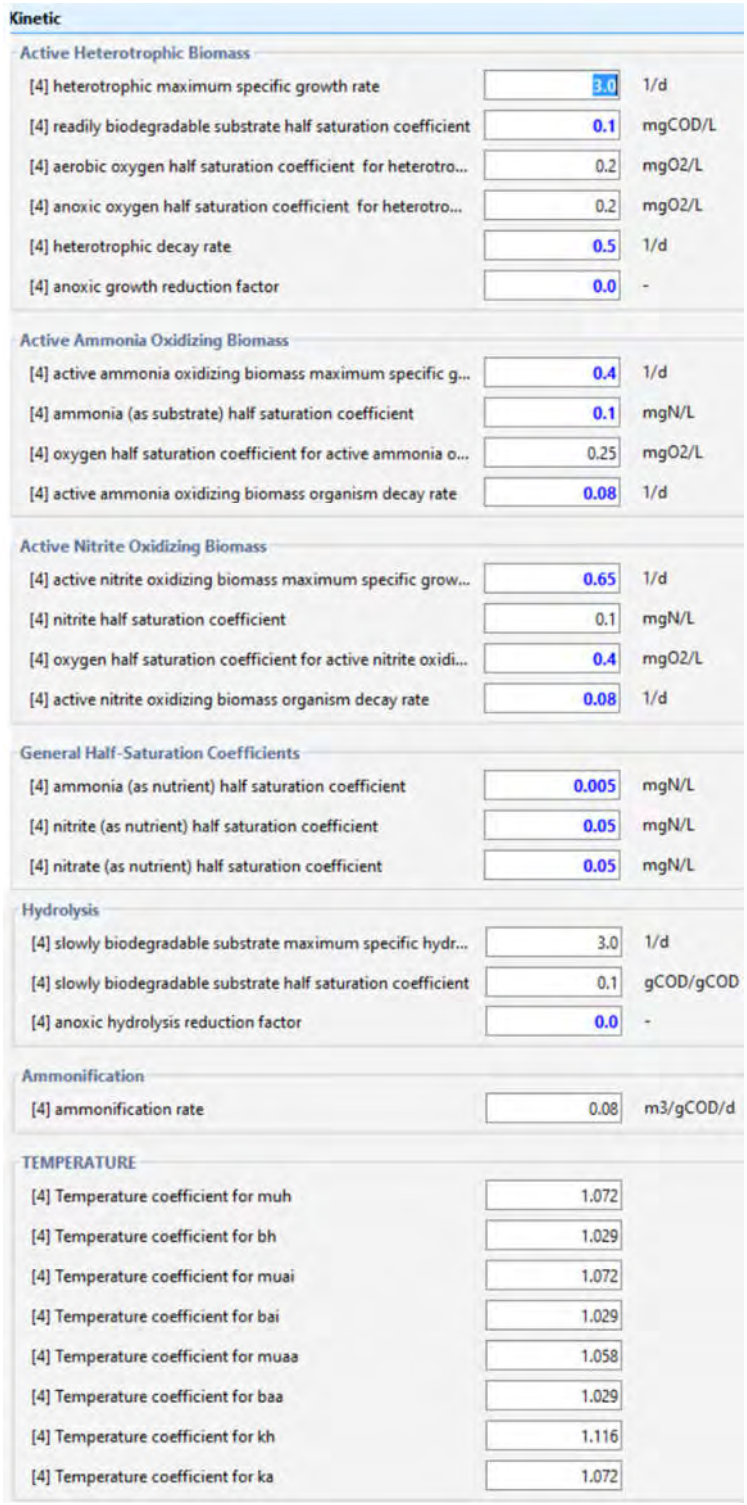

Kinetic		
Active Heterotrophic Biomass		
[4] heterotrophic maximum specific growth rate	3.0	1/d
[4] readily biodegradable substrate half saturation coefficient	0.1	mgCOD/L
[4] aerobic oxygen half saturation coefficient for heterotro...	0.2	mgO2/L
[4] anoxic oxygen half saturation coefficient for heterotro...	0.2	mgO2/L
[4] heterotrophic decay rate	0.5	1/d
[4] anoxic growth reduction factor	0.0	-
Active Ammonia Oxidizing Biomass		
[4] active ammonia oxidizing biomass maximum specific g...	0.4	1/d
[4] ammonia (as substrate) half saturation coefficient	0.1	mgN/L
[4] oxygen half saturation coefficient for active ammonia o...	0.25	mgO2/L
[4] active ammonia oxidizing biomass organism decay rate	0.08	1/d
Active Nitrite Oxidizing Biomass		
[4] active nitrite oxidizing biomass maximum specific grow...	0.65	1/d
[4] nitrite half saturation coefficient	0.1	mgN/L
[4] oxygen half saturation coefficient for active nitrite oxidi...	0.4	mgO2/L
[4] active nitrite oxidizing biomass organism decay rate	0.08	1/d
General Half-Saturation Coefficients		
[4] ammonia (as nutrient) half saturation coefficient	0.005	mgN/L
[4] nitrite (as nutrient) half saturation coefficient	0.05	mgN/L
[4] nitrate (as nutrient) half saturation coefficient	0.05	mgN/L
Hydrolysis		
[4] slowly biodegradable substrate maximum specific hydr...	3.0	1/d
[4] slowly biodegradable substrate half saturation coefficient	0.1	gCOD/gCOD
[4] anoxic hydrolysis reduction factor	0.0	-
Ammonification		
[4] ammonification rate	0.08	m3/gCOD/d
TEMPERATURE		
[4] Temperature coefficient for muh	1.072	
[4] Temperature coefficient for bh	1.029	
[4] Temperature coefficient for muai	1.072	
[4] Temperature coefficient for bai	1.029	
[4] Temperature coefficient for muaa	1.058	
[4] Temperature coefficient for baa	1.029	
[4] Temperature coefficient for kh	1.116	
[4] Temperature coefficient for ka	1.072	

Figure 65. Kinetic menu for five simulations

2.3. SIMULATON SCENARIOS

2.3.1. DATASET FOR LAB-SCALE START-UP PERIOD

t	snhcon1	sno1	snn1	so1	snh4	sno4	snn4	so4	snh1	temp
d	mgN/L	mgN/L	mgN/L	mgO2/L	mgN/L	mgN/L	mgN/L	mgO2/L	mgN/L	C
0	0.75	0.00	0.68	8.87	0.62	0.00	0.82	7.85	0.75	14.20
0.98	0.80	0.01	0.28	8.70	0.63	0.01	0.45	7.59	0.80	15.00
1.95	0.79	0.00	0.86	8.80	0.62	0.01	0.92	7.20	0.79	14.30
3	0.78	0.01	0.74	9.19	0.61	0.01	0.94	7.23	0.78	13.00
3.85	0.82	0.00	0.86	9.85	0.66	0.01	1.02	7.35	0.82	13.20
6	0.81	0.00	0.87	9.67	0.66	0.06	0.97	7.09	0.81	13.10
7.9	0.76	0.00	0.07	9.34	0.41	0.15	0.12	7.34	0.76	11.30
8.73	0.77	0.00	0.92	9.73	0.53	0.10	1.05	7.66	0.77	11.30
11.87	0.76	0.01	0.88	9.65	0.38	0.10	1.16	7.24	0.76	11.30
12.97	0.68	0.02	1.15	9.38	0.58	0.06	1.20	7.20	0.68	11.60
13.89	0.73	0.00	0.19	9.41	0.53	0.06	0.34	7.45	0.73	11.70
14.75	0.82	0.02	0.97	9.95	0.58	0.05	1.18	7.25	0.82	11.80
15.92	0.83	0.00	1.01	9.91	0.35	0.27	1.23	6.91	0.83	12.60
16.72	0.96	0.00	0.89	9.36	0.36	0.16	1.33	7.18	0.96	12.40
17.81	0.88	0.00	0.16	9.53	0.39	0.14	0.19	6.49	0.88	12.40
18.88	0.83	0.00	0.57	9.22	0.04	0.03	0.20	5.91	0.83	11.80
19.95	0.71	0.00	0.16	9.17	0.08	0.32	0.16	6.23	0.71	11.60
20.76	0.84	0.00	1.06	9.72	0.15	0.21	1.55	6.28	0.84	11.50
22	0.75	0.00	0.99	9.74	0.00	0.21	1.54	5.17	0.75	12.70
22.89	0.88	0.00	0.88	9.58	0.03	0.17	1.56	5.24	0.88	12.30
23.98	0.82	0.00	0.70	9.80	0.00	0.07	1.46	5.95	0.82	12.80
24.49	0.94	0.01	0.81	9.03	0.00	0.02	1.73	4.91	0.94	13.70
25.99	0.89	0.00	1.14	9.40	0.15	0.17	1.72	5.01	0.89	12.90
27.41	1.09	0.00	0.61	9.21	0.00	0.07	1.63	5.17	1.09	13.00
29.01	0.98	0.00	0.59	8.37	0.06	0.04	0.29	5.22	0.98	12.70
29.79	0.93	0.00	0.50	9.24	0.04	0.00	0.39	4.65	0.93	13.70
30.98	0.72	0.00	0.45	9.04	0.04	0.00	0.63	5.32	0.72	13.90
31.56	0.82	0.01	0.02	8.39	0.00	0.00	0.91	5.62	0.82	15.70
32.98	0.65	0.00	0.84	8.36	0.00	0.00	1.49	4.78	0.65	15.70
33.89	0.92	0.00	0.74	9.05	0.02	0.00	0.16	4.91	0.92	13.50
34.41	0.94	0.00	0.60	8.76	0.06	0.01	0.85	4.60	0.94	13.20
35.99	0.92	0.00	0.67	8.91	0.02	0.00	0.23	5.10	0.92	14.50
36.43	0.90	0.00	0.44	9.00	0.05	0.00	1.30	6.22	0.90	14.30
37.72	0.88	0.01	0.49	8.87	0.11	0.00	0.29	5.63	0.88	14.70
38.45	1.00	0.01	0.91	8.85	0.03	0.00	0.07	5.58	1.00	14.70
39.97	0.76	0.00	0.34	8.70	0.00	0.00	0.47	5.65	0.76	14.90
42.02	0.92	0.04	0.63	9.00	0.00	0.00	1.58	5.82	0.92	13.70
43	0.94	0.00	0.21	9.10	0.00	0.00	0.74	5.58	0.94	13.50
43.43	0.92	0.00	0.24	9.15	0.00	0.01	1.16	5.72	0.92	13.50
44.92	0.63	0.00	0.75	9.00	0.00	0.00	1.38	5.76	0.63	13.80
45.47	0.73	0.00	0.51	8.90	0.05	0.01	1.18	6.05	0.73	14.60
47.01	0.67	0.00	0.30	8.82	0.05	0.03	0.90	5.92	0.67	14.90
47.64	1.20	0.00	0.22	8.70	0.01	0.00	1.40	4.88	1.20	13.20
48.67	0.82	0.00	0.58	9.01	0.06	0.00	1.35	5.29	0.82	12.90
49.42	0.92	0.00	0.13	8.80	0.02	0.00	1.03	4.77	0.92	13.80
51.91	0.93	0.00	0.12	9.03	0.01	0.00	0.87	4.96	0.93	14.90
52.52	0.94	0.00	0.74	8.33	0.05	0.00	0.16	4.66	0.94	16.60
53.95	0.92	0.02	0.35	8.73	0.02	0.00	1.27	5.35	0.92	16.20
54.43	0.73	0.00	0.46	8.79	0.00	0.01	0.35	4.78	0.73	16.10
55.94	0.87	0.00	0.50	8.39	0.00	0.01	1.36	4.71	0.87	16.80
57.9	0.73	0.00	0.42	8.82	0.04	0.00	0.28	4.49	0.73	14.80
58.92	0.97	0.00	0.55	8.84	0.04	0.00	1.48	4.73	0.97	14.80
59.49	1.04	0.01	0.12	8.90	0.06	0.00	1.11	5.25	1.04	15.20
60.43	0.98	0.00	0.57	8.91	0.09	0.00	1.46	4.61	0.98	15.20
61.66	1.09	0.01	0.80	8.58	0.01	0.01	0.28	5.00	1.09	15.20
62.44	0.77	0.00	0.14	8.76	0.02	0.00	0.89	4.89	0.77	15.10
63.42	0.66	0.00	0.66	8.86	0.01	0.00	1.31	4.50	0.66	14.60
64.75	0.92	0.00	0.46	8.30	0.02	0.00	1.36	4.70	0.92	15.80
66.77	0.92	0.00	0.81	8.78	0.05	0.00	0.06	4.60	0.92	16.70
67.75	0.84	0.00	0.54	8.52	0.08	0.00	0.21	4.50	0.84	16.60
68.72	1.04	0.00	0.71	8.51	0.00	0.00	0.33	4.61	1.04	16.50
69.43	0.92	0.00	0.55	8.26	0.04	0.01	0.32	4.59	0.92	16.40
70.69	1.11	0.00	0.54	8.20	0.08	0.00	0.50	4.28	1.11	17.10
71.77	1.09	0.00	0.35	8.61	0.06	0.00	0.69	4.22	1.09	16.10
73.37	0.92	0.00	0.25	8.50	0.02	0.00	1.15	4.73	0.92	16.80
74.98	0.87	0.00	0.42	8.97	0.07	0.00	1.23	4.44	0.87	17.10
75.8	1.01	0.00	0.66	8.90	0.09	0.00	0.26	4.48	1.01	17.30
76.47	0.94	0.00	0.39	8.70	0.09	0.01	1.24	4.72	0.94	18.70
78.77	0.84	0.00	0.45	8.80	0.03	0.00	1.26	4.96	0.84	18.40
79.9	0.88	0.02	0.42	8.10	0.00	0.01	0.48	4.76	0.88	17.50
80.36	0.81	0.01	0.28	8.85	0.01	0.01	0.53	4.47	0.81	17.40
81.93	0.79	0.01	0.67	8.60	0.02	0.01	1.45	4.53	0.79	18.30
82.85	1.07	0.00	0.22	8.40	0.02	0.00	1.27	4.81	1.07	18.50
84.96	0.76	0.00	1.21	8.85	0.08	0.00	1.88	4.69	0.76	18.40
92.83	0.81	0.00	0.12	8.70	0.00	0.00	0.93	5.97	0.81	18.30
95.96	0.90	0.00	0.44	8.50	0.00	0.00	1.34	4.59	0.90	20.20

2.3.2. DATASET FOR LAB-SCALE CONTINOUS OPERATION

t	snhcon1	snh1	sno1	snn1	so1	snh4	sno4	snn4	so4	temp
d	mgN/L	mgN/L	mgN/L	mgN/L	mgO2/L	mgN/L	mgN/L	mgN/L	mgO2/L	C
0	1.00	1.00	0.00400	0.400	6	0.0500	0.00400	1.30	1.5	24.00
1	1.06	1.06	0.00400	0.359	6.1	0.0466	0.01890	1.47	1.48	23.90
2	1.07	1.07	0.00114	0.664	6.05	0.0710	0.01540	1.29	1.54	24.60
3	1.05	1.05	0.00286	0.383	6.08	0.1373	0.01540	1.46	1.5	25.50
4	0.95	0.95	0.00791	0.392	6.08	0.0189	0.02000	1.29	1.51	25.70
5	1.08	1.08	0.00384	0.810	6.06	0.1281	0.01860	1.41	1.63	25.40
6	1.10	1.10	0.00329	0.414	5.58	0.0751	0.01860	1.19	1.62	25.80
7	0.95	0.95	0.00819	0.384	5.59	0.0311	0.01860	1.54	1.56	26.40
8	1.02	1.02	0.00370	0.678	5.64	0.0622	0.01060	1.45	1.74	26.60
9	0.93	0.93	0.00687	0.544	5.82	0.1497	0.00950	1.15	1.82	26.60
10	0.93	0.93	0.00423	0.726	6.24	0.1660	0.00790	1.17	1.85	26.50
11	1.01	1.01	0.01098	0.215	6.19	0.0347	0.01650	1.47	1.75	26.30
12	0.92	0.92	0.01248	0.413	6.04	0.0543	0.01750	1.28	1.78	26.40
13	0.98	0.98	0.00394	0.471	6.03	0.2277	0.01130	1.24	1.74	26.50
14	1.00	1.00	0.00781	0.438	5.89	0.0492	0.00940	1.78	1.86	26.50
15	0.95	0.95	0.00365	0.301	5.93	0.0098	0.00570	1.18	1.82	26.50
16	0.99	0.99	0.00154	0.511	5.95	0.0823	0.00260	1.18	1.81	28.00
19	1.05	1.05	0.00402	0.327	7.43	0.0995	0.00350	1.16	2.19	28.10
20	0.98	0.98	0.00364	0.492	7.6	0.1038	0.00360	1.42	2.14	28.50
21	0.91	0.91	0.00312	0.151	7.25	0.0660	0.00310	1.40	2.05	29.00
22	1.47	1.47	0.02575	0.384	7.45	0.0502	0.01290	1.90	0.89	29.20
23	1.34	1.34	0.01318	0.383	7.85	0.0493	0.01120	1.81	0.88	29.50
24	1.38	1.38	0.00866	0.388	8.15	0.1656	0.00610	1.69	1.2	29.50
25	1.58	1.58	0.00514	0.497	8.15	0.2354	0.00210	1.89	1.15	29.50
26	1.52	1.52	0.00580	0.503	7.87	0.0413	0.00210	1.91	1.03	29.00
27	1.60	1.60	0.00369	0.689	7.86	0.0321	0.00260	2.03	0.95	29.50
28	1.51	1.51	0.00398	0.601	7.85	0.1325	0.01290	2.12	0.75	29.00
29	1.55	1.55	0.00696	0.563	7.82	0.1060	0.01090	1.96	0.78	28.90
30	1.46	1.46	0.01057	0.499	7.83	0.0549	0.01000	2.00	0.79	29.10
31	1.43	1.43	0.00899	0.614	7.82	0.0848	0.02750	2.01	0.89	29.50
32	1.39	1.39	0.00100	0.509	7.84	0.0501	0.00200	1.93	1.01	29.50
33	1.51	1.51	0.01397	0.509	7.9	0.0523	0.00700	1.93	1.24	29.00
34	1.44	1.44	0.00239	0.668	7.9	0.1269	0.00290	1.95	1.26	29.00
35	1.46	1.46	0.00096	0.751	7.85	0.0987	0.00050	1.91	1.08	28.90
36	1.52	1.52	0.00202	0.660	7.88	0.1064	0.00150	1.91	1.01	28.30
37	1.83	1.83	0.00050	0.542	7.95	0.1250	0.12150	2.19	0.1	28.40
38	1.91	1.91	0.00151	0.592	7.89	0.1157	0.10530	2.33	0.08	29.70
39	1.85	1.85	0.00261	0.598	7.89	0.0592	0.12270	2.39	0.1	29.70
40	1.89	1.89	0.00155	0.577	7.94	0.0861	0.09890	2.30	0.11	28.00
41	1.98	1.98	0.00156	0.604	8	0.1692	0.11880	2.24	0.24	28.30
43	2.05	2.05	0.00204	0.580	8.13	0.1905	0.20410	2.20	0.13	28.70
44	2.10	2.10	0.00459	0.610	8.21	0.0231	0.09490	1.95	0.22	28.20
45	2.06	2.06	0.00260	0.663	8.2	0.1786	0.32080	2.25	0.13	27.80
46	2.02	2.02	0.00099	0.635	8.23	0.1031	0.19930	2.30	0.07	27.20
47	2.05	2.05	0.00357	0.618	8.26	0.1755	0.28780	2.27	0.07	27.10
48	2.02	2.02	0.00523	0.579	8.3	0.2639	0.30040	2.18	0.06	25.40
49	2.12	2.12	0.00406	0.612	8.29	0.1038	0.29520	2.28	0.05	25.10
50	1.96	1.96	0.00309	0.548	8.3	0.0186	0.19440	2.22	0.07	25.00
51	1.97	1.97	0.00745	0.545	8.3	0.0710	0.12450	2.24	0.07	25.30
52	1.97	1.97	0.00483	0.460	8.28	0.0526	0.13950	2.19	0.05	24.20
53	2.04	2.04	0.00379	0.550	8.23	0.0737	0.23620	2.35	0.04	25.10
54	1.81	1.81	0.00461	0.501	8.27	0.0276	0.09940	2.28	0.16	25.00
55	1.91	1.91	0.00530	0.546	8.33	0.0331	0.17380	2.32	0.06	24.10
56	2.00	2.00	0.00518	0.532	8.39	0.0242	0.15380	2.24	0.11	24.30
57	1.95	1.95	0.00570	0.539	8.42	0.0242	0.23710	2.17	0.07	23.80
58	1.96	1.96	0.00725	0.493	8.44	0.0778	0.11860	2.19	0.1	24.10
59	2.02	2.02	0.00576	0.431	8.44	0.0687	0.21140	2.10	0.02	22.80
60	2.04	2.04	0.00665	0.388	8.35	0.1178	0.16990	2.03	0.07	23.80
61	2.00	2.00	0.00616	0.392	8.39	0.0343	0.17740	2.12	0.02	23.00
62	1.46	1.46	0.00625	0.411	8.65	0.0154	0.00110	1.84	1.78	22.90
63	1.47	1.47	0.00480	0.429	8.6	0.0212	0.00110	1.73	2.06	22.70
64	1.46	1.46	0.00669	0.500	8.63	0.0148	0.00170	1.83	2.06	22.30
65	1.47	1.47	0.02954	0.527	8.88	0.0146	0.00210	1.94	1.83	22.00
66	1.51	1.51	0.00666	0.517	8.72	0.0889	0.00200	1.93	1.88	22.30
67	1.48	1.48	0.00681	0.553	8.76	0.0222	0.00160	1.90	1.87	22.70
68	1.49	1.49	0.00566	0.550	8.76	0.0286	0.00210	1.94	2.1	22.00
69	1.50	1.50	0.00549	0.537	8.9	0.0238	0.00160	1.85	2.38	21.50
71	1.44	1.44	0.00611	0.506	8.98	0.0140	0.00100	1.85	2.34	22.30
72	1.48	1.48	0.00684	0.520	8.98	0.0227	0.00110	1.89	2.34	22.00
73	1.48	1.48	0.00585	0.554	8.63	0.0623	0.00110	1.99	2.29	21.50
74	1.47	1.47	0.00616	0.503	8.9	0.0623	0.00150	1.99	2.4	21.50
75	1.52	1.52	0.00761	0.489	8.89	0.0312	0.00100	1.93	2.53	21.90
76	1.11	1.11	0.00409	0.463	8.89	0.0172	0.00260	1.53	4.4	21.20
77	1.00	1.00	0.00308	0.525	9.15	0.0263	0.00050	1.55	4.22	21.40
78	1.00	1.00	0.00419	0.520	8.8	0.0175	0.00100	1.50	3.84	21.10
79	0.99	0.99	0.00421	0.624	9.07	0.0356	0.00110	1.35	4.47	20.00
80	0.75	0.75	0.00818	0.647	8.91	0.1850	0.00050	1.25	5.4	20.50
81	0.81	0.81	0.00586	0.647	8.6	0.0273	0.00110	1.38	4.7	20.00
82	0.96	0.96	0.00734	0.645	9.09	0.0538	0.00260	1.39	4.67	20.50
83	0.97	0.97	0.00726	0.655	8.96	0.0486	0.00100	1.40	4.72	21.80
84	0.99	0.99	0.00690	0.645	8.9	0.0802	0.00050	1.41	4.63	20.00
85	0.68	0.68	0.00800	0.609	9.02	0.0231	0.00160	1.61	4.3	17.80
86	1.02	1.02	0.00803	0.639	8.99	0.0292	0.00160	1.58	4.36	19.20
87	0.68	0.68	0.00540	0.646	9	0.0231	0.00050	1.23	5.59	19.70
88	1.00	1.00	0.00796	0.654	8.96	0.0392	0.00320	1.54	4.43	19.70
89	0.98	0.98	0.00702	0.632	9.12	0.0238	0.00160	1.52	4.26	18.00

2.3.3. DATASET FOR PILOT-SCALE HOA PHU WTP

t	so1	so4	snh1	snhcon1	snh4	snd1	sscon1	ss1	temp
d	mgO2/L	mgO2/L	mgN/L	mgN/L	mgN/L	mgN/L	mgCOD/L	mgCOD/L	C
std	6.45	3.42	0.2	0.2	0.02	0.2	3	3	30.2
0.000	6.45	3.42	0.11	0.11	0.02	0.15	3.00	3.00	30.2
0.006	6.42	3.39	0.11	0.11	0.02	0.15	3.00	3.00	30.2
0.010	6.38	3.35	0.10	0.10	0.02	0.15	3.00	3.00	30.2
0.016	6.35	3.33	0.09	0.09	0.02	0.15	3.00	3.00	30.2
0.021	6.32	3.31	0.07	0.07	0.02	0.15	3.00	3.00	30.2
0.026	6.29	5.36	0.05	0.05	0.02	0.15	3.00	3.00	30.7
0.031	6.25	7.40	0.05	0.05	0.01	0.15	3.00	3.00	31.2
0.037	6.21	7.22	0.05	0.05	0.01	0.15	3.00	3.00	32.5
0.042	6.16	7.03	0.06	0.06	0.01	0.15	3.00	3.00	33.7
0.047	6.20	5.51	0.06	0.06	0.01	0.15	3.00	3.00	32.1
0.052	6.23	3.98	0.07	0.07	0.01	0.15	3.00	3.00	30.4
0.058	5.85	4.01	0.07	0.07	0.01	0.15	3.00	3.00	30.3
0.062	5.47	4.04	0.06	0.06	0.01	0.15	3.00	3.00	30.2
0.068	5.39	3.47	0.06	0.06	0.01	0.15	3.00	3.00	30.1
0.073	5.31	2.90	0.06	0.06	0.01	0.15	3.00	3.00	30.0
0.079	5.25	2.80	0.06	0.06	0.01	0.15	3.00	3.00	30.0
0.083	5.19	2.70	0.07	0.07	0.01	0.20	3.00	3.00	29.9
0.089	5.16	2.66	0.07	0.07	0.01	0.20	3.00	3.00	29.9
0.094	5.13	2.61	0.08	0.08	0.01	0.20	3.00	3.00	29.9
0.099	5.09	2.60	0.08	0.08	0.01	0.20	3.00	3.00	30.0
0.104	5.05	2.58	0.08	0.08	0.01	0.20	3.00	3.00	30.0
0.110	5.03	2.57	0.09	0.09	0.01	0.20	3.00	3.00	29.9
0.122	5.01	2.56	0.10	0.10	0.01	0.20	3.00	3.00	29.8
0.132	4.97	2.55	0.09	0.09	0.01	0.20	3.00	3.00	29.6
0.135	4.95	2.56	0.09	0.09	0.01	0.20	3.00	3.00	29.6
0.143	4.93	2.56	0.09	0.09	0.01	0.20	3.00	3.00	29.6
0.145	4.89	2.54	0.09	0.09	0.01	0.20	3.00	3.00	29.8
0.153	4.85	2.51	0.10	0.10	0.01	0.20	3.00	3.00	30.0
0.156	4.86	2.48	0.10	0.10	0.01	0.20	3.00	3.00	30.0
0.163	4.87	2.45	0.14	0.14	0.01	0.20	3.00	3.00	30.0
0.174	4.84	2.45	0.16	0.16	0.01	0.20	3.00	3.00	29.8
0.184	4.88	2.56	0.18	0.18	0.02	0.20	3.00	3.00	29.7
0.195	4.83	2.48	0.21	0.21	0.02	0.20	3.00	3.00	29.6
0.205	4.90	2.50	0.25	0.25	0.02	0.20	3.00	3.00	29.4
0.215	4.90	2.49	0.29	0.29	0.03	0.20	3.00	3.00	29.3
0.219	4.83	2.42	0.33	0.33	0.03	0.20	3.00	3.00	29.2
0.226	4.76	2.34	0.22	0.22	0.03	0.20	3.00	3.00	29.1
0.230	4.78	2.35	0.14	0.14	0.02	0.20	3.00	3.00	29.1
0.236	4.79	2.35	0.12	0.12	0.02	0.20	3.00	3.00	29.0
0.240	4.75	2.38	0.10	0.10	0.02	0.20	3.00	3.00	29.0
0.247	4.71	2.41	0.11	0.11	0.01	0.20	3.00	3.00	29.0
0.251	5.09	2.60	0.11	0.11	0.01	0.20	3.00	3.00	30.0
0.257	4.70	2.39	0.12	0.12	0.01	0.20	3.00	3.00	28.8
0.261	4.73	2.39	0.13	0.13	0.01	0.20	3.00	3.00	28.8
0.268	4.75	2.38	0.13	0.13	0.01	0.15	3.00	3.00	28.7
0.272	4.81	2.50	0.14	0.14	0.01	0.15	3.00	3.00	28.7
0.278	4.87	2.62	0.23	0.23	0.01	0.15	3.00	3.00	28.6
0.288	4.86	2.39	0.40	0.40	0.02	0.15	3.00	3.00	28.5
0.299	4.89	2.32	0.22	0.22	0.01	0.15	3.00	3.00	28.4
0.309	4.82	2.30	0.20	0.20	0.01	0.15	2.00	2.00	28.4
0.320	4.88	2.36	0.19	0.19	0.01	0.15	2.00	2.00	28.4
0.330	4.92	2.42	0.19	0.19	0.01	0.15	2.00	2.00	28.3
0.340	4.93	2.50	0.19	0.19	0.01	0.15	2.00	2.00	28.3
0.351	5.01	2.56	0.19	0.19	0.01	0.15	2.00	2.00	28.2
0.361	5.05	2.66	0.19	0.19	0.01	0.15	2.00	2.00	28.2
0.372	5.11	2.80	0.16	0.16	0.01	0.15	2.00	2.00	28.1
0.382	5.14	2.86	0.15	0.15	0.01	0.15	2.00	2.00	28.1
0.393	5.16	2.92	0.14	0.14	0.01	0.15	2.00	2.00	28.1
0.403	5.14	2.96	0.14	0.14	0.01	0.15	2.00	2.00	28.0
0.413	5.15	2.93	0.14	0.14	0.01	0.15	2.00	2.00	28.0
0.424	5.19	3.00	0.14	0.14	0.01	0.15	2.00	2.00	28.0
0.434	5.17	2.99	0.15	0.15	0.01	0.15	2.00	2.00	27.9
0.445	5.15	2.93	0.15	0.15	0.01	0.15	2.00	2.00	27.9
0.455	5.14	2.91	0.15	0.15	0.01	0.15	2.00	2.00	27.9
0.465	5.09	2.88	0.16	0.16	0.01	0.15	2.00	2.00	27.9
0.476	5.01	2.81	0.17	0.17	0.01	0.15	2.00	2.00	27.8
0.486	4.97	2.77	0.17	0.17	0.01	0.15	2.00	2.00	27.8
0.497	4.93	2.74	0.17	0.17	0.01	0.15	3.00	3.00	27.8
0.507	4.87	2.70	0.18	0.18	0.01	0.15	3.00	3.00	27.8
0.518	4.88	2.72	0.18	0.18	0.01	0.15	3.00	3.00	27.8
0.528	4.86	2.66	0.18	0.18	0.01	0.15	3.00	3.00	27.7
0.538	4.87	2.70	0.18	0.18	0.01	0.15	3.00	3.00	27.7
0.549	4.87	2.69	0.19	0.19	0.01	0.15	3.00	3.00	27.7
0.559	4.85	2.67	0.19	0.19	0.01	0.15	3.00	3.00	27.7
0.570	4.82	2.66	0.19	0.19	0.01	0.15	3.00	3.00	27.8
0.580	4.78	2.67	0.19	0.19	0.01	0.15	3.00	3.00	27.8
0.590	4.77	2.61	0.19	0.19	0.01	0.15	3.00	3.00	27.8
0.601	4.74	2.61	0.20	0.20	0.01	0.15	3.00	3.00	27.8
0.611	4.67	2.58	0.21	0.21	0.01	0.15	3.00	3.00	27.8
0.622	4.65	2.47	0.22	0.22	0.01	0.15	3.00	3.00	27.8
0.632	4.63	2.41	0.24	0.24	0.01	0.15	3.00	3.00	27.8
0.643	4.63	2.37	0.26	0.26	0.01	0.15	3.00	3.00	27.7
0.653	4.61	2.21	0.29	0.29	0.01	0.15	3.00	3.00	27.7
0.663	4.56	2.14	0.32	0.32	0.01	0.15	3.00	3.00	27.6
0.674	4.59	2.06	0.35	0.35	0.01	0.15	3.00	3.00	27.7
0.684	4.56	1.96	0.37	0.37	0.01	0.15	3.00	3.00	27.6
0.695	4.55	1.83	0.41	0.41	0.01	0.15	3.00	3.00	27.6
0.705	4.51	1.78	0.44	0.44	0.01	0.15	3.00	3.00	27.6
0.715	4.52	1.68	0.46	0.46	0.01	0.15	3.00	3.00	27.6
0.726	4.57	1.67	0.48	0.48	0.01	0.15	3.00	3.00	27.6
0.736	4.62	1.69	0.50	0.50	0.01	0.15	3.00	3.00	27.6
0.747	4.69	1.68	0.51	0.51	0.01	0.05	0.20	0.20	27.5
0.757	4.73	1.65	0.52	0.52	0.01	0.05	0.20	0.20	27.5
0.768	4.77	1.66	0.55	0.55	0.01	0.05	0.20	0.20	27.5
0.778	4.79	1.65	0.55	0.55	0.01	0.05	0.20	0.20	27.5
0.788	4.91	1.73	0.55	0.55	0.01	0.05	0.20	0.20	27.5
0.799	4.90	1.85	0.52	0.52	0.01	0.05	0.20	0.20	27.5

0.809	4.94	1.89	0.46	0.46	0.01	0.05	0.20	0.20	27.5
0.820	4.98	2.01	0.40	0.40	0.01	0.05	0.20	0.20	27.5
0.830	5.09	2.23	0.35	0.35	0.01	0.05	0.20	0.20	27.5
0.840	5.09	2.35	0.27	0.27	0.01	0.05	0.20	0.20	27.7
0.851	5.15	2.47	0.22	0.22	0.01	0.05	0.20	0.20	28.0
0.861	5.17	2.61	0.19	0.19	0.01	0.05	0.20	0.20	28.3
0.872	5.22	2.73	0.17	0.17	0.01	0.05	0.20	0.20	28.5
0.882	5.32	2.87	0.16	0.16	0.01	0.05	0.20	0.20	28.5
0.893	5.34	2.99	0.15	0.15	0.01	0.05	0.20	0.20	28.7
0.905	5.44	3.01	0.14	0.14	0.01	0.05	0.20	0.20	28.9
0.910	5.56	3.05	0.14	0.14	0.01	0.05	0.20	0.20	29.0
0.915	5.67	3.08	0.14	0.14	0.01	0.05	0.20	0.20	29.1
0.921	5.66	3.19	0.14	0.14	0.01	0.05	0.20	0.20	29.2
0.926	5.64	3.29	0.14	0.14	0.01	0.05	0.20	0.20	29.3
0.931	5.75	3.28	0.14	0.14	0.01	0.05	0.20	0.20	29.4
0.936	5.85	3.26	0.18	0.18	0.01	0.05	0.20	0.20	29.4
0.942	5.81	3.29	0.24	0.24	0.01	0.05	0.20	0.20	29.5
0.947	5.76	3.31	0.25	0.25	0.01	0.05	0.20	0.20	29.5
0.952	5.79	3.36	0.25	0.25	0.01	0.05	0.20	0.20	29.6
0.957	5.81	3.41	0.29	0.29	0.01	0.05	0.20	0.20	29.6
0.963	5.82	3.36	0.34	0.34	0.01	0.05	0.20	0.20	29.7
0.967	5.83	3.31	0.31	0.31	0.01	0.05	0.20	0.20	29.7
0.973	5.84	3.31	0.28	0.28	0.01	0.05	0.20	0.20	29.7
0.978	5.84	3.31	0.22	0.22	0.01	0.05	0.20	0.20	29.7
0.983	5.79	3.30	0.18	0.18	0.01	0.05	0.20	0.20	29.8
0.988	5.73	3.29	0.17	0.17	0.01	0.05	0.20	0.20	29.8
0.994	5.67	3.22	0.15	0.15	0.01	0.05	0.20	0.20	29.9
0.999	5.60	3.14	0.16	0.16	0.01	0.25	3.00	3.00	29.9
1.004	5.57	3.17	0.06	0.06	0.01	0.25	3.00	3.00	30.0
1.009	5.53	3.20	0.07	0.07	0.01	0.25	3.00	3.00	30.0
1.015	5.50	3.08	0.07	0.07	0.01	0.25	3.00	3.00	30.1
1.020	5.47	2.95	0.07	0.07	0.01	0.25	3.00	3.00	30.1
1.025	5.38	2.92	0.08	0.08	0.01	0.25	3.00	3.00	30.1
1.030	5.28	2.88	0.08	0.08	0.01	0.25	3.00	3.00	30.1
1.035	5.22	2.80	0.09	0.09	0.01	0.25	3.00	3.00	30.1
1.040	5.16	2.71	0.09	0.09	0.01	0.25	3.00	3.00	30.1
1.046	5.12	2.61	0.08	0.08	0.01	0.25	3.00	3.00	30.1
1.051	5.08	2.50	0.08	0.08	0.01	0.25	3.00	3.00	30.0
1.056	5.06	2.49	0.08	0.08	0.01	0.25	3.00	3.00	30.1
1.061	5.04	2.48	0.07	0.07	0.01	0.25	3.00	3.00	30.2
1.067	5.02	2.46	0.07	0.07	0.01	0.25	3.00	3.00	30.2
1.072	4.99	2.43	0.07	0.07	0.01	0.25	3.00	3.00	30.2
1.077	4.94	2.37	0.07	0.07	0.01	0.25	3.00	3.00	30.2
1.082	4.88	2.30	0.07	0.07	0.01	0.25	3.00	3.00	30.2
1.088	4.83	2.31	0.07	0.07	0.01	0.25	3.00	3.00	30.3
1.092	4.78	2.32	0.07	0.07	0.01	0.25	3.00	3.00	30.3
1.098	4.76	2.25	0.07	0.07	0.01	0.25	3.00	3.00	30.4
1.103	4.73	2.17	0.06	0.06	0.01	0.25	3.00	3.00	30.4
1.108	4.71	2.11	0.06	0.06	0.01	0.25	3.00	3.00	30.4
1.113	4.68	2.05	0.06	0.06	0.01	0.25	3.00	3.00	30.3
1.119	4.64	2.09	0.06	0.06	0.01	0.25	3.00	3.00	30.3
1.124	4.60	2.12	0.06	0.06	0.01	0.25	3.00	3.00	30.3
1.129	4.57	2.08	0.06	0.06	0.01	0.25	3.00	3.00	30.2
1.134	4.54	2.04	0.06	0.06	0.01	0.25	3.00	3.00	30.0
1.140	4.54	2.00	0.07	0.07	0.01	0.25	3.00	3.00	29.8
1.145	4.53	1.96	0.07	0.07	0.01	0.25	3.00	3.00	29.5
1.155	4.50	2.17	0.07	0.07	0.01	0.25	3.00	3.00	29.2
1.165	4.52	2.07	0.07	0.07	0.01	0.25	3.00	3.00	29.4
1.176	4.48	2.05	0.06	0.06	0.02	0.25	3.00	3.00	29.0
1.197	4.43	2.03	0.07	0.07	0.02	0.25	3.00	3.00	29.1
1.218	4.38	2.05	0.09	0.09	0.02	0.25	3.00	3.00	28.9
1.239	4.35	2.17	0.07	0.07	0.02	0.25	3.00	3.00	28.7
1.259	4.36	2.23	0.09	0.09	0.02	0.25	3.00	3.00	28.6
1.280	4.31	2.13	0.17	0.17	0.02	0.25	3.00	3.00	28.4
1.301	4.28	1.68	0.25	0.25	0.02	0.25	3.00	3.00	28.4
1.322	4.33	1.66	0.27	0.27	0.02	0.25	3.00	3.00	28.3
1.343	4.34	1.54	0.30	0.30	0.01	0.25	3.00	3.00	28.2
1.364	4.35	1.53	0.32	0.32	0.01	0.25	3.00	3.00	28.2
1.384	4.50	1.58	0.33	0.33	0.01	0.18	1.00	1.00	28.1
1.405	4.53	1.72	0.31	0.31	0.01	0.18	1.00	1.00	28.0
1.426	4.61	1.90	0.28	0.28	0.01	0.18	1.00	1.00	28.0
1.447	4.71	2.12	0.22	0.22	0.01	0.18	1.00	1.00	28.0
1.468	4.78	2.39	0.18	0.18	0.02	0.18	1.00	1.00	27.9
1.489	4.74	2.44	0.15	0.15	0.02	0.18	1.00	1.00	27.8
1.509	4.66	2.48	0.14	0.14	0.02	0.18	1.00	1.00	27.8
1.530	4.51	2.38	0.14	0.14	0.02	0.18	1.00	1.00	27.8
1.551	4.45	2.29	0.14	0.14	0.02	0.18	1.00	1.00	27.7
1.572	4.35	2.19	0.14	0.14	0.02	0.18	3.00	3.00	27.8
1.593	4.26	2.12	0.15	0.15	0.02	0.18	3.00	3.00	27.8
1.614	4.26	2.18	0.15	0.15	0.02	0.18	3.00	3.00	27.7
1.634	4.25	2.09	0.16	0.16	0.02	0.18	3.00	3.00	27.7
1.655	4.24	2.03	0.17	0.17	0.02	0.20	3.00	3.00	27.7
1.676	4.13	1.88	0.21	0.21	0.02	0.20	3.00	3.00	27.6
1.697	4.10	1.66	0.26	0.26	0.02	0.20	3.00	3.00	27.6
1.718	4.04	1.52	0.30	0.30	0.02	0.20	3.00	3.00	27.6
1.739	4.06	1.36	0.36	0.36	0.02	0.20	3.00	3.00	27.6
1.759	4.11	1.29	0.42	0.42	0.02	0.20	3.00	3.00	27.5
1.780	4.17	1.29	0.43	0.43	0.02	0.20	3.00	3.00	27.5
1.801	4.23	1.25	0.45	0.45	0.02	0.20	2.00	2.00	27.5
1.822	4.32	1.32	0.29	0.29	0.02	0.20	2.00	2.00	27.6
1.843	4.43	1.55	0.19	0.19	0.02	0.20	2.00	2.00	27.7
1.864	4.48	1.81	0.10	0.10	0.02	0.20	2.00	2.00	28.0
1.884	4.66	2.03	0.07	0.07	0.02	0.20	2.00	2.00	28.5
1.905	3.99	7.53	0.01	0.01	0.04	0.20	2.00	2.00	27.8
1.926	3.96	4.28	0.03	0.03	0.06	0.20	2.00	2.00	28.4
1.947	3.77	2.36	0.05	0.05	0.03	0.20	2.00	2.00	28.5
1.968	3.50	2.07	0.07	0.07	0.03	0.20	2.00	2.00	29.1
1.989	3.40	1.89	0.08	0.08	0.03	0.20	2.00	2.00	29.5
2.009	3.39	1.77	0.10	0.10	0.02	0.20	0.10	0.10	29.4
2.030	3.33	1.79	0.18	0.18	0.02	0.15	0.10	0.10	29.6

2.051	3.28	1.71	0.13	0.13	0.02	0.15	0.10	0.10	29.9
2.072	3.30	1.66	0.16	0.16	0.02	0.15	0.10	0.10	30.1
2.093	3.57	2.03	0.10	0.10	0.02	0.15	0.10	0.10	30.2
2.114	3.74	2.16	0.11	0.11	0.02	0.15	0.10	0.10	30.4
2.134	4.57	2.69	0.14	0.14	0.02	0.15	0.10	0.10	30.0
2.155	4.89	2.65	0.09	0.09	0.02	0.15	0.10	0.10	30.2
2.176	5.03	2.77	0.04	0.04	0.02	0.15	0.10	0.10	30.4
2.197	5.09	3.08	0.05	0.05	0.02	0.15	0.10	0.10	30.1
2.218	5.01	3.18	0.06	0.06	0.02	0.15	0.10	0.10	29.8
2.239	5.11	3.27	0.05	0.05	0.02	0.15	0.10	0.10	29.6
2.259	5.11	3.34	0.04	0.04	0.02	0.25	2.00	2.00	29.5
2.280	4.89	3.07	0.04	0.04	0.02	0.25	2.00	2.00	29.3
2.301	4.45	2.84	0.03	0.03	0.02	0.25	2.00	2.00	29.0
2.322	4.45	2.31	0.03	0.03	0.02	0.25	2.00	2.00	28.8
2.343	3.90	2.43	0.04	0.04	0.02	0.25	2.00	2.00	28.6
2.364	3.86	2.05	0.07	0.07	0.02	0.25	2.00	2.00	28.4
2.384	3.90	2.24	0.05	0.05	0.02	0.25	2.00	2.00	28.3
2.405	3.86	2.16	0.04	0.04	0.02	0.25	2.00	2.00	28.2
2.426	3.93	2.14	0.07	0.07	0.02	0.25	2.00	2.00	28.2
2.447	3.98	2.23	0.06	0.06	0.02	0.25	2.00	2.00	28.2
2.468	3.90	2.21	0.08	0.08	0.02	0.25	2.00	2.00	28.2
2.489	3.83	2.12	0.07	0.07	0.02	0.25	2.00	2.00	28.2
2.509	3.61	2.06	0.09	0.09	0.02	0.25	2.00	2.00	28.2
2.530	3.45	1.87	0.12	0.12	0.02	0.25	2.00	2.00	28.2
2.551	3.15	1.70	0.13	0.13	0.02	0.25	2.00	2.00	28.1
2.572	3.00	1.50	0.14	0.14	0.02	0.25	2.00	2.00	28.1
2.593	2.97	1.37	0.10	0.10	0.02	0.25	2.00	2.00	28.0
2.614	2.89	1.33	0.08	0.08	0.02	0.25	2.00	2.00	27.9
2.634	2.85	1.23	0.10	0.10	0.02	0.25	2.00	2.00	27.9
2.655	2.86	1.15	0.09	0.09	0.02	0.25	2.00	2.00	27.9
2.676	3.01	1.25	0.08	0.08	0.02	0.15	0.50	0.50	27.8
2.697	3.17	1.59	0.07	0.07	0.02	0.15	0.50	0.50	27.6
2.718	3.39	1.82	0.10	0.10	0.02	0.15	0.50	0.50	27.5
2.739	3.66	2.13	0.10	0.10	0.02	0.15	0.50	0.50	27.5
2.759	4.42	2.11	0.09	0.09	0.02	0.15	0.50	0.50	27.4
2.780	4.59	2.44	0.08	0.08	0.02	0.15	0.50	0.50	27.5
2.801	4.63	2.48	0.06	0.06	0.02	0.15	0.50	0.50	27.4
2.822	4.27	2.34	0.05	0.05	0.02	0.25	1.50	1.50	27.3
2.843	3.86	2.32	0.04	0.04	0.02	0.25	1.50	1.50	27.3
2.864	4.14	2.28	0.05	0.05	0.02	0.25	1.50	1.50	27.2
2.884	4.16	2.42	0.07	0.07	0.02	0.25	1.50	1.50	27.2
2.905	4.14	2.37	0.06	0.06	0.02	0.25	1.50	1.50	27.8
2.926	4.25	2.42	0.07	0.07	0.02	0.25	1.50	1.50	28.0
2.947	4.28	2.41	0.04	0.04	0.02	0.25	1.50	1.50	28.3
2.968	4.26	2.31	0.12	0.12	0.03	0.25	1.50	1.50	28.3
2.989	4.23	2.36	0.11	0.11	0.03	0.25	1.50	1.50	28.6
3.009	4.19	2.26	0.09	0.09	0.03	0.25	1.50	1.50	29.3
3.030	4.11	2.18	0.08	0.08	0.03	0.25	1.50	1.50	29.9
3.051	4.13	2.18	0.16	0.16	0.03	0.25	1.50	1.50	29.9
3.072	4.09	2.19	0.13	0.13	0.03	0.25	1.50	1.50	30.0
3.093	4.18	2.19	0.11	0.11	0.03	0.25	1.50	1.50	30.3
3.114	4.65	7.03	0.08	0.08	0.03	0.25	1.50	1.50	34.3
3.134	4.92	4.53	0.07	0.07	0.03	0.25	1.50	1.50	30.6
3.155	4.86	3.27	0.07	0.07	0.03	0.25	1.50	1.50	30.7
3.176	4.97	3.04	0.08	0.08	0.03	0.25	1.50	1.50	30.7
3.197	5.11	3.01	0.09	0.09	0.03	0.25	1.50	1.50	30.6
3.218	5.04	2.99	0.10	0.10	0.03	0.25	1.50	1.50	30.7
3.239	5.06	2.99	0.08	0.08	0.03	0.25	1.50	1.50	30.6
3.259	5.01	2.96	0.09	0.09	0.03	0.25	1.50	1.50	30.5
3.280	5.01	2.99	0.12	0.12	0.03	0.25	1.50	1.50	30.1
3.301	4.74	2.97	0.14	0.14	0.03	0.25	3.00	3.00	29.8
3.322	4.49	2.77	0.15	0.15	0.03	0.25	3.00	3.00	29.4
3.343	4.20	2.63	0.17	0.17	0.03	0.25	3.00	3.00	29.1
3.364	3.89	2.23	0.17	0.17	0.03	0.25	3.00	3.00	28.9
3.384	3.68	1.93	0.18	0.18	0.03	0.25	3.00	3.00	28.8
3.405	3.57	1.95	0.19	0.19	0.03	0.25	3.00	3.00	28.7
3.426	3.56	1.73	0.22	0.22	0.03	0.25	3.00	3.00	28.6
3.447	3.62	1.89	0.20	0.20	0.03	0.25	1.50	1.50	28.5
3.468	3.68	1.87	0.19	0.19	0.03	0.25	1.50	1.50	28.4
3.489	3.68	1.91	0.18	0.18	0.03	0.25	1.50	1.50	28.3
3.509	3.69	1.92	0.17	0.17	0.03	0.25	1.50	1.50	28.3
3.530	3.61	1.87	0.18	0.18	0.03	0.15	1.50	1.50	28.2
3.551	3.38	1.72	0.22	0.22	0.03	0.15	1.50	1.50	28.2
3.572	3.29	1.66	0.20	0.20	0.03	0.15	1.50	1.50	28.2
3.593	3.16	1.54	0.21	0.21	0.03	0.15	1.50	1.50	28.2
3.614	3.17	1.52	0.22	0.22	0.03	0.15	1.50	1.50	28.1
3.634	3.14	1.52	0.17	0.17	0.03	0.15	1.50	1.50	28.0
3.655	2.95	1.38	0.18	0.18	0.03	0.15	1.50	1.50	27.9
3.676	3.15	1.40	0.20	0.20	0.03	0.15	0.05	0.05	27.8
3.697	3.32	1.55	0.20	0.20	0.03	0.15	0.05	0.05	27.7
3.718	3.67	1.72	0.19	0.19	0.03	0.15	0.05	0.05	27.6
3.739	4.24	2.01	0.23	0.23	0.03	0.05	0.05	0.05	27.6
3.759	4.08	2.32	0.25	0.25	0.04	0.05	0.05	0.05	27.5
3.780	4.20	2.45	0.38	0.38	0.03	0.05	0.05	0.05	27.5
3.801	4.18	2.54	0.37	0.37	0.03	0.05	0.05	0.05	27.5
3.822	5.22	2.55	0.36	0.36	0.03	0.05	0.05	0.05	27.5
3.843	4.66	2.49	0.32	0.32	0.03	0.05	0.05	0.05	27.5
3.864	4.66	2.71	0.28	0.28	0.03	0.05	0.05	0.05	27.4
3.884	4.38	2.55	0.26	0.26	0.03	0.05	0.05	0.05	27.5
3.905	4.78	2.48	0.24	0.24	0.03	0.05	0.05	0.05	27.6
3.926	4.15	2.41	0.22	0.22	0.03	0.05	0.05	0.05	28.4
3.947	4.17	2.20	0.15	0.15	0.03	0.05	0.05	0.05	28.8
3.968	4.11	2.06	0.14	0.14	0.03	0.05	0.05	0.05	29.6
3.989	4.11	2.17	0.13	0.13	0.02	0.05	0.05	0.05	29.3
4.009	4.11	2.05	0.13	0.13	0.02	0.05	0.05	0.05	29.4
4.030	4.16	7.39	0.15	0.15	0.02	0.20	0.05	0.05	31.2
4.051	4.09	3.08	0.12	0.12	0.02	0.20	0.05	0.05	30.0
4.072	4.20	2.66	0.09	0.09	0.02	0.20	0.05	0.05	30.1
4.093	4.19	2.74	0.09	0.09	0.02	0.20	0.05	0.05	30.1
4.114	4.17	2.89	0.08	0.08	0.02	0.20	0.05	0.05	30.2
4.134	4.23	2.89	0.07	0.07	0.02	0.20	0.05	0.05	30.3
4.155	5.02	2.86	0.06	0.06	0.02	0.20	0.05	0.05	30.8
4.176	4.35	2.92	0.05	0.05	0.02	0.20	0.05	0.05	31.0
4.197	4.93	2.85	0.06	0.06	0.02	0.20	0.05	0.05	30.4
4.218	5.05	3.48	0.06	0.06	0.02	0.20	0.05	0.05	30.0
4.239	5.13	3.58	0.06	0.06	0.02	0.20	0.05	0.05	29.8
4.259	5.05	3.32	0.06	0.06	0.02	0.20	3.00	3.00	29.6
4.280	5.01	3.39	0.08	0.08	0.02	0.25	3.00	3.00	29.4
4.301	4.88	3.43	0.09	0.09	0.02	0.25	3.00	3.00	29.3
4.322	4.74	3.05	0.10	0.10	0.02	0.25	3.00	3.00	29.1
4.343	4.46	2.97	0.12	0.12	0.02	0.25	3.00	3.00	28.9
4.364	4.38	2.86	0.13	0.13	0.03	0.25	3.00	3.00	28.8
4.384	4.76	2.66	0.15	0.15	0.03	0.25	3.00	3.00	28.7
4.405	3.94	2.19	0.20	0.20	0.03	0.25	3.00	3.00	28.7
4.426	4.54	2.23	0.26	0.26	0.03	0.25	3.00	3.00	28.6
4.447	3.80	2.34	0.24	0.24	0.03	0.25	3.00	3.00	28.6
4.468	3.84	2.37	0.17	0.17	0.03	0.25	3.00	3.00	28.6
4.489	3.84	2.33	0.17	0.17	0.03	0.25	3.00	3.00	28.6
4.509	3.86	2.28	0.18	0.18	0.03	0.25	3.00	3.00	28.6

2.3.4. DATASET FOR FULL-SCALE VINH BAO WTP (D)

t	snhcon1	snh1	snd1	so1	sscon1	snh4	so4	temp
d	mgN/L	mgN/L	mgN/L	mgO2/L	mgCOD/L	mgN/L	mgO2/L	C
std	0.51	0.51	0.50	7.57	8.00	0.15	0.03	20.70
0.000	0.51	0.51	0.75	7.57	8.00	0.15	0.03	20.70
0.010	0.30	0.30	0.75	7.60	8.00	0.05	0.05	20.70
0.021	0.22	0.22	0.75	7.65	8.00	0.03	0.10	20.70
0.031	0.19	0.19	0.75	7.67	8.00	0.02	0.11	20.70
0.042	0.17	0.17	0.75	7.65	8.00	0.02	0.05	20.70
0.052	0.17	0.17	0.75	7.68	8.00	0.01	0.03	20.70
0.063	0.15	0.15	0.75	7.73	8.00	0.01	0.11	20.80
0.073	0.14	0.14	0.75	7.73	8.00	0.01	0.03	20.80
0.083	0.18	0.18	0.75	7.72	8.00	0.01	0.18	20.80
0.094	0.20	0.20	0.75	7.74	8.00	0.01	0.00	20.80
0.104	0.22	0.22	0.75	7.74	8.00	0.02	0.20	20.80
0.115	0.24	0.24	0.75	7.75	8.00	0.03	0.04	20.80
0.125	0.25	0.25	0.75	7.71	8.00	0.04	0.12	20.80
0.138	0.26	0.26	0.75	7.67	8.00	0.05	0.20	20.80
0.148	0.21	0.21	0.75	7.58	8.00	0.03	0.35	20.80
0.158	0.19	0.19	0.75	7.59	8.00	0.02	0.51	20.80
0.169	0.17	0.17	0.75	7.58	8.00	0.01	0.33	20.80
0.179	0.16	0.16	0.75	7.61	8.00	0.01	0.33	20.80
0.190	0.15	0.15	0.75	7.60	8.00	0.01	0.35	20.80
0.200	0.15	0.15	0.75	7.58	8.00	0.01	0.31	20.80
0.210	0.14	0.14	0.75	7.54	8.00	0.01	0.27	20.80
0.221	0.14	0.14	0.50	7.55	8.00	0.01	0.28	20.70
0.231	0.14	0.14	0.50	7.52	8.00	0.01	0.35	20.70
0.242	0.13	0.13	0.50	7.51	8.00	0.01	0.46	20.70
0.252	0.10	0.10	0.50	7.52	8.00	0.01	0.52	20.70
0.262	0.10	0.10	0.50	7.50	8.00	0.01	0.34	20.70
0.273	0.10	0.10	0.50	7.47	8.00	0.01	0.54	20.70
0.283	0.10	0.10	0.50	7.47	8.00	0.01	0.47	20.70
0.294	0.11	0.11	0.50	7.45	8.00	0.01	0.54	20.70
0.304	0.11	0.11	0.50	7.47	8.00	0.01	0.59	20.70
0.315	0.11	0.11	0.50	7.47	8.00	0.01	0.57	20.70
0.325	0.11	0.11	0.50	7.44	8.00	0.01	0.67	20.70
0.335	0.11	0.11	0.50	7.42	8.00	0.01	0.90	20.70
0.346	0.11	0.11	0.50	7.42	8.00	0.01	0.99	20.70
0.356	0.12	0.12	0.50	7.42	8.00	0.01	0.95	20.69
0.367	0.12	0.12	0.50	7.42	8.00	0.01	0.92	20.68
0.377	0.12	0.12	0.50	7.42	8.00	0.01	0.88	20.66
0.387	0.12	0.12	0.50	7.43	8.00	0.02	0.85	20.65
0.398	0.12	0.12	0.50	7.43	8.00	0.02	0.81	20.64
0.408	0.12	0.12	0.50	7.43	8.00	0.02	0.77	20.63
0.419	0.13	0.13	0.50	7.43	8.00	0.02	0.74	20.61
0.429	0.13	0.13	0.50	7.43	8.00	0.02	0.72	20.61
0.435	0.13	0.13	0.50	7.43	8.00	0.02	0.70	20.60
0.446	0.11	0.11	0.50	7.46	8.00	0.02	0.87	20.60
0.456	0.10	0.10	0.50	7.44	5.00	0.01	1.05	20.60
0.466	0.08	0.08	0.50	7.43	5.00	0.01	1.44	20.60
0.477	0.08	0.08	0.50	7.46	5.00	0.01	1.23	20.60
0.487	0.08	0.08	0.50	7.42	5.00	0.01	1.48	20.60
0.498	0.07	0.07	0.50	7.43	5.00	0.01	1.41	20.60
0.508	0.07	0.07	0.50	7.41	5.00	0.01	1.64	20.60
0.519	0.07	0.07	0.50	7.39	5.00	0.01	1.79	20.60
0.529	0.06	0.06	0.50	7.39	5.00	0.01	1.64	20.60
0.539	0.06	0.06	0.50	7.38	5.00	0.01	1.50	20.60
0.550	0.06	0.06	0.50	7.38	5.00	0.01	1.80	20.60
0.560	0.06	0.06	0.50	7.35	5.00	0.01	1.83	20.50
0.571	0.06	0.06	0.50	7.35	5.00	0.00	1.62	20.50
0.581	0.06	0.06	0.50	7.35	5.00	0.00	1.70	20.50
0.591	0.05	0.05	0.50	7.34	5.00	0.00	1.67	20.50
0.602	0.05	0.05	0.50	7.34	5.00	0.00	1.69	20.50
0.612	0.05	0.05	0.50	7.33	5.00	0.00	1.86	20.50
0.623	0.05	0.05	0.50	7.33	5.00	0.00	1.83	20.50
0.633	0.05	0.05	0.50	7.32	5.00	0.00	1.78	20.50
0.644	0.05	0.05	0.50	7.33	5.00	0.00	1.74	20.50
0.654	0.05	0.05	0.50	7.31	5.00	0.00	1.97	20.50
0.664	0.05	0.05	0.50	7.32	5.00	0.00	1.94	20.50
0.675	0.05	0.05	0.50	7.32	5.00	0.00	1.97	20.50
0.685	0.04	0.04	0.50	7.31	5.00	0.00	1.85	20.50
0.696	0.04	0.04	0.50	7.31	5.00	0.00	1.87	20.50
0.706	0.04	0.04	0.50	7.31	5.00	0.00	1.92	20.50
0.716	0.04	0.04	0.50	7.32	5.00	0.00	2.05	20.50
0.727	0.04	0.04	0.50	7.32	5.00	0.00	1.99	20.50
0.737	0.04	0.04	0.50	7.30	5.00	0.00	2.00	20.50
0.748	0.04	0.04	0.50	7.30	5.00	0.00	2.28	20.40
0.758	0.04	0.04	0.50	7.30	5.00	0.00	2.18	20.40
0.769	0.04	0.04	0.50	7.27	5.00	0.00	2.04	20.40
0.779	0.04	0.04	0.50	7.29	5.00	0.00	2.04	20.40
0.789	0.04	0.04	0.50	7.29	5.00	0.00	2.13	20.40
0.800	0.03	0.03	0.50	7.26	5.00	0.00	2.05	20.40
0.810	0.03	0.03	0.50	7.26	5.00	0.00	2.08	20.40
0.821	0.03	0.03	0.50	7.25	5.00	0.00	2.18	20.40
0.831	0.03	0.03	0.50	7.25	5.00	0.00	2.11	20.40
0.841	0.03	0.03	0.50	7.25	5.00	0.00	2.18	20.40
0.852	0.03	0.03	0.50	7.24	5.00	0.00	2.14	20.50
0.862	0.03	0.03	0.50	7.23	5.00	0.00	2.04	20.50
0.883	0.02	0.02	0.50	7.23	5.00	0.00	2.28	20.50
0.894	0.02	0.02	0.50	7.23	5.00	0.00	2.11	20.50
0.904	0.02	0.02	0.50	7.23	5.00	0.00	2.47	20.50
0.915	0.02	0.02	0.50	7.22	5.00	0.00	2.09	20.50
0.925	0.02	0.02	0.50	7.21	5.00	0.00	2.26	20.50
0.935	0.02	0.02	0.50	7.21	5.00	0.00	2.07	20.60
0.946	0.02	0.02	0.50	7.21	5.00	0.00	2.12	20.60
0.956	0.02	0.02	0.50	7.21	5.00	0.00	2.07	20.60
0.967	0.02	0.02	0.50	7.20	5.00	0.00	2.01	20.60
0.977	0.02	0.02	0.50	7.20	5.00	0.00	2.06	20.70
0.987	0.01	0.01	0.50	7.21	5.00	0.00	1.99	20.70
0.998	0.01	0.01	0.50	7.21	5.00	0.00	2.31	20.70
1.008	0.01	0.01	0.50	7.19	5.00	0.00	2.13	20.70

1.019	0.01	0.01	0.50	7.19	5.00	0.00	2.07	20.70
1.029	0.01	0.01	0.50	7.20	5.00	0.00	2.37	20.80
1.040	0.02	0.02	0.50	7.20	5.00	0.00	2.08	20.80
1.050	0.02	0.02	0.50	7.21	5.00	0.00	2.09	20.80
1.060	0.02	0.02	0.50	7.21	5.00	0.01	2.05	20.90
1.071	0.02	0.02	0.50	7.22	5.00	0.01	2.09	20.90
1.081	0.02	0.02	0.50	7.21	5.00	0.01	2.10	20.90
1.092	0.02	0.02	0.50	7.24	5.00	0.01	2.14	20.90
1.102	0.03	0.03	0.50	7.24	5.00	0.02	2.25	20.90
1.112	0.03	0.03	0.50	7.24	5.00	0.02	2.01	20.90
1.121	0.03	0.03	0.50	7.23	5.00	0.02	2.08	20.90
1.132	0.02	0.02	0.50	7.23	5.00	0.01	2.05	21.00
1.142	0.02	0.02	0.50	7.25	5.00	0.01	2.06	21.00
1.152	0.02	0.02	0.50	7.26	5.00	0.01	2.13	21.00
1.163	0.01	0.01	0.50	7.26	5.00	0.01	2.19	21.00
1.173	0.01	0.01	0.50	7.27	5.00	0.00	2.37	21.00
1.184	0.01	0.01	0.50	7.27	5.00	0.00	2.19	21.00
1.194	0.01	0.01	0.50	7.28	5.00	0.00	2.20	21.00
1.204	0.01	0.01	0.50	7.27	5.00	0.00	2.36	21.00
1.215	0.01	0.01	0.50	7.27	5.00	0.00	2.30	21.00
1.225	0.01	0.01	0.50	7.30	5.00	0.00	1.94	21.00
1.236	0.01	0.01	0.50	7.28	5.00	0.00	2.00	21.00
1.246	0.01	0.01	0.50	7.29	5.00	0.00	2.17	21.00
1.257	0.01	0.01	0.50	7.30	5.00	0.00	2.41	21.00
1.267	0.01	0.01	0.50	7.30	5.00	0.00	2.25	21.00
1.277	0.01	0.01	0.50	7.29	5.00	0.00	1.91	21.00
1.288	0.01	0.01	0.50	7.29	5.00	0.00	2.16	21.00
1.298	0.01	0.01	0.50	7.28	5.00	0.00	2.13	21.00
1.309	0.02	0.02	0.50	7.27	5.00	0.00	2.06	21.00
1.325	0.03	0.03	0.50	7.26	5.00	0.00	2.00	21.00
1.335	0.04	0.04	0.50	7.28	5.00	0.00	2.25	21.00
1.345	0.05	0.05	0.50	7.27	5.00	0.00	2.09	21.00
1.356	0.11	0.11	0.50	7.23	5.00	0.00	2.05	21.00
1.366	0.12	0.12	0.50	7.23	5.00	0.00	2.02	21.00
1.377	0.12	0.12	0.50	7.24	5.00	0.00	2.07	21.00
1.387	0.12	0.12	0.50	7.22	5.00	0.00	2.12	21.00
1.397	0.12	0.12	0.50	7.21	5.00	0.00	1.86	21.00
1.408	0.12	0.12	0.50	7.30	5.00	0.00	1.74	21.00
1.418	0.12	0.12	0.50	7.24	5.00	0.00	1.69	21.00
1.429	0.13	0.13	0.50	7.22	5.00	0.00	1.75	21.00
1.439	0.13	0.13	0.50	7.23	5.00	0.00	1.84	21.00
1.450	0.13	0.13	0.50	7.23	5.00	0.00	1.79	21.00
1.460	0.11	0.11	0.50	7.22	5.00	0.00	1.80	21.00
1.470	0.10	0.10	0.50	7.22	5.00	0.00	1.77	21.00
1.481	0.08	0.08	0.50	7.21	5.00	0.00	1.79	21.00
1.491	0.08	0.08	0.50	7.22	5.00	0.00	1.75	21.00
1.502	0.08	0.08	0.50	7.20	5.00	0.00	1.84	21.00
1.512	0.07	0.07	0.50	7.20	5.00	0.00	2.01	21.00
1.522	0.07	0.07	0.50	7.17	5.00	0.00	1.71	21.00
1.533	0.07	0.07	0.50	7.17	5.00	0.00	1.73	21.00
1.543	0.06	0.06	0.50	7.16	5.00	0.00	1.81	21.00
1.554	0.06	0.06	0.50	7.16	5.00	0.00	1.93	21.00
1.564	0.06	0.06	0.50	7.14	5.00	0.00	2.05	21.00
1.575	0.06	0.06	0.50	7.15	5.00	0.00	1.96	20.90
1.585	0.06	0.06	0.50	7.13	5.00	0.00	1.68	20.90
1.595	0.06	0.06	0.50	7.11	5.00	0.00	1.83	20.90
1.606	0.05	0.05	0.50	7.10	5.00	0.00	1.87	20.90
1.616	0.05	0.05	0.50	7.10	5.00	0.00	1.72	20.90
1.627	0.05	0.05	0.50	7.07	5.00	0.00	2.02	20.90
1.637	0.05	0.05	0.50	7.08	5.00	0.00	1.74	20.90
1.647	0.05	0.05	0.50	7.08	5.00	0.00	1.70	20.90
1.658	0.05	0.05	0.50	7.05	5.00	0.00	1.81	20.90
1.668	0.05	0.05	0.50	7.05	5.00	0.00	1.67	20.90
1.679	0.05	0.05	0.50	7.09	5.00	0.00	1.60	20.90
1.689	0.05	0.05	0.50	7.11	5.00	0.00	1.53	20.90
1.700	0.04	0.04	0.50	6.87	5.00	0.00	1.53	20.9
1.710	0.04	0.04	0.50	6.82	5.00	0.00	1.54	20.9
1.720	0.04	0.04	0.50	6.77	5.00	0.00	1.01	20.9
1.731	0.04	0.04	0.50	6.77	5.00	0.00	0.99	20.9
1.741	0.04	0.04	0.50	6.75	5.00	0.00	1.59	20.9
1.752	0.04	0.04	0.50	6.75	5.00	0.00	1.54	20.9
1.762	0.04	0.04	0.50	6.77	5.00	0.00	1.20	20.9
1.772	0.04	0.04	0.50	6.74	5.00	0.00	1.22	20.9
1.783	0.04	0.04	0.50	6.72	5.00	0.00	1.13	20.9
1.793	0.04	0.04	0.50	6.71	5.00	0.00	1.45	20.9
1.804	0.04	0.04	0.50	6.71	5.00	0.00	0.96	20.9
1.814	0.03	0.03	0.50	6.66	5.00	0.00	1.24	20.9
1.825	0.03	0.03	0.50	6.66	5.00	0.00	1.44	20.9
1.835	0.03	0.03	0.50	6.66	5.00	0.00	1.05	20.9
1.845	0.03	0.03	0.50	6.68	5.00	0.00	1.30	20.9
1.856	0.03	0.03	0.50	6.62	5.00	0.00	1.25	20.9
1.866	0.03	0.03	0.50	6.62	5.00	0.00	1.50	21
1.877	0.03	0.03	0.50	6.61	5.00	0.00	1.28	21
1.887	0.01	0.01	0.50	6.64	7.00	0.00	1.51	21
1.897	0.01	0.01	0.50	6.66	7.00	0.00	1.23	21
1.908	0.01	0.01	0.50	6.64	7.00	0.00	1.39	21
1.918	0.01	0.01	0.50	6.66	7.00	0.00	1.06	21
1.929	0.01	0.01	0.50	6.64	7.00	0.00	1.26	21
1.939	0.01	0.01	0.50	6.64	7.00	0.00	1.56	21.1
1.950	0.01	0.01	0.50	6.64	7.00	0.00	1.70	21.1
1.960	0.01	0.01	0.50	6.63	7.00	0.00	1.59	21.1
1.970	0.01	0.01	0.50	6.65	7.00	0.00	1.46	21.1
1.981	0.01	0.01	0.50	6.68	7.00	0.00	1.43	21.1125
1.991	0.01	0.01	0.50	6.71	7.00	0.00	1.41	21.125
2.002	0.02	0.02	0.50	6.73	7.00	0.00	1.38	21.1375
2.012	0.02	0.02	0.50	6.76	7.00	0.00	1.35	21.15
2.022	0.02	0.02	0.50	6.79	7.00	0.01	1.32	21.1625
2.033	0.02	0.02	0.60	6.82	7.00	0.01	1.30	21.175
2.043	0.02	0.02	0.60	6.84	7.00	0.01	1.27	21.1875
2.054	0.02	0.02	0.60	6.87	7.00	0.01	1.24	21.2

2.061	0.03	0.03	0.60	6.91	7.00	0.02	0.86	21.20
2.071	0.03	0.03	0.60	6.91	7.00	0.01	0.99	21.20
2.082	0.03	0.03	0.60	6.89	7.00	0.01	1.05	21.20
2.092	0.03	0.03	0.60	6.88	7.00	0.01	0.88	21.20
2.102	0.03	0.03	0.60	6.86	7.00	0.01	0.93	21.10
2.113	0.04	0.04	0.60	6.87	7.00	0.01	0.73	21.10
2.123	0.04	0.04	0.60	6.86	7.00	0.00	0.98	21.10
2.134	0.04	0.04	0.60	6.85	7.00	0.00	1.10	21.10
2.144	0.04	0.04	0.60	6.84	7.00	0.00	1.21	21.10
2.154	0.04	0.04	0.60	6.83	7.00	0.00	1.21	21.10
2.165	0.04	0.04	0.60	6.82	7.00	0.00	1.03	21.10
2.175	0.05	0.05	0.60	6.79	7.00	0.00	1.01	21.00
2.186	0.05	0.05	0.60	6.78	7.00	0.00	0.94	21.00
2.196	0.05	0.05	0.60	6.75	7.00	0.00	1.09	21.00
2.207	0.05	0.05	0.60	6.72	7.00	0.00	1.15	21.00
2.217	0.05	0.05	0.60	6.74	7.00	0.00	0.93	21.00
2.227	0.05	0.05	0.60	6.71	7.00	0.00	0.90	20.90
2.238	0.05	0.05	0.60	6.72	7.00	0.00	1.15	20.90
2.248	0.05	0.05	0.60	6.73	7.00	0.00	1.18	20.90
2.259	0.05	0.05	0.60	6.73	7.00	0.00	1.05	20.90
2.269	0.06	0.06	0.60	6.72	7.00	0.00	0.98	20.90
2.279	0.06	0.06	0.60	6.71	7.00	0.00	1.24	20.80
2.290	0.06	0.06	0.60	6.74	7.00	0.00	1.06	20.80
2.300	0.06	0.06	0.60	6.73	7.00	0.00	1.03	20.80
2.311	0.06	0.06	0.60	6.73	7.00	0.00	0.91	20.80
2.321	0.06	0.06	0.60	6.74	7.00	0.00	1.17	20.80
2.332	0.07	0.07	0.60	6.73	7.00	0.00	0.90	20.70
2.342	0.07	0.07	0.60	6.72	7.00	0.00	0.78	20.70
2.352	0.07	0.07	0.60	6.75	7.00	0.00	0.87	20.70
2.363	0.07	0.07	0.60	6.77	7.00	0.00	0.97	20.68
2.373	0.07	0.07	0.60	6.79	7.00	0.00	1.06	20.66
2.384	0.07	0.07	0.60	6.83	7.00	0.00	1.26	20.63
2.394	0.08	0.08	0.60	6.85	7.00	0.00	1.35	20.61
2.404	0.08	0.08	0.60	6.87	7.00	0.00	1.45	20.59
2.415	0.08	0.08	0.40	6.91	7.00	0.00	1.64	20.55
2.425	0.08	0.08	0.40	6.92	7.00	0.00	1.74	20.53
2.436	0.09	0.09	0.40	6.94	7.00	0.00	1.83	20.51
2.446	0.09	0.09	0.40	6.98	7.00	0.00	2.03	20.48
2.457	0.09	0.09	0.40	7.00	7.00	0.00	2.12	20.46
2.467	0.09	0.09	0.40	7.02	7.00	0.00	2.22	20.44
2.477	0.09	0.09	0.40	7.06	7.00	0.00	2.41	20.40
2.488	0.10	0.10	0.40	7.06	7.00	0.00	1.35	20.40
2.499	0.15	0.15	0.40	7.06	7.00	0.00	1.46	20.30
2.509	0.20	0.20	0.40	7.05	7.00	0.00	1.42	20.30
2.519	0.23	0.23	0.40	7.07	7.00	0.00	1.19	20.20
2.530	0.24	0.24	0.40	7.06	7.00	0.00	1.50	20.20
2.540	0.26	0.26	0.40	7.06	7.00	0.00	1.35	20.20
2.551	0.26	0.26	0.40	7.07	7.00	0.00	1.22	20.20
2.561	0.26	0.26	0.40	7.09	7.00	0.00	1.29	20.10
2.572	0.27	0.27	0.40	7.07	7.00	0.00	1.23	20.10
2.582	0.27	0.27	0.40	7.08	7.00	0.00	1.27	20.10
2.592	0.29	0.29	0.40	7.08	7.00	0.00	1.30	20.00
2.603	0.29	0.29	0.40	7.09	7.00	0.00	1.30	20.00
2.613	0.29	0.29	0.40	7.10	8.00	0.00	1.32	20.00
2.624	0.31	0.31	0.40	7.08	8.00	0.00	1.26	19.90
2.634	0.31	0.31	0.40	7.10	8.00	0.00	1.28	19.90
2.644	0.31	0.31	0.40	7.08	8.00	0.00	1.44	19.90
2.655	0.31	0.31	0.40	7.08	8.00	0.00	1.35	19.80
2.665	0.31	0.31	0.40	7.09	8.00	0.00	1.26	19.80
2.676	0.32	0.32	0.40	7.10	8.00	0.00	1.14	19.80
2.686	0.32	0.32	0.40	7.10	8.00	0.00	1.37	19.70
2.697	0.32	0.32	0.40	7.09	8.00	0.00	1.21	19.70
2.707	0.32	0.32	0.40	7.09	8.00	0.00	1.22	19.70
2.717	0.34	0.34	0.40	7.10	8.00	0.00	1.28	19.60
2.728	0.34	0.34	0.40	7.11	8.00	0.00	1.27	19.60
2.738	0.34	0.34	0.40	7.11	8.00	0.00	1.27	19.60
2.749	0.34	0.34	0.40	7.11	8.00	0.00	1.37	19.50
2.759	0.34	0.34	0.40	7.11	8.00	0.00	1.29	19.50
2.769	0.34	0.34	0.40	7.15	8.00	0.00	1.23	19.50
2.780	0.36	0.36	0.40	7.16	8.00	0.00	1.25	19.40
2.790	0.34	0.34	0.40	7.04	8.00	0.00	1.16	19.40
2.801	0.34	0.34	0.40	7.10	8.00	0.00	1.20	19.40
2.811	0.32	0.32	0.40	7.10	8.00	0.00	1.16	19.30
2.822	0.31	0.31	0.40	7.12	8.00	0.00	1.22	19.30
2.832	0.31	0.31	0.40	7.14	8.00	0.00	1.28	19.30
2.842	0.31	0.31	0.40	7.17	8.00	0.00	1.18	19.30
2.853	0.29	0.29	0.40	7.17	8.00	0.00	1.23	19.30
2.863	0.29	0.29	0.40	7.17	8.00	0.00	1.18	19.20
2.874	0.29	0.29	0.40	7.21	8.00	0.00	1.29	19.20
2.884	0.27	0.27	0.40	7.23	8.00	0.00	1.27	19.20
2.894	0.27	0.27	0.40	7.24	8.00	0.00	1.31	19.20
2.905	0.26	0.26	0.40	7.27	8.00	0.00	1.45	19.20
2.915	0.26	0.26	0.40	7.29	8.00	0.00	1.46	19.20
2.926	0.24	0.24	0.40	7.32	8.00	0.00	1.51	19.20
2.936	0.24	0.24	0.40	7.36	8.00	0.00	1.54	19.20
2.947	0.24	0.24	0.40	7.41	8.00	0.00	1.57	19.20
2.957	0.23	0.23	0.40	7.46	8.00	0.00	1.61	19.30
2.967	0.23	0.23	0.40	7.50	8.00	0.00	1.61	19.30
2.978	0.23	0.23	0.40	7.54	8.00	0.00	1.76	19.30
2.988	0.23	0.23	0.40	7.61	8.00	0.00	1.81	19.30
2.999	0.23	0.23	0.40	7.64	8.00	0.00	1.77	19.30
3.009	0.22	0.22	0.40	7.68	8.00	0.00	1.83	19.30
3.019	0.22	0.22	0.40	7.70	8.00	0.00	1.75	19.30
3.030	0.22	0.22	0.40	7.72	8.00	0.00	1.84	19.30
3.040	0.22	0.22	0.40	7.79	8.00	0.00	1.92	19.40
3.051	0.22	0.22	0.40	7.85	8.00	0.00	1.88	19.40
3.061	0.20	0.20	0.40	7.89	8.00	0.00	2.00	19.40
3.072	0.20	0.20	0.40	7.91	8.00	0.00	2.07	19.40
3.082	0.19	0.19	0.40	7.93	8.00	0.00	1.94	19.40
3.092	0.18	0.18	0.40	8.02	8.00	0.00	2.21	19.40
3.103	0.19	0.19	0.40	8.04	8.00	0.00	2.11	19.40

2.3.5. DATASET FOR FULL-SCALE VINH BAO WTP (R)

t	snhcon1	snh1	sno1	snn1	so1	xiicon1	si1	sscon1	xicon1	snh4	sno4	snn4	so4	xii4	xil1	ss1	temp
h	mgN/L	mgN/L	mgN/L	mgN/L	mgO2/L	mg/L	mgCOD/L	mgCOD/L	mgCOD/L	mgN/L	mgN/L	mgN/L	mgO2/L	mg/L	mg/L	mgCOD/L	C
std	4.17	4.17	0.00	0.00	5.40	50.00	8.50	4.50	8.00	3.19	0.90	0.27	0.01	51.28	40.32	4.50	30.60
0	4.36	4.36	0.00	0.00	6.00	40.32	5.52	4.00	8.48	3.19	0.90	0.27	0.01	51.28	40.32	4.00	30.60
1	4.80	4.80	0.00	0.00	6.00	37.92	7.02	4.00	8.88	4.21	0.71	0.27	0.01	28.00	37.92	4.00	30.80
2	4.80	4.80	0.00	0.00	6.07	41.40	7.70	4.00	10.60	3.70	0.58	0.51	0.01	26.48	41.40	4.00	30.80
3	4.07	4.07	0.00	0.00	6.08	41.20	4.80	4.00	8.00	3.70	0.61	0.51	0.01	12.20	41.20	4.00	30.80
4	4.94	4.94	0.00	0.00	6.17	36.80	6.50	4.00	8.00	3.85	0.69	0.41	0.01	11.40	36.80	4.00	30.70
5	5.02	5.02	0.00	0.88	5.92	53.56	4.86	4.00	10.84	3.63	0.61	1.66	0.01	16.32	53.56	4.00	30.70
6	4.14	4.14	0.00	0.00	5.79	39.08	4.38	4.00	9.32	3.34	0.58	0.22	0.01	21.84	39.08	4.00	30.70
7	5.09	5.09	0.00	0.00	5.77	42.76	5.36	4.00	9.64	3.78	0.53	0.79	0.01	11.24	42.76	4.00	30.60
8	5.02	5.02	0.00	0.00	5.66	31.72	4.52	4.00	6.68	4.43	0.56	0.03	0.01	18.04	31.72	4.00	30.60
9	5.16	5.16	0.00	0.00	5.56	31.24	4.64	4.00	7.56	4.36	0.61	0.20	0.01	12.72	31.24	4.00	30.50
10	5.46	5.46	0.00	0.00	5.18	43.04	5.74	4.00	7.76	5.16	0.63	0.20	0.00	12.68	43.04	4.00	30.50
11	4.87	4.87	0.00	0.00	5.13	37.96	3.06	4.00	8.44	3.99	0.56	0.32	0.00	12.28	37.96	4.00	30.50
12	4.29	4.29	0.00	0.00	5.13	41.32	14.52	4.00	7.48	3.96	0.50	1.18	0.00	19.92	41.32	4.00	30.40
13	5.16	5.16	0.00	0.00	4.98	31.88	9.38	4.00	7.32	4.10	0.50	1.40	0.00	8.28	31.88	4.00	30.40
14	5.16	5.16	0.00	0.00	4.88	45.28	5.68	4.00	8.72	4.36	0.43	0.38	0.00	14.52	45.28	4.00	30.30
15	6.48	6.48	0.00	0.00	4.78	21.68	6.78	4.00	6.32	4.00	0.48	2.30	0.01	22.48	21.68	4.00	30.20
16	4.80	4.80	0.00	0.00	4.65	41.24	9.54	4.00	7.56	4.00	0.45	1.74	0.01	36.96	41.24	4.00	30.00
17	5.31	5.31	0.00	0.00	4.59	28.24	2.64	4.00	8.16	4.58	0.45	0.28	0.01	19.36	28.24	4.00	30.00
18	5.89	5.89	0.00	0.00	4.43	27.20	0.00	4.00	12.00	5.16	0.45	0.28	0.01	20.40	27.20	4.00	30.00
19	5.16	5.16	0.00	0.00	4.45	30.24	3.84	4.00	6.96	4.43	0.45	0.28	0.00	25.16	30.24	4.00	30.00
20	5.02	5.02	0.00	0.00	4.49	14.68	2.88	4.00	7.32	4.29	0.43	0.31	0.01	19.56	14.68	4.00	30.00
21	5.60	5.60	0.00	0.00	4.48	27.96	4.36	4.00	7.64	3.70	0.50	1.40	0.01	22.52	27.96	4.00	30.00
22	4.65	4.65	0.00	0.00	4.60	31.92	4.12	4.00	7.28	3.60	0.50	1.40	0.01	20.40	31.92	4.00	30.00
23	4.58	4.58	0.00	0.00	4.70	35.36	3.36	4.00	7.44	4.58	0.45	1.40	0.00	15.72	35.36	4.00	30.20
24	5.31	5.31	0.00	0.00	4.87	32.52	3.22	4.00	8.28	4.87	0.48	0.23	0.01	21.48	32.52	4.00	30.30
25	4.87	4.87	0.00	0.00	5.07	39.96	3.66	4.00	8.44	4.14	0.50	0.23	0.00	24.20	39.96	4.00	30.40
26	5.02	5.02	0.00	0.00	5.20	38.44	3.74	4.00	7.96	4.29	0.50	0.23	0.01	22.84	38.44	4.00	30.40
27	5.31	5.31	0.00	0.00	5.19	41.48	2.88	4.00	9.32	4.58	0.48	0.25	0.00	21.60	41.48	4.00	30.40
28	5.02	5.02	0.00	0.00	5.32	43.92	2.32	4.00	8.88	5.02	0.45	0.25	0.00	22.72	43.92	4.00	30.40
29	5.46	5.46	0.00	0.00	5.36	41.08	3.88	4.00	8.12	4.43	0.45	0.57	0.00	27.08	41.08	4.00	30.30
30	5.60	5.60	0.00	0.00	5.30	42.72	4.12	4.00	7.68	4.87	0.43	0.31	0.00	30.60	42.72	4.00	30.20
31	4.94	4.94	0.00	0.00	5.30	35.60	6.00	1.00	7.20	4.00	0.37	1.75	0.01	44.80	35.60	1.00	30.20
32	4.73	4.73	0.00	0.00	5.30	33.20	6.90	1.00	7.60	3.99	0.45	0.28	0.01	31.96	33.20	1.00	30.10
33	4.43	4.43	0.00	0.00	5.14	31.76	5.56	1.00	7.04	4.14	0.45	0.28	0.00	25.20	31.76	1.00	30.00
34	4.58	4.58	0.00	0.00	5.04	36.04	8.54	1.00	7.56	4.00	0.43	1.33	0.00	23.64	36.04	1.00	29.90
35	5.02	5.02	0.00	0.00	5.05	37.04	7.44	1.00	7.36	3.99	0.35	0.68	0.00	22.92	37.04	1.00	29.80
36	5.16	5.16	0.00	0.00	5.26	38.28	7.38	1.00	6.52	4.73	0.48	0.68	0.00	28.20	38.28	1.00	29.60
37	5.89	5.89	0.00	0.00	5.26	40.44	5.84	1.00	7.16	4.87	0.29	0.73	0.00	19.48	40.44	1.00	29.40
38	4.58	4.58	0.00	0.00	5.36	37.04	3.24	1.00	7.76	4.14	0.40	0.04	0.00	25.20	37.04	1.00	29.30
39	3.34	3.34	0.00	0.00	5.37	44.36	12.16	1.00	8.44	2.61	0.45	0.28	0.00	20.96	44.36	1.00	29.10
40	3.56	3.56	0.00	0.68	5.41	47.32	14.72	1.00	7.48	3.26	0.43	0.55	0.00	23.44	47.32	1.00	29.10
41	2.02	2.02	0.00	1.07	5.35	46.60	1.90	1.00	8.60	1.87	0.50	0.72	0.01	15.08	46.60	1.00	29.10
42	2.09	2.09	0.00	0.88	5.38	38.28	9.48	1.00	7.32	1.66	0.36	0.76	0.01	41.20	38.28	1.00	29.10
43	3.12	3.12	0.00	0.68	5.39	37.40	12.70	1.00	6.80	2.39	0.57	1.04	0.27	151.40	37.40	1.00	29.10
44	2.68	2.68	0.00	0.00	5.48	35.52	9.02	5.00	7.48	1.87	0.35	0.46	0.25	97.80	35.52	5.00	29.90
45	4.14	4.14	0.00	0.00	5.89	32.40	11.90	5.00	8.80	3.12	0.32	0.70	0.20	37.60	32.40	5.00	29.40
46	4.36	4.36	0.00	0.00	5.42	40.68	11.58	5.00	8.92	3.20	0.55	1.04	0.20	41.36	40.68	5.00	29.60
47	4.36	4.36	0.00	0.00	5.41	42.80	1.40	5.00	8.60	3.20	0.38	1.77	0.10	38.96	42.80	5.00	29.70
48	4.36	4.36	0.00	0.00	5.94	41.06	1.40	5.00	9.60	3.09	0.41	1.77	0.38	460.47	41.06	5.00	29.35
49	4.14	4.14	0.00	0.00	5.72	39.52	2.82	5.00	9.08	2.97	0.48	0.69	0.38	108.84	39.52	5.00	30.00
50	4.36	4.36	0.00	0.68	5.90	37.84	2.54	5.00	8.56	3.10	0.32	1.75	0.47	32.92	37.84	5.00	30.00
51	4.58	4.58	0.00	0.00	5.91	34.72	3.22	5.00	7.88	3.48	0.38	0.75	0.28	42.48	34.72	5.00	29.90
52	4.38	4.38	0.00	0.00	5.87	43.28	2.08	5.00	8.72	3.19	0.58	0.82	0.12	18.20	43.28	5.00	29.90
53	3.99	3.99	0.00	0.68	5.83	38.92	1.83	5.00	7.88	3.48	0.32	0.88	0.09	31.24	38.92	5.00	29.80
54	4.38	4.38	0.00	0.00	5.84	37.64	0.00	5.00	7.98	3.48	0.27	0.88	0.07	31.84	37.64	5.00	29.70
55	5.02	5.02	0.00	0.68	5.51	38.56	1.89	5.00	8.54	4.03	0.48	0.84	0.08	30.04	38.56	5.00	29.70
56	4.73	4.73	0.00	0.00	5.43	36.24	2.44	5.00	7.76	4.14	0.27	0.52	0.07	34.96	36.24	5.00	29.70
57	5.09	5.09	0.00	0.68	5.34	36.72	3.12	5.00	7.28	3.40	0.00	3.02	0.03	33.72	36.72	5.00	29.60
58	4.58	4.58	0.00	0.00	5.28	33.84	2.44	5.00	8.56	4.38	0.52	0.98	0.15	36.72	33.84	5.00	29.60
59	5.02	5.02	0.00	0.00	5.27	37.20	2.40	5.00	8.80	4.38	0.25	0.96	0.11	31.96	37.20	5.00	29.90
60	4.29	4.29	0.00	0.68	5.21	34.20	0.90	5.00	8.20	4.00	0.00	3.02	0.12	33.52	34.20	5.00	29.50
61	4.73	4.73	0.00	0.00	5.15	38.92	2.63	5.00	8.08	3.92	0.00	0.80	0.08	32.88	38.92	5.00	29.40
62	4.43	4.43	0.00	0.00	5.10	37.28	0.78	5.00	8.32	3.90	0.00	0.80	0.08	33.12	37.28	5.00	29.40
63	3.48	3.48	0.00	0.88	4.85	42.44	2.24	5.00	8.36	3.20	0.00	0.51	0.06	38.92	42.44	5.00	29.30
64	3.41	3.41	0.00	0.88	4.76	45.96	1.16	5.00	8.04	3.19	0.27	0.83	0.05	33.44	45.96	5.00	29.20
65	3.70	3.70	0.00	1.07	4.77	40.68	0.76	5.00	8.12	2.61	0.27	1.90	0.04	24.58	40.68	5.00	29.20
66	2.73	2.73	0.00	0.88	4.83	40.16	19.66	5.00	8.24	2.17	0.32	1.14	0.21	36.28	40.16	5.00	29.30
67	2.61	2.61	0.00	0.88	5.26	32.80	19.50	5.00	7.20	2.10	0.00	5.12	0.26	0.00	32.80	5.00	29.40
68	2.61	2.61	0.00	0.88	5.23	38.12	17.22	5.00	8.88	2.00	0.00	5.44	0.13	0.00	38.12	5.00	29.90
69	3.53	3.53	0.00	1.27	5.48	31.40	21.00	5.00	7.40	2.02	0.00	1.78	0.18	18.08	31.40	5.00	29.50
70	2.31	2.31	0.00	1.07	5.70	34.08	22.08	5.00	7.52	1.89	0.00	5.34	0.19	0.00	34.08	5.00	29.70
71	1.95	1.95	0.00	0.88	5.74	37.88	22.88	5.00	8.72	1.70	0.00	2.76	0.20	0.00	37.88	5.00	29.90

t	rattach4(1	rattach4(2	rattach4(3	rattach4(4	rattach4(5	rattach4(6	rattach4(7	rattach4(8	rattach4(9	rattach4(1	rattach4(1	rdetach	rdetach	rdetach	rdetach	rdetach	rdetach	rdetach	rdetach	rdetach	rdetach	rdetach
h	m/d	m/d	m/d	m/d	m/d	m/d	m/d	m/d	m/d	m/d	m/d	g/m2/d	g/m2/d	g/m2/d	g/m2/d	g/m2/d	g/m2/d	g/m2/d	g/m2/d	g/m2/d	g/m2/d	g/m2/d
std	0.30	0.30	0.30	0.30	0.30	0.30	0.30	0.30	0.30	0.30	0.30	10	10	10	10	10	10	10	10	10	10	10
0	0.65	0.65	0.65	0.65	0.65	0.65	0.65	0.65	0.65	0.65	0.65	10	10	10	10	10	10	10	10	10	10	10
1	0.65	0.65	0.65	0.65	0.65	0.65	0.65	0.65	0.65	0.65	0.65	10	10	10	10	10	10	10	10	10	10	10
2	0.55	0.55	0.55	0.55	0.55	0.55	0.55	0.55	0.55	0.55	0.55	10	10	10	10	10	10	10	10	10	10	10
3	0.55	0.55	0.55	0.55	0.55	0.55	0.55	0.55	0.55	0.55	0.55	10	10	10	10	10	10	10	10	10	10	10
4	0.55	0.55	0.55	0.55	0.55	0.55	0.55	0.55	0.55	0.55	0.55	10	10	10	10	10	10	10	10	10	10	10
5	0.65	0.65	0.65	0.65	0.65	0.65	0.65	0.65	0.65	0.65	0.65	10	10	10	10	10	10	10	10	10	10	10
6	0.60	0.60	0.60	0.60	0.60	0.60	0.60	0.60	0.60	0.60	0.60	10	10	10	10	10	10	10	10	10	10	10
7	0.65	0.65	0.65	0.65	0.65	0.65	0.65	0.65	0.65	0.65	0.65	10	10	10	10	10	10	10	10	10	10	10
8	0.70	0.70	0.70	0.70	0.70	0.70	0.70	0.70	0.70	0.70	0.70	10	10	10	10	10	10	10	10	10	10	10
9	0.75	0.75	0.75	0.75	0.75	0.75	0.75	0.75	0.75	0.75	0.75	10	10	10	10	10	10	10	10	10	10	10
10	0.75	0.75	0.75	0.75	0.75	0.75	0.75	0.75	0.75	0.75	0.75	10	10	10	10	10	10	10	10	10	10	10
11	0.80	0.80	0.80	0.80	0.80	0.80	0.80	0.80	0.80	0.80	0.80	10	10	10	10	10	10	10	10	10	10	10
12	0.85	0.85	0.85	0.85	0.85	0.85	0.85	0.85	0.85	0.85	0.85	10	10	10	10	10	10	10	10	10	10	10
13	0.65	0.65	0.65	0.65	0.65	0.65	0.65	0.65	0.65	0.65	0.65	10	10	10	10	10	10	10	10	10	10	10
14	0.65	0.65	0.65	0.65	0.65	0.65	0.65	0.65	0.65	0.65	0.65	10	10	10	10	10	10	10	10	10	10	10
15	0.60	0.60	0.60	0.60	0.60	0.60	0.60	0.60	0.60	0.60	0.60	10	10	10	10	10	10	10	10	10	10	10
16	0.60	0.60	0.60	0.60	0.60	0.60	0.60	0.60	0.60	0.60	0.60	10	10	10	10	10	10	10	10	10	10	10
17	0.65	0.65	0.65	0.65	0.65	0.65	0.65	0.65	0.65	0.65	0.65	10	10	10	10	10	10	10	10	10	10	10
18	0.65	0.65	0.65	0.65	0.65	0.65	0.65	0.65	0.65	0.65	0.65	10	10	10	10	10	10	10	10	10	10	10
19	0.70	0.70	0.70	0.70	0.70	0.70	0.70	0.70	0.70	0.70	0.70	10	10	10	10	10	10	10	10	10	10	10
20	0.70	0.70	0.70	0.70	0.70	0.70	0.70	0.70	0.70	0.70	0.70	10	10	10	10	10	10	10	10	10	10	10
21	0.70	0.70	0.70	0.70	0.70	0.70	0.70	0.70	0.70	0.70	0.70	10	10	10	10	10	10	10	10	10	10	10
22	0.68	0.68	0.68	0.68	0.68	0.68	0.68	0.68	0.68	0.68	0.68	10	10	10	10	10	10	10	10	10	10	10
23	0.66	0.66	0.66	0.66	0.66	0.66	0.66	0.66	0.66	0.66	0.66	10	10	10	10	10	10	10	10	10	10	10
24	0.64	0.64	0.64	0.64	0.64	0.64	0.64	0.64	0.64	0.64	0.64	10	10	10	10	10	10	10	10	10	10	10
25	0.62	0.62	0.62	0.62	0.62	0.62	0.62	0.62	0.62	0.62	0.62	10	10	10	10	10	10	10	10	10	10	10
26	0.60	0.60	0.60	0.60	0.60	0.60	0.60	0.60	0.60	0.60	0.60	10	10	10	10	10	10	10	10	10	10	10
27	0.58	0.58	0.58	0.58	0.58	0.58	0.58	0.58	0.58	0.58	0.58	10	10	10	10	10	10	10	10	10	10	10
28	0.56	0.56	0.56	0.56	0.56	0.56	0.56	0.56	0.56	0.56	0.56	10	10	10	10	10	10	10	10	10	10	10
29	0.49	0.49	0.49	0.49	0.49	0.49	0.49	0.49	0.49	0.49	0.49	10	10	10	10	10	10	10	10	10	10	10
30	0.47	0.47	0.47	0.47	0.47	0.47	0.47	0.47	0.47	0.47	0.47	10	10	10	10	10	10	10	10	10	10	10
31	0.47	0.47	0.47	0.47	0.47	0.47	0.47	0.47	0.47	0.47	0.47	10	10	10	10	10	10	10	10	10	10	10
32	0.55	0.55	0.55	0.55	0.55	0.55	0.55	0.55	0.55	0.55	0.55	10	10	10	10	10	10	10	10	10	10	10
33	0.55	0.55	0.55	0.55	0.55	0.55	0.55	0.55	0.55	0.55	0.55	10	10	10	10	10	10	10	10	10	10	10
34	0.60	0.60	0.60	0.60	0.60	0.60	0.60	0.60	0.60	0.60	0.60	10	10	10	10	10	10	10	10	10	10	10
35	0.60	0.60	0.60	0.60	0.60	0.60	0.60	0.60	0.60	0.60	0.60	10	10	10	10	10	10	10	10	10	10	10
36	0.60	0.60	0.60	0.60	0.60	0.60	0.60	0.60	0.60	0.60	0.60	10	10	10	10	10	10	10	10	10	10	10
37	0.60	0.60	0.60	0.60	0.60	0.60	0.60	0.60	0.60	0.60	0.60	10	10	10	10	10	10	10	10	10	10	10
38	0.60	0.60	0.60	0.60	0.60	0.60	0.60	0.60	0.60	0.60	0.60	10	10	10	10	10	10	10	10	10	10	10
39	0.62	0.62	0.62	0.62	0.62	0.62	0.62	0.62	0.62	0.62	0.62	10	10	10	10	10	10	10	10	10	10	10
40	0.65	0.65	0.65	0.65	0.65	0.65	0.65	0.65	0.65	0.65	0.65	10	10	10	10	10	10	10	10	10	10	10
41	0.70	0.70	0.70	0.70	0.70	0.70	0.70	0.70	0.70	0.70	0.70	10	10	10	10	10	10	10	10	10	10	10
42	0.30	0.30	0.30	0.30	0.30	0.30	0.30	0.30	0.30	0.30	0.30	10	10	10	10	10	10	10	10	10	10	10
43	0.40	0.40	0.40	0.40	0.40	0.40	0.40	0.40	0.40	0.40	0.40	10	10	10	10	10	10	10	10	10	10	10
44	0.15	0.15	0.15	0.15	0.15	0.15	0.15	0.15	0.15	0.15	0.15	10	10	10	10	10	10	10	10	10	10	10
45	0.48	0.48	0.48	0.48	0.48	0.48	0.48	0.48	0.48	0.48	0.48	10	10	10	10	10	10	10	10	10	10	10
46	0.50	0.50	0.50	0.50	0.50	0.50	0.50	0.50	0.50	0.50	0.50	10	10	10	10	10	10	10	10	10	10	10
47	0.30	0.30	0.30	0.30	0.30	0.30	0.30	0.30	0.30	0.30	0.30	10	10	10	10	10	10	10	10	10	10	10
48	0.70	0.70	0.70	0.70	0.70	0.70	0.70	0.70	0.70	0.70	0.70	250	250	250	250	250	250	250	250	250	250	250
49	0.40	0.40	0.40	0.40	0.40	0.40	0.40	0.40	0.40	0.40	0.40	10	10	10	10	10	10	10	10	10	10	10
50	0.40	0.40	0.40	0.40	0.40	0.40	0.40	0.40	0.40	0.40	0.40	10	10	10	10	10	10	10	10	10	10	10
51	0.40	0.40	0.40	0.40	0.40	0.40	0.40	0.40	0.40	0.40	0.40	10	10	10	10	10	10	10	10	10	10	10
52	0.39	0.39	0.39	0.39	0.39	0.39	0.39	0.39	0.39	0.39	0.39	10	10	10	10	10	10	10	10	10	10	10
53	0.38	0.38	0.38	0.38	0.38	0.38	0.38	0.38	0.38	0.38	0.38	10	10	10	10	10	10	10	10	10	10	10
54	0.36	0.36	0.36	0.36	0.36	0.36	0.36	0.36	0.36	0.36	0.36	10	10	10	10	10	10	10	10	10	10	10
55	0.34	0.34	0.34	0.34	0.34	0.34	0.34	0.34	0.34	0.34	0.34	10	10	10	10	10	10	10	10	10	10	10
56	0.32	0.32	0.32	0.32	0.32	0.32	0.32	0.32	0.32	0.32	0.32	10	10	10	10	10	10	10	10	10	10	10
57	0.37	0.37	0.37	0.37	0.37	0.37	0.37	0.37	0.37	0.37	0.37	10	10	10	10	10	10	10	10	10	10	10
58	0.42	0.42	0.42	0.42	0.42	0.42	0.42	0.42	0.42	0.42	0.42	10	10	10	10	10	10	10	10	10	10	10
59	0.42	0.42	0.42	0.42	0.42	0.42	0.42	0.42	0.42	0.42	0.42	10	10	10	10	10	10	10	10	10	10	10
60	0.42	0.42	0.42	0.42	0.42	0.42	0.42	0.42	0.42	0.42	0.42	10	10	10	10	10	10	10	10	10	10	10
61	0.42	0.42	0.42	0.42	0.42	0.42	0.42	0.42	0.42	0.42	0.42	10	10	10	10	10	10	10	10	10	10	10
62	0.42	0.42	0.42	0.42	0.42	0.42	0.42	0.42	0.42	0.42	0.42	10	10	10	10	10	10	10	10	10	10	10
63	0.38	0.38	0.38	0.38	0.38	0.38	0.38	0.38	0.38	0.38	0.38	10	10	10	10	10	10	10	10	10	10	10
64	0.58	0.58	0.58	0.58	0.58	0.58	0.58	0.58	0.58	0.58	0.58	10	10	10	10	10	10	10	10	10	10	10
65	0.63	0.63	0.63	0.63	0.63	0.63	0.63	0.63	0.63	0.63	0.63	10	10	10	10	10	10	10	10	10	10	10
66	0.67	0.67	0.67	0.67	0.67	0.67	0.67	0.67	0.67	0.67	0.67	10	10	10	10	10	10	10	10	10	10	10
67	0.72	0.72	0.72	0.72	0.72	0.72	0.72	0.72	0.72	0.72	0.72	10	10	10	10	10	10	10	10	10	10	10
68	0.60	0.60	0.60	0.60	0.60	0.60	0.60	0.60	0.60	0.60	0.60	10	10	10	10	10	10	10	10	10	10	10
69	0.58	0.58	0.58	0.58	0.58	0.58	0.58	0.58	0.58	0.58	0.58	10	10	10	10	10	10	10	10	10	10	10
70	0.57	0.57	0.57	0.57	0.57	0.57	0.57	0.57	0.57	0.57	0.57	10	10	10	10	10	10	10	10	10	10	10
71	0.57	0.57	0.57	0.57	0.57	0.57	0.57	0.57	0.57	0.57	0.57	10	10	10	10	10	10	10	10	10	10	10

t	x1	vss1	cod1	x4	vss4	cod4
h	mg/L	mg/L	mgCOD/L	mg/L	mg/L	mgCOD/L
std	48.8	8.48	18	60.4	9.12	18.3
0	48.8	8.48	18	60.4	9.12	18.3
1	46.8	8.88	19.9	35.2	7.2	18.8
2	52	10.6	22.3	32.8	6.32	14.7
3	49.2	8	16.8	16.8	4.6	12.2
4	44.8	8	18.5	16	4.6	12.7
5	64.4	10.84	19.7	20.8	4.48	13.1
6	48.4	9.32	17.7	27.6	5.76	14.1
7	52.4	9.64	19	17.6	6.36	15.7
8	38.4	6.68	15.2	24.8	6.76	45.6
9	38.8	7.56	16.2	17.6	4.88	9.9
10	50.8	7.76	17.5	18	5.32	13.5
11	46.4	8.44	15.5	18.4	6.12	45.8
12	48.8	7.48	26	26.4	6.48	26.6
13	39.2	7.32	20.7	14.4	6.12	20.7
14	54	8.72	18.4	19.6	5.08	19.5
15	28	6.32	17.1	28.8	6.32	18.5
16	48.8	7.56	21.1	45.6	8.64	13.6
17	36.4	8.16	14.8	25.6	6.24	14.8
18	39.2	12	13.4	27.6	7.2	15.3
19	37.2	6.96	14.8	31.6	6.44	13.8
20	22	7.32	14.2	22.8	3.24	15
21	35.6	7.64	16	28.4	5.88	12.8
22	39.2	7.28	15.4	26.4	6	12.8
23	42.8	7.44	14.8	21.6	5.88	12.5
24	40.8	8.28	15.5	27.6	6.12	12.8
25	48.4	8.44	16.1	31.6	7.4	13.9
26	46.4	7.96	15.7	26.8	3.96	13.4
27	50.8	9.32	16.2	27.2	5.6	13.9
28	52.8	8.88	15.2	27.6	4.88	12.2
29	49.2	8.12	16	33.6	6.52	13.7
30	50.4	7.68	15.8	37.2	6.6	12.2
31	42.8	7.2	14.2	54.4	9.6	14
32	40.8	7.6	15.5	38.8	6.84	12
33	38.8	7.04	13.6	31.6	6.4	12.2
34	43.6	7.56	17.1	27.6	3.96	12.6
35	44.4	7.36	15.8	28.4	5.48	14.3
36	44.8	6.52	14.9	34	5.8	13.4
37	47.6	7.16	14	25.2	5.72	13.2
38	44.8	7.76	12	31.2	6	12.2
39	52.8	8.44	21.6	26	5.04	20.5
40	54.8	7.48	23.2	29.6	6.16	20.3
41	55.2	8.6	11.5	19.6	4.52	12.2
42	45.6	7.32	17.8	45.6	4.4	18.1
43	44	6.6	20.3	172.4	31	29.4
44	42.8	7.48	21.3	110.8	13.2	25.2
45	39.2	8.8	23.7	89.2	11.6	22.2
46	49.6	8.92	25.6	50	8.44	24.7
47	50.4	9.6	16	42.8	7.24	13.6
48	52.4	9.6	16	534.4979	74.02724	13.6
49	48.4	9.08	16.9	124.4	17.56	16.6
50	46.4	6.56	15.9	40.8	8.48	14.2
51	42.4	7.68	15.9	52	9.92	14.4
52	52	8.72	15.8	35.6	7.4	13.5
53	46.8	7.88	14.5	38.8	7.56	15.1
54	43.6	7.96	11.2	40	8.16	15.4
55	47.2	8.64	13.5	37.6	7.56	13.6
56	44	7.76	15.2	43.2	8.84	15.1
57	44	7.28	15.4	41.6	7.88	14.2
58	42.4	8.36	16	45.6	8.88	14.6
59	48	8.8	18.2	39.6	7.64	15
60	42.4	8.2	14.1	44.4	9.08	16.9
61	48	8.08	15.7	41.6	8.72	16.1
62	43.6	8.32	14.1	41.6	8.48	14
63	50.8	6.36	15.6	48	9.08	13
64	54	8.04	14.2	41.2	7.76	13.4
65	48.8	6.12	13.9	31.6	6.92	11.8
66	48.4	8.24	32.9	105	8.72	33.4
67	40	7.2	31.5	-1	-1	33.4
68	48	9.88	32.1	-1	-1	33.4
69	38.8	7.4	33.4	20.4	6.32	31.7
70	41.8	7.52	34.8	-1	-1	31.7
71	46.4	8.72	36.8	-1	-1	35.5

72	1.80	1.80	0.00	1.07	6.12	36.56	22.56	5.00	9.04	1.50	0.00	2.83	0.23	0.00	36.56	5.00	30.30	0.56	0.56	0.56	0.56	0.56	0.56	0.56	0.56	0.56	0.56	0.56	10	10	10	10	10	10	10	10	10	10	10	45.6	9.04	36.6	-1	-1	35.5
73	1.36	1.36	0.00	1.27	6.37	39.08	19.08	5.00	8.92	0.78	0.27	1.58	0.26	22.24	39.08	5.00	30.40	0.56	0.56	0.56	0.56	0.56	0.56	0.56	0.56	0.56	0.56	0.56	10	10	10	10	10	10	10	10	10	10	10	48	8.92	33	26.4	4.16	35.5
74	1.66	1.66	0.00	1.07	6.46	42.08	11.68	5.00	8.72	1.00	0.29	1.44	0.14	27.08	42.08	5.00	30.30	0.55	0.55	0.55	0.55	0.55	0.55	0.55	0.55	0.55	0.55	0.55	10	10	10	10	10	10	10	10	10	10	10	50.8	8.72	25.4	33.6	6.52	23.1
75	1.36	1.36	0.00	1.07	6.49	41.60	12.10	5.00	8.80	0.71	0.27	1.46	0.14	28.48	41.60	5.00	30.10	0.54	0.54	0.54	0.54	0.54	0.54	0.54	0.54	0.54	0.54	0.54	10	10	10	10	10	10	10	10	10	10	10	50.4	8.8	25.9	35.2	6.72	24.7
76	1.44	1.44	0.00	1.07	6.43	45.00	0.00	0.50	8.32	0.56	0.27	1.68	0.12	32.72	45.00	0.50	29.90	0.51	0.51	0.51	0.51	0.51	0.51	0.51	0.51	0.51	0.51	0.51	10	10	10	10	10	10	10	10	10	10	10	53.32	8.32	10.9	39.84	7.12	9.1
77	1.14	1.14	0.00	1.27	6.12	40.88	0.00	0.50	7.72	0.56	0.27	1.58	0.15	33.28	40.88	0.50	29.70	0.49	0.49	0.49	0.49	0.49	0.49	0.49	0.49	0.49	0.49	0.49	10	10	10	10	10	10	10	10	10	10	10	48.6	7.72	12.7	40.72	7.44	9
78	1.14	1.14	0.00	1.27	6.01	55.84	0.00	0.50	9.52	0.27	0.00	2.14	0.09	32.60	55.84	0.50	29.50	0.46	0.46	0.46	0.46	0.46	0.46	0.46	0.46	0.46	0.46	0.46	10	10	10	10	10	10	10	10	10	10	10	65.36	9.52	10.7	39.28	6.68	10
79	1.22	1.22	0.00	0.68	5.92	38.12	0.00	0.50	7.00	0.19	0.00	1.71	0.11	40.32	38.12	0.50	29.40	0.44	0.44	0.44	0.44	0.44	0.44	0.44	0.44	0.44	0.44	0.44	10	10	10	10	10	10	10	10	10	10	10	45.12	7	9.1	48.4	8.08	13.4
80	1.14	1.14	0.00	1.07	5.87	40.24	0.00	0.50	7.20	0.05	0.00	2.17	0.14	41.60	40.24	0.50	29.30	0.41	0.41	0.41	0.41	0.41	0.41	0.41	0.41	0.41	0.41	0.41	10	10	10	10	10	10	10	10	10	10	10	47.44	7.2	10.8	49.6	8	9.6
81	0.85	0.85	0.00	1.07	6.00	41.40	0.00	5.00	7.20	0.05	0.00	1.88	0.36	48.60	41.40	5.00	29.20	0.39	0.39	0.39	0.39	0.39	0.39	0.39	0.39	0.39	0.39	0.39	10	10	10	10	10	10	10	10	10	10	10	48.6	7.2	11.5	57.24	8.64	9.7
82	0.92	0.92	0.00	1.27	6.02	46.96	0.00	5.00	6.68	0.05	0.00	2.14	0.41	41.52	46.96	5.00	29.10	0.37	0.37	0.37	0.37	0.37	0.37	0.37	0.37	0.37	0.37	0.37	10	10	10	10	10	10	10	10	10	10	10	53.64	6.68	8.3	47.2	5.68	11.2
83	0.93	0.93	0.00	1.46	5.99	40.80	0.00	5.00	7.24	0.05	0.00	2.41	0.64	45.12	40.80	5.00	29.10	0.41	0.41	0.41	0.41	0.41	0.41	0.41	0.41	0.41	0.41	0.41	10	10	10	10	10	10	10	10	10	10	10	48.04	7.24	7.8	52.56	7.44	9.5
84	0.92	0.92	0.00	0.88	6.02	41.64	0.00	5.00	7.52	0.30	0.00	2.12	0.62	39.84	41.64	5.00	29.00	0.37	0.37	0.37	0.37	0.37	0.37	0.37	0.37	0.37	0.37	0.37	10	10	10	10	10	10	10	10	10	10	10	49.16	7.52	11.4	47.4	7.56	9
85	0.95	0.95	0.00	1.46	6.01	44.04	0.00	5.00	7.20	0.30	0.00	2.70	0.81	43.44	44.04	5.00	28.90	0.35	0.35	0.35	0.35	0.35	0.35	0.35	0.35	0.35	0.35	0.35	10	10	10	10	10	10	10	10	10	10	10	51.24	7.2	9.9	51.32	7.88	7.8
86	0.97	0.97	0.00	1.27	6.00	44.52	0.00	5.00	8.08	0.35	0.00	2.51	0.86	39.12	44.52	5.00	28.80	0.31	0.31	0.31	0.31	0.31	0.31	0.31	0.31	0.31	0.31	0.31	10	10	10	10	10	10	10	10	10	10	10	52.6	8.08	7.2	46.92	7.8	9.1
87	0.94	0.94	0.00	1.07	5.93	49.16	0.00	5.00	8.72	0.25	0.00	2.17	0.87	46.32	49.16	5.00	28.80	0.31	0.31	0.31	0.31	0.31	0.31	0.31	0.31	0.31	0.31	0.31	10	10	10	10	10	10	10	10	10	10	10	57.88	8.72	7.5	55.12	8.8	7.6
88	0.92	0.92	0.00	1.07	5.91	53.56	0.00	5.00	8.36	0.24	0.00	1.95	0.86	45.76	53.56	5.00	28.70	0.31	0.31	0.31	0.31	0.31	0.31	0.31	0.31	0.31	0.31	0.31	10	10	10	10	10	10	10	10	10	10	10	61.92	8.36	9.8	53.6	7.84	7.5
89	0.85	0.85	0.00	1.27	5.88	54.16	0.00	5.00	9.96	0.05	0.00	2.07	0.79	45.28	54.16	5.00	28.70	0.30	0.30	0.30	0.30	0.30	0.30	0.30	0.30	0.30	0.30	0.30	10	10	10	10	10	10	10	10	10	10	10	64.12	9.96	12.1	53.48	8.2	6.8
90	1.07	1.07	0.00	1.07	5.86	50.76	0.00	5.00	8.64	0.05	0.00	2.10	0.62	50.24	50.76	5.00	29.00	0.30	0.30	0.30	0.30	0.30	0.30	0.30	0.30	0.30	0.30	0.30	10	10	10	10	10	10	10	10	10	10	10	59.4	8.64	8.9	59.48	9.24	8.4
91	0.71	0.71	0.00	1.27	5.91	49.92	0.00	5.00	8.72	0.05	0.00	1.93	0.74	52.56	49.92	5.00	29.10	0.30	0.30	0.30	0.30	0.30	0.30	0.30	0.30	0.30	0.30	0.30	10	10	10	10	10	10	10	10	10	10	10	58.64	8.72	11.6	62.12	9.56	9.7
92	0.78	0.78	0.00	1.07	5.87	57.04	2.18	5.00	10.24	0.05	0.00	1.80	0.84	56.84	57.04	5.00	29.10	0.27	0.27	0.27	0.27	0.27	0.27	0.27	0.27	0.27	0.27	0.27	10	10	10	10	10	10	10	10	10	10	10	67.28	10.24	17.42	67.24	10.4	8.5
93	0.34	0.34	0.00	1.27	5.86	47.48	0.00	9.00	8.72	0.05	0.00	1.56	0.64	36.92	47.48	9.00	29.50	0.27	0.27	0.27	0.27	0.27	0.27	0.27	0.27	0.27	0.27	0.27	10	10	10	10	10	10	10	10	10	10	10	56.2	8.72	13	44.2	7.28	8.3
94	0.63	0.63	0.00	1.27	6.07	53.88	0.00	9.00	8.88	0.05	0.00	1.85	0.60	31.28	53.88	9.00	29.80	0.37	0.37	0.37	0.37	0.37	0.37	0.37	0.37	0.37	0.37	0.37	10	10	10	10	10	10	10	10	10	10	10	62.76	8.88	13	37.08	5.8	8.8
95	0.56	0.56	0.00	1.27	6.12	51.84	1.00	9.00	9.00	0.05	0.00	1.78	0.81	35.04	51.84	9.00	29.80	0.35	0.35	0.35	0.35	0.35	0.35	0.35	0.35	0.35	0.35	0.35	10	10	10	10	10	10	10	10	10	10	10	60.84	9	19	41.44	6.4	7.8
96	0.71	0.71	0.00	1.27	6.05	49.12	2.10	9.00	9.20	0.05	0.00	1.93	0.76	41.96	49.12	9.00	29.60	0.34	0.34	0.34	0.34	0.34	0.34	0.34	0.34	0.34	0.34	0.34	10	10	10	10	10	10	10	10	10	10	10	58.32	9.2	20.3	49.4	7.44	7.6
97	0.71	0.71	0.00	1.27	6.18	51.84	1.00	9.00	9.88	0.05	0.00	1.93	0.62	35.84	51.84	9.00	29.80	0.32	0.32	0.32	0.32	0.32	0.32	0.32	0.32	0.32	0.32	0.32	10	10	10	10	10	10	10	10	10	10	10	61.72	9.88	19.88	43.76	7.92	8.5
98	0.63	0.63	0.00	1.27	6.06	66.64	1.00	9.00	11.68	0.05	0.00	1.85	0.63	63.04	66.64	9.00	29.80	0.30	0.30	0.30	0.30	0.30	0.30	0.30	0.30	0.30	0.30	0.30	10	10	10	10	10	10	10	10	10	10	10	78.32	11.68	21.68	73.64	10.6	9.5
99	0.63	0.63	0.00	1.27	6.10	46.84	1.00	9.00	9.44	0.05	0.00	1.85	0.69	40.28	46.84	9.00	29.60	0.28	0.28	0.28	0.28	0.28	0.28	0.28	0.28	0.28	0.28	0.28	10	10	10	10	10	10	10	10	10	10	10	56.28	9.44	19.44	49.64	9.36	7.1
100	0.63	0.63	0.00	1.27	5.79	50.36	1.00	9.00	8.96	0.05	0.00	1.85	0.55	45.56	50.36	9.00	29.50	0.27	0.27	0.27	0.27	0.27	0.27	0.27	0.27	0.27	0.27	0.27	10	10	10	10	10	10	10	10	10	10	10	59.32	8.96	18.96	53.48	7.92	8.3
101	0.71	0.71	0.00	1.07	5.78	49.32	1.00	9.00	9.56	0.05	0.00	1.73	0.67	46.92	49.32	9.00	29.50	0.25	0.25	0.25	0.25	0.25	0.25	0.25	0.25	0.25	0.25	0.25	10	10	10	10	10	10	10	10	10	10	10	58.88	9.56	19.56	55.8	8.88	6.4
102	0.78	0.78	0.00	1.27	5.80	43.28	0.00	9.00	8.08	0.05	0.00	2.00	1.03	46.00	43.28	9.00	29.40	0.31	0.31	0.31	0.31	0.31	0.31	0.31	0.31	0.31	0.31	0.31	10	10	10	10	10	10	10	10	10	10	10	51.36	8.08	16.38	54.24	8.24	10.5
103	0.56	0.56	0.00	1.27	5.74	48.28	0.00	9.00	2.20	0.05	0.00	1.78	1.03	74.92	48.28	9.00	29.40	0.32	0.32	0.32	0.32	0.32	0.32	0.32	0.32	0.32	0.32	0.32	10	10	10	10	10	10	10	10	10	10	10	50.48	2.2	10.2	89.4	14.48	8.6
104	0.56	0.56	0.00	1.27	5.74	41.52	5.42	0.10	9.12	0.05	0.00	1.78	1.29	42.48	41.52	0.10	29.40	0.33	0.33	0.33	0.33	0.33	0.33	0.33	0.33	0.33	0.33	0.33	10	10	10	10	10	10	10	10	10	10	10	50.64	9.12	14.64	53.6	11.12	8.4
105	0.56	0.56	0.00	1.27	5.73	45.36	4.94	0.10	9.52	0.05	0.00	1.78	1.24	47.96	45.36	0.10	29.30	0.34	0.34	0.34	0.34	0.34	0.34	0.34	0.34	0.34	0.34	0.34	10	10	10	10	10	10	10	10	10	10	10	54.88	9.52	14.56	58.28	10.32	6
106	0.63	0.63	0.00	1.27	5.47	48.16	5.06	0.10	9.84	0.05	0.00	1.85	1.27	43.92	48.16	0.10	29.30	0.35	0.35	0.35	0.35	0.35	0.35	0.35	0.35	0.35	0.35	0.35	10	10	10	10	10	10	10	10	10	10	10	58	9.84	15	53.32	9.4	7.9
107	0.71	0.71	0.00	1.27	5.42	37.00	5.18	0.10	8.24	0.05	0.00	1.93	1.16	62.24	37.00	0.10	29.30	0.37	0.37	0.37	0.37	0.37	0.37	0.37	0.37	0.37	0.37	0.37	10	10	10	10	10	10	10	10	10	10	10	45.24	8.24	13.52	74.6	12.36	9.9
108	0.78	0.78	0.00	1.46	5.34	50.80	5.05	0.10	9.68	0.05	0.00	2.19	1.25	43.72	50.80	0.10	29.20	0.33	0.33	0.33	0.33	0.33	0.33	0.33	0.33	0.33	0.33	0.33	10	10	10	10	10	10	10	10	10	10	10	60.48	9.68	14.83	51.28	7.56	10.9
109	0.78	0.78	0.00	1.46	5.26	48.44	5.57	0.10	9.28	0.05	0.00	2.19	1.11	59.72	48.44	0.10	29.20	0.34	0.34	0.34	0.34	0.34	0.34	0.34	0.34	0.34	0.34	0.34	10	10	10	10	10	10	10	10	10	10	10	57.72	9.28	14.95	71.24	11.52	11
110	0.71	0.71	0.00	1.46	5.21	47.32	5.48	0.10	9.72	0.05	0.00	2.12	1.17	55.28	47.32	0.10	29.10	0.34	0.34	0.34	0.34	0.34	0.34	0.34	0.34	0.34	0.34	0.34	10	10	10	10	10	10	10	10	10	10	10	57.04	9.72	15.3	65.68	10.4	9.8
111	0.78	0.78	0.00	1.27	5.16	50.48	1.48	0.10	9.80	0.05	0.00	2.00	1.17	51.16	50.48	0.10	29.10	0.35	0.35	0.35	0.35	0.35	0.35	0.35	0.35	0.35	0.35	0.35	10	10	10	10	10	10	10	10	10	10	10	60.28	9.8	11.375	61.64	10.48	9.3
112	0.78	0.78	0.00	1.27	5.17	45.44	2.20	0.10	9.88	0.19	0.00	1.85	1.01	43.24	45.44	0.10	29.10	0.35	0.35	0.35	0.35	0.35	0.35	0.35	0.35	0.35	0.35	0.35	10	10	10	10	10	10	10	10	10	10	10	55.32	9.88	12.18	53.64	10.4	8.8
113	0.85	0.85	0.00	1.27	5.13	41.32	1.92	0.10	8.28	0.27	0.00	1.85	1.08	44.44	41.32	0.10	29.20	0.36	0.36	0.36	0.36	0.36	0.36	0.36	0.36	0.36	0.36	0.36	10	10	10	10	10	10	10	10	10	10	10	49.6	8.28	10.3	54.44	10	10.7
114	0.71	0.71	0.00	1.27	5.16	45.16	1.78	0.10	9.16	0.05	0.00	1.93	0.95	11.92	45.16	0.10	29.30	0.36	0.36	0.36	0.36	0.36	0.36	0.36	0.36	0.36	0.36	0.36	10	10	10	10	10	10	10	10	10	10	10	54.32	9.16	11.04	61.8	49.88	9.9
115	0.71	0.71	0.00	1.46	5.18	46.64	2.04	0.10	8.44	0.19	0.27	1.71	1.06	33.84	46.64	0.10	29.60	0.39	0.39	0.39	0.39	0.39	0.39	0.39	0.39	0.39	0.39	0.39	10	10	10	10	10	10	10	10	10	10	10	55.08	8.44	10.58	41.56	7.72	8.9
116	0.92	0.92	0.00	1.46	5.45	44.08	2.54	0.10	10.16	0.05	0.29	2.05	1.07	37.56	44.08	0.10	29.80	0.40	0.40	0.40	0.40	0.40	0.40	0.40	0.40	0.40	0.40	0.40	10	10	10	10	10	10	10	10	10	10	10	54.24	10.16	12.8	46.72	9.16	10.2
117	0.92	0.92	0.00	1.66	5.50	43.00	1.78	0.10	11.00	0.05	0.29	2.24	1.01	43.28	43.00	0.10	30.10	0.41	0.41	0.41	0.41	0.41	0.41	0.41	0.41	0.41	0.41	0.41	10	10	10	10	10	10	10	10	10	10	10	54	11	12.88	52.96	9.68	8.7
118	0.85	0.85	0.40	1.85	5.57	43.80	2.44	0.10	11.16	0.19	0.32	2.59	1.06	28.44	43.80	0.10	30.50	0.43	0.43	0.43	0.43	0.43	0.43	0.43	0.43	0.43	0.43	0.43	10	10	10	10	10	10	10	10	10	10	10	54.96	11.16	13.7	36.36	7.92	8.6
119	1.14	1.14	0.43	1.66	5.85	44.20	7.67	0.10	9.88	0.05	0.32	2.86	0.88	28.20	44.20	0.10	30.80	0.44	0.44	0.44	0.44	0.44	0.44	0.44	0.44	0.44	0.44	0.44	10	10	10	10	10	10	10	10	10	10	10	54.08	9.88	17.65	36.6	8.4	8.9
120	0.92	0.92	0.00	1.66	6.11	42.88	7.38	0.10	9.84	0.05	0.32	2.21	0.90	34.04	42.88	0.10	31.00	0.50	0.50	0.50	0.50	0.50	0.50	0.50	0.50	0.50	0.50	0.50	10	10	10	10	10	10	10	10	10	10	10	52.72	9.84	17.32	42.32	8.28	9.4
121	1.41	1.41	0.00	1.46	6.40	25.44	7.74	0.10	7.84	0.05	0.27	2.22	1.11	20.68	25.44	0.10	31.20	0.50	0.50	0.50	0.50	0.50	0.50	0.50	0.50	0.50	0.50	0.50	10	10	10	10	10	10	10	10	10	10	10	33.28	7.84	15.68	28.64	7.96	13
122	1.42	1.42	0.00	1.27	6.59	33.18	7.74	0.10	7.84	0.12	0.29	2.22	0.36	722.09	33.18	0.10	31.10	0.65	0.65	0.65	0.65	0.65	0.65	0.65	0.65	0.65	0.65	0.65	250	250	250	250	250	250	250	250	250	250	250	33.28	7.84	15.68	788.9513	66.85649	13
123	1.45	1.45	0.00	1.07	6.61	40.92	5.49	2.00	9.96	0.19	0.32	1.63	0.36	1,149.10	40.92	2.00	31.10	0.20	0.20	0.20	0.20	0.20	0.20	0.20	0.20	0.20	0.20	0.20	10	10	10	10	10	10	10	10	10	10	10	50.88	9.96	17.45	1199.1	50	25.5
124	1.17	1.17	0.00	1.27	6.63	42.44	5.77	2.00	10.80	0.19	0.27	1.80	0.85	269.40	42.44	2.00	30.90	0.20	0.20	0.20	0.20	0.20	0.20	0.20	0.20	0.20	0.20	0.20	10	10	10	10	10	10	10	10	10	10	10	53.24	10.8	18.57	310.64	41.24	25.5
125	1.14	1.14	0.00	1.07	6.36	40.08	7.44	2.00	9.48	0.05	0.00	2.17	0.24	87.00	40.08	2.00	30.80	0.20	0.20	0.20	0.20	0.20	0.20	0.20	0.20	0.20	0.20	0.20	10	10	10	10	10	10	10	10	10	10	10	49.56	9.48	18.915	103.52	16.52	13.9
126	0.63	0.63	0.00	1.66	6.49	44.16	7.35	2.00	8.88	0.05	0.00	2.24	0.21	87.88	44.16	2.00	30.80	0.20	0.20	0.20	0.20	0.20	0.20	0.20	0.20	0.20	0.20	0.20	10	10	10	10	10	10	10	10	10	10	10	53.04	8.88	18.23	100.28	12.4	12.9
127	0.71	0.71	0.00	1.66	6.40	44.68	0.10	9.00	10.20	0.19	0.00	2.17	0.91	72.04	44.68	9.00	30.80	0.25	0.25	0.25	0.25	0.25	0.25	0.25	0.25	0.25	0.25	0.25	10	10	10	10	10	10	10	10	10	10	10	54.88	10.2	19.3	85.4	13.36	12.8
128	0.92	0.92	0.00	1.46	6.52	42.96	0.09	9.00	10.64	0.05	0.00	2.34	1.05	56.04	42.96	9.00	30.80	0.30	0.30	0.30	0.30	0.30	0.30	0.30	0.30	0.30	0.30	0.30	10	10	10	10	10	10	10	10	10	10	10	53.6	10.64	19.735	68.44	12.4	12.8
129	0.85	0.85	0.00	1.46	6.40	41.12	0.48	9.00	11.04	0.05	0.27	2.00	0.95	49.84	41.12	9.00	30.80	0.25	0.25	0.25	0.25	0.25	0.25	0.25	0.25	0.25	0.25	0.25	10	10	10	10	10	10	10	10	10	10	10	52.16	11.04	20.5175	60.76	10.92	10
130	0.41	0.41	0.00	1.27	6.44	43.60	0.86	9.00	10.64	0.05	0.00	1.63	1.16	54.80	43.60	9.00	30.70	0.18	0.18	0.18	0.18	0.18	0.18	0.18	0.18	0.18	0.18	0.18	10	10	10	10	10	10	10	10	10	10	10	54.24	10.64	20.5	67.92	13.12	10.3
131	0.56	0.56	0.00	1.07	6.46	40.28	0.00	9.00	9.40	0.05	0.00	1.58	1.75	82.92	40.28	9.00	30.70	0.19	0.19	0.19	0.19	0.19	0.19	0.19	0.19	0.19	0.19	0.19	10	10	10	10	10	10	10	10	10	10	10	49.68	9.4	18.805	98.44	15.52	13.6
132	0.71	0.71	0.00	1.46	6.37	41.56	1.64	9.00	10.00	0.05	0.00	2.12	1.11	83.72	41.56	9.00	30.70	0.21	0.21	0.21	0.21	0.21	0.21	0.21	0.21	0.21	0.21	0.21	10	10	10	10	10	10	10	10	10	10	10	51.56	10	20.64	99.8	16.08	13.9
133	0.85	0.85	0.00	1.46	6.24	45.64	0.00	9.00	17.56	0.05	0.00	2.27	0.54	59.80	45.64	9.00	30.70	0.21	0.21	0.21	0.21	0.21	0.21	0.21	0.21	0.21	0.21	0.21	10	10	10	10	10	10	10	10	10	10	10	63.2	17.56	26.73	72.32	12.52	12.8
134	1.22	1.22	0.00	1.46	6.10	44.20	0.73	9.00	8.92	0.05	0.00	2.63	0.34	68.00	44.20	9.00	30.60	0.22	0.22	0.22	0.22	0.22	0.22	0.22	0.22	0.22	0.22	0.22	10	10	10	10	10	10	10	10	10	10	10	53.12	8.92	18.65	81.44	13.44	13.4
135	1.66	1.66	0.27	1.07	5.99	56.48	0.00	9.00	9.36	0.35	0.35	2.46	0.29	67.72	56.48	9.00	30.60	0.22	0.22	0.22	0.22	0.22	0.22	0.22	0.22	0.22	0.22	0.22	10	10	10	10	10	10	10	10	10	10	10	65.84	9.36	18.46	80.32	12.6	15.1
136	1.22	1.22	0.00	1.27	5.85	52.04	0.52	9.00	13.08	0.19	0.29	2.00	0.21	42.24	52.04	9.00	30.50	0.23	0.23	0.23	0.23	0.23	0.23	0.23	0.23	0.23	0.23	0.23	10	10	10	10	10	10	10	10	10	10	10	65.12	13.08	22.6	53.28	11.04	12.8
137	0.92	0.92	0.00	1.27	5.94	48.36	0.17	9.00	11.60	0.05	0.29	1.85	0.28	63.36	48.36	9.00	30.40	0.23	0.23	0.23	0.23	0.23	0.23	0.23	0.23	0.23	0.23	0.23	10	10	10	10	10	10	10	10	10	10	10	59.96	11.6	20.77	77.64	14.28	12.8
138	0.92	0.92	0.00	1.46	5.97	60.52	0.10	9.00	11.28	0.05	0.00	2.34	0.32	43.28	60.52	9.00	30.20	0.24	0.24	0.24	0.24	0.24	0.24	0.24	0.24	0.24	0.24	0.24	10	10	10	10	10	10	10	10	10	10	10	71.8	11.28	20.38	53.96	10.68	12.1
139	0.85	0.85	0.00	1.46	6.31	65.40	0.00	9.00	13.16	0.05	0.00	2.27	0.64	53.52	65.40	9.00	30.00	0.24	0.24	0.24	0.24	0.24	0.24	0.24	0.24	0.24	0.24	0.24	10	10	10	10	10	10	10	10	10	10	10	78.56	13.16	22.16	65.56	12.04	12.8
140	0.63	0.63	0.00	1.46	6.63	76.60	0.04	9.00	13.16	0.05	0.00	2.05	0.87	62.04	76.60	9.00	29.70	0.25	0.25	0.25	0.25	0.25	0.25	0.25	0.25	0.25	0.25	0.25	10	10	10	10	10	10	10	10	10	10	10	89.76	13.16	22.2	73.52	11.48	12.7
141	0.71	0.71	0.00	1.27	6.94	68.40	0.20	9.00	10.92	0.05	0.00	1.93	0.98	55.16	68.40	9.00	29.70	0.25	0.25	0.25	0.25	0.25	0.25	0.25	0.25	0.25	0.25	0.25	10	10	10	10	10	10	10	10	10	10	10	79.32	10.92	20.12	65.36	10.2	9.5

142	0.41	0.41	0.00	1.27	7.24	87.48	0.09	9.00	13.84	0.05	0.00	1.63	1.39	55.48	87.48	9.00	29.70	0.26	0.26	0.26	0.26	0.26	0.26	0.26	0.26	0.26	0.26	0.26	10	10	10	10	10	10	10	10	10	10	10	101.32	13.84	22.93	65.36	9.88	10.7
143	0.34	0.34	0.00	1.46	7.49	79.24	0.28	9.00	10.92	0.05	0.00	1.75	1.66	78.96	79.24	9.00	29.90	0.26	0.26	0.26	0.26	0.26	0.26	0.26	0.26	0.26	0.26	0.26	10	10	10	10	10	10	10	10	10	10	10	90.16	10.92	20.2	91.08	12.12	9.7
144	0.41	0.41	0.00	1.27	7.75	72.88	0.54	9.00	11.64	0.05	0.00	1.63	2.03	47.60	72.88	9.00	30.00	0.27	0.27	0.27	0.27	0.27	0.27	0.27	0.27	0.27	0.27	0.27	10	10	10	10	10	10	10	10	10	10	10	84.52	11.64	21.18	56.88	9.28	7.9
145	0.34	0.34	0.00	1.46	7.89	57.48	0.31	9.00	10.56	0.05	0.00	1.75	2.22	61.36	57.48	9.00	29.80	0.25	0.25	0.25	0.25	0.25	0.25	0.25	0.25	0.25	0.25	0.25	10	10	10	10	10	10	10	10	10	10	10	68.04	10.56	19.875	70.96	9.6	8
146	0.27	0.27	0.00	1.46	7.88	59.56	0.09	9.00	10.28	0.05	0.00	1.68	2.24	58.92	59.56	9.00	29.50	0.25	0.25	0.25	0.25	0.25	0.25	0.25	0.25	0.25	0.25	0.25	10	10	10	10	10	10	10	10	10	10	10	69.84	10.28	19.37	70.72	11.8	9.5
147	0.34	0.34	0.00	1.07	7.66	67.16	0.00	9.00	9.92	0.05	0.00	1.37	2.35	62.24	67.16	9.00	29.30	0.25	0.25	0.25	0.25	0.25	0.25	0.25	0.25	0.25	0.25	0.25	10	10	10	10	10	10	10	10	10	10	10	77.08	9.92	18.92	72.24	10	10
148	0.41	0.41	0.00	1.27	7.48	74.72	0.00	9.00	11.76	0.05	0.00	1.63	2.55	83.32	74.72	9.00	29.10	0.25	0.25	0.25	0.25	0.25	0.25	0.25	0.25	0.25	0.25	0.25	10	10	10	10	10	10	10	10	10	10	10	86.48	11.76	20.76	95.16	11.84	10.1
149	0.27	0.27	0.00	1.46	7.31	63.60	0.00	9.00	10.56	0.05	0.00	1.68	2.27	58.60	63.60	9.00	28.90	0.25	0.25	0.25	0.25	0.25	0.25	0.25	0.25	0.25	0.25	0.25	10	10	10	10	10	10	10	10	10	10	10	74.16	10.56	19.56	68.84	10.24	6.1
150	0.27	0.27	0.00	1.07	7.08	64.04	0.00	9.00	10.36	0.05	0.00	1.29	2.20	56.92	64.04	9.00	28.70	0.25	0.25	0.25	0.25	0.25	0.25	0.25	0.25	0.25	0.25	0.25	10	10	10	10	10	10	10	10	10	10	10	74.4	10.36	19.36	65.68	8.76	9.7
151	0.19	0.19	0.00	1.27	6.98	105.24	0.27	9.00	14.32	0.05	0.00	1.41	2.52	80.64	105.24	9.00	28.70	0.25	0.25	0.25	0.25	0.25	0.25	0.25	0.25	0.25	0.25	0.25	10	10	10	10	10	10	10	10	10	10	10	119.56	14.32	23.585	93.52	12.88	8.9
152	0.27	0.27	0.00	1.07	6.73	62.68	0.00	9.00	10.84	0.05	0.00	1.29	2.35	55.12	62.68	9.00	28.70	0.24	0.24	0.24	0.24	0.24	0.24	0.24	0.24	0.24	0.24	0.24	10	10	10	10	10	10	10	10	10	10	10	73.52	10.84	18.54	65.4	10.28	7
153	0.05	0.05	0.00	1.07	6.71	59.52	0.00	9.00	10.52	0.05	0.00	1.07	2.06	41.72	59.52	9.00	28.60	0.27	0.27	0.27	0.27	0.27	0.27	0.27	0.27	0.27	0.27	0.27	10	10	10	10	10	10	10	10	10	10	10	70.04	10.52	17.52	50.08	8.36	8
154	0.05	0.05	0.00	1.07	6.72	57.56	0.00	9.00	10.28	0.05	0.00	1.07	1.97	38.24	57.56	9.00	28.60	0.28	0.28	0.28	0.28	0.28	0.28	0.28	0.28	0.28	0.28	0.28	10	10	10	10	10	10	10	10	10	10	10	67.84	10.28	17.48	46.4	8.16	7
155	0.05	0.05	0.00	0.88	6.66	56.00	1.50	9.00	10.16	0.05	0.00	0.88	2.05	45.80	56.00	9.00	28.50	0.28	0.28	0.28	0.28	0.28	0.28	0.28	0.28	0.28	0.28	0.28	10	10	10	10	10	10	10	10	10	10	10	66.16	10.16	20.66	54.32	8.52	13
156	0.05	0.05	0.00	1.07	6.61	55.48	0.10	9.00	9.00	0.05	0.00	1.07	2.22	49.16	55.48	9.00	28.50	0.29	0.29	0.29	0.29	0.29	0.29	0.29	0.29	0.29	0.29	0.29	10	10	10	10	10	10	10	10	10	10	10	64.48	9	18.1	57.8	8.64	9
157	0.19	0.19	0.00	1.07	6.57	54.24	0.00	9.00	9.84	0.05	0.00	1.22	2.27	42.76	54.24	9.00	28.40	0.29	0.29	0.29	0.29	0.29	0.29	0.29	0.29	0.29	0.29	0.29	10	10	10	10	10	10	10	10	10	10	10	64.08	9.84	16.84	51.08	8.32	12
158	0.19	0.19	0.00	1.27	6.53	54.76	0.00	9.00	9.84	0.05	0.00	1.41	2.31	37.32	54.76	9.00	28.40	0.30	0.30	0.30	0.30	0.30	0.30	0.30	0.30	0.30	0.30	0.30	10	10	10	10	10	10	10	10	10	10	10	64.6	9.84	17.04	50.28	12.96	12
159	0.05	0.05	0.00	1.27	6.48	62.52	2.20	9.00	10.20	0.05	0.00	1.27	2.33	49.48	62.52	9.00	28.40	0.30	0.30	0.30	0.30	0.30	0.30	0.30	0.30	0.30	0.30	0.30	10	10	10	10	10	10	10	10	10	10	10	72.72	10.2	21.4	58.6	9.12	8
160	0.19	0.19	0.00	1.27	6.43	64.68	2.90	9.00	9.88	0.05	0.00	1.41	2.39	42.00	64.68	9.00	28.30	0.31	0.31	0.31	0.31	0.31	0.31	0.31	0.31	0.31	0.31	0.31	10	10	10	10	10	10	10	10	10	10	10	74.56	9.88	21.78	50.04	8.04	9
161	0.19	0.19	0.00	1.07	6.39	57.24	1.50	9.00	9.20	0.05	0.00	1.22	2.76	46.64	57.24	9.00	28.30	0.31	0.31	0.31	0.31	0.31	0.31	0.31	0.31	0.31	0.31	0.31	10	10	10	10	10	10	10	10	10	10	10	66.44	9.2	19.7	56.04	9.4	7

2.4. LIST OF FIGURES

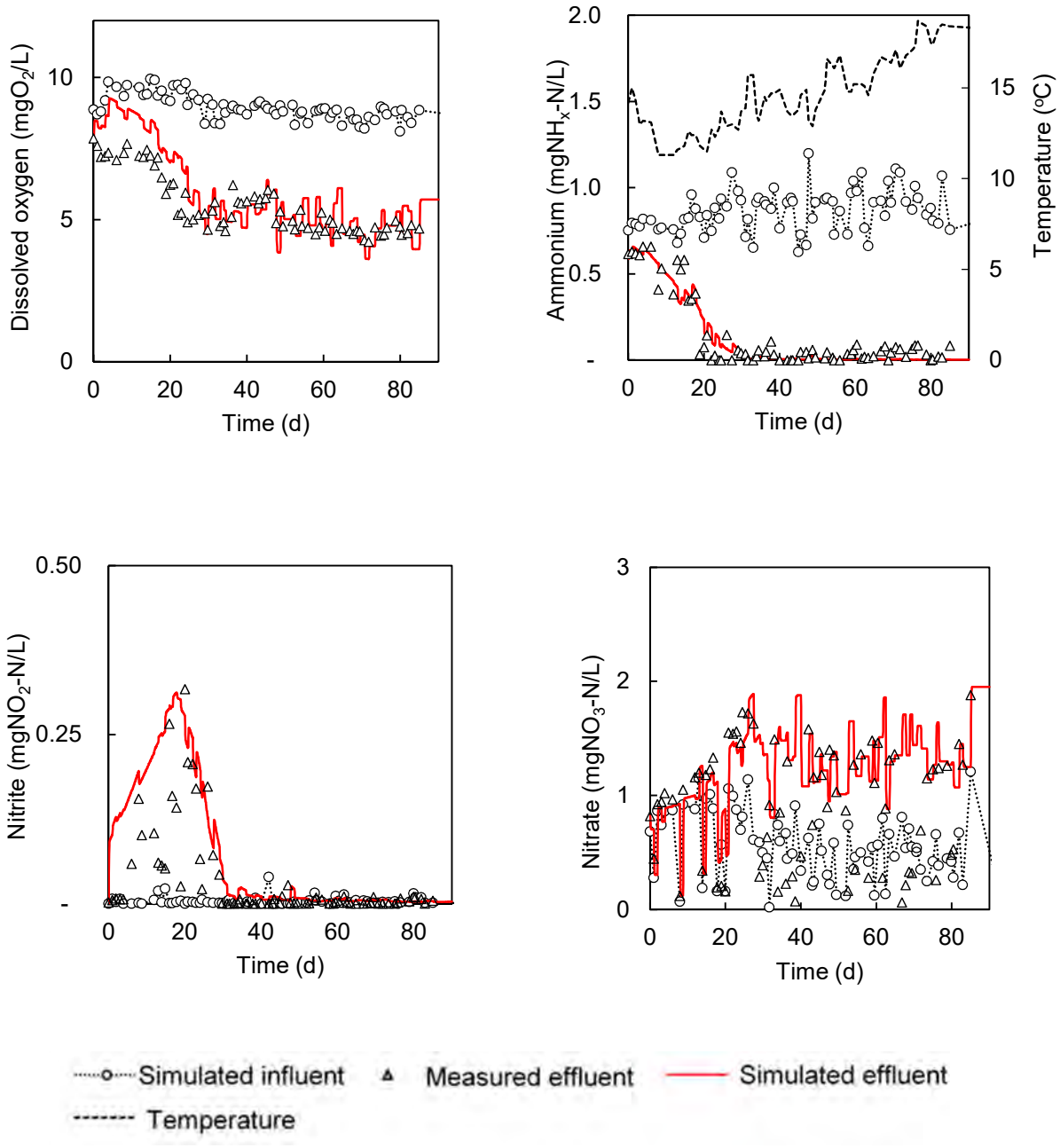

Figure S 1. Measured and simulated results for the lab-scale reactor in the start-up period

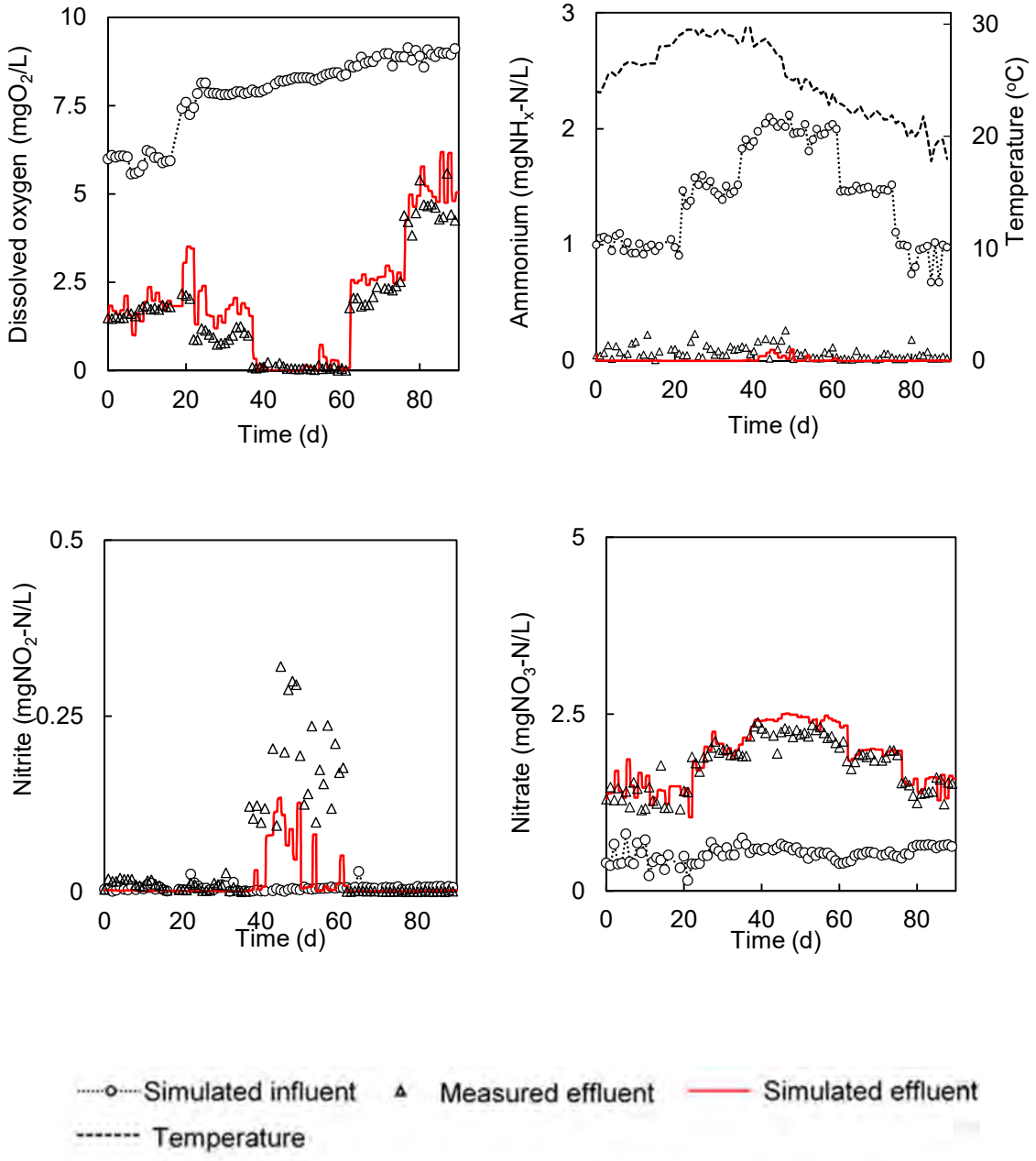

Figure S 2. Measured and simulated results for the lab-scale reactor in the continuous operation

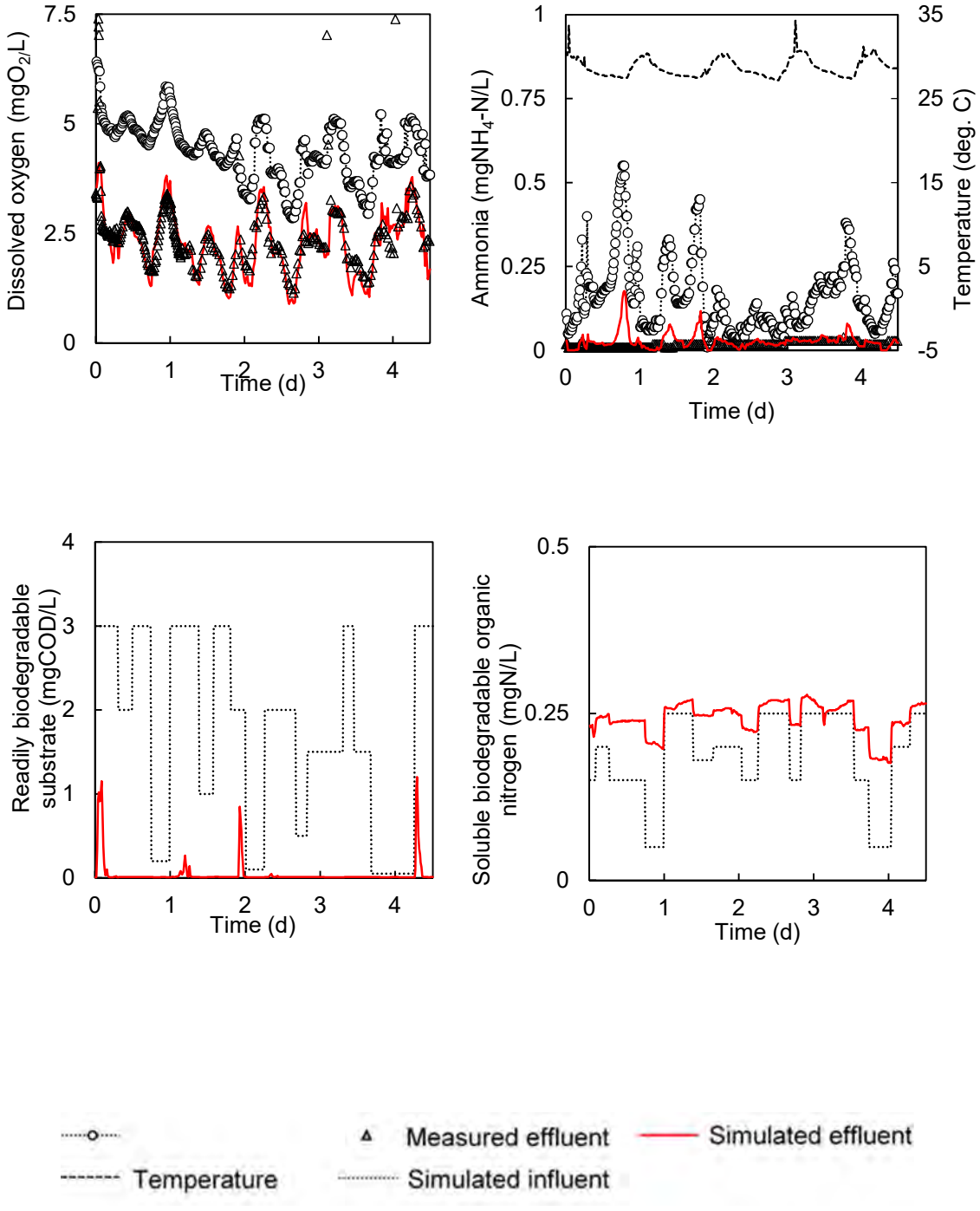

Figure S 3. Measured and simulated results for the pilot-scale reactor in Hoa Phu WTP

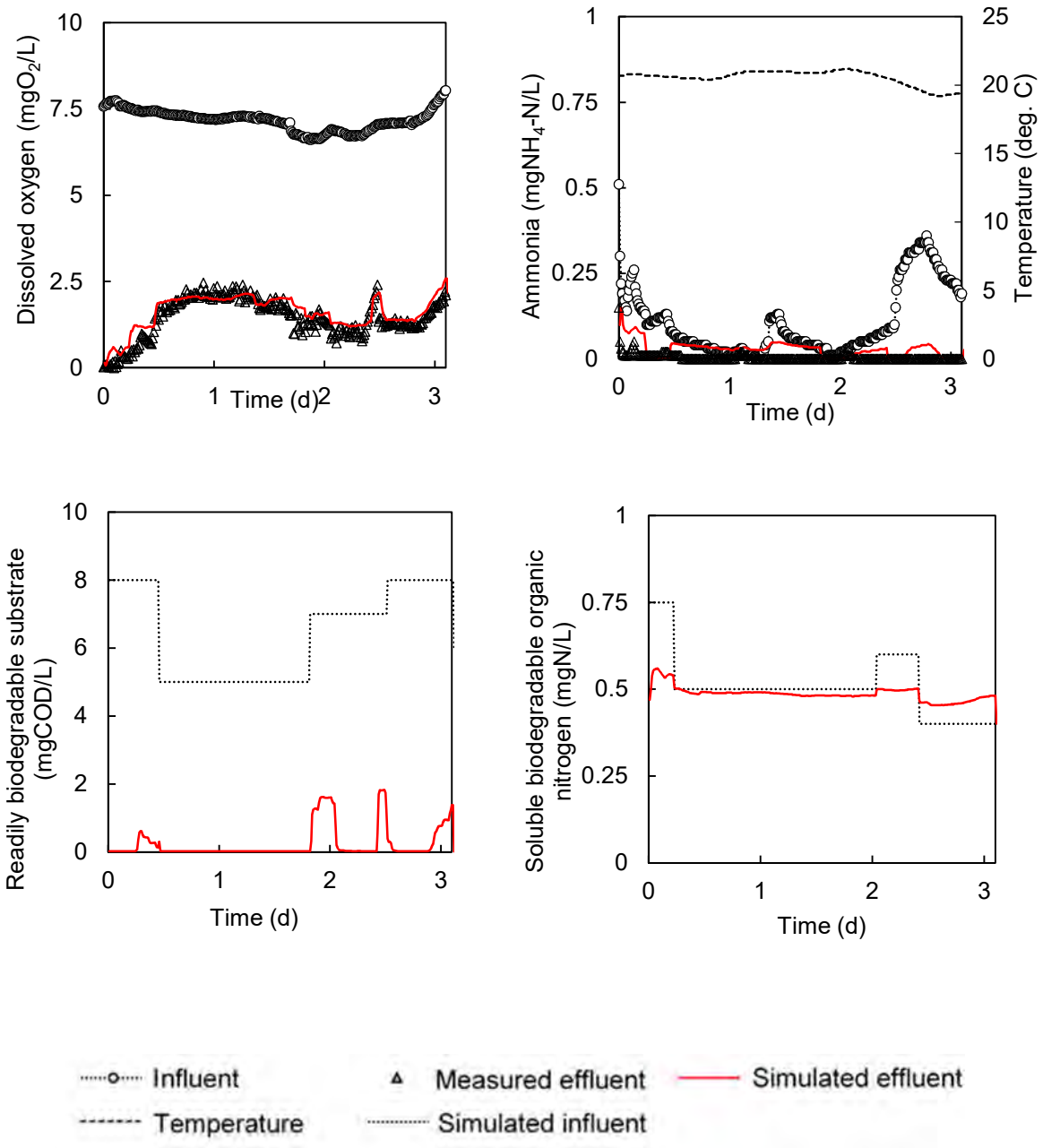

Figure S 4. Measured and simulated results for the full-scale reactor in Vinh Bao WTP (D)

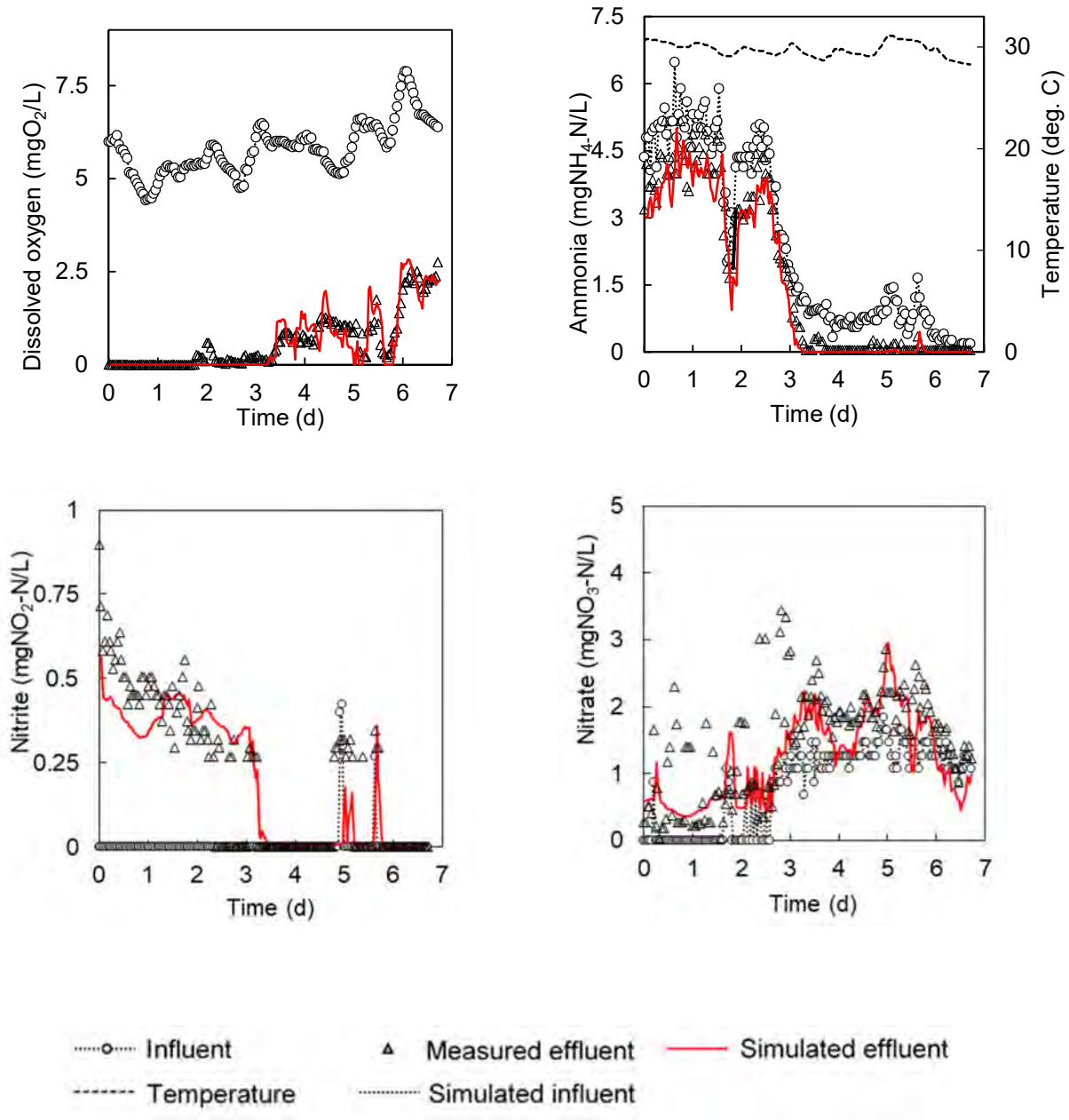

Figure S 5. Measured and simulated results for the full-scale reactor in Vinh Bao WTP (R)

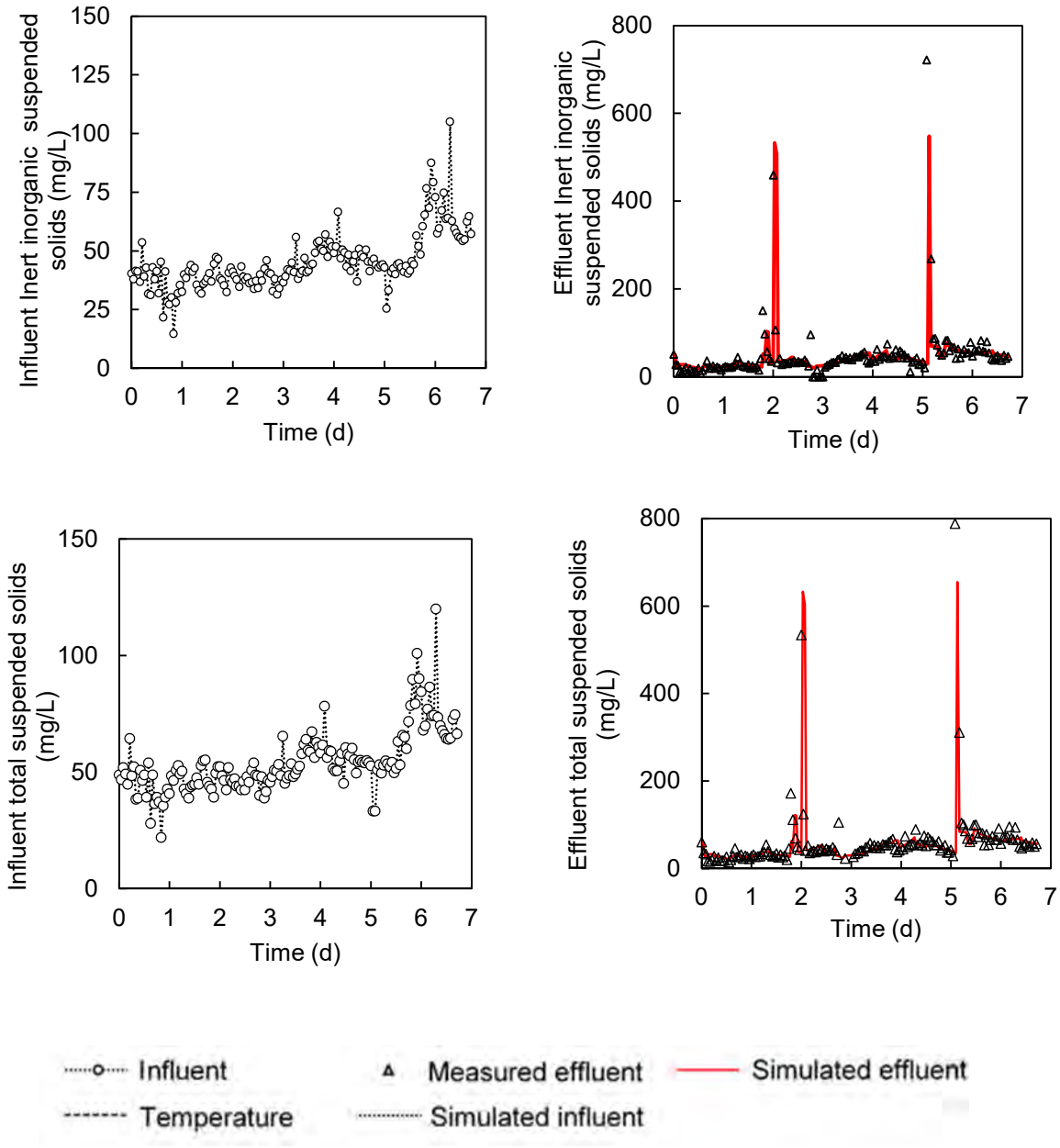

Figure S 6. Measured and simulated results for the full-scale reactor in Vinh Bao WTP (R)

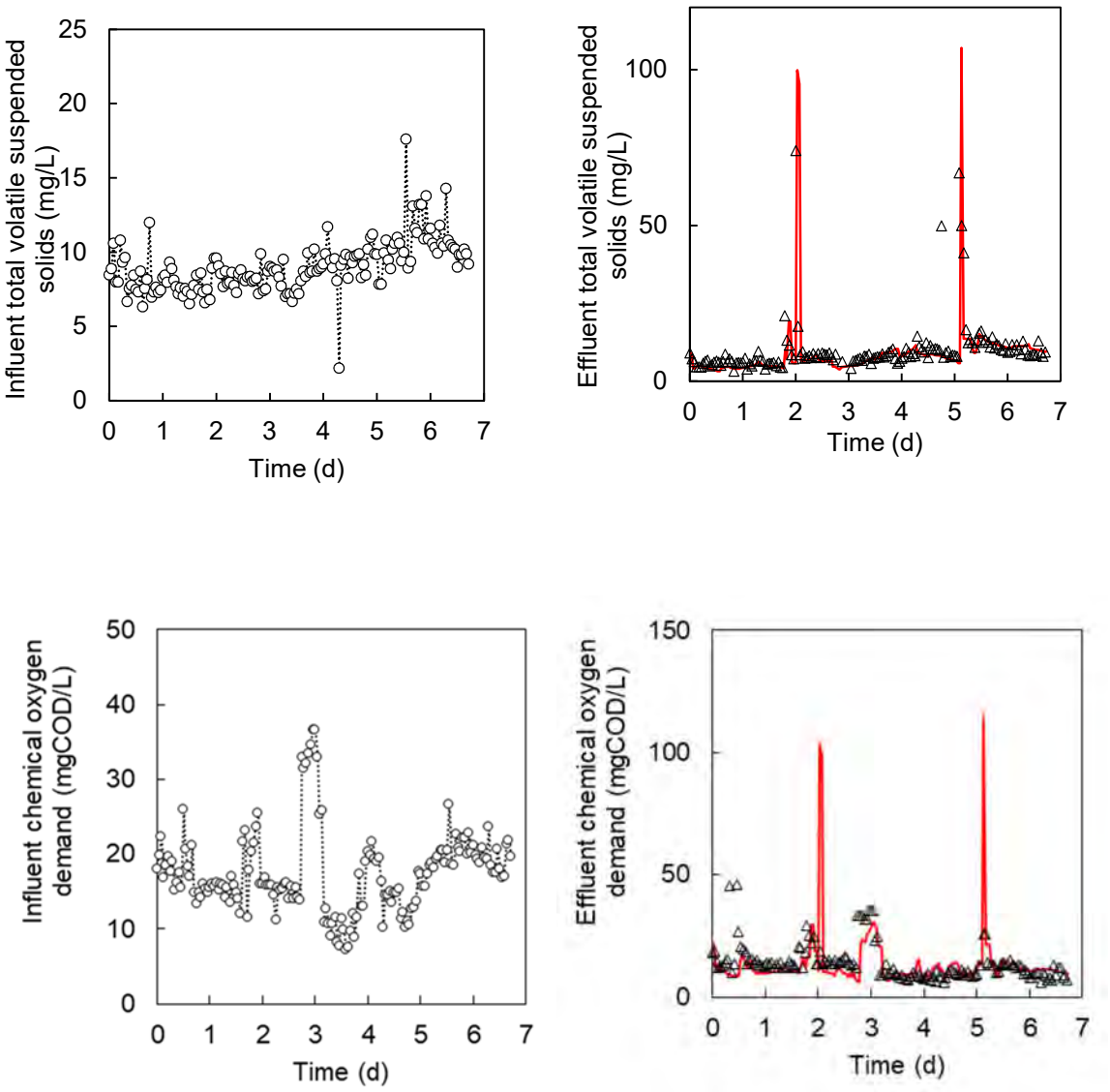

Figure S 7. Measured and simulated results for the full-scale reactor in Vinh Bao WTP (R)

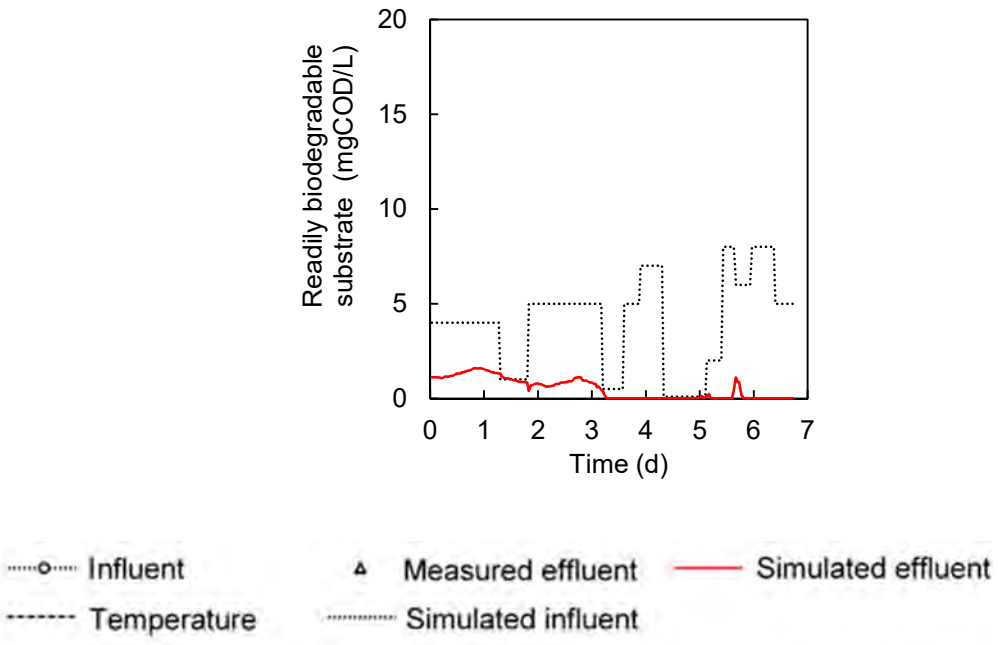

Figure S 8. Measured and simulated results for the full-scale reactor in Vinh Bao WTP (R)

LIST OF PUBLICATIONS

1. **Nguyet Thi-Minh Dao**, The-Anh Nguyen, Viet-Anh Nguyen, Mitsuharu Terashima, Rajeev Goel, and Hidenari Yasui, "A mathematical model of a nitrifying expanded-bed reactor for the pretreatment of drinking water", Biochemical Engineering Journal, vol. 158, 2020.

2. **Nguyet Thi-Minh Dao**, The-Anh Nguyen, Viet-Anh Nguyen, Mitsuharu Terashima, and Hidenari Yasui, "Pesticide removals in the nitrifying expanded-bed filter at drinking water treatment plant", Journal of Science and Technology in Civil Engineering, vol. 15, No 1/1-2021.

PARTICIPATION TO INTERNATIONAL CONFERENCES

1. **Nguyet Thi-minh Dao**, The-anh Nguyen, Mitsuharu Terashima, Hidenari Yasui. Possible degradation of pesticides in the nitrifying expanded-bed filter for drinking water treatment. *Water and Environment Technology Conference 2019,* 13-14 July, Osaka, Japan, 2019.

2. **Nguyet Thi-minh Dao**, The-anh Nguyen, Mitsuharu Terashima, Hidenari Yasui. Pesticide removal in the expanded-bed biofilter at drinking water plant. *The 9th International Forum on Green Technology and Management (IFGTM 2019),* 27-28 September, Hanoi, Vietnam, 2019.

3. **Nguyet Thi-minh Dao**, The-anh Nguyen, Mitsuharu Terashima, Hidenari Yasui. A hydraulic model for the expanded-bed reactor for the pretreatment of drinking water. *2019 Japan/Taiwan/Korea Chemical Engineering conference,* 13-15 November, Beppu, Japan, 2019.